NASA CR 174685
SCT 5471 FR

NASA

IDENTIFICATION OF QUASI-STEADY COMPRESSOR CHARACTERISTICS FROM TRANSIENT DATA

FINAL REPORT

Prepared by

K.B. Nunes
S.M. Rock

September 1984

Prepared for

NATIONAL AERONAUTICS AND SPACE ADMINISTRATION
Lewis Research Center
21000 Brookpark Road
Cleveland, Ohio 44135

Under Contract No. NAS3-23537

1. Report No.	2. Government Accession No.	3. Recipient's Catalog No.
NASA CR 174685		

4. Title and Subtitle	5. Report Date
IDENTIFICATION OF QUASI-STEADY COMPRESSOR CHARACTERISTICS FROM TRANSIENT DATA	September 1984
	6. Performing Organization Code: 5471 FR

7. Author(s)	8. Performing Organization Report No.
K.B. Nunes S.M. Rock	
	10. Work Unit No.

9. Performing Organization Name and Address	11. Contract or Grant No.
Systems Control Technology, Inc. 1801 Page Mill Road Palo Alto, CA 94304	NAS3-23537
	13. Type of Report and Period Covered: Contractor Report

12. Sponsoring Agency Name and Address	14. Sponsoring Agency Code
NASA Lewis Research Center Cleveland, Ohio 44135	

15. Supplementary Notes

Project Manager, Leon M. Wenzel, NASA Lewis Research Center, Cleveland, Ohio 44135

16. Abstract

This is the final report for the program entitled "Development of a Technique to Identify Quasi-Steady In-Stall Compressor Maps from Transient Data," sponsored by NASA LeRC. The principal goal of this program was to demonstrate that nonlinear compressor map parameters, which govern an in-stall response, can be identified from test data using parameter identification techniques. The program tasks included developing and then applying an identification procedure to data generated by NASA LeRC on a hybrid computer.

Two levels of model detail were employed. First was a lumped compressor rig model; second was a simplified turbofan model.

The main outputs of this program are the tools and procedures generated to accomplish the identification.

17. Key Words (Suggested by Author(s))	18. Distribution Statement
parameter identification system identification compressor modeling nonrecoverable stall	UNCLASSIFIED - Unlimited

19. Security Classif. (of this report)	20. Security Classif. (of this page)	21. No. of pages	22. Price*
UNCLASSIFIED	UNCLASSIFIED		

*For sale by the National Technical Information Service, Springfield, Virginia 22161

TABLE OF CONTENTS

TABLE OF CONTENTS (Continued)

TABLE OF CONTENTS (Concluded)

LIST OF FIGURES

LIST OF FIGURES (Continued)

LIST OF FIGURES (Continued)

LIST OF FIGURES (Continued)

LIST OF FIGURES (Concluded)

LIST OF TABLES

LIST OF TABLES (Continued)

FOREWORD

The work described in this report was performed under Contract NAS3-23537 for the NASA Lewis Research Center. The technical monitor for NASA is Mr. Leon Wenzel. The principal author from Systems Control Technology, Inc. is Mr. Kenneth Nunes. The program manager for the Identification of Quasi- Steady Compressor Characteristics Program is Dr. Stephen Rock. Report preparation efforts were directed by Ms. Clare Walker.

I. INTRODUCTION AND SUMMARY

1.1 INTRODUCTION

All engines occasionally stall. This is a result of their operating with minimum stall margins to maximize performance and economy. In recent years, a considerable number of data gathering and analysis techniques have been used to derive engine designs that attempt to minimize the occurrence of stalls. Obviously, when stalling does occur, it is desired that the stalls be only momentary disruptions of the performance of the engine and that they may be self-recovering with no action required of the pilot. Unfortunately, some modern turbofans, after one or more surge/stall cycles, stabilize at an operating point of low speeds and high turbine temperatures. This situation is termed nonrecoverable stall [1,2]. In some cases, it has led to loss of the turbine. The situation almost invariably requires shutdown and restart in order to clear the engine of this condition.

Current design techniques do not provide adequate insight into the sensitivity or susceptibility to nonrecoverable stall. Consequently, since neither the physical mechanism nor the influence factors triggering or exciting the phenomena are clearly understood, satisfactory technical guidelines to assure avoidance of or recovery from this behavior do not exist.

One of the most important and least well-known parameters governing stall behavior is the quasi-steady in-stall compressor performance. Identifying the parameters which describe this performance characteristic is a non-trivial problem. Data are scarce and models have not been verified.

The solution to nonrecoverable stall most probably involves both component and system redesign. Compression system characteristics may be altered either through component redesign or innovative uses of bleeds and variable geometries. System changes may involve parameter changes (volumes, etc.) and/or innovative uses of multivariable control theory. In short, interactions among the compression components, bleeds, ducting, splitters, volumes, and controls are all potentially significant factors governing the nonrecoverability of engine stalls. Investigating these interactions and the effectiveness of proposed solutions required validated engine stall models.

In the past 10 years, system analysis tools have been fully developed and implemented which are directed toward system identification [3-21]. The tools include algorithms for mathematical model structure determination, parameter estimation, and test planning. These tools, when properly applied, provide the test engineer and engine designer with the vaidated data and test results to make critical assessments and evaluations of design decisions directed toward the alleviation of nonrecoverable stall.

1.2 PROGRAM GOALS

This is the final report the program entitled "Development of a Technique to Identify Quasi-Steady In-Stall Compressor Maps from Transient Data," sponsored by NASA LeRC. The principal goal of this program was to demonstrate that nonlinear compressor map parameters, which govern an in-stall response, can be identified from test data using parameter identification techniques. The program tasks included developing and then applying an identification procedure to data generated by NASA LeRC on a hybrid computer. This provided a means of verifying the technique since the exact parameter values were known (although they were not known beforehand by SCT).

Two levels of model detail were employed. First, the procedure was applied to a lumped compressor rig model that was derived from Ref. 3. This model is presented schematically in Figures 1.1 and 1.2, and described in detail in Chapter IV and Appendix A. Second, a simplified turbofan model was used. This model was also taken from Ref. 3. It is presented schematically in Figure 1.3 and is discussed in Chapters VI and Appendix B.

The main outputs of this program are the tools and procedures generated to accomplish the identification.

1.3 SUMMARY OF RESULTS

The program goals were accomplished. For both the simulated rig data and the turbofan data, not only were the compressor characteristics identified successfully, but also other engine parameters (e.g., flow resistances and volumes). This success is a major step towards the development of a procedure applicable to real test data.

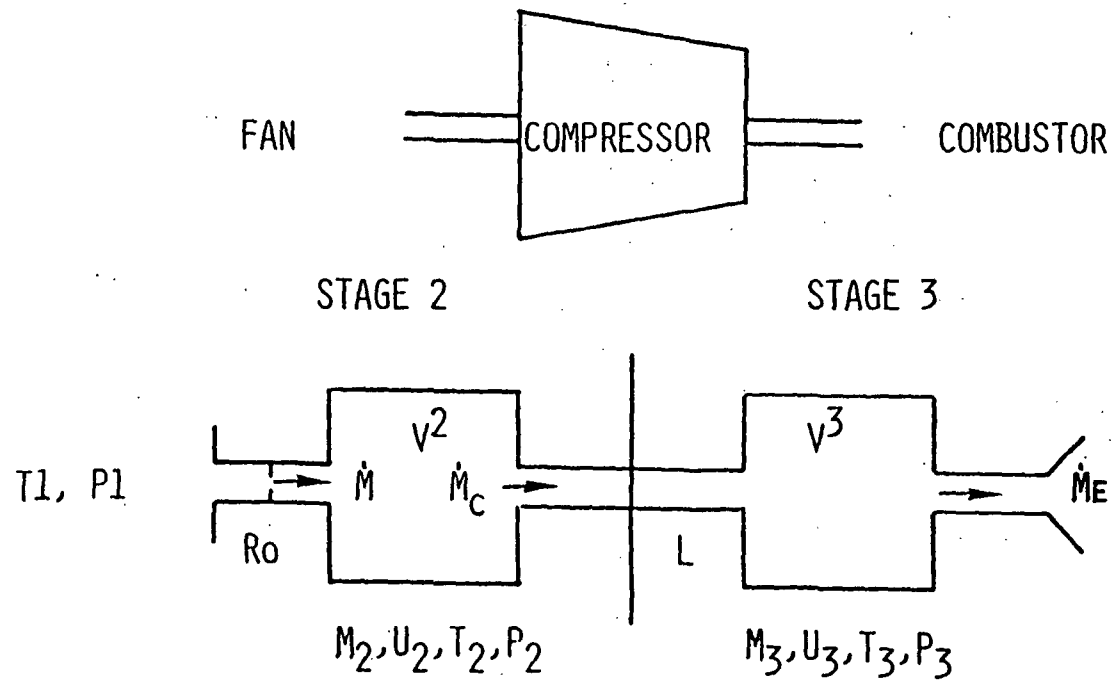

STAGE *

- RESISTIVE INLET
- STAGE 2 & 3 CONSTANT VOLUME, ADIABATIC
- STAGE 2 & 3 MASS CONSERVATION
- TEMPERATURE & PRESSURE f(u,m)
- COMPRESSOR MAP AT STAGE *
- INDUCTIVE FLOW INTO STAGE 3
- THROTTLED, ADIABATIC EXIT FLOW
- CONSTANT SPEED

Figure 1.1 Compressor Rig Lumped Parameter Model

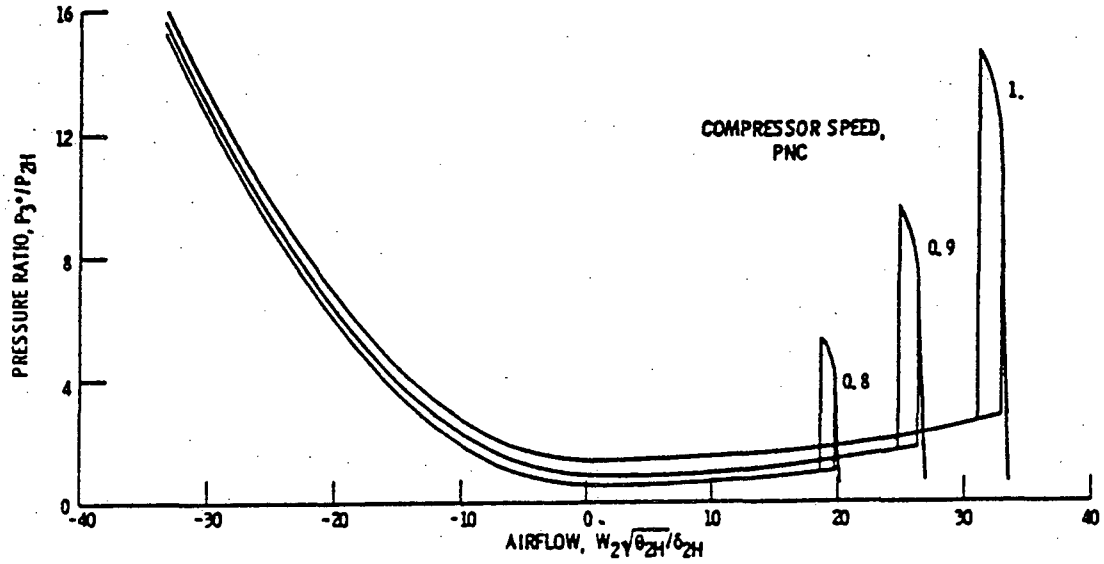

Figure 1.2 Pressure Performance Map for Compressor

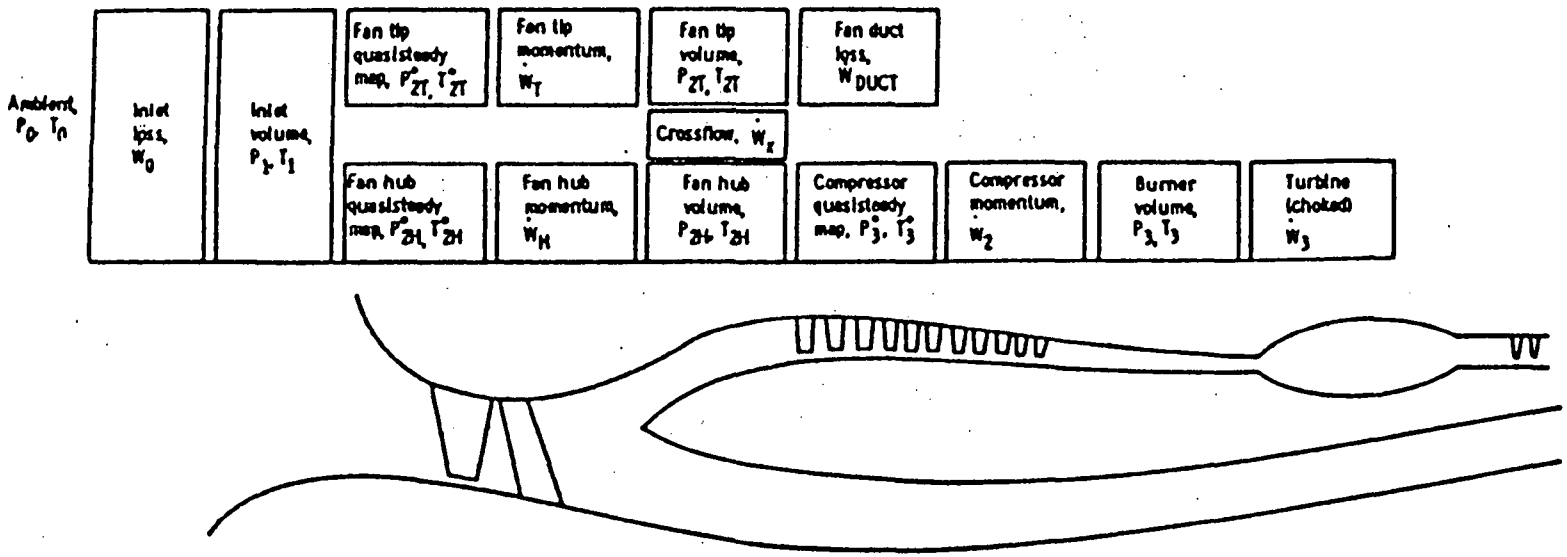

Figure 1.3 Schematic Diagram of the Turbofan Model (from Reference 1)

In future efforts, SCT plans to extend these results to actual compressor rig and turbofan test data.

One important difference between the work accomplished in this program and that proposed for future studies is that the correct model structure was known in this program. It will not generally be known for actual compressor rigs and turbofans. This added complexcity will add to the challenge of those future efforts; however, it also helps justify this current effort.

1.4 SUMMARY

This final report documents all program results and includes general conclusions and recommendations. It is arranged around the program outline. After background and details of parameter estimation are discussed in Chapters II and III, the results of the compressor rig study are examined in Chapter IV. The identifiability/sensitivity study of the turbofan study are documented in Chapters V and VI. Chapter VII summarizes all results and documents general conclusions and specific recommendations.

II. BACKGROUND

2.1 INTRODUCTION

The primary objective of this program is to develop and demonstrate techniques to identify engine parameters. In this program, the parameters studied represent the characterisitics of an engine compressor during recoverable or non-recoverable stall.

The method being used to study these parameters is parameter estimation (or identification). Parameter identification is used because of its uniquely effective ability to evaluate real, transient data and to extract model information.

In this program, parameter identification is used to identify four parameters: Kp (compressor positive flow characteristics), Kn (compressor negative flow characteristics), Rx (cross-flow resistance) and V3 (lumped parameter value of stage 3 volumes). Program focus, however, is upon the two parameters which define a quasi-steady in-stall compressor map: Kp and Kn. These parameters define the shape of the compressor map during an in-stall condition for positive (Kp) and negative (Kn) compressor flows. An example of how the parameters affect the in-stall compressor map is shown in Figure 2.1.

The interest in Kp and Kn comes from their effect on the stall response of the engine [3]. Some Kp and Kn values allow the engine to recover from the stall simply by the nature of the in-stall compressor maps. Alternately, other Kp and Kn values produce non-recoverable stall responses in the engine (Figure 2.2). While the immediate goal of the program is to identify these in-stall parameters from simulated engine data, a long-term goal is to study what in the engine build determines these Kp and Kn values.

Because this program is intended to demonstrate an ability to identify these parameters, the work was done in a controlled situation. Instead of using real engine data to identify the parameters, synthesized data were used. This way, noise and sensor characteristics could be added and removed

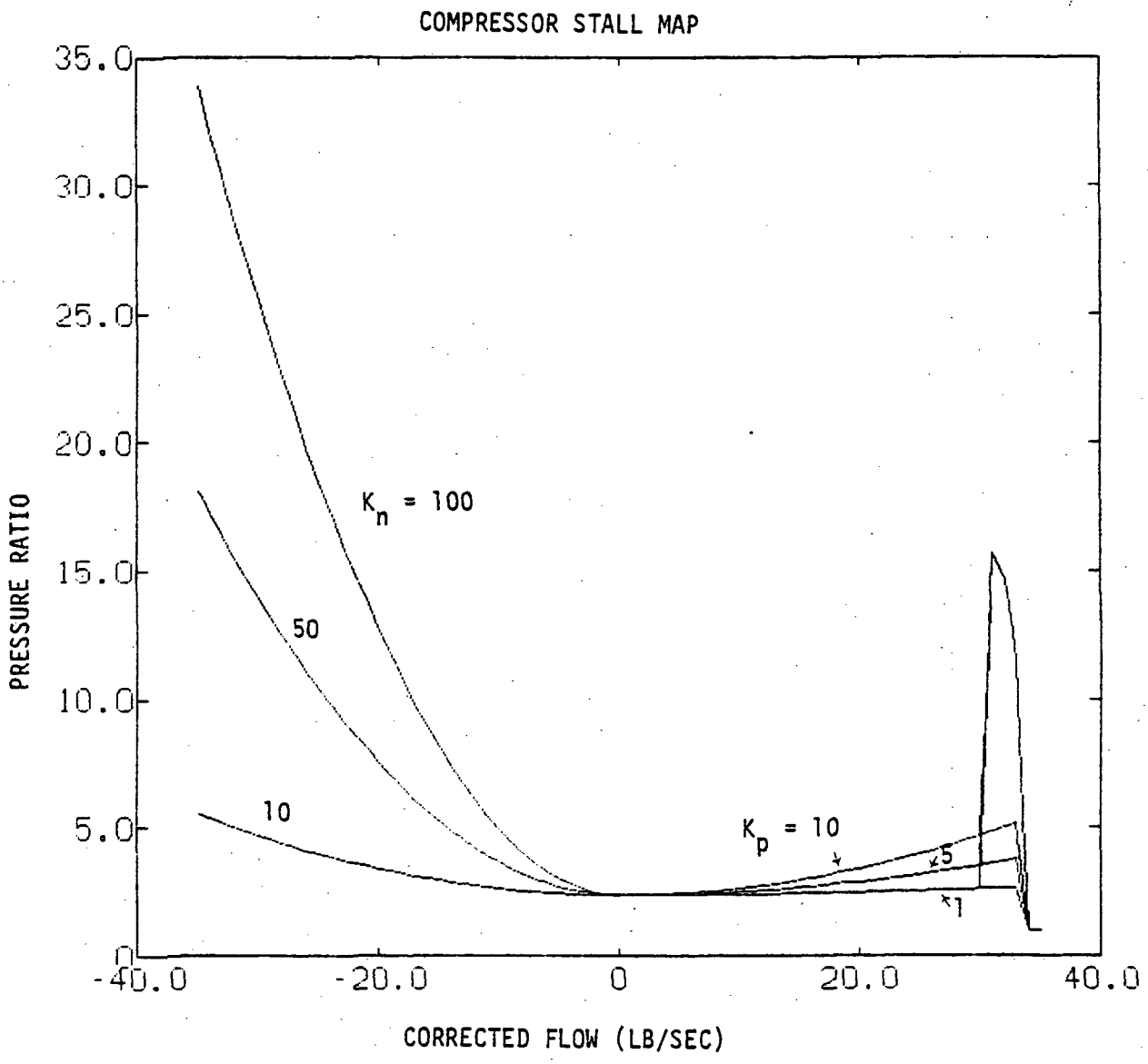

Figure 2.1 Compressor Stall Map Parameter Variations

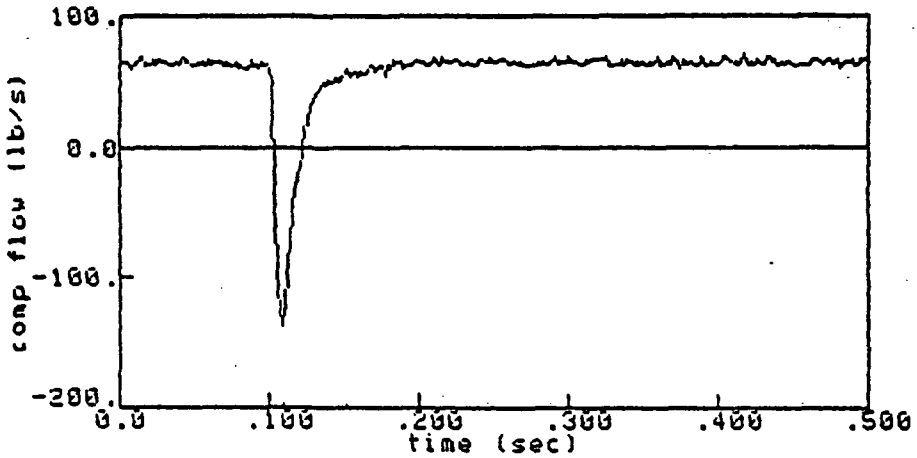

(a) Recoverable Stall

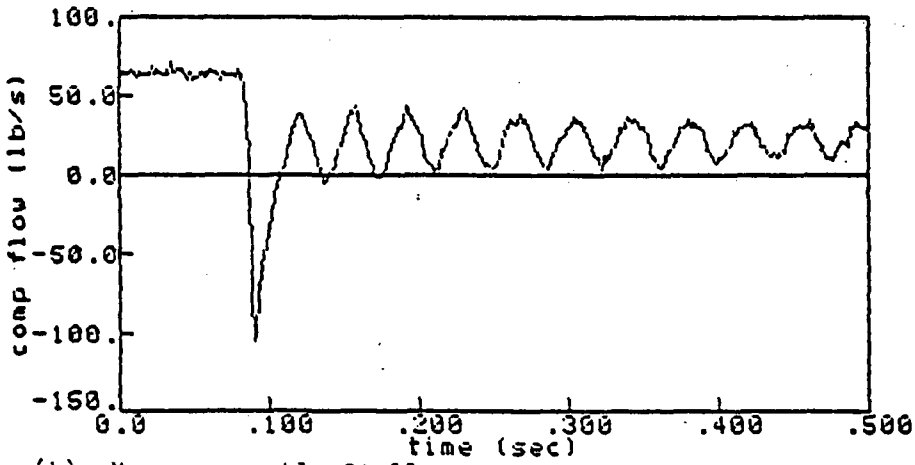

(b) Nonrecoverable Stall

Figure 2.2 Effect of K_p and K_n on Stall Trajectory

from the synthetic data to see how they affect identification. Follow-on efforts are expected to apply these results to actual engine test data.

Synthesized data were provided by the hybrid computing facilities at NASA LeRC. The hybrid computer implements low-order stand-alone compressor rig and turbofan models characterisitic of the Pratt Whitney TF-34 engine. Both models are capable of producing recoverable and non-recoverable stall.

Synthesized data representing both non-recoverable and recoverable stall were generated by encoding different Kp and Kn values into the hybrid model compressor maps. The hybrid models were perturbed to initiate stall and the resulting data are recorded on tape with an FM multiplexer, filtered and eventually digitally recorded on another tape. That digital tape was then sent to SCT for processing. The whole recording process and the use of the hybrid computer are emulating the steps that normally occur during an engine test. Figure 2.3 illustrates how the information flows through the recording and analysis system.

Once the data arrived at SCT, it was processed using an SCT-developed software package called SCIDNT. SCIDNT uses parameter estimation theory developed at SCT over the past ten years to identify the engine parameters. (Details on the workings of SCIDNT are found in Chapter III.)

The basic idea in system parameter identification is to find model parameters that cause the model to reproduce and predict plant responses as accurately as possible. Parameters identified by SCIDNT represent maximum likelihood values which are most likely to be the actual parameter values of the plant. In terms of the Kp and Kn identifications, the identified values have the highest probability of being the same as those used to produce the data. In a real engine test, the identified parameters would be those values that most likely describe the true characteristics of the engine.

A few examples of the identifications from the program are shown in Figures 2.4 through 2.6. Notice that SCT's initial model (represented by the solid, noise-free line) disagrees with the NASA data which has had noise added to it. As SCIDNT evaluates and compares the NASA data to the SCT model, it changes the values of Kp and Kn until the model and plant responses become as close as possible. Finally, SCIDNT converges to a solution (a new in-stall compressor map) which is the best estimate of the actual characteristic of the engine.

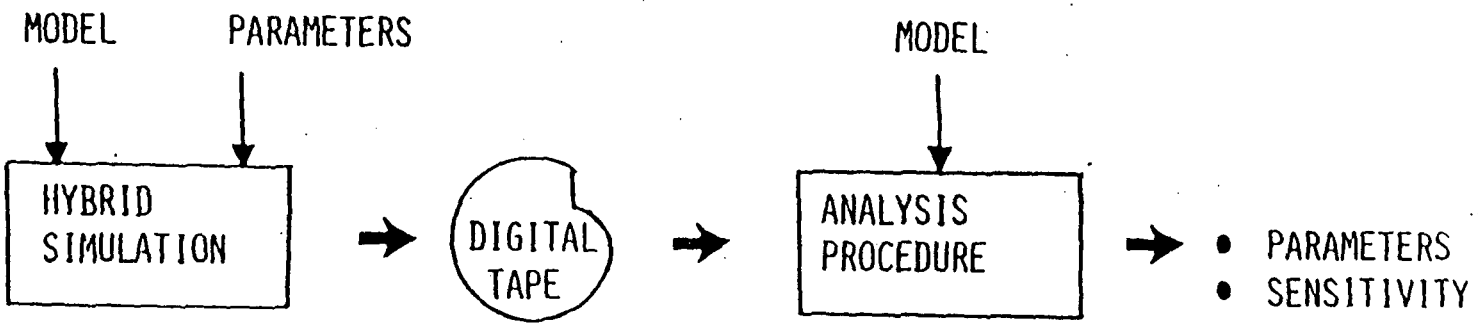

- RIG
- TURBOFAN

"MYSTERY" PARAMETERS

Figure 2.3 Program Approach

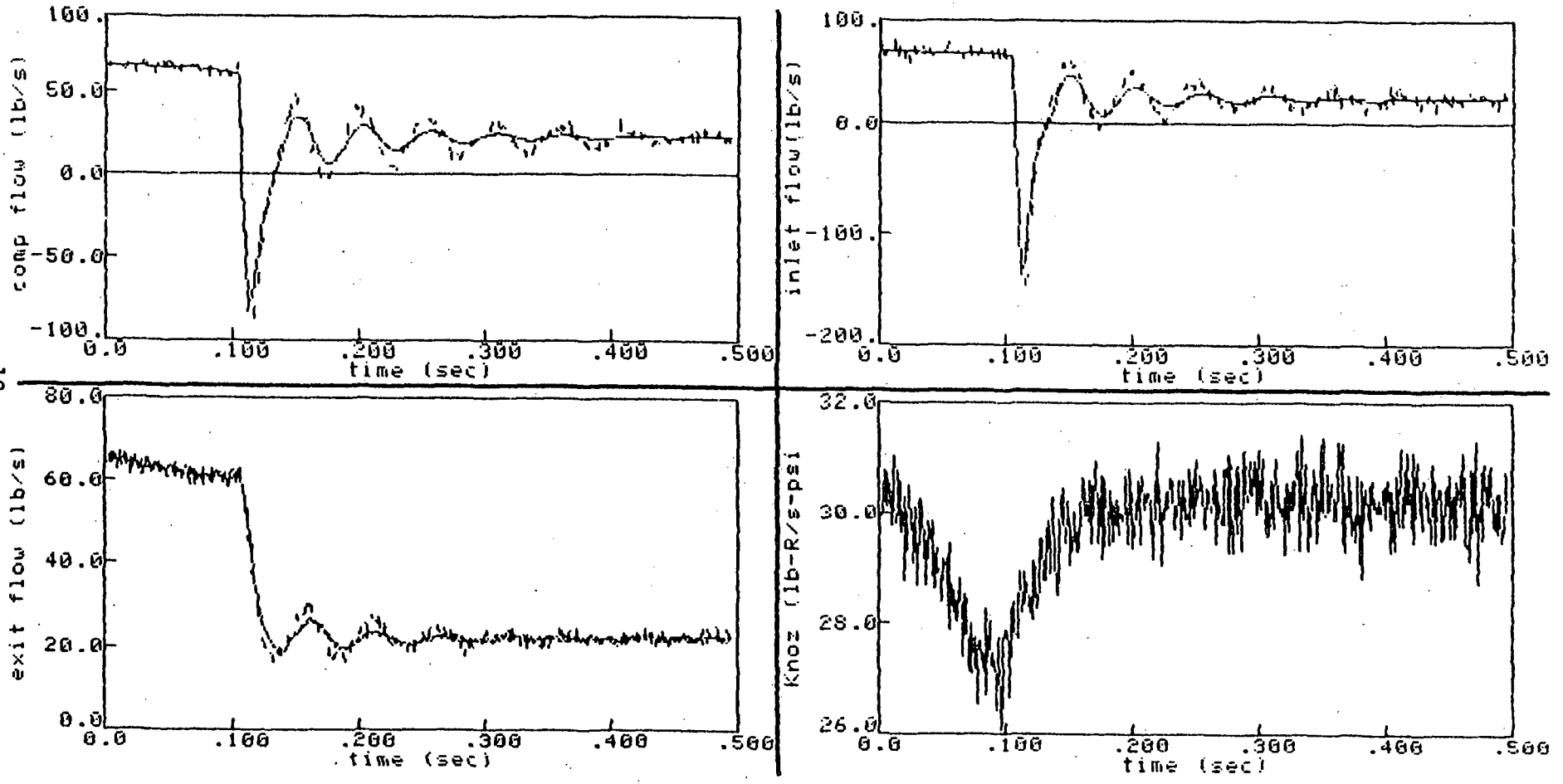

Figure 2.4 Comparison of Initial Parameter Curves with Data

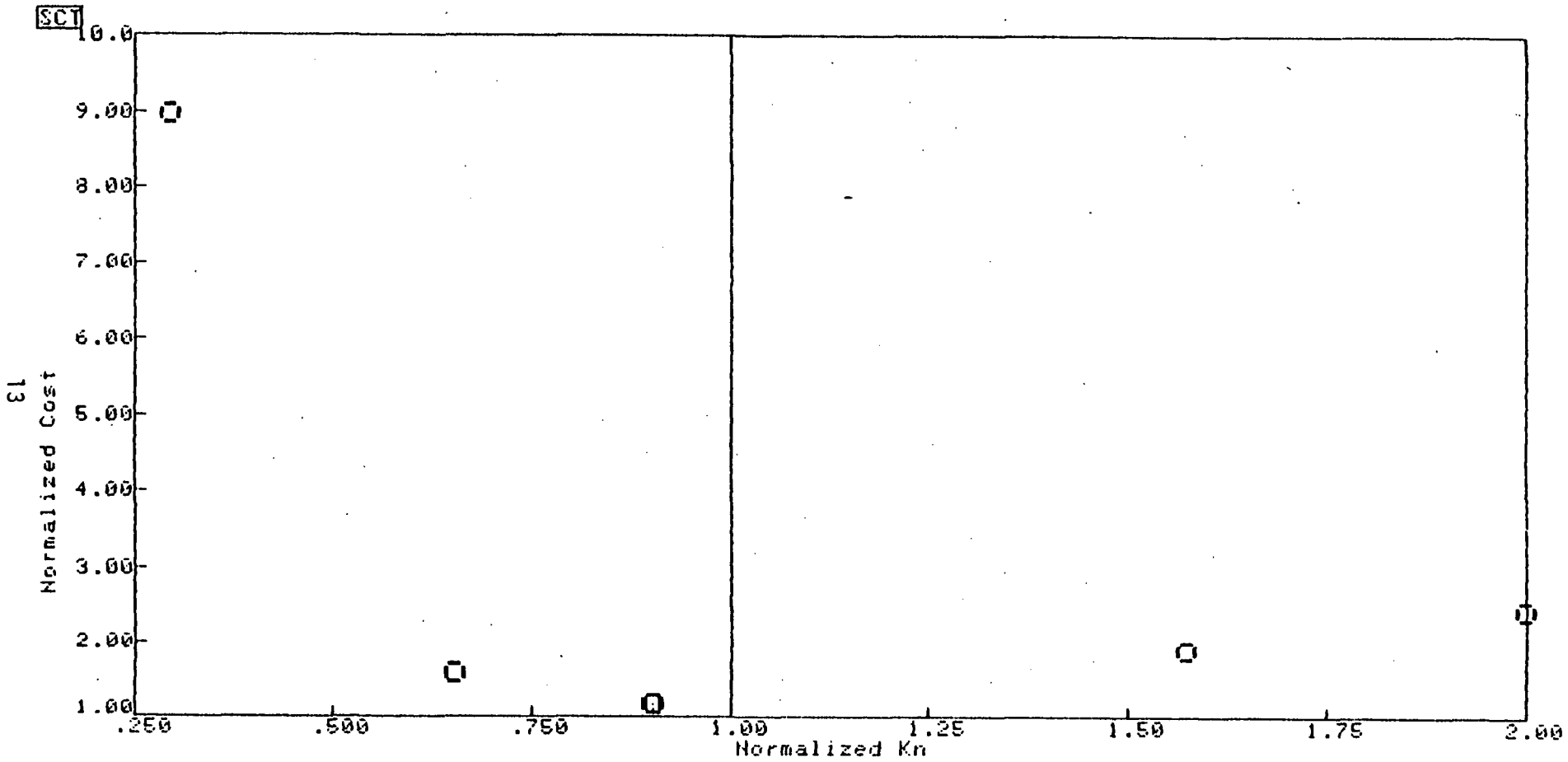

Figure 2.5 Convergence of K_n Identification

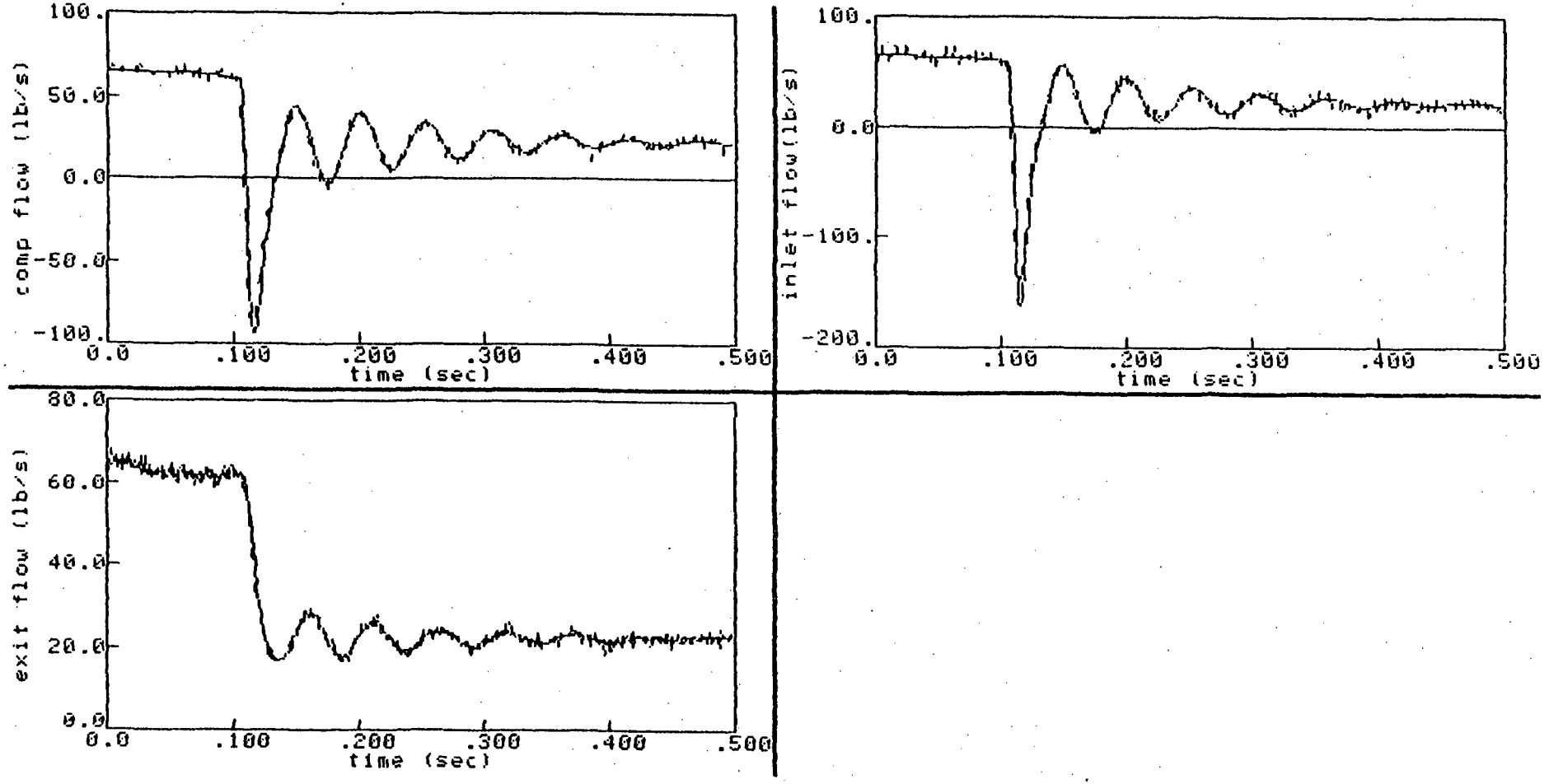

Figure 2.6 Comparison of Final Parameter Curves with Data
(estimate solid line; data dashed line)

Convergence to the best estimates is illustrated graphically in Figure 2.5. Notice that the original guess of Kn was twice what was used in the NASA engine. SCIDNT determined that decreasing the Kn value would decrease the model-plant errors and a new guess was made at a lower parameter value. Eventually, a final value is settled upon which cannot be changed without increasing model-plant errors. This value is the maximum likelihood parameter value.

A comparison of the NASA model and the final SCT model is shown in Figure 2.6. At this point the newly identified parameter values are very close to the actual values, and the identification is complete.

2.2 PROGRAM OUTLINE

2.2.1 Task A: Compressor Rig Identification

This first phase of Task A satisfied the primary program objective: demonstration of compressor parameter identification techniques. The demonstration was based upon parameter identifications made from simulated data of a TF-34 Compressor Rig. However, the focus in this particular task was not only to demonstrate, but to identify those areas of identification that required further investigation for improved identification accuracy.

Task A also provided needed experience with an engine model having an unusual structure: two modes for unstalled and stalled operation. Experience was gained by attempting a variety of identification techniques using the compressor rig model. At the conclusion of the task and experience gathering, areas for improvement and further investigation were identified for use in Task B, and experiences were summarized for use in Task C.

2.2.2 Task B: Identifiability/Sensitivity Study

Using the compressor rig model developed under Task A, an identifiability/sensitivity (I/S) study was performed. The study investigated the ability to identify engine and compressor parameters under differing instrumentation conditions (sensor noise, sensor sets, sensor lags) and plant

responses (recoverable vs. nonrecoverable)). These results were used to improve the compressor parameter identification process and in the turbofan study make recommendations for engine test instrumentations.

The I/S study also investigated how engine and compressor parameter identifications are sensitive to modeling errors. Modeling errors include structural errors (e.g., lumped parameter assumption), instrumentation modeling errors (unmodeled or poorly modeled sensor lags), and recording modeling errors (time skews between recorded channels.) These results were also used to improve the identification process and point out potential sources of difficulty for future identifications.

2.2.3 Task C: Turbofan Identification

This final program task combined knowledge gained in Tasks A and B (identification experience and instrumentation effects) to demonstrate advanced procedures for stall parameter identifications. Three subobjectives were used to accomplish Task C. First, the identification experiences from Task A were used to develop a streamlined identification procedure. Second, a turbofan was developed and identified using these new procedures to achieve maximum accuracy. Finally, the turbofan results and future results were predicted using the tools developed under the I/S study.

2.3 SUMMARY OF FINDINGS

All tasks mentioned above were completed successfully. A few details and results are summarized below.

2.3.1 Task A: Preliminary Demonstration

Task A preliminarily demonstrated the identification of compressor map parameters. A major subobjective in Task A was the acquisition of identification experience. This experience was used to find problem areas requiring further investigation in Task B and to improve identification techniques for use in Task C.

Kn and Kp were successfully identified using the compressor rig. Kn was more accurately identified than Kp and that Kp is only marginally identifiable in recoverable stall runs. Both Kn and Kp identifiability improved as more data were used, particularly data on the positive stalled flow periods. Kn and Kp identifiability was influenced by the quality of information, which was determined in part by the noise levels present.

Several special considerations had to be made when identifying compressor parameters. Among the considerations are stall synchronization, algorithm precision and integration procedures.

2.3.2 Task B: Identifiability/Sensitivity Study

Task B, the I/S study, explained the results of the compressor rig identifications and developed tools that can generally be used in all types of engine identifications. One of these tools quantitatively explains the relationship between identifiability (a statistical measure of the accuracy of an identified parameter) under a variety of data conditions including sample frequency, number maneuvers, noise level, number of maneuvers, type of stall, and available sensors. Another tool indicates which sensors are necessary to identification and which are marginal.

The sensitivity portion of the study focused on parameter susceptibility to biasing due to model errors. For example, if Kn were in error, then its effect on the model would cause estimates of Kp to be in error. Kp would be in error because parameter estimation seeks to minimize a cost function and that function is mathematically related to all engine parameters; this is what is meant by sensitivity.

Sensitivity relationships were derived from identification theory to explain these error and biasing effects and improve identification procedures. Strong biasing relationships were found between errors in several engine parameters and the compressor map parameters, Kn and Kp. The discovery of these relationships affected the philosophies used to develop identification techniques and had a significant impact upon the methods used in the turbofan identifications.

The experiences gained in Tasks A and B were instrumental in streamlining procedures used in the turbofan identifications. The final task, Task C, was aimed at refining these procedures and producing an effective set of guidelines for use in future compressor parameter identifications while also achieving maximum identification accuracy.

2.3.3 Task C: Final Demonstration

The identifications achieved in Task C were very accurate as a result of the techniques developed during Tasks A and B. As expected from Task B results, accuracy was dependent upon the noise levels present. I/S tools predicted that KPC would be marginally identifiable in recoverable stall for the given turbofan model, noise level, etc. I/S tools also indicated that KPC would be readily identifiable in nonrecoverable stall. Both predictions proved to be correct.

Several identifications were made without the use of flow measurements and satisfactory accuracy was achieved. I/S tools determined that flow measurements would not be necessary to attain satisfactory results in the identification of compressor stall parameters. However, these results are dependent upon sensor time constants and noise conditions present in the other sensors.

2.3.4 Conclusion

The NAS3-23537 program has accomplished it objectives. Identification of compressor map parameters from transient data was demonstrated. Experience was gained in map parameter identification, new tools were developed, and a logical, efficient identification procedure was outlined.

III. PARAMETER IDENTIFICATION

3.1 THEORY AND CONCEPTS

The techniques used by SCT to identify model parameters from transient data are drawn directly from parameter estimation theory developed at SCT. This chapter summarizes the concepts of parameter estimation and begins the development of some identification and sensitivity tools.

The basic idea in system parameter estimation is to find model parameters that force the model's response to match that of the plant (e.g., energy). Parameters identified by SCT's parameter estimation algorithm, SCIDNT, represent maximum likelihood values of the model parameters. The identified parameters make the model follow the engine as well as possible and are the most likely plant parameters given the plant model.

3.1.1 Cost Function

The goal of parameter estimation is to estimate model parameters in such a way that the model reproduces the results of the unknown system as closely as possible. This is illustrated graphically in Figure 3.1, where the goal would be to eliminate the differences between the two responses highlighted by the slanted lines. Stated mathematically, the problem is equivalent to minimizing a performance index, the error between measured plant outputs and corresponding model outputs.

$$L_s(\theta) = \sum^{N} [\hat{y} - y(t, \theta, y)] \tag{3.1}$$

where

$$x = f(x, u, w, t, \theta) - K(\hat{y} - y)$$

and

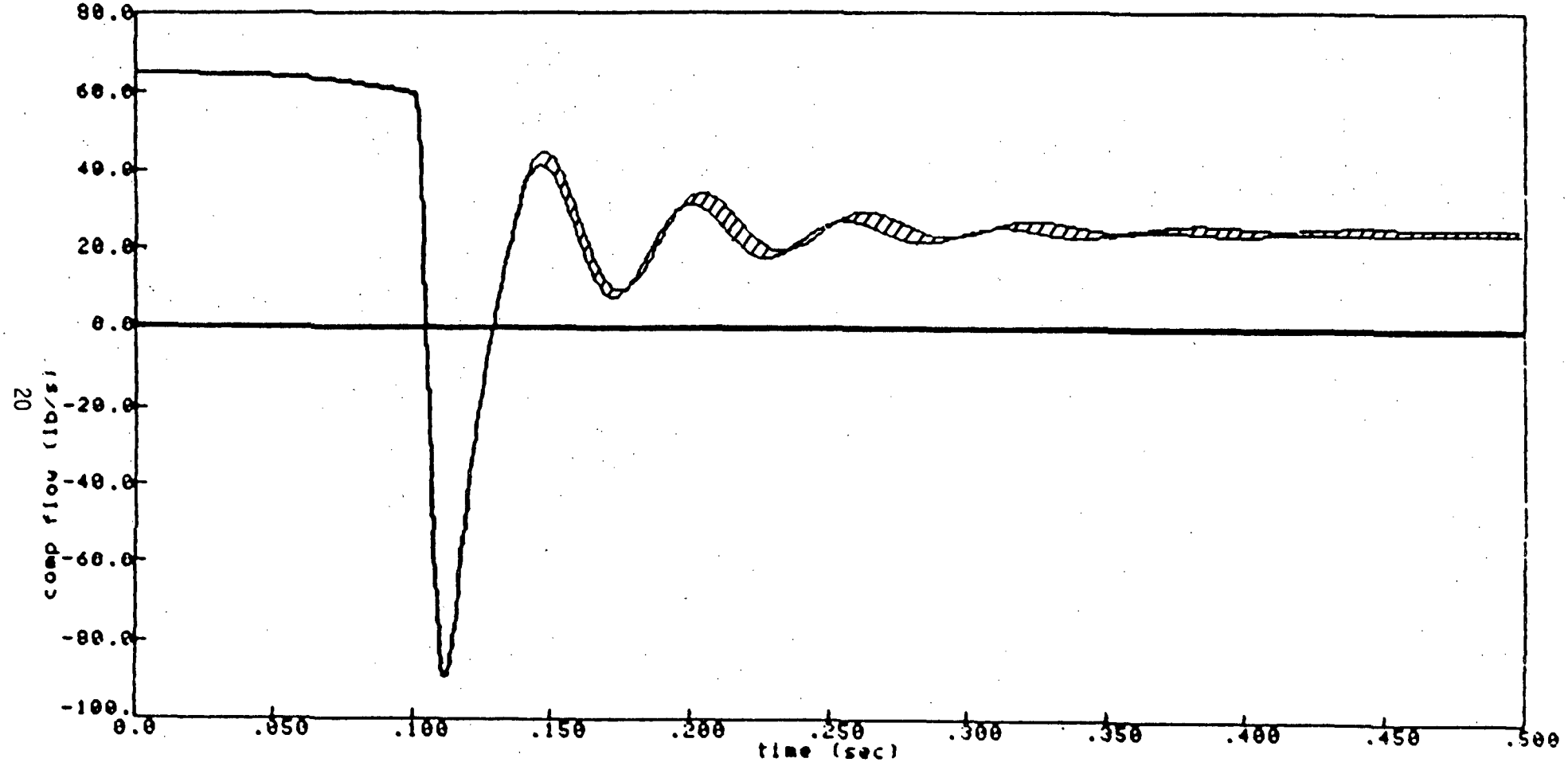

Figure 3.1 Model-Plant Errors

$y = h(x, u, t, \theta) + v$

N = number of data points

x = nx states

y = ny outputs

u = nu inputs

θ = np parameters

t = time

w = nx process noise vector

v = ny output noise vector

$$E\{w\} = 0 \qquad E\{w\ w'\} = Q$$

$$E\{v\} = 0 \qquad E\{v\ v'\} = R$$

where

E is the expected value

and

$E\{x\ x'\}$ is the covariance matrix

The estimated plant outputs are determined by using both state equations and output measurements (typically a Kalman filter.) When a Kalman filter is used, minimizing the performance index produces maximum likelihood parameter estimates. (Kalman filters were not used in this program.)

If w and v are Gaussian then the performance index in Eq. (3.1), can be expressed as a likelihood function (Eq. (3.2)). This likelihood function is Gaussian and indicates the likelihood (probability) that a certain parameter set, θ, has produced the measured data, y. Since θ is the random variable here, the likelihood function covers np-space, and, instead of a single normal curve, the function is actually an np-space surface.

$$L(\theta) = \frac{N \exp(-\nu^2 / 2\sigma^2)}{\sqrt{2\pi}\ \sigma} \qquad (3.2)$$

To find an optimal set of parameters, the likelihood function in Eq. (3.2) must be maximized, i.e., a θ must be found which gives the largest value of L. Eq. (3.2) can be maximized as is, but a simpler approach considers the negative log of Eq. (3.2). Finding the minimum of the negative log likelihood function is equivalent to finding the maximum of the likelihood function.

$$J(\theta) = - \ln L(\theta)$$

$$\min J(\theta) = \max L(\theta)$$

where

$$J(\theta) = 1/2 \sum^{N} \{ v'v\, R^{-1} + 2*\ln R^{1/2} \} \qquad (3.3)$$

J = negative log likelihood (cost function)

$v = Y - Y(\theta)$

$Y(\theta)$ = model outputs

θ = model parameters,

Y = plant measured outputs,

$R = E\{v\ v'\}$ = covariance of measurement noise

Minimizing the negative log likelihood is a least squares problem, very similar in form to Eq. (3.1), the general optimization problem. Because v and w are Gaussian, the relationship in Eq. (3.3) still produces maximum likelihood parameter estimates. One example of a negative log likelihood function for a single parameter is shown in Figure 3.2.

3.1.2 Gradient Search

The maximum likelihood parameters occur where J is at a minimum. Finding this minimum requires the use of the gradient of J since the minimum of J occurs where the gradient (slope) of J is zero (see Figure 3.3.) Parameter identification algorithms are based upon finding where the gradient of J is nearest to zero:

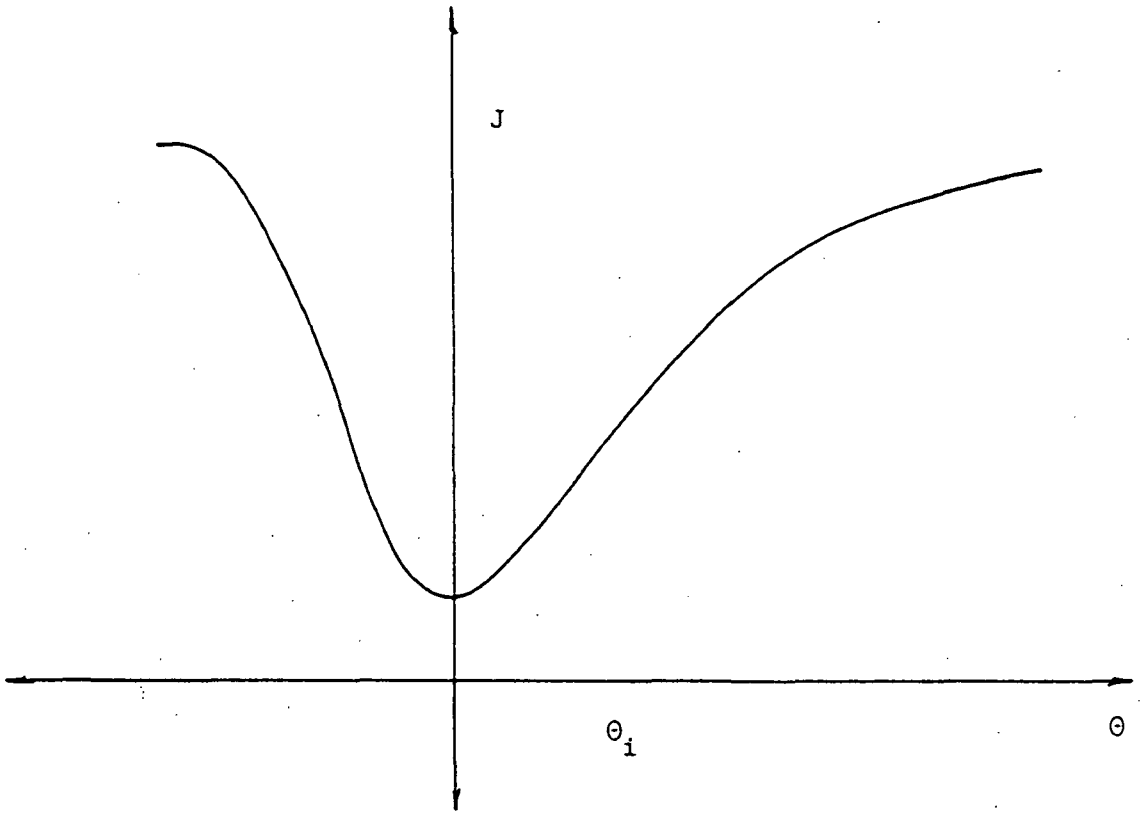

Figure 3.2 Example Cost Function

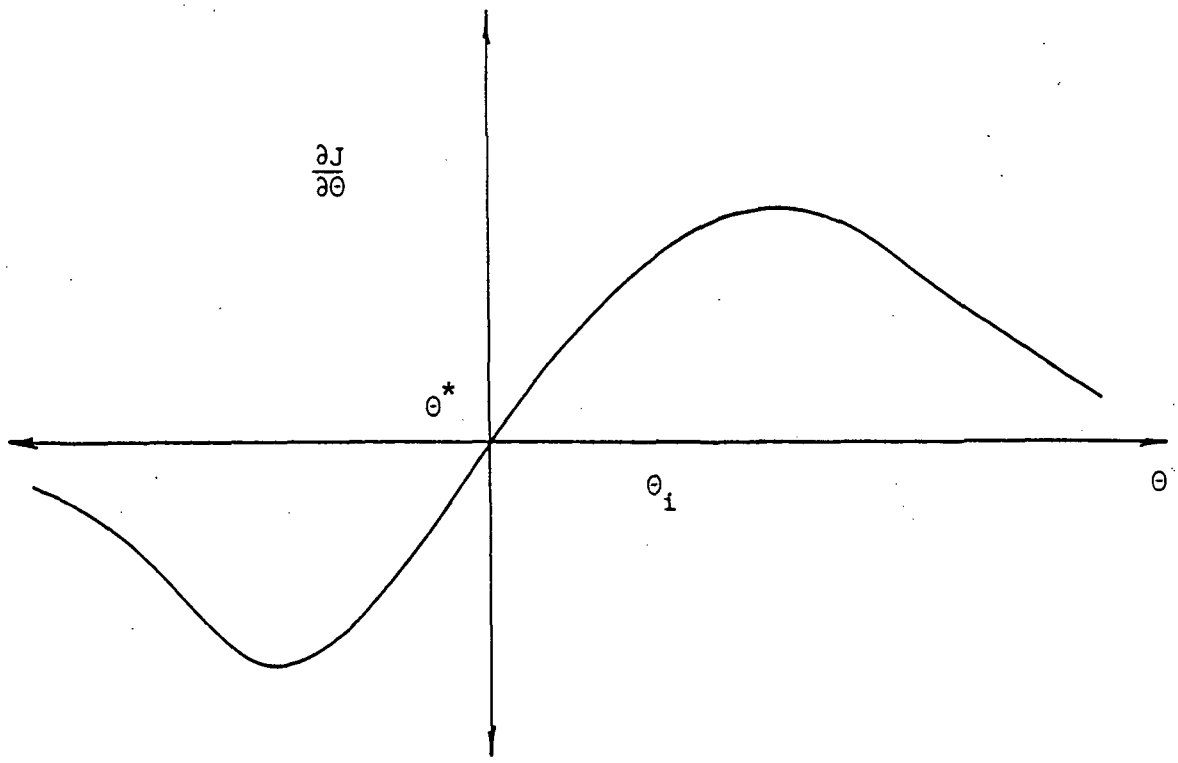

Figure 3.3 Cost Function Gradient

$$\frac{\partial J}{\partial \theta}_{final} = 0 \tag{3.4}$$

The SCT algorithm, SCIDNT, uses a Gauss-Newton method to converge to gradient zeros. The convergence follows a first-order iterative algorithm.

First, an initial parameter guess, θi, is made. The cost function value, $J(\theta i)$ is measured based upon the plant response and the model's response given the model parameters, θi. Next, the gradient and Hessian are measured at θi. The gradient is the first partial of J with respect to θ at θi and the Hessian is the second partial. The Hessian is used to predict where the gradient is zero; this is done with a first-order estimate (see Figure 3.4).

$$\theta_{i+1} = \theta_i - pM^{-1} * g \tag{3.5}$$

where

θ = np x 1 parameter vector

g = gradient of J

M = gradient of g

= 2nd partial of J

p = a user-defined scalar (< 1.) used to control rate of convergence.

If the overall costs (value of J) decrease at θ_{i+1}, then the new parameter estimate is accepted. If the costs increase, a smaller step is tried.

Once a new parameter is accepted, a new cost value, gradient and Hessian are measured for θ_{i+1} and another step is calculated. The whole process is repeated several times until convergence is achieved. The iterative nature of the process is illustrated in Figure 3.5. Convergence is determined by the size of the step. If the parameter estimate is so close to the actual value that the step sizes are less than .001 percent, identification is stopped. (SCIDNT users can use step thresholds other that .001 percent according to precision requirements.)

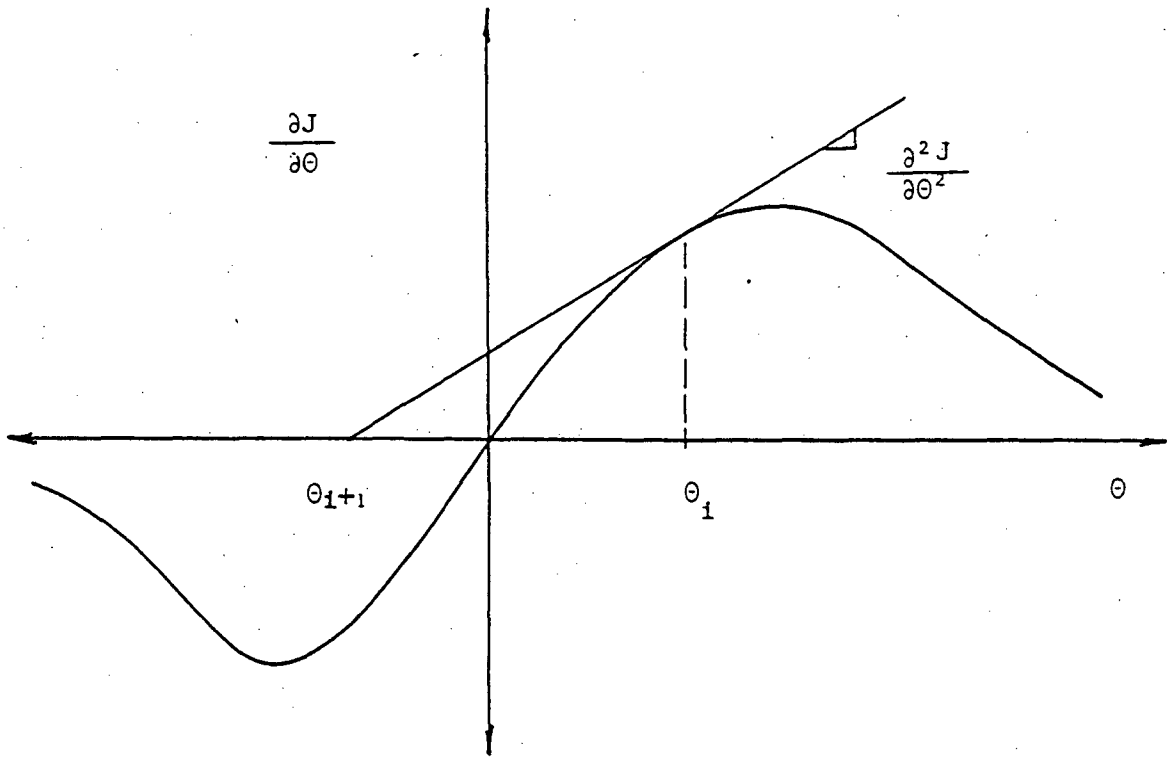

Figure 3.4 Parameter Stepping Using Gradient and Hessian

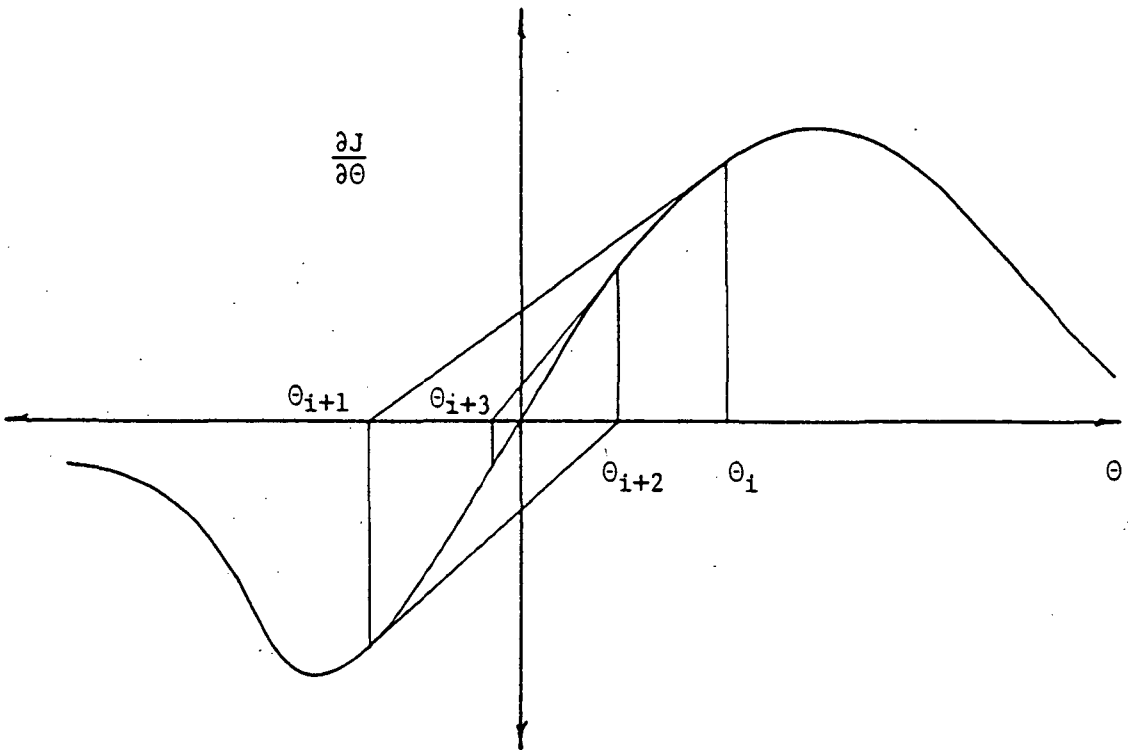

Figure 3.5 Parameter Iteration

3.1.3 Perturbational Techniques

The critical problem at this point is the determination of the gradient and Hessian for what could be a highly nonlinear model. Differentiating Eq. (3.3) with respect to θ yields the following relationships for the gradient and Hessian (written in matrix form).

$$g = \sum^{N} \{ \nu' R^{-1} \frac{\partial \nu}{\partial \theta} - (1/2)\ \nu' R^{-1} \frac{\partial R^{-1}}{\partial \theta} R^{-1} \nu + (1/2)\ \mathrm{Tr}(R^{-1} \frac{\partial R}{\partial \theta}) \} \tag{3.6}$$

$$M \sum^{N} - \sum^{N} \{ \frac{\partial \nu}{\partial \theta} R^{-1} \frac{\partial \nu}{\partial \theta} + \mathrm{Tr}(R^{-1} \frac{\partial R}{\partial \theta} R^{-1} \frac{\partial R}{\partial \theta}) \} \tag{3.7}$$

$$M \sum^{N} - \sum^{N} \{ \frac{\partial \nu}{\partial \theta} R^{-1} \frac{\partial \nu}{\partial \theta} \} \tag{3.8}$$

The SCT solution to the gradient determination relies upon the use of approximations of the gradient using estimates of the ν and R partials produced via a perturbational technique for each parameter $\theta(j)$:

$$\frac{\partial \nu}{\partial \theta(j)} \sum^{N} \frac{[\hat{y}\theta + \Delta\theta - y] - [\hat{y}(\theta) - y]}{\Delta\theta(j)}$$

$$= \frac{(\hat{y}(\theta) + \Delta\theta) - \hat{y}(\theta)}{\Delta\theta(j)} \tag{3.9}$$

In effect, SCIDNT propagates two output models, one at $\theta + \Delta\theta$ and one at θ. The partial of R is found in a manner similar to that used above. SCIDNT produces maximum likelihood parameter estimates using these approximations and the stepping algorithm. Additional information and

background on parameter estimation and applicable algorithms can be found in Refs. 2 through 12.

3.1.4 Other Considerations

Thus far, the question of the accuracy of these identifications has not been posed. But accuracy is indeed and important concern in parameter estimation. Several clues to factors affecting accuracy can be found upon examining Eqs. (3.6) and (3.7). To understand better how external factors (e.g., noise, sample rates, time lags, etc.) affect identification accuracy, Sections 3.1.4.1 and 3.1.4.2 introduce the concepts of identifiability and sensitivity. These concepts are drawn directly from parameter estimation theory and form the basis of the I/S studies discussed in Chapter V where parameter identifiabilities and sensitivities are fully interpreted and examined.

3.1.4.1 Identifiability

The concepts of identifiability and sensitivity are both derived from the Hessian. The Hessian is the second partial of the cost function with respect to the estimate parameter(s) and is also known as the Fisher information matrix.

The Hessian is a weighted measure of the information content of each measurement in matrix form. It is an indication of how much the model will change (or how much the model-plant costs will change) given a change in parameter values. The measure is weighted by the noise levels associated with each measurement. For example, if a parameter has a large effect on the model outputs, then the outputs have a high information content. But this content may be offset by the fact that the measured signal has a great deal of noise. This can be seen physically by considering the model-plant error demonstrated in Figure 3.1. Assuming that the errors indicate how much the model changes under a change in parameters, consider what the error would look like if the measured signal contained a large amount of noise. The greater the noise, the

less obvious and significant the model-plant errors become, and the weaker the parameter-cost function relationship in the Hessian becomes.

Thus, the amount of noise determines how much information each measurement can contribute and also determines the overall strength of the measured parameter-cost function relationship. It is this relationship between the parameter values and the measured cost function (the Hessian) which determines how well a parameter can be identified, i.e., parameter identifiability.

Parameter identifiability is measured by the inverse of the Fisher information matrix. Also known as a measure of parameter uncertainty, the inverse matrix is a covariance matrix indicating the expected covariance in the estimated parameters.

$$M^{-1} = E\{\theta\,\theta'\} \tag{3.10}$$

$$\text{diag}\ M^{-1/2} = E\{\theta\}\ \sigma(\theta) \tag{3.11}$$

Because M inverse is the parameter covariance matrix, it is a measure of the likelihood that a estimated parameter is within a certain range of the actual value. In regards to identifiability, the values of greatest concern are the square roots of the diagonal elements of M inverse. These values are the standard deviations of each of the parameters being estimated.

The standard deviation indicates the confidence regions for an estimated parameter. If $\sigma(Kp)$ is 0.1, then there is a 68 percent probability that the actual KP is within 10 percent of the estimated value, and, there is a 95 percent probability that the actual parameter is within 20 percent of the estimated value (2σ rule). Thus, standard deviations can provide a measure of the confidence or uncertainty in an estimated parameter.

These measured uncertainties can be used to determine how reliable an estimate might be (given that noise can cloud an identification). Uncertainties can also be determined without measured data by using only estimated noise levels. This is done extensively in Chapter V to study how parameter uncertainties change under various noise conditions. It is also

done while considering limited numbers of sensors, slow sample rates, etc., all of which affect uncertainty. (Note: uncertainty is alternately referred to as identifiability throughout this text. Identifiability is equally appropriate since the measure also indicates the likelihood that a parameter will be accurately identified.)

As a final note, the uncertainty relationship in Eq. (3.11) is an ideal; that is, the uncertainty predicted by the information matrix is a minimal value based upon exact model and plant agreement. Any disagreement between model and plant in form or parameter values will be reflected as an increase in uncertainty. Once the model and plant disagree, the inverse square-root of M is no longer a mathematically correct prediction of uncertainty and the values predicted by M will be below actual uncertainties.

3.1.4.2 Sensitivity

The Fisher information matrix indicates how much the plant-model errors change given a change in the estimate parameters. Not only can a measure of identifiability be drawn from the Fisher matrix, but a measure of sensitivity can also be determined.

Sensitivity is defined as the anticipated change in an estimated parameter based upon a unit change in another parameter. It is a critical measure since it indicates how much an estimate might be biased when a model parameter is wrong. For example, if a modeled inlet resistance is only 90 percent of the actual value, then the estimated value of Kp might be biased due to the 10 percent error. The estimate would be biased because parameter estimation theory attempts to compensate for errors resulting from the bad resistance by over compensating with the Kp estimate.

All of this sensitivity information can be found in the information matrix. The matrix indicates how much model-plant errors change due to changes in the parameters. Sensitivities are determined by equating these changes. The idea is that if an X change in parameter A produces a Y change in the plant and so does a Z change in parameter B, then an X error in A will produce a Z error in the estimate of B.

The mathematics of sensitivity theory are saved for Chapter V. The common measures used in sensitivity analysis is called a bias matrix. The bias matrix is used extensively in the results sections in Chapter V to investigate the bias-inducing effects of modeling errors (e.g., resistance errors, volume errors, etc.), sensor errors (time lag errors, drift, etc.), and recording errors (channel to channel time skews).

Sensitivity results were used to modify the identification procedures to avoid problems areas in the turbofan identifications. The greatest use of sensitivity tools has yet to be fully realized and will probably come in evaluating proposed models in future engine identifications in the context of parameter uncertainties (e.g., how accurately must the resistance value be known) and instrumentation (e.g., how much drift can be allowed or how accurately must a time constant be modeled).

3.2 PARAMETER IDENTIFICATION ALGORITHM: SCIDNT

SCIDNT is the acronym given to SCT's parameter estimation algorithm. The algorithm implements the estimation theory discussed in the preceding sections along with additional features not previously mentioned. The purpose of this brief subsection is to discuss some of SCIDNT's special features that are particularly relevant to considerations involved in compressor map identifications.

3.2.1 Background

SCIDNT was designed with modularity in mind. This is in part due to foresight, in part due to necessity. Out of necessity, SCIDNT had to be able to work with any type of dynamic model. This meant that the model subroutines had to be modular and generic so that they could be easily incorprated. The format chosen for SCIDNT is simple yet effective. Three subroutines are used: MEAS, STATIC and STATE. MEAS takes as inputs the current state (X), state derivatives (XDOT), control input values (U), and the vector of model parameters (P)(any one of which can be identified.) MEAS's output is the output vector of measurements (Y). STATIC is the initial condition module.

It is only called at the beginning of a propagation to determine the initial states. Its inputs are the input control vector (U) and the model parameter vector (P). Its outputs are the initial state values (X), state derivatives (XDOT), and outputs (Y). The third module, STATE, calculates the state derivatives. The inputs are the past state values (X), the vector of model parameters (P), and the input control vector (U). Output of STATE is the vector of state derivatives (XDOT)

3.2.2 Variable Step Integration

In keeping with its modular philosophy, SCIDNT is equipped with a integration subroutine. The routine updates the value of X using the state derivative vector, XDOT. The method used is fairly involved but important to the program.

The unique feature of this integration routine is its ability to do variable-step integration. This is convenient especially for nonlinear models since the model time constants may vary significantly over a maneuver. The routine uses an integration step only as small as is needed at any given time; thus, small time steps are only used when absolutely necessary thereby saving computation time. An example of how the time step can change over a maneuver is shown in Figure 3.6.

The user is given some control over the routine by means of tolerable error specifications. Maximum allowable percent errors in the states are specified by the user (commonly on the order of .001 percent). Thus, when the user specifies a small error tolerance, the time steps generally are smaller.

3.2.3 Error Weighting

Recall from Eq. (3.3) that model-plant errors are weighted, or normalized, according to the amount of measurement noise on a signal. In SCIDNT, there are two ways in which to specify the error weighting terms. In the first and most common method, weight is determined by the RMS error between the plant and model evaluated over the entire maneuver. At the onset of identification this error consists of both modeling error effects and noise

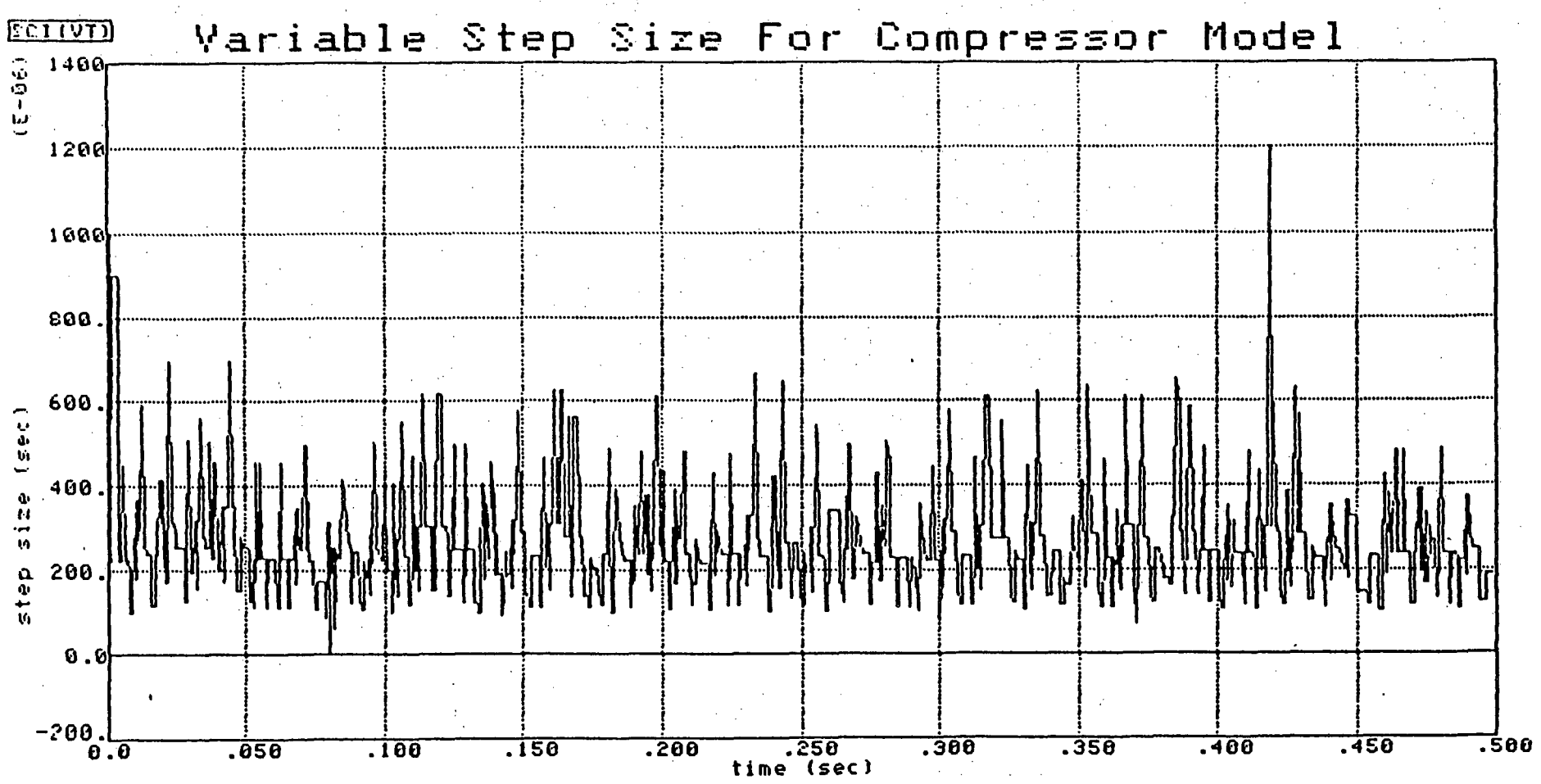

Figure 3.6 Variable Step Sizes used by SCIDNT Integration Package

errors. As the model comes closer to the actual plant, model errors are reduced and weighting is almost entirely due to noise. An important point here is that the weights change as the identification procedes.

The second method of error weighting is user-specified. The user estimates (or measures in some way) the RMS values or standard deviations of the measurement noise. These values can then be specified to SCIDNT and the cost function will be weighted according to these values. These values remain fixed over the maneuver.

The fact of whether the weights are fixed or floating is important to the compressor map identifications. Some parameters have only slight effects on the model response and thus have numerically small normalized gradients. When the measurement weightings are allowed to vary (as they are in the first method), the weighted gradient can end up varying a great deal. Thus, from one iteration to the next, the normalized gradient may change drastically (even change signs), while the true gradient is much more stable and predictable. The result is that convergence can be destroyed because the parameter step calculations are disrupted. Consequently, the fixed weighting method was used in most of the identifications.

3.2.4 Simultaneous Identifications

SCIDNT is capable of identifying up to 50 parameters simultaneously. This means that for each calculated parameter step (see Eq. 3.5), up to 50 parameters may be changed. It also means the gradient vector has 50 values and the Hessian is 50x50. Although these are large structures to manipulate in a program, there are significant advantages to simultaneous identifications. Basically, simultaneous identifications produce more accurate identifications using less computations. The alternative is to identify one parameter and then the next. The problem with this approach is that one parameter might bias the other, so the process must be iterated through several times in order to reduce the biasing effects.

Normally, simultaneous identifications are used. The point about individual identifications is mentioned here because some of the unique features of the stalling compressor model required that individual identifications be made at times. This had some significant effects on the compressor map identifications, the consequences of which are fully discussed in Chapter IV.

IV. PRELIMINARY DEMONSTRATION WITH COMPRESSOR RIG

4.1 BACKGROUND

Task A demonstrates parameter identification techniques on transient, in-stall compressor rig data. The demonstration was designed to mimic those procedures that would be followed in any engine identification. The only exception was that the data were simulated instead of measured directly from an engine. An outline of the major procedures is given below:

(1) NASA LeRC implemented a fifth-order, lumped-parameter model of a compressor rig on a hybrid digital/analog computer.

(2) Using several different Kp, Kn, V and L parameters, NASA LeRC obtained a variety of recoverable and nonrecoverable stall signatures.

(3) These signatures were recorded on analog tape and consisted of flow, pressure, and temperature signals.

(4) The analog results were filtered and recorded digitally at 5 kHz.

(5) The digital tapes were sent to SCT for processing.

(6) SCT developed a second compressor rig model, identical to the first, but strictly a digital version.

(7) The SCT model was used in conjunction with SCIDNT to identify the parameters used in producing the various stall signatures recorded on the NASA Lewis digital tapes. (Note: the SCT model was perturbed by the recorded input signal, a throttling disturbance knoz. As a result, the model response was dependent upon the condition of this recorded signal, the significance of which becomes more apparent when model-plant synchronization are discussed in Section 4.5.3.)

4.2 COMPRESSOR MODEL DEVELOPMENT

The compressor rig model is a fifth-order, lumped-parameter model taken from a NASA-developed TF-34 model [1]. The major features of the model are summarized in schematic form in Figure 4.1 and are listed below:

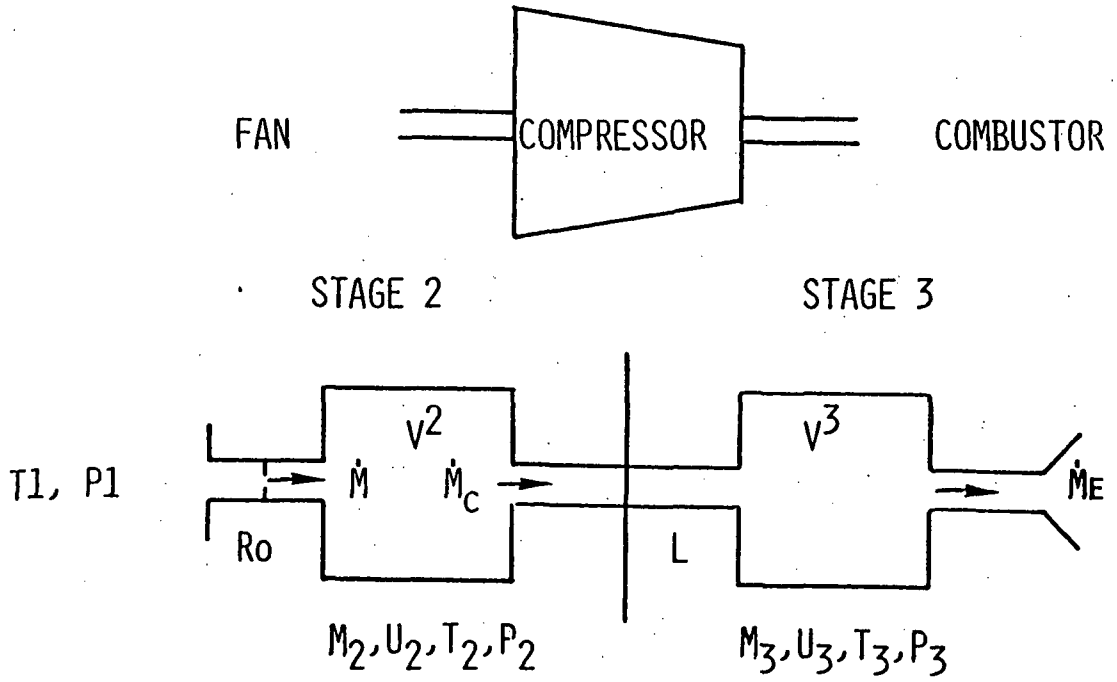

STAGE *

- RESISTIVE INLET
- STAGE 2 & 3 CONSTANT VOLUME, ADIABATIC
- STAGE 2 & 3 MASS CONSERVATION
- TEMPERATURE & PRESSURE f(u,m)
- COMPRESSOR MAP AT STAGE *
- INDUCTIVE FLOW INTO STAGE 3
- THROTTLED, ADIABATIC EXIT FLOW
- CONSTANT SPEED

Figure 4.1 Compressor Rig Lumped Parameter Model

(1) Resistive inlet.

(2) Stages 2 and 3 are constant volume and adiabatic.

(3) Mass conservation is maintained at Stages 2 and 3.

(4) Temperature and pressure at Stages 2 and 3 are functions of the accumulated mass and internal energy.

(5) A volumeless compressor is assumed at Stage *. This compressor operates in both unstalled and stalled conditions depending upon the compressor flow and speed.

(6) Inductive flow into stage 3.

(7) Throttled, adiabatic exit flow.

(8) Compressor speed is constant, although corrected speed may vary.

A detailed mathematical description of the model is in Appendix A. The compressor map at stage * is shown in Figure 4.2. The parameters of interest in this program, Kp and Kn, define the shape of the map during stalled positive and negative flow respectively. The curves are quadratic functions of corrected compressor flow and speed. The map is shown in a 3-dimensional representation in Figure 4.3.

Two examples of how the model responds during stall are shown in Figures 4.4 and 4.5. The first is a recoverable stall, the second is nonrecoverable. The only diffence in the model between these two responses is that Kp was increased to produce the recoverable stall. The goal of task A was to identify what Kp and Kn parameters produce a given stall signature such as those shown in these figures.

4.3 IDENTIFICATION OF Kp AND Kn WITH NASA DATA

SCT identified Kp and Kn for several NASA stalled compressor runs and the results were quite successful. First of all, the identifications demonstrated the ability to identify compressor parameters using SCIDNT. Second, the identifications presented some typical difficulities that may be encountered in more real situations and indicated approaches that could be used to overcome the difficulites. These experiences were the most valuable results of the compressor identification task. Using the experiences gained here, new

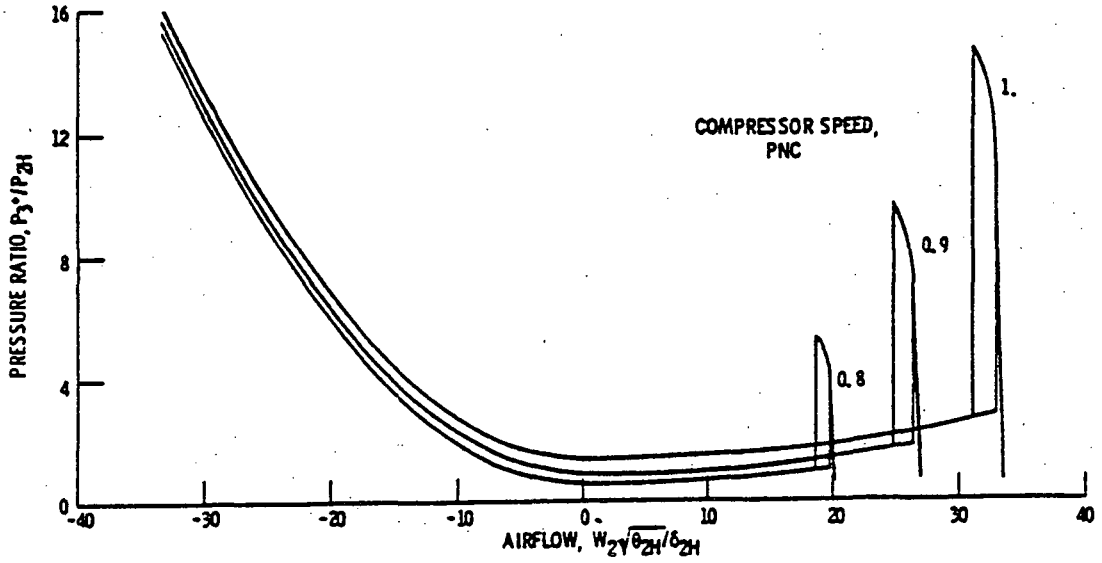

Figure 4.2 Pressure Performance Map for Compressor

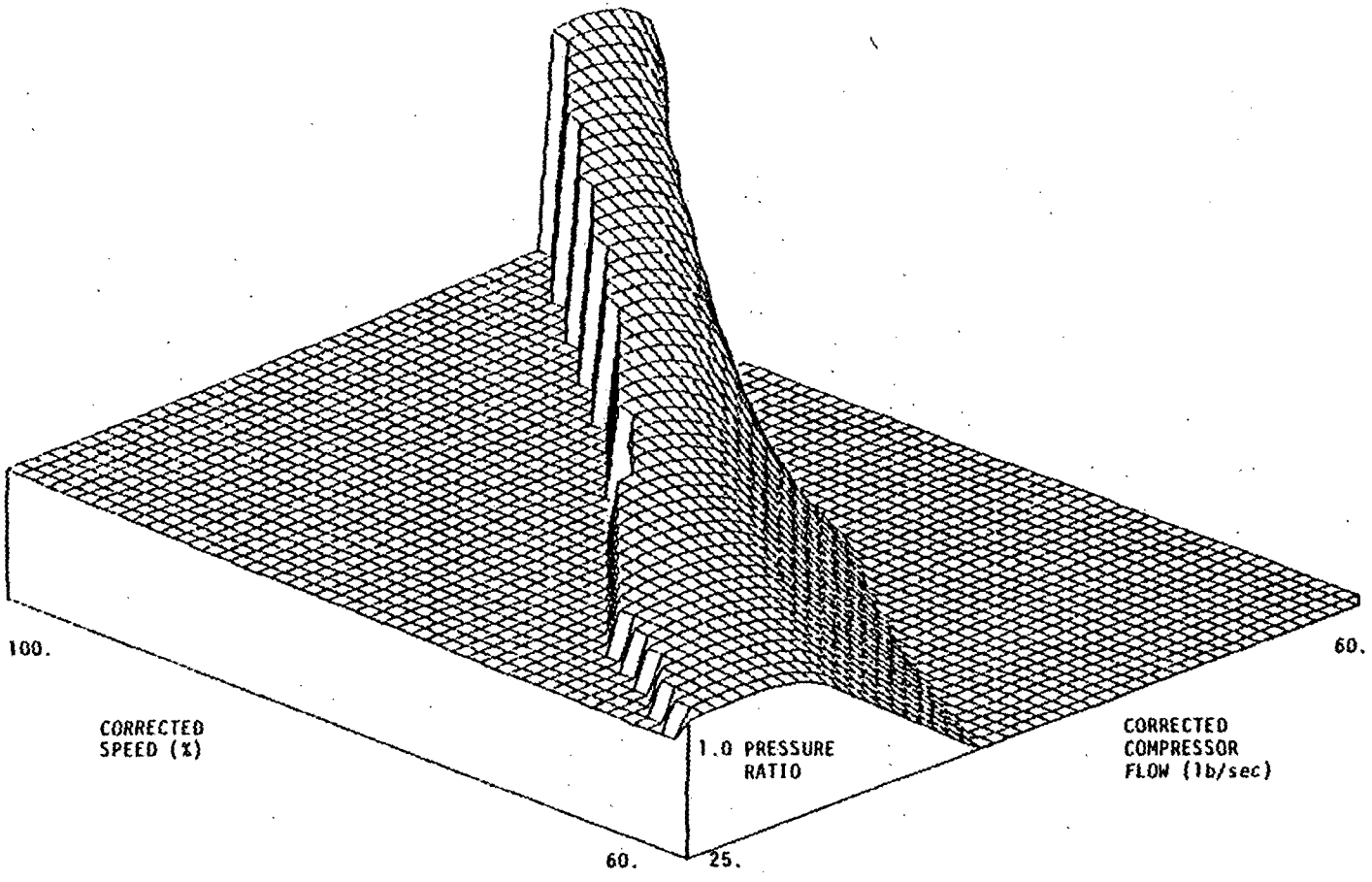

Figure 4.3 Stalled and Unstalled Compressor Map

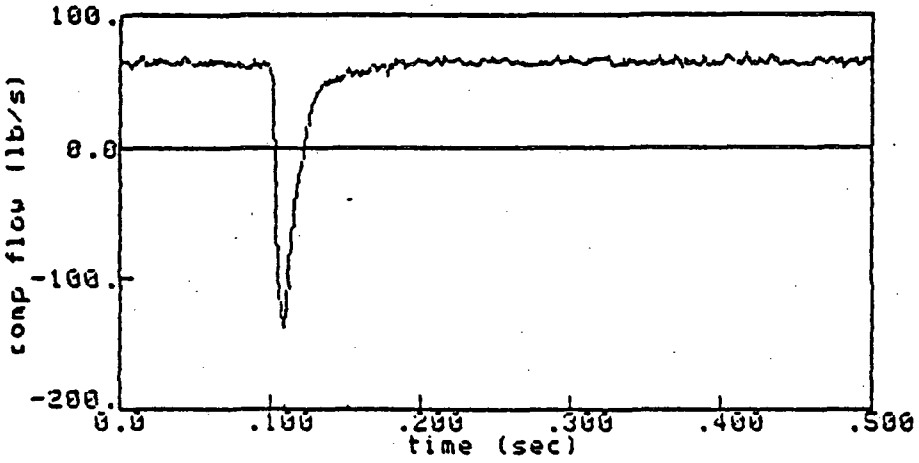

Figure 4.4 Compressor Rig Model Response — Recoverable Stall

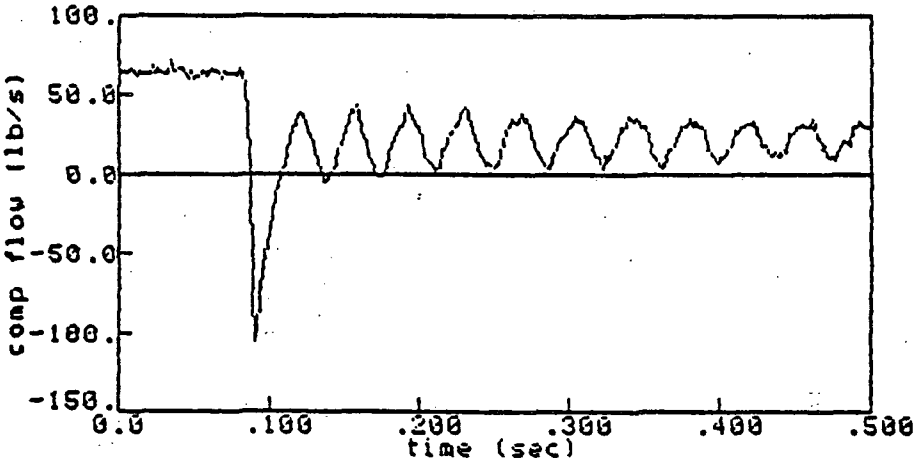

Figure 4.5 Compressor Rig Model Response — Nonrecoverable Stall

studies were fostered to quantify the effects of the difficulties (Task B), and these studies were used to define a comprehensive set of guidelines for achieving maximum identification accuracy in Task C. The identification results and experiences are related in Sections 4.4 through 4.6 and are summarized and interpreted in Section 4.7.

The goals of the compressor rig study are to demonstrate identifiability and gain understanding of the intricacies of compressor map parameter identification. Because of these goals, a minimal effort was made to improve the less successful identifications even though there were means available to do this. In this task, maximizing identification accuracy was not a specific goal.

The following sections document all the results of the identifications runs under four headings: the identification runs, general identification details, general identification results, and case-specific details and results.

4.4 THE IDENTIFICATION RUNS

Eight of 18 possible compressor stall runs were selected for use in the parameter identification studies based upon their diverse characteristics. The remaining 10 runs were omitted from the identification because they were either too similar to other runs or began in a transient mode, making initialization difficult.

Note: Runs 2, 8, 12, 18 were characterized by a Knoz that was throttled before data recording started. Because the throttling began too early, the compressor was in a transient mode at t=0. The compressor model was incapable of initializing in a transient, and, consequently, these runs could not be used for identification. This situation may be avoided in the future by using only data which begins in a steady state mode or by configuring models to initialize in a transient mode.)

The runs selected for identification are shown in Figures 4.6 through 4.21. The parameters used in each run and their major characteristics are summarized in Table 4.1. These runs provide a diverse test bed for the identification study as seen by their descriptions.

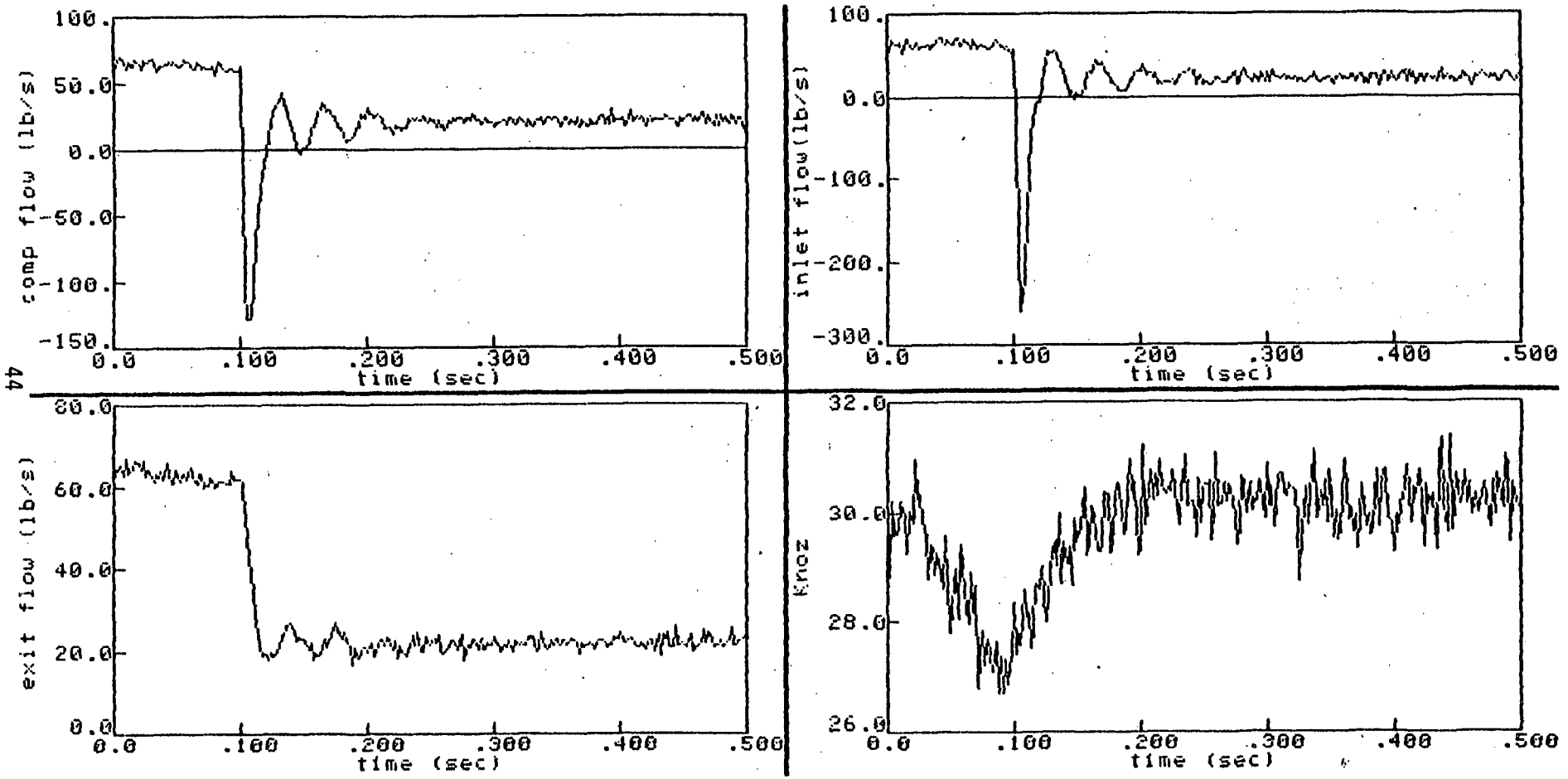

Figure 4.6 Compressor Rig, NASA Run 5

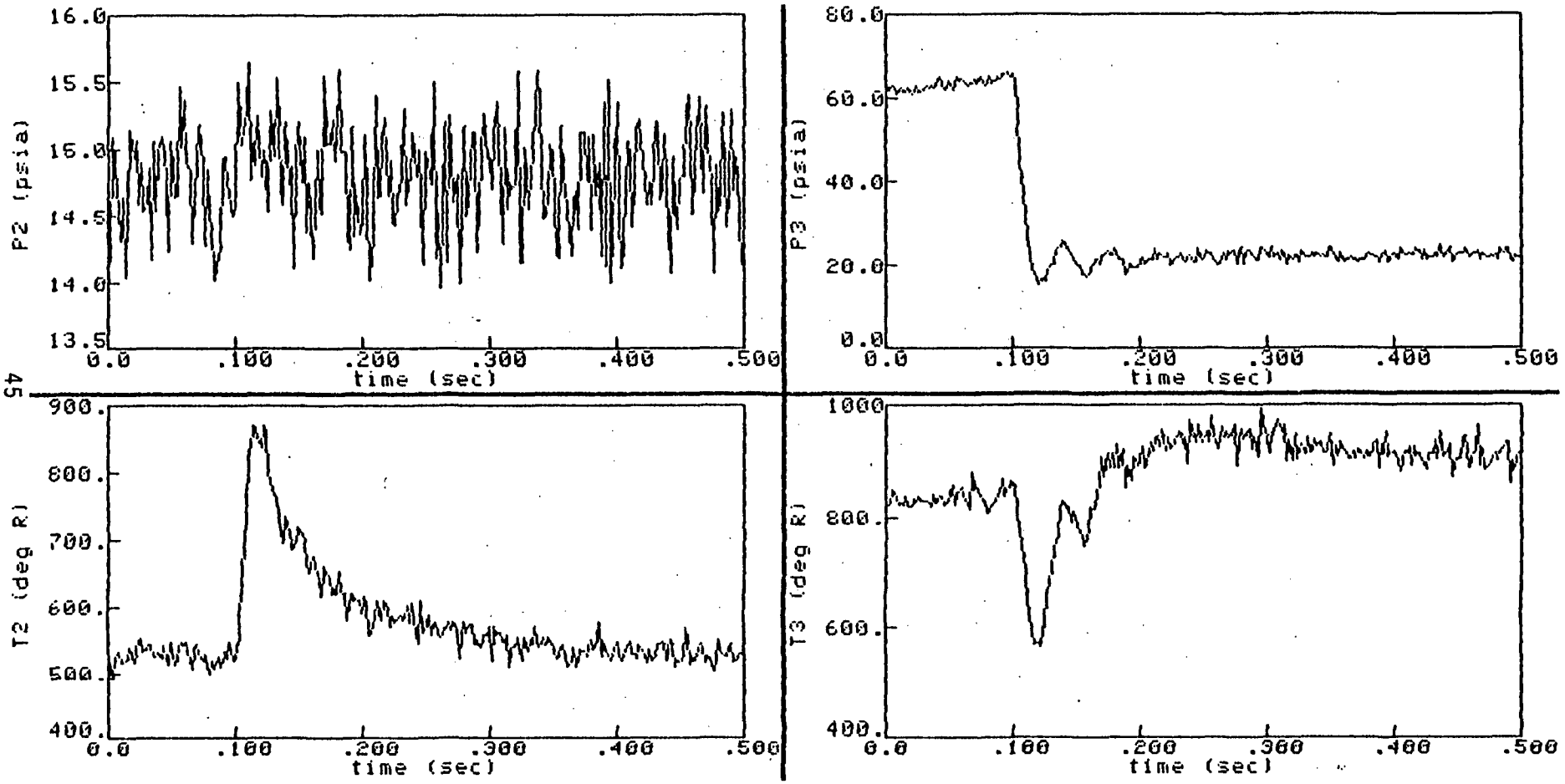

Figure 4.7 Compressor Rig, NASA Run 5

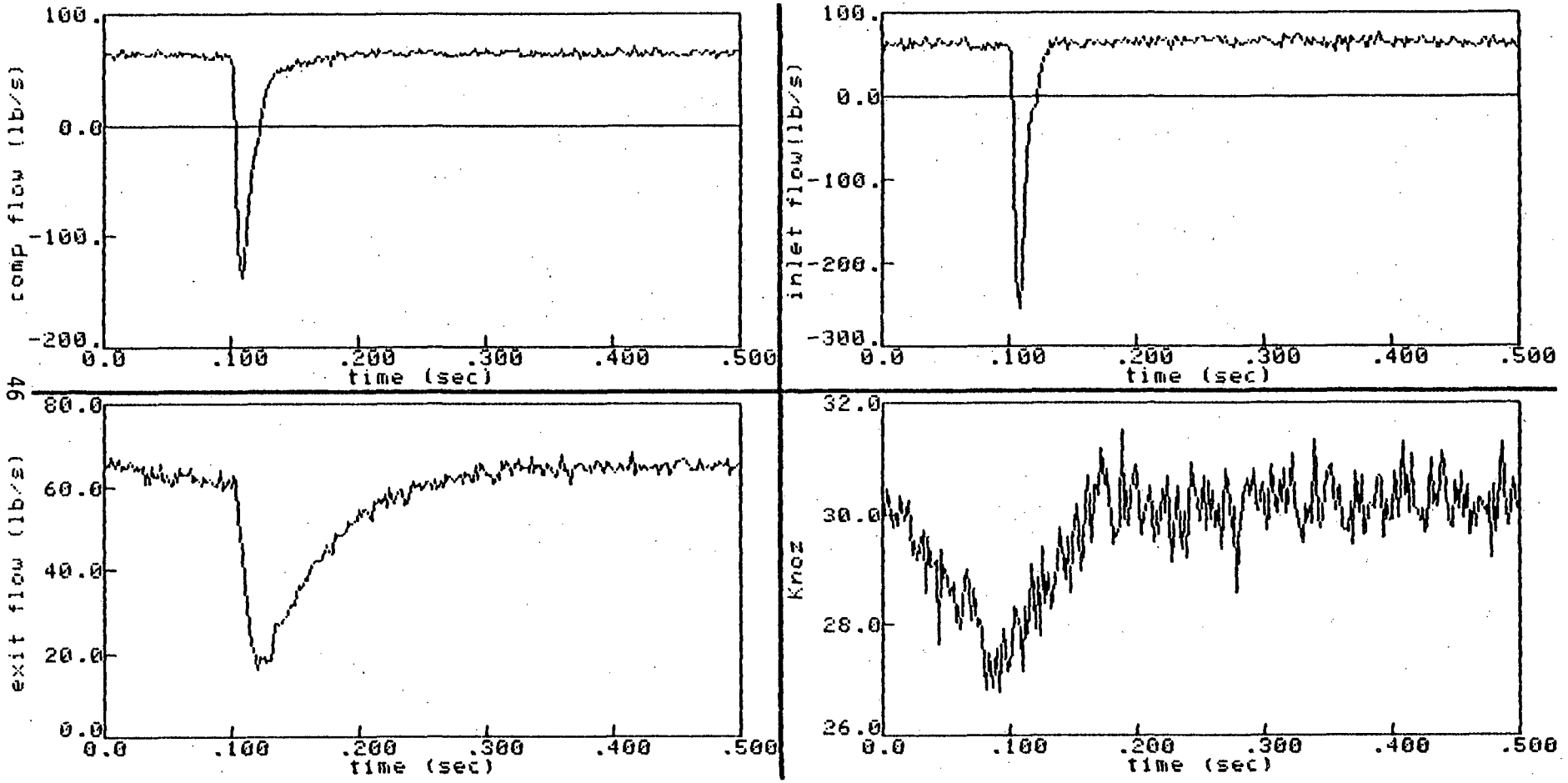

Figure 4.8 Compressor Rig, NASA Run 7

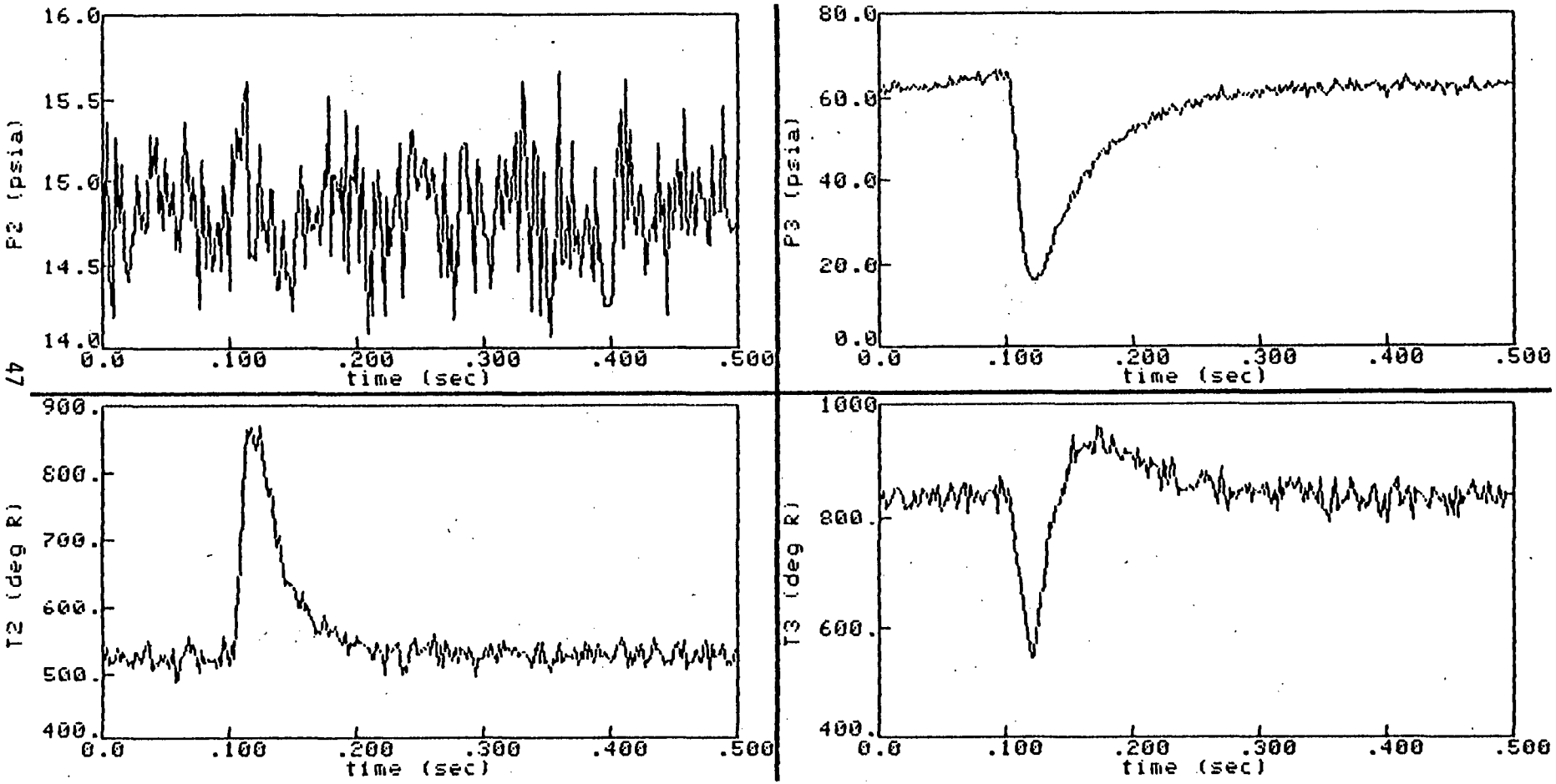

Figure 4.9 Compressor Rig, NASA Run 7

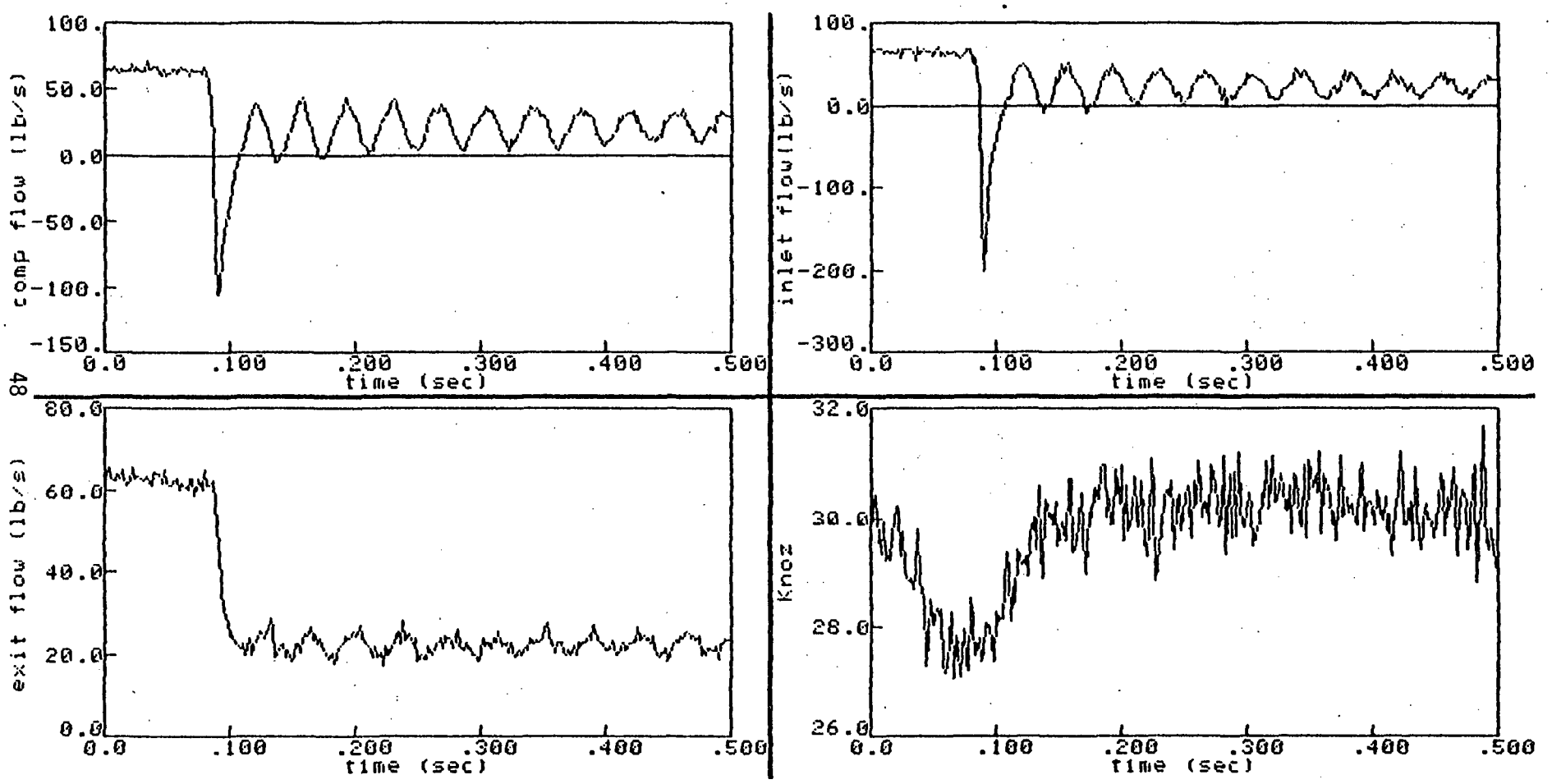

Figure 4.10 Compressor Rig, NASA Run 9

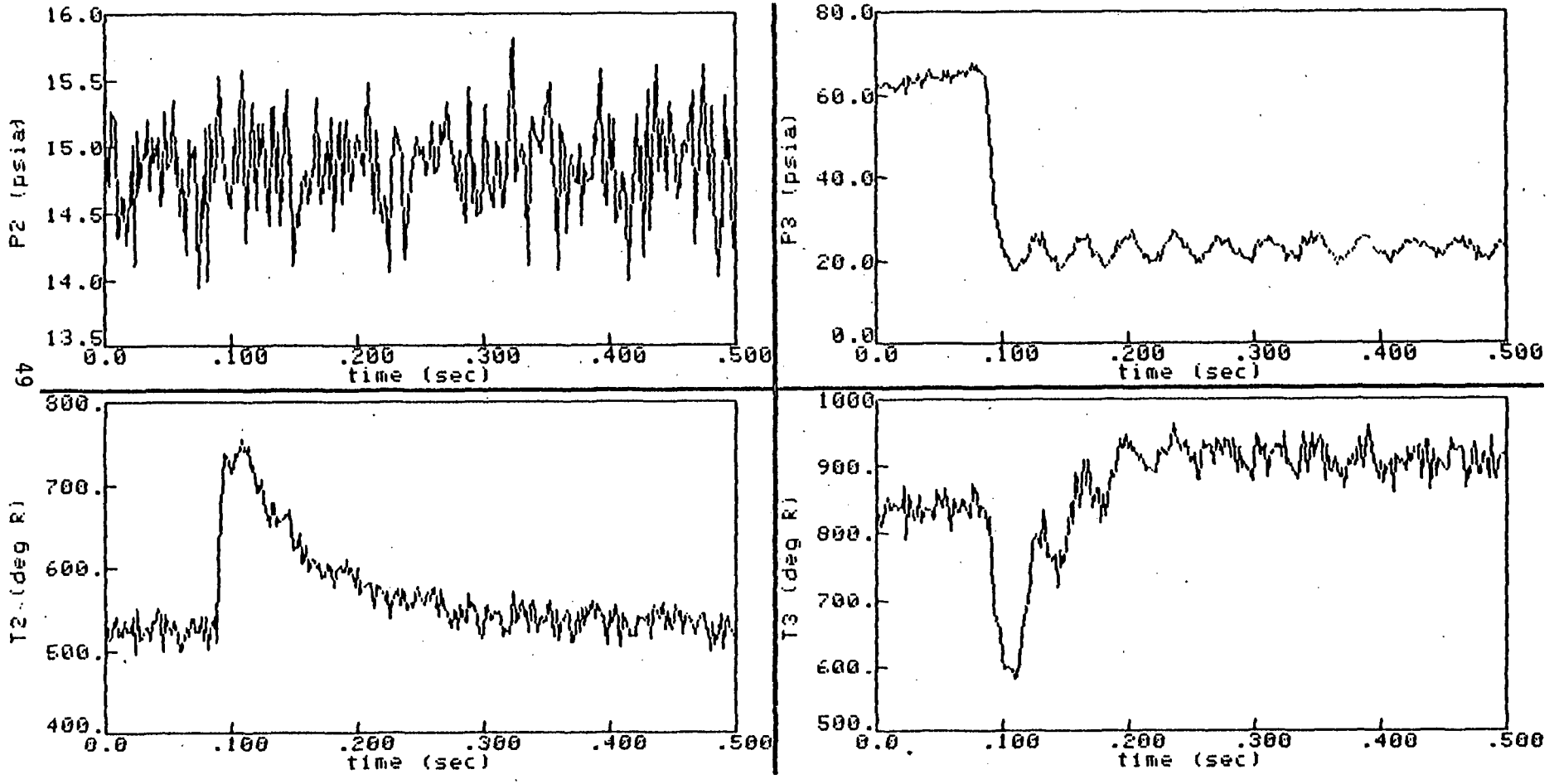

Figure 4.11 Compressor Rig, NASA Run 9

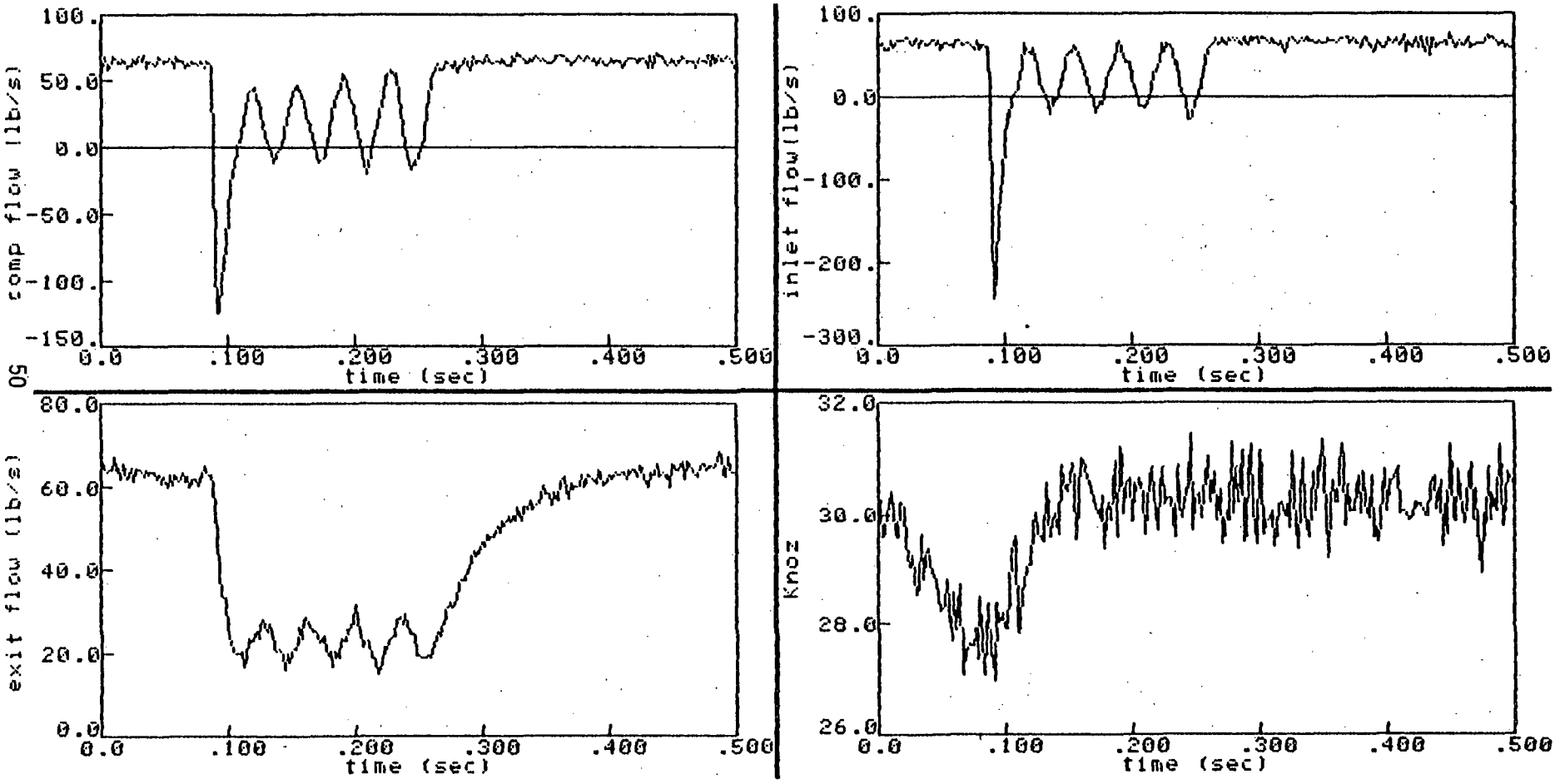

Figure 4.12 Compressor Rig, NASA Run 10

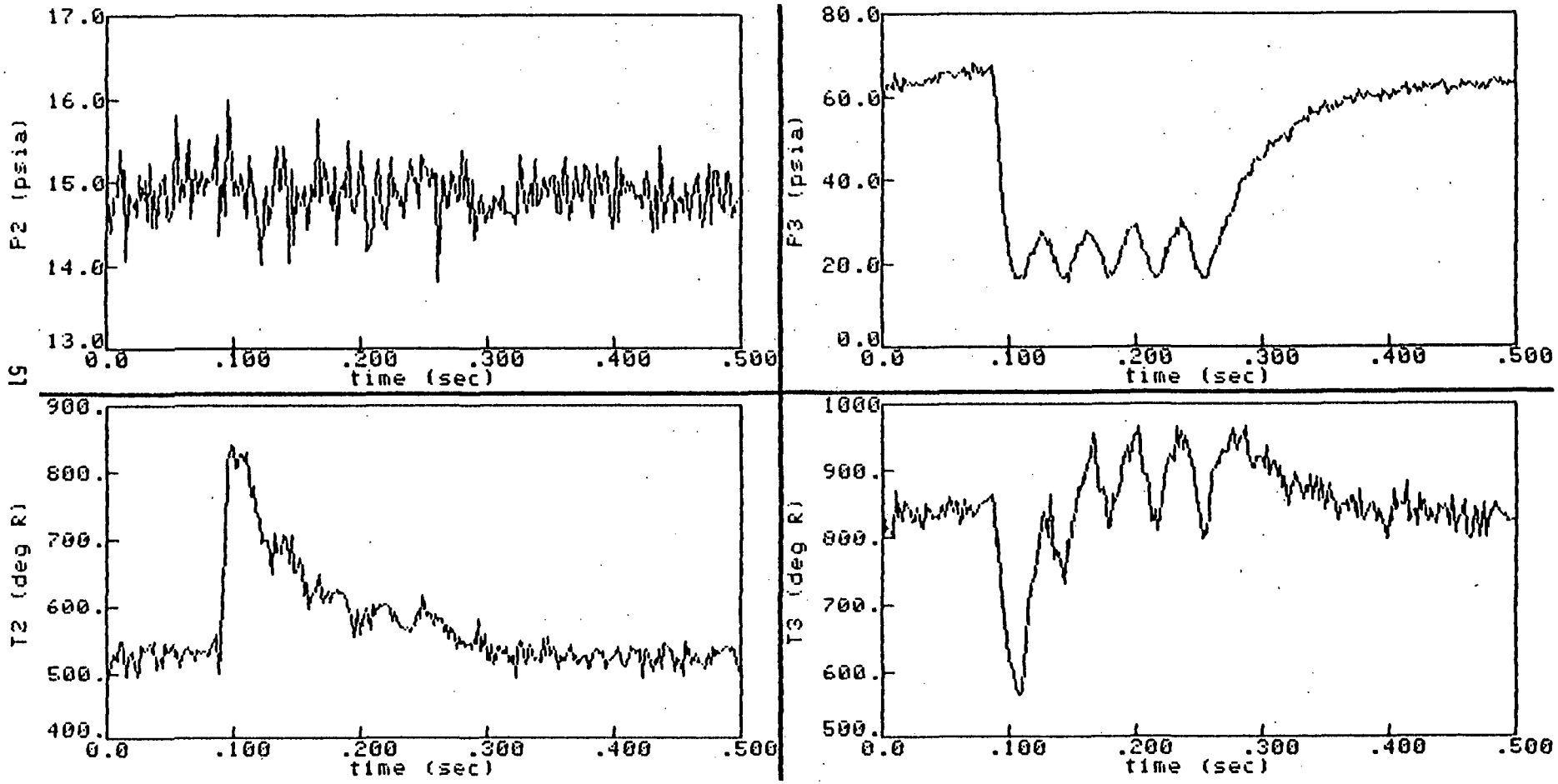

Figure 4.13 Compressor Rig, NASA Run 10

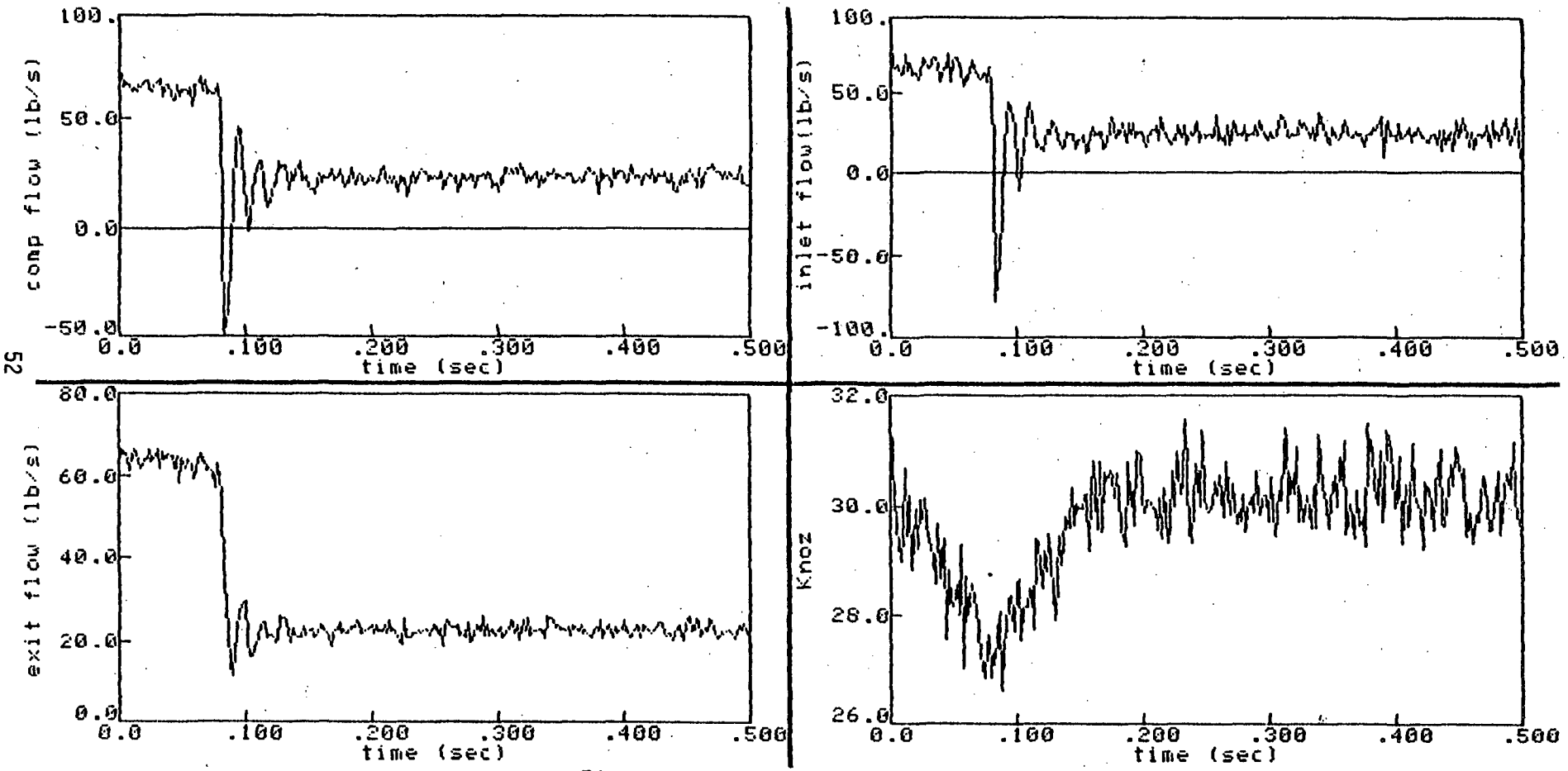

Figure 4.14 Compressor Rig, NASA Run 11

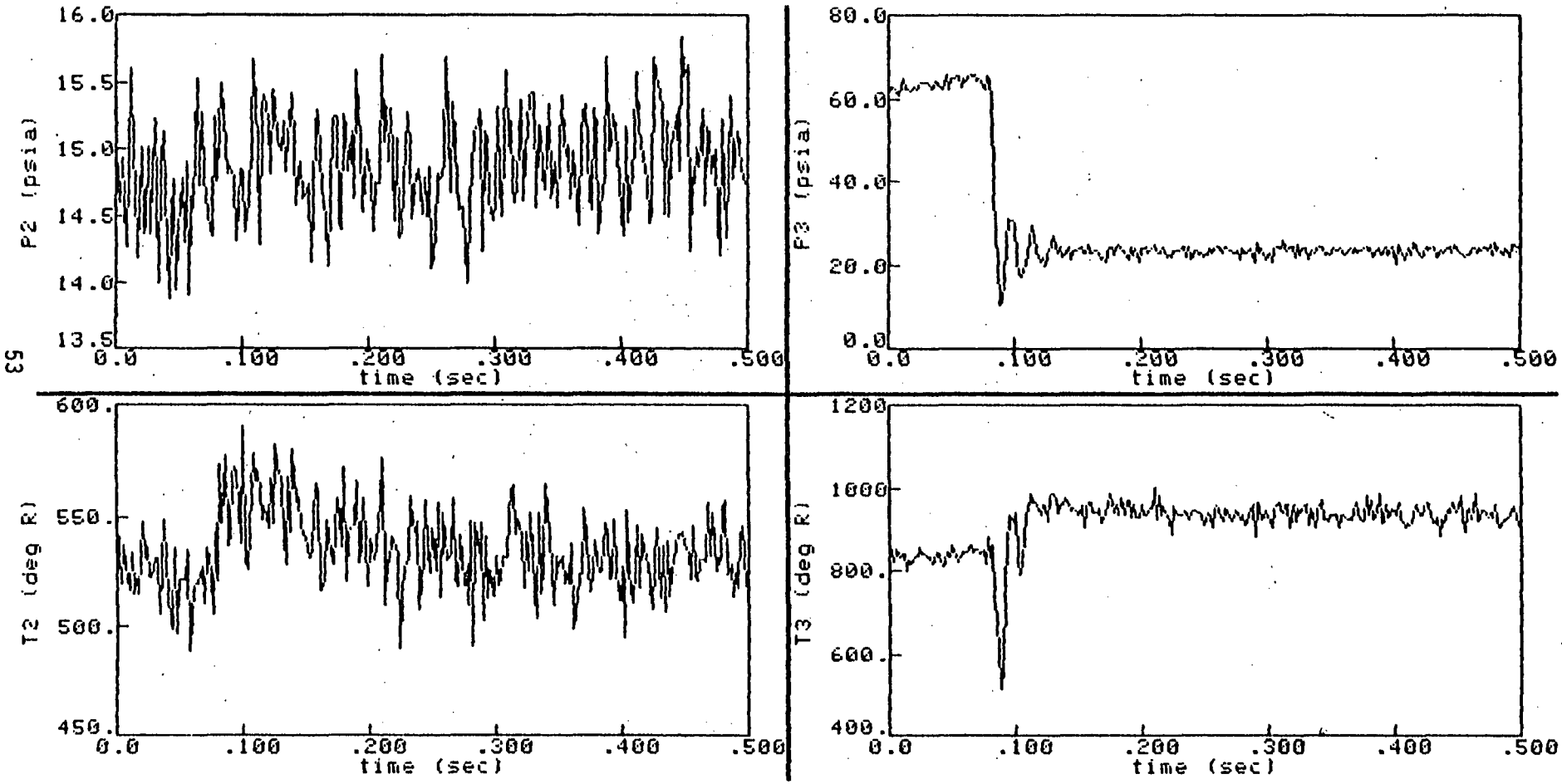

Figure 4.15 Compressor Rig, NASA Run 11

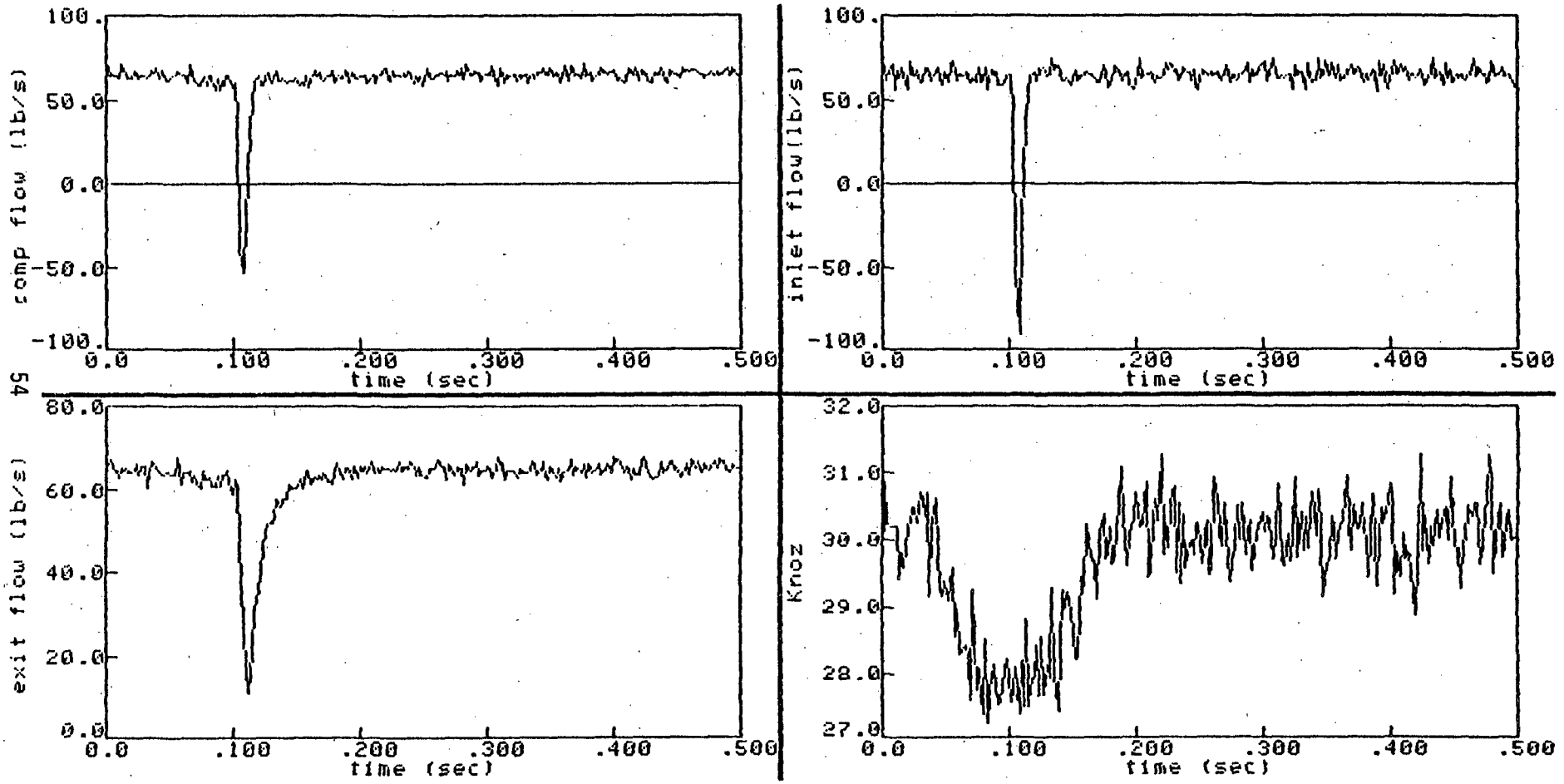

Figure 4.16 Compressor Rig, NASA Run 13

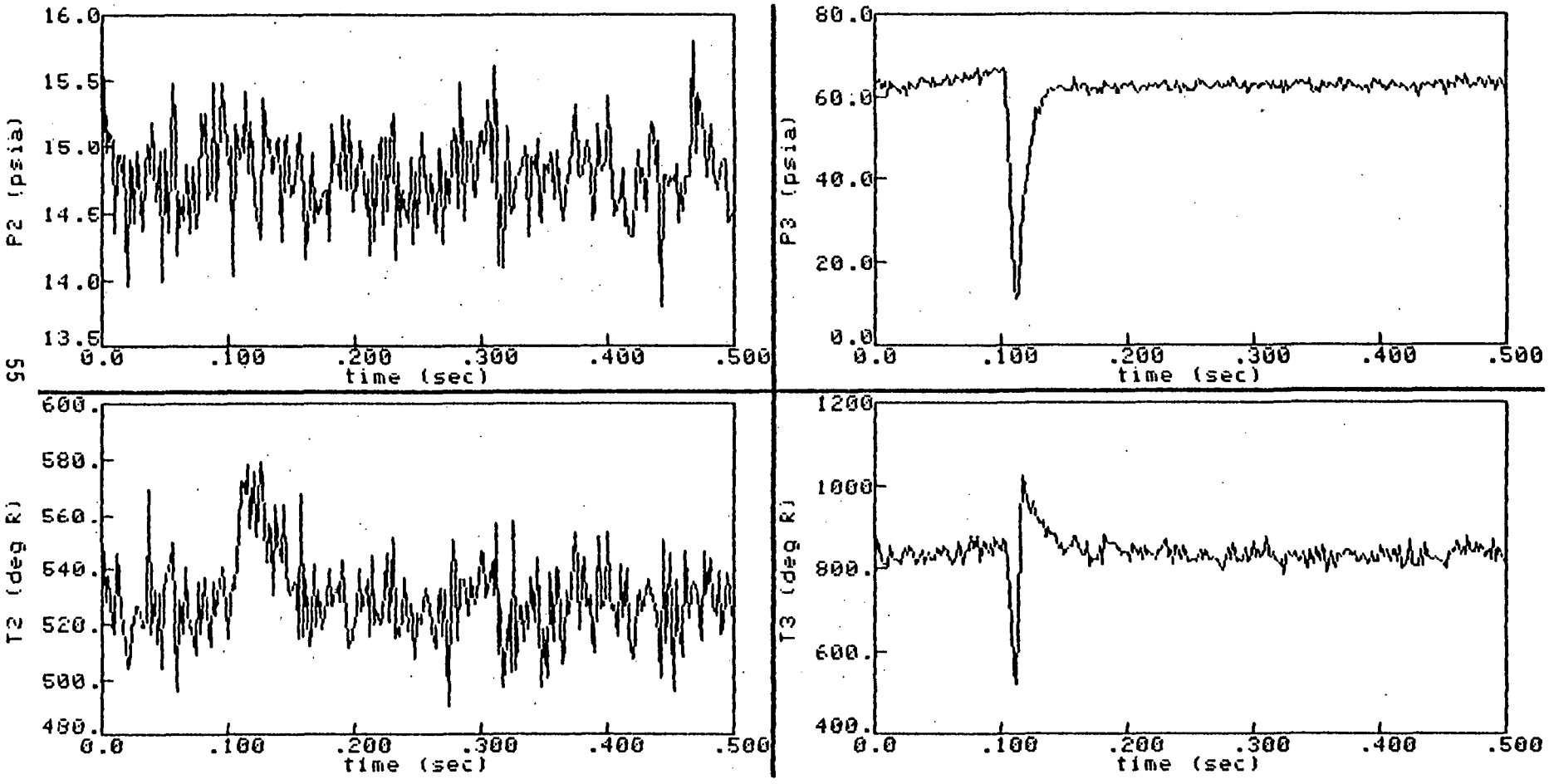

Figure 4.17 Compressor Rig, NASA Run 13

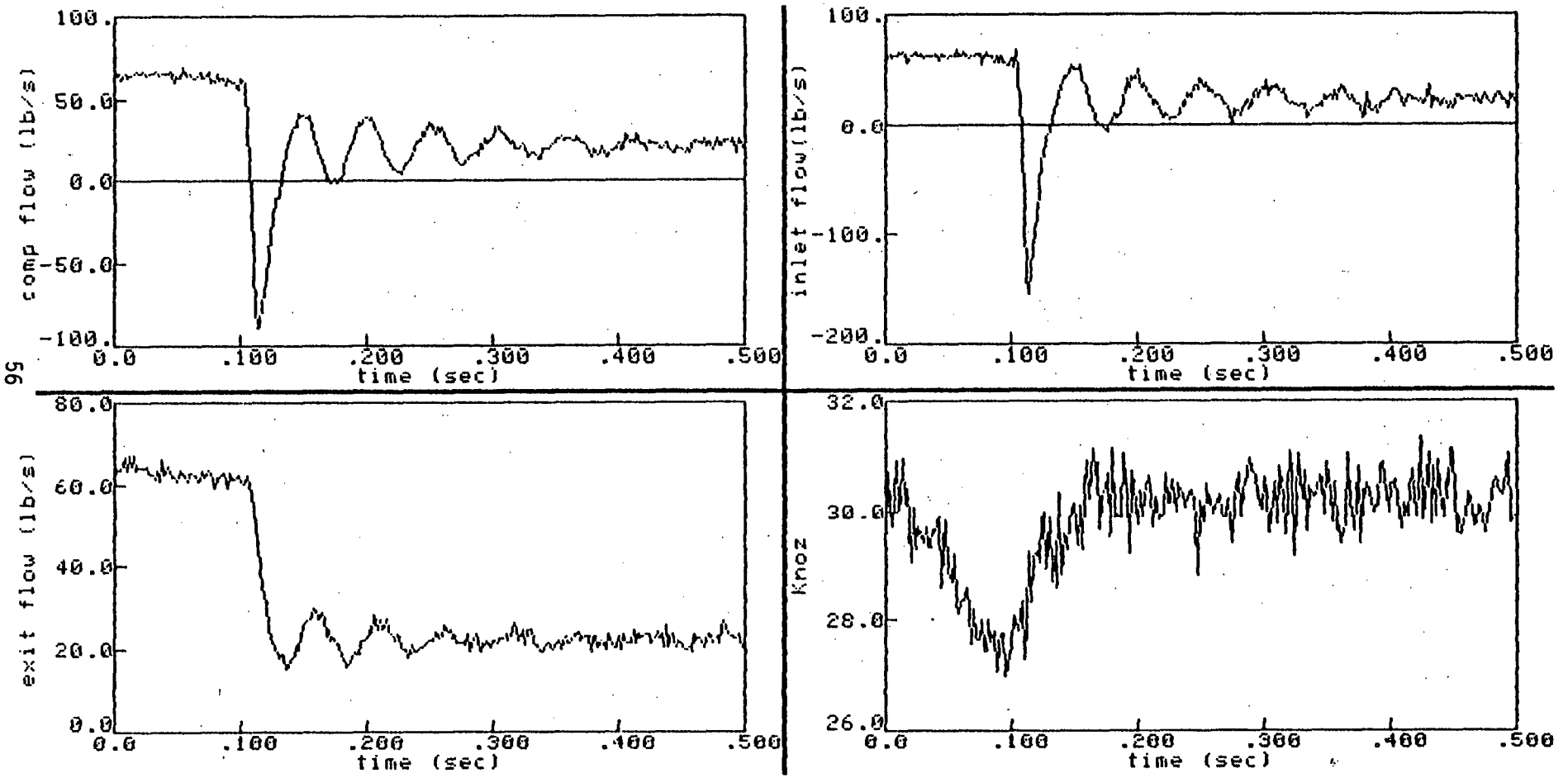

Figure 4.18 Compressor Rig, NASA Run 15

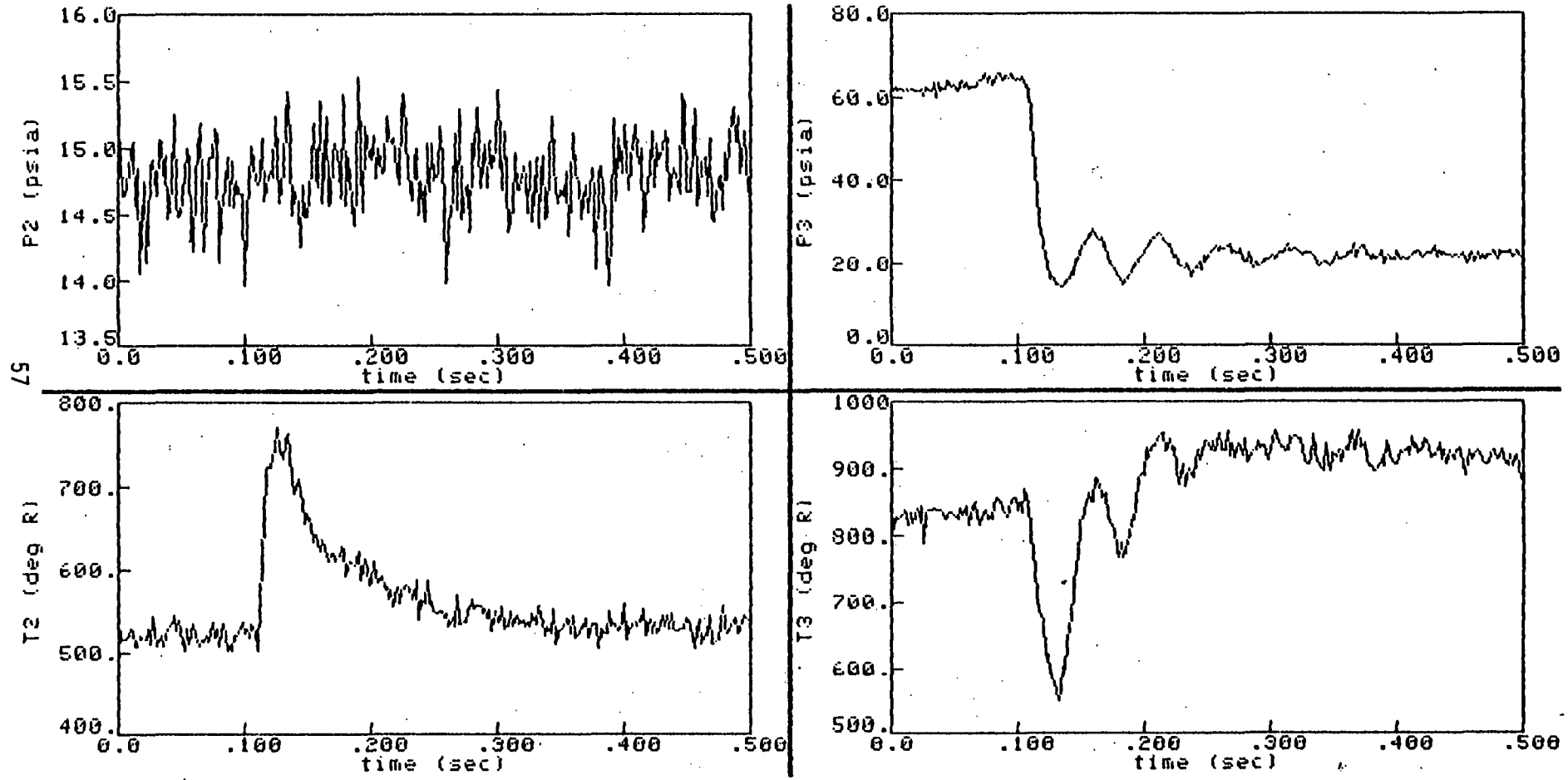

Figure 4.19 Compressor Rig, NASA Run 15

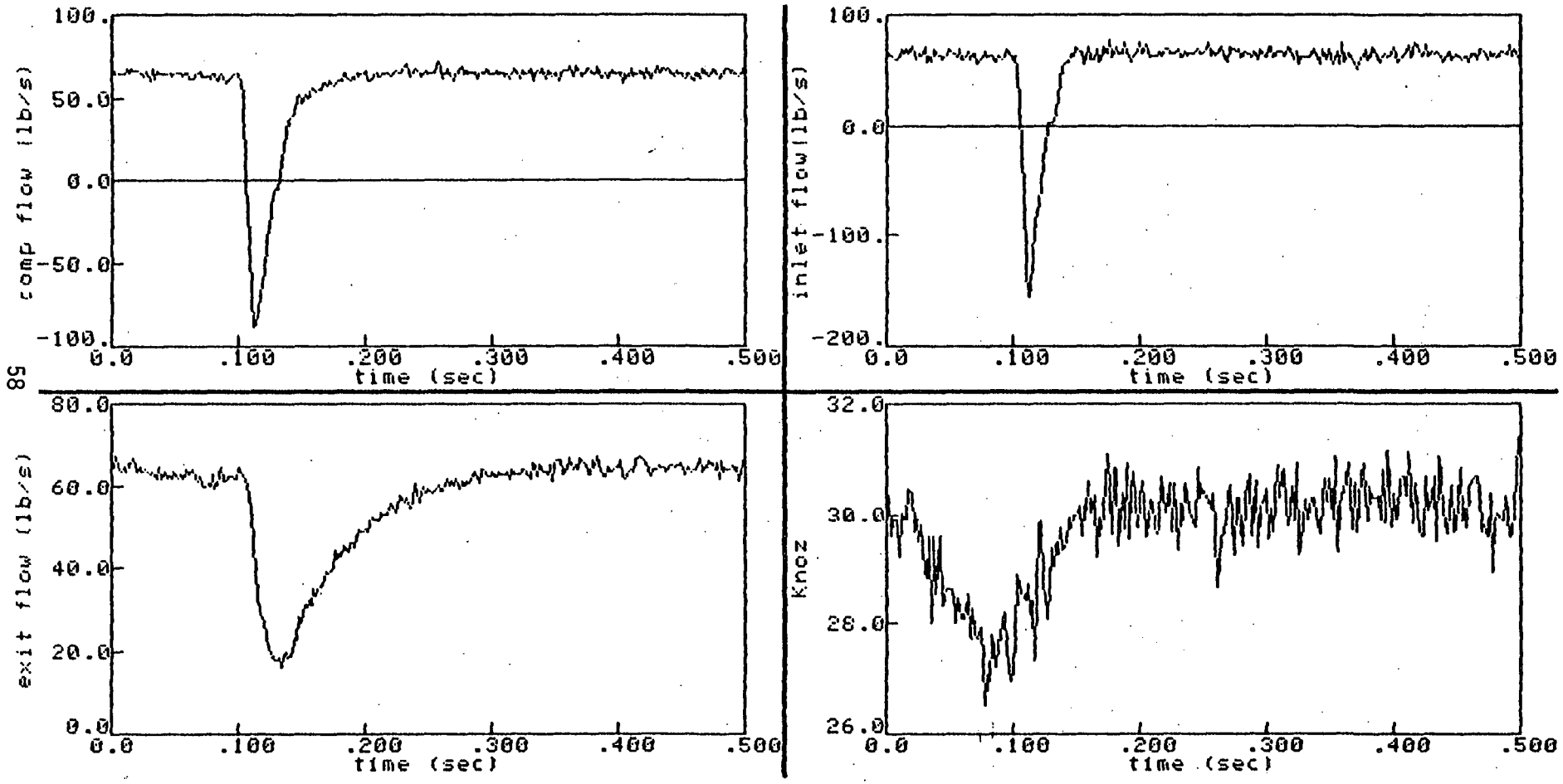

Figure 4.20 Compressor Rig, NASA Run 17

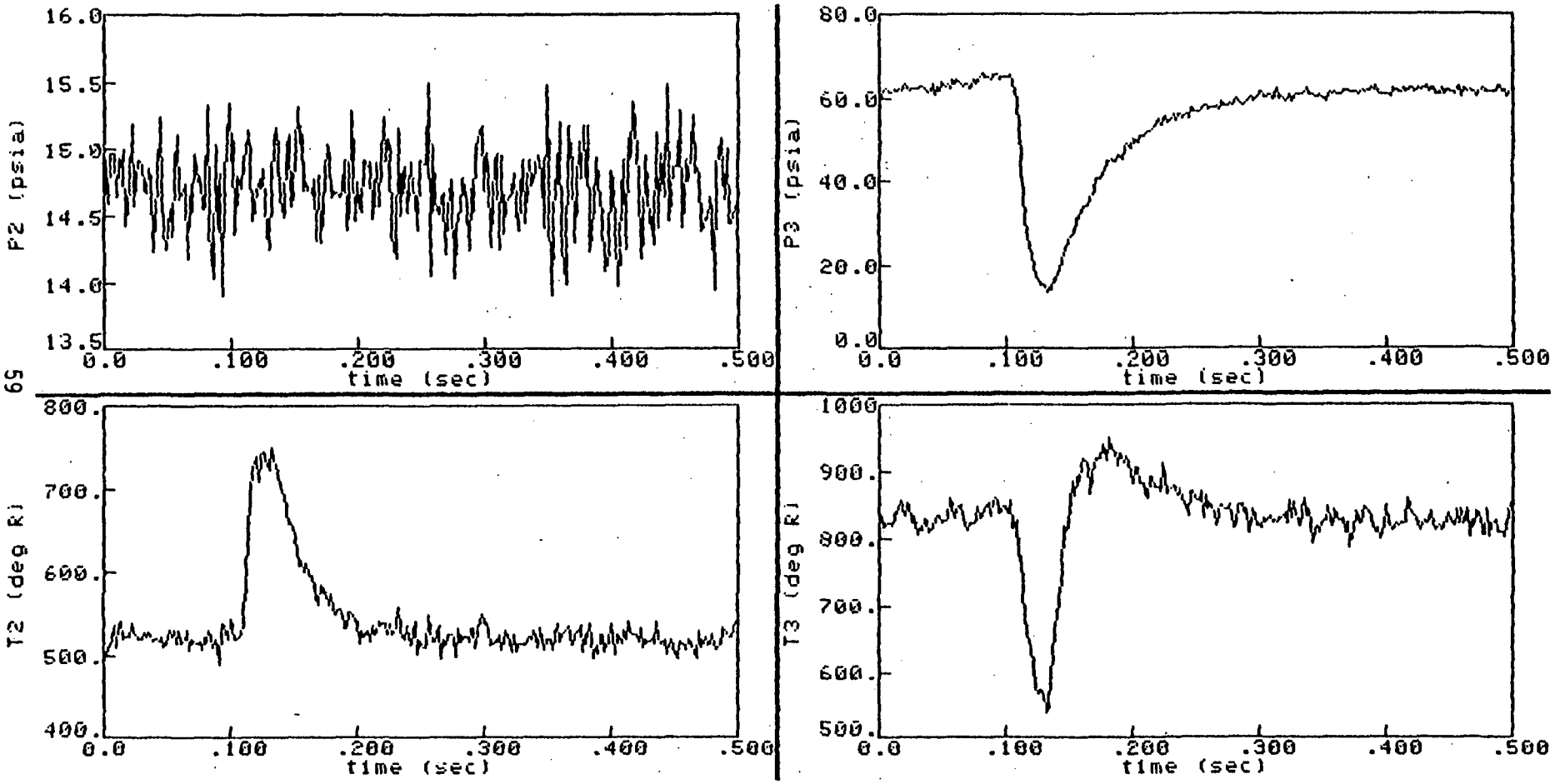

Figure 4.21 Compressor Rig, NASA Run 17

Table 4.1
Run Descriptions

Run	V3 x	L x	Kn	Kp	Description
5	10	1	8.0	0.1	Non-recoverable, medium damping, medium frequency.
7	10	1	8.0	0.5	Recoverable in 1 cycle, medium frequency.
9	10	1	20.0	0.8	Non-recoverable. light damping, medium frequency.
10	10	1	10.0	0.8	Recoverable in 5 cycles, medium frequency.
11	2	1	15.0	2.0	Non-recoverable, medium damping, high frequency.
13	2	1	15.0	4.25	Recoverable in 1 cycle, high frequency.
15	10	2	15.0	1.0	Non-recoverable, light damping, low frequency.
17	10	2	15.0	2.0	Recoverable in 1 cycle, low frequency.

Note: In many of the runs, the NASA measurements (T2, T3, P2, P3,...) were biased above the identified initial conditions. These biases affected the identifications. To what extent is unknown, but in future identifications, identification of sensor bias levels should be considered. Effects of sensor biases can be studied with sensitivity tools (from Chapter V). See Section 4.7, Identification Experiences, for further discussion.

4.5 SPECIAL CONSIDERATIONS

Several identifications were made for each run as needed. In many cases the identification had to be tailored for a particular type of stall characteristic and required special consideration. For example, in the recoverable stall runs, it was beneficial to use only a portion of the data such as the positive flow stalled region for identification. This technique

eliminated the use of unnecessary, noisy data and improved overall convergence properties. Some of these special treatments are discussed on a case by case basis in Section 4.6.1. More general details are discussed in this section and are used in Section 4.7 for defining a comprehensive approach to future parameter identifications.

This section examines four special considerations: number of data points needed for each identification, the need for separate Kp and Kn identifications, a procedure for synchronizing the onset of stall between model and data, and the need for a fixed-step integration routine in SCIDNT.

4.5.1 5-kHz Data versus 1-kHz Data

The primary frequency of the stalling compressor model is in the area of 20 to 100 kHz, depending on volume and inductance parameters. The exception occurs at the onset of stall, where the compressor flow becomes negative and the model eigenvalues are briefly near -7000 rad/sec. Using this information, SCT determined that a 1-kHz signal could be used with reasonable success in identification. Thus, most identifications used only one out of every five NASA-recorded data points.

A need for higher frequency data signals does exist, however. A significant improvement in identification accuracy was noticed when 5-kHz data were used instead of 1-kHz data. In some cases the improvement was marginal. In other cases the improvement was more substantial, particularly where the amount of time spent in stalled flow was limited due to the speed of the model (e.g. run 13).

Identification improvement was brought about because the 5-kHz signal provides more noise and signal information, and SCIDNT is better able to distinguish between the two. If less noise information is available, then estimate uncertainty will increase, as will estimate biases. The NASA data have a significant amount of noise since were passed through a relatively high-frequency filter (16 kHz) before the signal was recorded. Subsequently, there remains a fair amount of noise (approximately 10 percent) on each of the channels. When a 1-kHz sampling frequency is used with the noisy data, SCIDNT is less able to distinguish between noise and signal, while a 5-kHz sample

rate provides much more information about the noise and the signal. Using a 1-kHz signal did not make identification impossible, but it did impede identification under difficult conditions.

The sample rate consideration prompted, in part, the Task B I/S study. Chapter V develops mathematical relationships between sample rate and identifiability which explain these observations.

For the cases discussed below, some loss in identification was expected because the 1-kHz signal was used. The loss was considered acceptable because the identification goals (to demonstrate identifiability and provide experience) do not require identification accuracy. A few special cases were done with the 5-kHz signal to demonstrate improved convergence, but generally, 5-kHz runs were avoided because of extended computation times. Using an improved signal type (e.g. a 5-kHz signal or better) may be mandatory for proper convergence in more critical identifications.

4.5.2 The Need for, and Consequences of, Separate Kp and Kn Identifications

SCIDNT is capable of identifying several parameters at the same time, allowing the parameters to converge simultaneously to their maximum likelihood values. This is an advantageous feature since it saves iterating between one parameter identification and another. But the feature has its limitations too. Parameters being identified must have certain relationships among themselves, if they do not, they must be identified separately. Kp and Kn lack this relationship.

4.5.2.1 Poorly Conditioned Hessian

Kp and Kn had to be identified separately in the compressor rig study for two reasons. The first reason is related to the information matrix, M. The second reason is related to the nature of the stalled compressor model. The discussion begins with the information matrix.

The information matrix is used to define how parameters converge to their maximum likelihood values. Rewriting Eq. (3.5) from Chapter III reveals the relationship:

$$M * g = - \Delta\theta \tag{4.1}$$

or, solving for the parameter step size:

$$= - M^{-1} g \tag{4.2}$$

Equation (4.1) indicates that if M is poorly conditioned or nearly singular, forming the inverse and $\Delta\theta$ will be difficult. This is in fact what happens with simultaneous Kn and Kp identifications. The two eigenvalues of M related to Kn and Kp are separated by approximately 6 orders of magnitude in the compressor model. Given the numerical precision of a 32-bit computer, such a difference makes inverting M very difficult. To SCIDNT this means that Kn converges while Kp doesn't; Kp is dominated by the Kn convergence. Increasing the precision of the computer would help the situation, but still there is the second reason for separate identifications (compressor model nature) that makes simultaneous identifications difficult. This second aspect is discussed in Section 4.5.2.3.

4.5.2.2 Consequences of Separate Identifications

Important consequences regarding the accuracy of identified parameters appear because Kp and Kn must be identified separately. Since they can no longer converge simultaneously, as Kn is identified, Kp does not improve, and Kn is identified with an uncertain value of Kp. This situation causes a bias in the estimate of Kn. Such biases can be eliminated by identifying iteratively. For example, first identify Kn, then identify Kp with the new Kn, then identify Kn with the new Kp, and so on. By this procedure, the maximum-likelihood solution would eventually be reached since the biases diminish with each iteration. In simultaneous identification, this iterative process occurs naturally; with the separate identifications, the process is done artificially and is more time-consuming.

In all of the compressor rig cases, only a single step iteration was carried out because additional iterations produced minimal accuracy improvement. This was due to the identification sequence and the fact that Kn could be identified accurately regardless of Kp errors. However, if the Kn

identification was inaccurate because of uncertainties introduced through sensor noise, Kp could be biased by the Kn errors.

To obtain a greater understanding for the extent of the biases, a sensitivity analysis was performed. (The details of this analysis are not given until Chapter V, but results are presented here to explain the Kn and Kp relationships.) The relationship being studied is the sensitivity of Kn to errors in Kp and vice versa.

The test case uses NASA run 5 data with a nominal parameter set. The analysis results are shown in Table 4.2. First-order approximations of estimated biases are made for a 10 percent nuisance bias level. The approximations should be taken with prejudice, yet they do indicate a magnitude for the expected errors.

Table 4.2
Kp and Kn Parameter Biases

	for Kn/Kp	for Kp/Kn
Bias sensitivity	2.4779	-0.0529
Bias sensitivity (normalized)	0.0309	-4.2320

+10 percent bias in	produces bias of	in estimated
Kn	-42.3 percent	Kp
Kp	+0.31 percent	Kn

Consider a physical interpretation of the above results. In the case of an error in Kn, physically, that error increases or decreases the amount of time spent in negative flow. Since negative flow typically occurs at the beginning of a stall (before the positive stalled flow), the effect is to shift the positive flow model in time. For example, if Kn were 10 percent above the nominal value, the model would spend less time in the negative flow region. Then modeled positive flow would begin before the data indicates, and the model and data would appear to be skewed. In a non-recoverable stall, this makes the model appear to be phase-shifted with respect to the data.

Such a serious disagreement between model and data could produce dramatic biases in an estimated Kp as reflected by the large predicted biases in Kp due to Kn.

So even though Kp and Kn are used at different times by the model, one is able to have a dramatic effect on the other because of a time relationship in the model. If the physical argument is logically extended to consider estimated Kn biases, the situation is completely reversed. Here, the positive flow response will have practically no effect on the negative flow response. The only exception is found in some non-recoverable cases where the oscillatory response occasionally dips into negative flow. Other than this exception, it is not surprising that the predicted Kn biases are quite small for Kp errors.

The important result is the consequence on Kn and Kp identifications. Since Kp has a minimal effect on Kn, an identified Kn should be unbiased by Kp, and a subsequently identified Kp should be unbiased as well. So, for a single step iteration (separate identifications), the results should ideally be the maximum-likelihood values and there will be no need for further iteration, as long as the Kn identification is accurate.

4.5.2.3 Bimodal Model Effects

The physical analysis presented above helps explain the other reason why it is so difficult to identify Kn and Kp simultaneously. If Kn is allowed to change and converge during an identification, then the time relationship between the positive flow model and data is also changing. This means that SCIDNT has to hit a moving target: the Kp information (gradient, etc.) changes while Kn is allowed to vary. Unlike the first aspect (numerical difficulties) which could be corrected by improved precision, there seems to be no such solution to this obstacle other than separate identifications or the situation where Kn is very close to its actual value.

Choosing to identify Kn before Kp in the separated identifications comes from this physical analysis. Simply put, Kn was chosen for identification ahead of Kp, because it is fairly independent of Kp. The sensitivity results and predicted biases simply verify these qualitative interpretations and

support the decision for separate identifications. In the future, when 10 parameters, not 2, will be identified, the condition of the information matrix will be the primary method for determining if simultaneous identifications are possible. The M-matrix tool is very powerful. The physical analysis is helpful to conceptualize why separate identifications are necessary, but fundamentally, the M matrix supplies the needed information.

4.5.3 Synchronizing Model and Data

The third consideration pertaining to these identifications is the synchonization of the SCT model with the NASA data. There are two phases to this problem.

First, it was found that the recorded NASA throttle disturbance (Knoz) was not vigorous enough to initiate stall when used as an input to the SCT model. This was not entirely unexpected. Earlier results with the SCT model indicated that a throttle coefficient of approximately 40.3 (vs. NASA's 40.0) was needed to initiate stall. In response to the situation, a scaling parameter was inserted into the model, "AT". The new scaling parameter made the measured throttle channel data appear as if a larger "AT" coefficient were used (see Figure 4.22). The fix worked well for initiating stall, but it also pointed out a strong relationship between the time of stall onset and the SCT value of AT. It was found that if the new AT was too large, even by a half percent, stall would begin too early, and the SCT model would be skewed with respect to the data (see Figures 4.23 and 4.24). If new AT's were to be used, a method had to be developed to ensure synchronization between model and data. This method is the second part of the synchronization problem.

This problem has a familiar aspect: find a suitable AT that will make SCT's model fit the hybrid data — simply a problem of parameter identification. SCIDNT was used to identify a new AT for each of the 8 runs, a new AT that both initiates stall and synchronizes the data. The results are in Table 4.3. A comparison between different AT's is demonstrated in Figures 4.23 and 4.24.

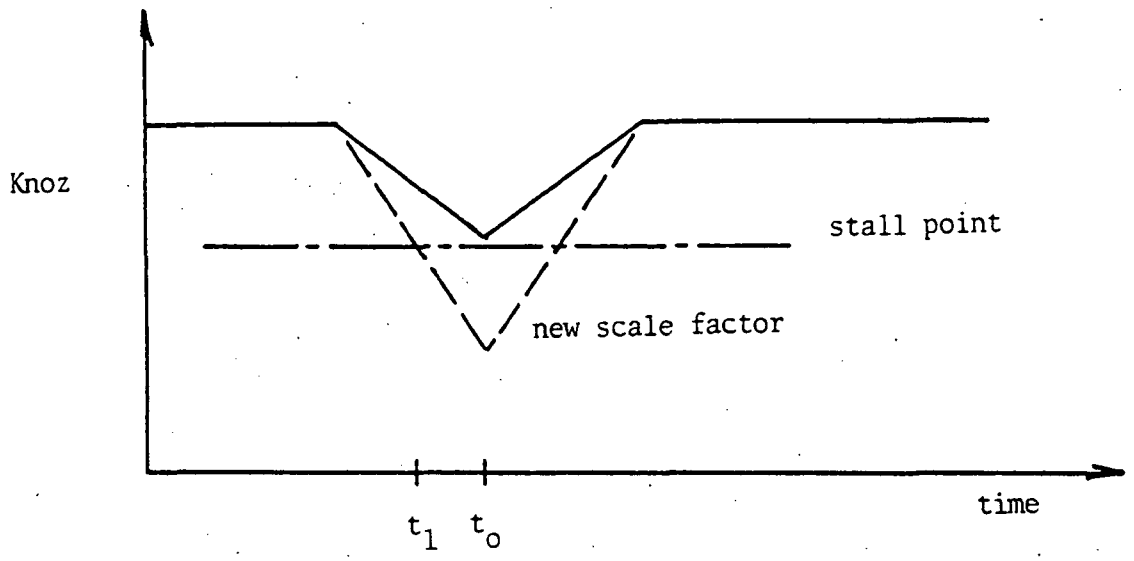

Figure 4.22 Scaling of Knoz Disturbance with AT

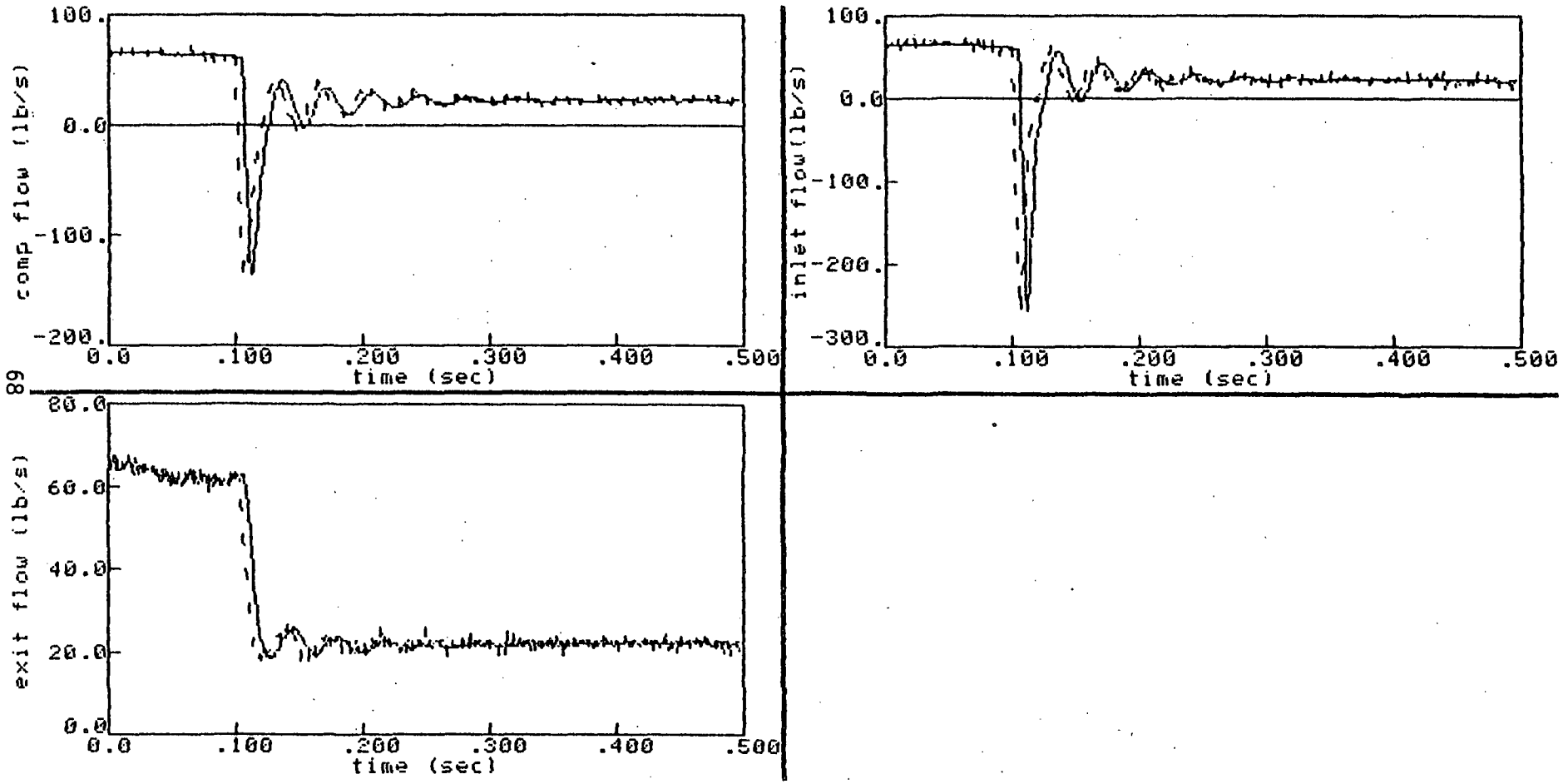

Figure 4.23 Run 5 AT = 40.07 (actual = 40.17): Model Follows Data

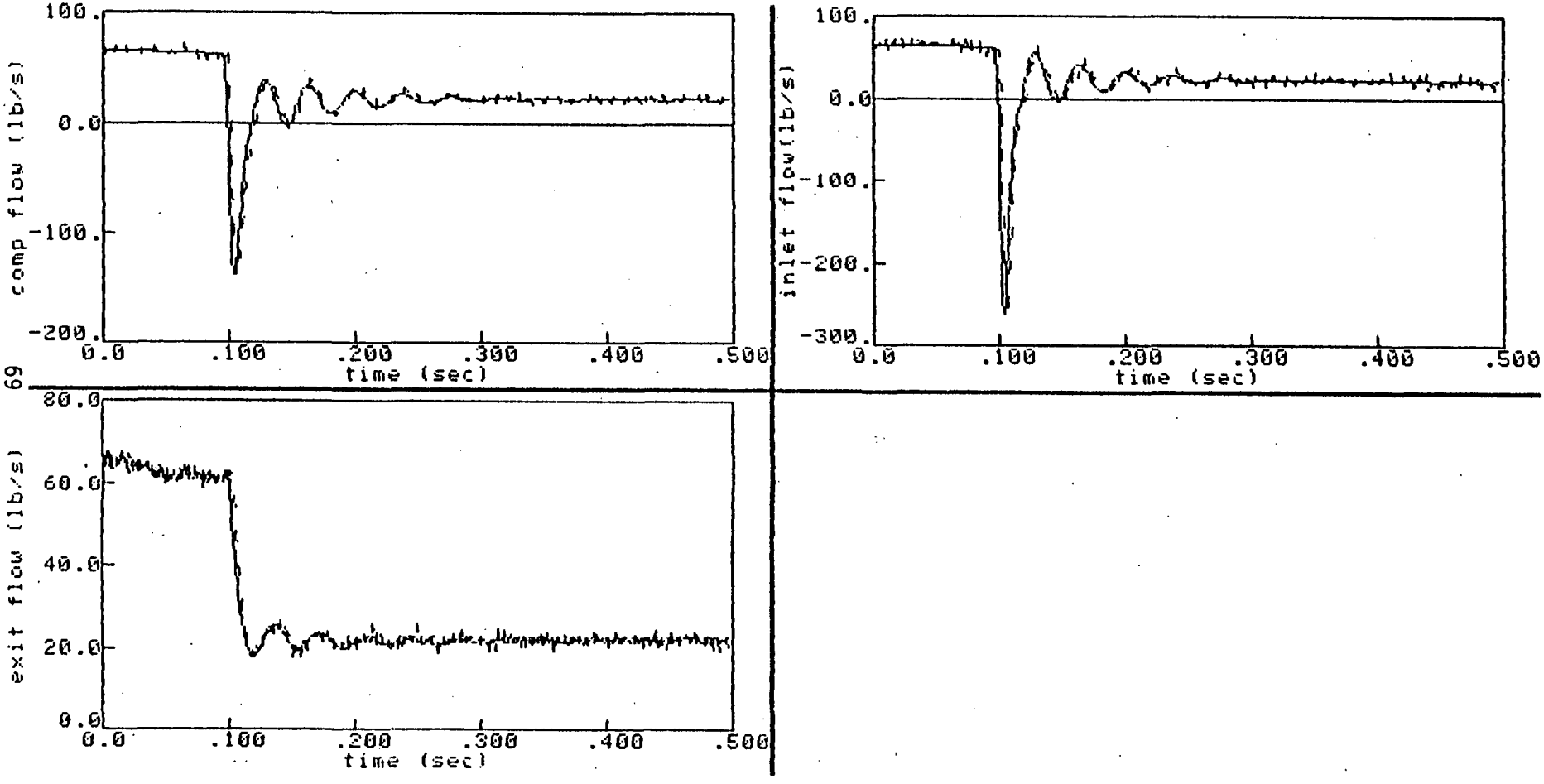

Figure 4.24 Run 5 AT = 40.27 (actual = 40.17): Model Leads Data

Table 4.3
Identified Throttle Coefficients

Run	5	7	9	10	11	13	15	17
AT	40.168	40.147	40.379	40.288	40.930	40.468	40.524	40.448

Note that these new values are only 1/10 to 1/2 percent from the NASA values. This may indicate the initialization problem is related to numerical or precision differences rather than any gross model structure anomaly.

4.5.4 Fixed Integration Routine in SCIDNT

In Chapter III, the advantages of using a variable step integration routine in SCIDNT were discussed (mainly in decreasing computer costs.) Unfortunately, it turns out that the variable integration routine is not precise enough in single-precision form to supply the accuracy needed for Kp identifications. It was observed that Kp cost errors were changing more drastically with different integration step size histories than they were with parameter steps. Efforts were made to improve precision by decreasing error tolerances, but they were to no avail. As a result, SCIDNT was converted a fixed step integration routine.

4.6 COMPRESSOR RIG IDENTIFICATIONS SUMMARY

Table 4.4 summarizes the results of the identification study. In general, SCIDNT successfully identified the Kp and Kn parameters; however, the degree of success varied from case to case. The case to case variances contain useful information since they demonstrate limitations in identification and also suggest methods for improving the identification process. General items of the identifications are discussed below. More specific details are discussed on a case by case basis in the following eight subsections.

The general conclusion of these results is that two factors dominate the success of identification: (1) the amount of information available, i.e.

simply the number of data points available for a given scenario, and (2) the stall trajectory or path followed on the stalled compressor map.

Table 4.4
Identification Summary

Run	Kn Initial	Kn	percent error	Kp Initial	Kp	percent error	
5	16.	7.94	-0.75	0.5	.115	+15.0	N
7	4.0	8.22	+2.75	1.0	.983	+96.7	R
9	14.0	17.9	-10.5	0.5	.755	-5.60	N
10	16.0	9.32	-6.8	0.5	.669	-16.4	R
11	8.0	20.2	+34.5	3.0	2.055	+2.75	N
13	16.0	20.88	+39.2	5.0	4.807	+13.0	R
15	30.0	12.78	-14.8	0.5	0.899	-10.1	N
17	30.0	15.6	+4.0	3.0	2.026	+1.30	R

Regarding the number of data points, one significant trend indicates that Kp identification is more difficult in recoverable runs (7, 10, 13, and 17) than in non-recoverable runs. The problem here is not the recoverable/non-recoverable nature of the stall phenomenon but simply the amount of positive stalled flow information. In each non-recoverable stall case there are about 350 milliseconds (or 1750 points/channel) of data. In each recovery case there are only about 15-20 milliseconds, or 1/20 of the information. The lack of information in the recovery cases is primarily responsible for the poorer identifications. This fact is supported by Kn results which show no particular sensitivity to the recoverable/non-recoverable character of the runs. Both types of runs have approximately equivalent amounts of negative stalled-flow information, and Kn was equally indentifiable in each type.

A related trend is found in Kn identification for runs 11 and 13. In these cases, the increased inductance (L = Lnom x 2) caused the stall response to speed up significantly and thus decreased the ratio between response

frequency and sample rate. Again, there is less information content and Kn identifications suffer as a result. This conclusion is supported by the fact that runs 5 and 11, and 7 and 13 are so similar. Both sets of runs have identical stall characteristics except runs 11 and 13 are faster and thus have less information and fewer data points.

The information content argument is supported further by cases where more data were used for identification -- more data meaning use of a 5-kHz signal instead of a 1-kHz signal. A 5-kHz signal was used instead of a 1-kHz signal in several cases, and these cases showed improved identification and demonstrate that increasing the amount of information increases identifiability.

(There are ways, other than just using higher frequency signals, to increase the amount of information where information content is poor. Content can be increased by using several measurement sets for a single run or by using several single measurement sets for several similar runs. For example, if several independent measurements from the same run were available, these measurements could be used in unison to increase information content and thus identifiability.)

The second factor affecting identifiability is the type of stall being studied. As mentioned above, non-recoverable stalls are more identifiable than recoverable stalls because of the increased amount of time spent in positive stalled flow. Similarly, those non-recoverable stalls which exhibit light damping in the stall oscillations (runs 9 and 15) are more easily identified than the heavily damped runs (runs 5 and 11.) The basic reason again is information. The lightly damped runs have trajectories that cover a larger portion of the stalled compressor map. Because they cover more of the map, they provide more information and better definition of the map. It is analogous to rolling a marble in a bowl. If the marble circles the bowl several times before settling at the bottom, the path it follows gives a good definition of the shape of the bowl. On the other hand, if the marble circles the bowl only once or twice and the path is more uncertain because of noise, the definition of the bowl shape becomes more ambiguous.

In conclusion, the compressor model parameter identifications in Table 4.4 are determined by the amount of information available. Information content can be increased under several conditions:

(1) Non-recoverable stalls provide more positive stall flow information.

(2) Lightly damped non-recoverable stalls also provide more information.

(3) Information can be increased by using higher frequency signals.

(4) Information can also be increased by using several measurement sets for a single run or several runs with a single set of measurements.

Information is the key to identification. Identifications will be most accurate when optimal measurement sets and stall trajectories are used in data recording. Therefore, it is extremely valuable to consider a priori to identification what arrangements (stall trajectories and measurement sets) would yield the greatest payoff in information and identifiability. Further discussion of these needs is found in Section 4.7 and are studied in detail in Chapter V.

4.6.1 Specific Identification Details and Results

All runs followed the same single step iteration: AT (throttling coefficient) and Kn were identified simultaneously, then Kp was identified with the identified AT and Kp. The identified AT synchronizes data and model, the identified Kn defines negative flow characteristics and places the model at a proper state for the positive flow identification. The identified Kp completes the identified model. The steps are summarized below:

(1) Synchronize model and define negative flow — identify AT and Kn.

(2) Complete model identification — identify Kp.

These steps form the single-step iterative process used by SCT. In some cases steps, 1 and 2 were repeated several times under different conditions to resolve difficulties or provide experience.

4.6.1.1 Run 5 (Figures 4.25 and 4.26)

Run 5 is a non-recoverable stall with medium damping (see Figures 4.6 and 4.7). The identification followed the basic outline sketched above. To begin the identification process, two K-parameters were chosen as initial values (Table 4.5.) Before the parameters were identified, the model and data were synchronized by identifying a new AT. To simulate as real a situation as possible, the new AT was identified using the initial (incorrect) K-parameters in the model. The identified AT is shown in Table 4.3., the new Kn and Kp are shown in Table 4.5.

Table 4.5
K-Parameter Identification for Run 5

Run	Initial Kn	Final Kn	Actual Kn	Initial Kp	Final Kp	Actual Kp	Comments
n05a	16.0	7.82	8.00	0.05		0.10	1 kHz
p05a		7.82	8.00	0.05	0.132	0.10	1 kHz

To demonstrate the SCIDNT identification algorithm, a plot of each of the Kn and Kp values tested by SCIDNT is shown in Figures 4.27 and 4.28. The figures illustrate the progression of SCIDNT-selected parameters towards the maximum-likelihood values. Normalized K-parameters (normalized to actual values, 8.0, and 0.1) are plotted versus normalized RMS errors in W2dot (uncorrected compressor flow). W2dot was chosen to represent a cost value because it is fairly indicative of Kp and Kn errors. The W2dot error is normalized to the RMS error present when actual parameter values are used in the model, i.e., the nominal error represents noise only.

In the first figure, Figure 4.27, Kn moves in one step from its initial value to within 10 percent of actual. Such a rapid convergence indicates that the gradient is fairly constant in this region. Kn progresses from this value to a new value at 97.75 percent of actual. At this point the gradient is near zero, i.e. the amount that model-data errors are changed by changing Kn is practically nil, so the identification is halted. (SCIDNT terminates the

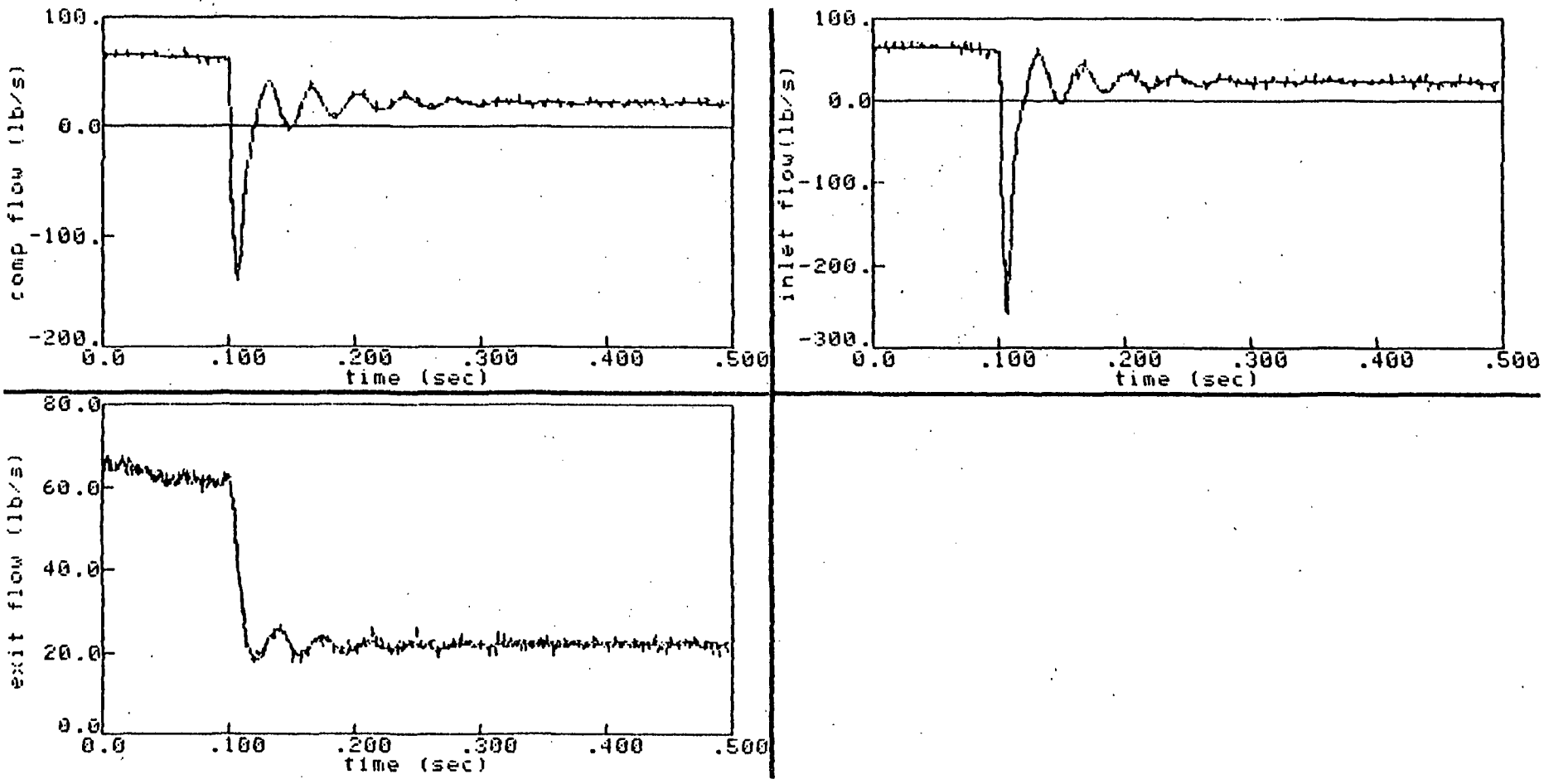

Figure 4.25 Run 5 Identification
(—— identified model)
(--- NASA data)

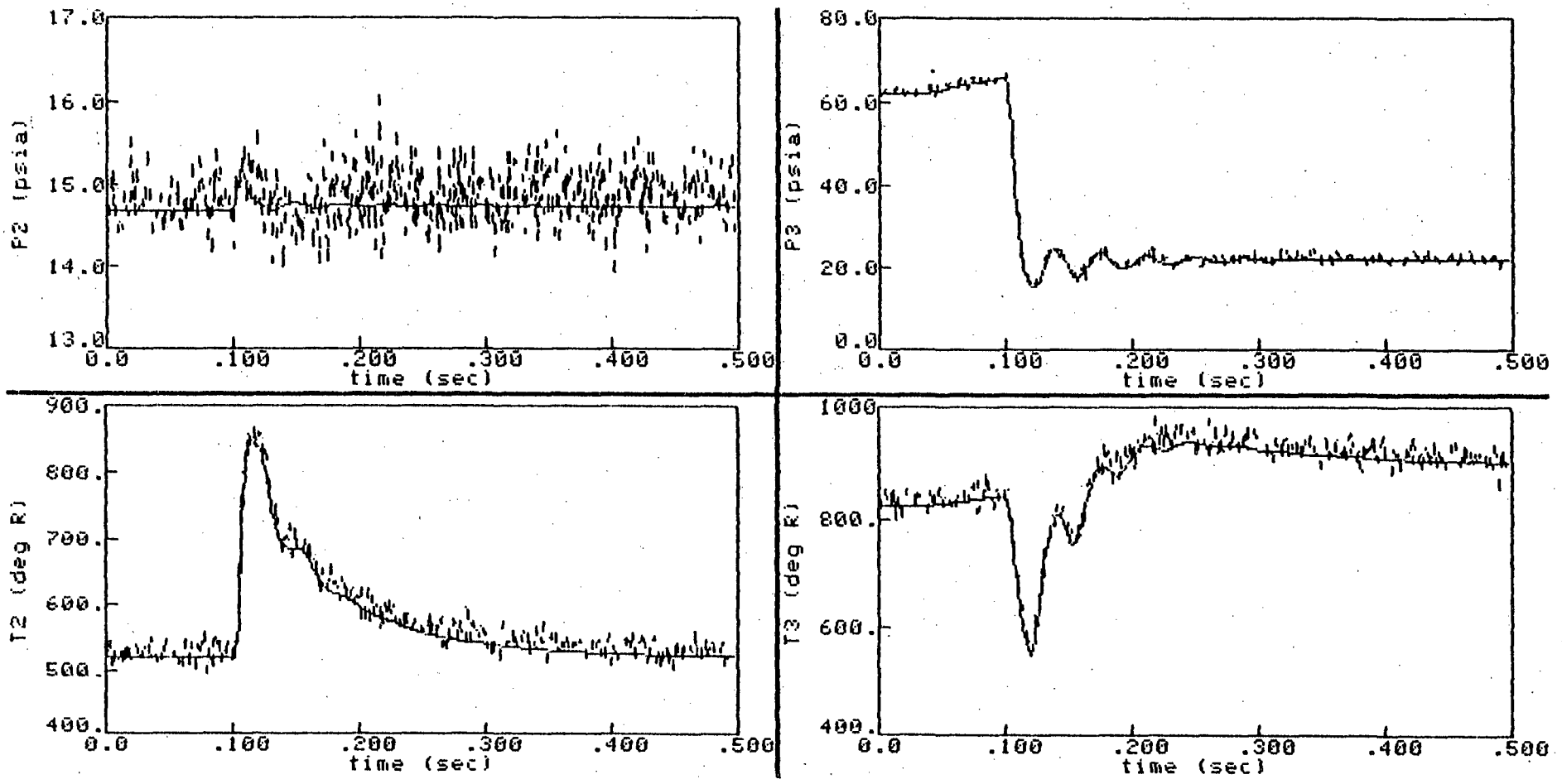

Figure 4.26 Run 5 Identification
(SCT, solid line; NASA, dashed line)

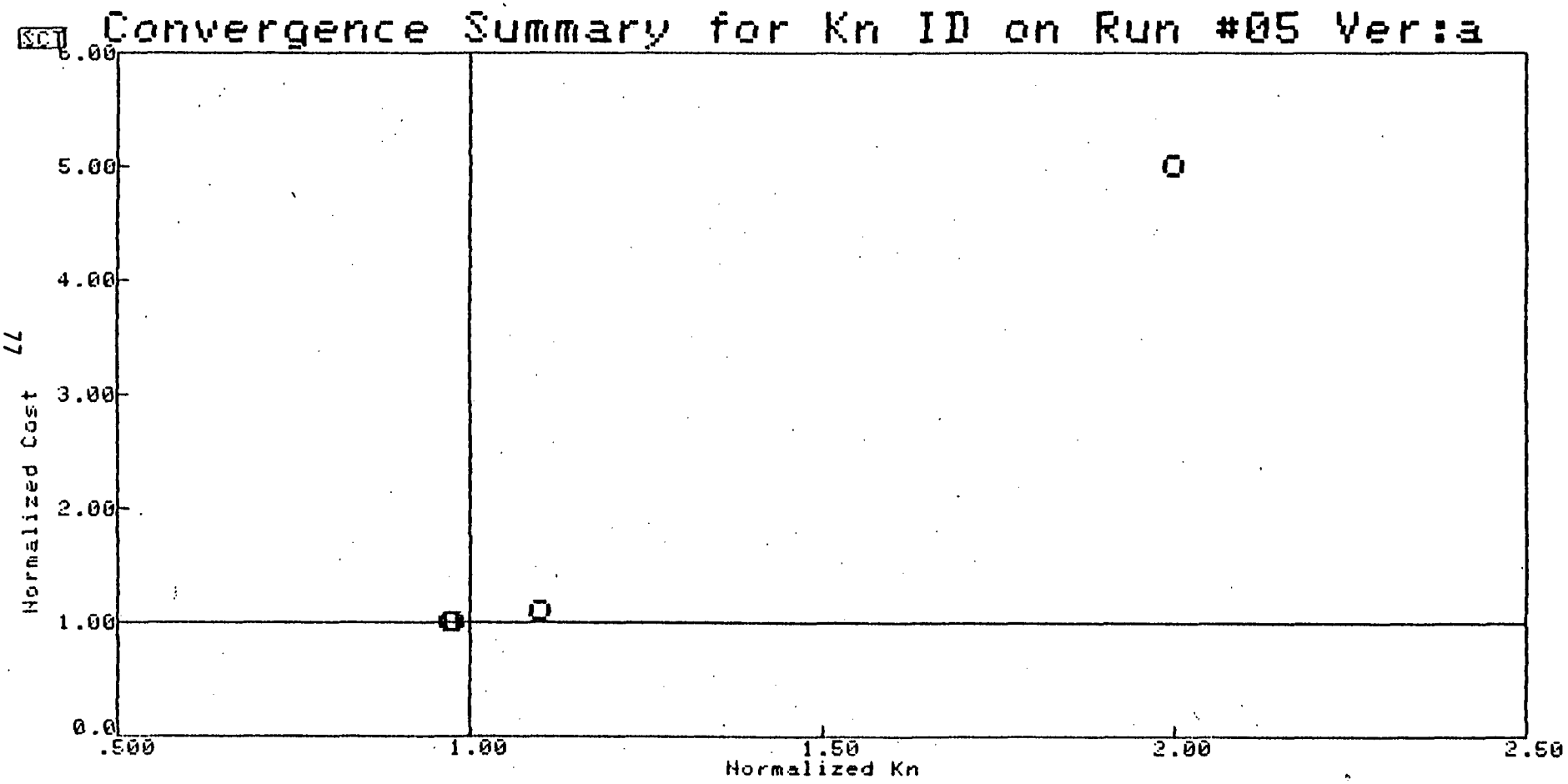

Figure 4.27 Run 5 Kn Convergence (1 kHz data)

search for more-likely parameter values when the parameter step size drops below a low threshold value specified by the user, in this case, 0.001 percent.)

To this point, even though SCIDNT has identified Kn, there still are model-data (W2dot) errors remaining. These errors are too small to be seen in Figure 4.27, but they are present. The errors are due to the incorrect Kp value being used in the model and possibly due to an incorrectly identified (or biased) estimate of Kn. They can be seen more clearly in Figure 4.28. In this figure, the scale of normalized cost (W2dot) is much narrower than in the Kn figure, simply because the errors due to incorrect Kp are quite small in comparison to errors due to Kn.

This difference in error magnitudes is significant. Because the normalized errors due to Kp are so small, the normalized gradient and information matrix (a scalar in this case) are also small. This means that there are precison problems in determining a parameter step size for Kp (see Eq. (3.13)). There was no such problem with Kn, because its gradient is steeper and the information matrix is thus better conditioned. But this is not the case with Kp. The difficulty with Kp was alleviated to some extent in the turbofan study by switching to a double-precision algorithm.

Note that the final solution, indicated by the vertical line, is not the lowest cost. This is because the plotted cost is only the W2dot RMS error. The actual cost used by SCIDNT is a weighted sum of all RMS errors and may therefore be slightly different. It is apparent in this example that the W2dot error gives a better indication of cost, suggesting that a weighting system other than what is currently used may increase accuracy.

The run 5 identification showed improvement when the amount of information was increased. The same identifications for Run 5 were repeated using a 5-kHz signal instead of a 1-kHz signal. As expected, the identification improved significantly. The new results are shown in Table 4.6 and in Figures 4.29 and 4.30.

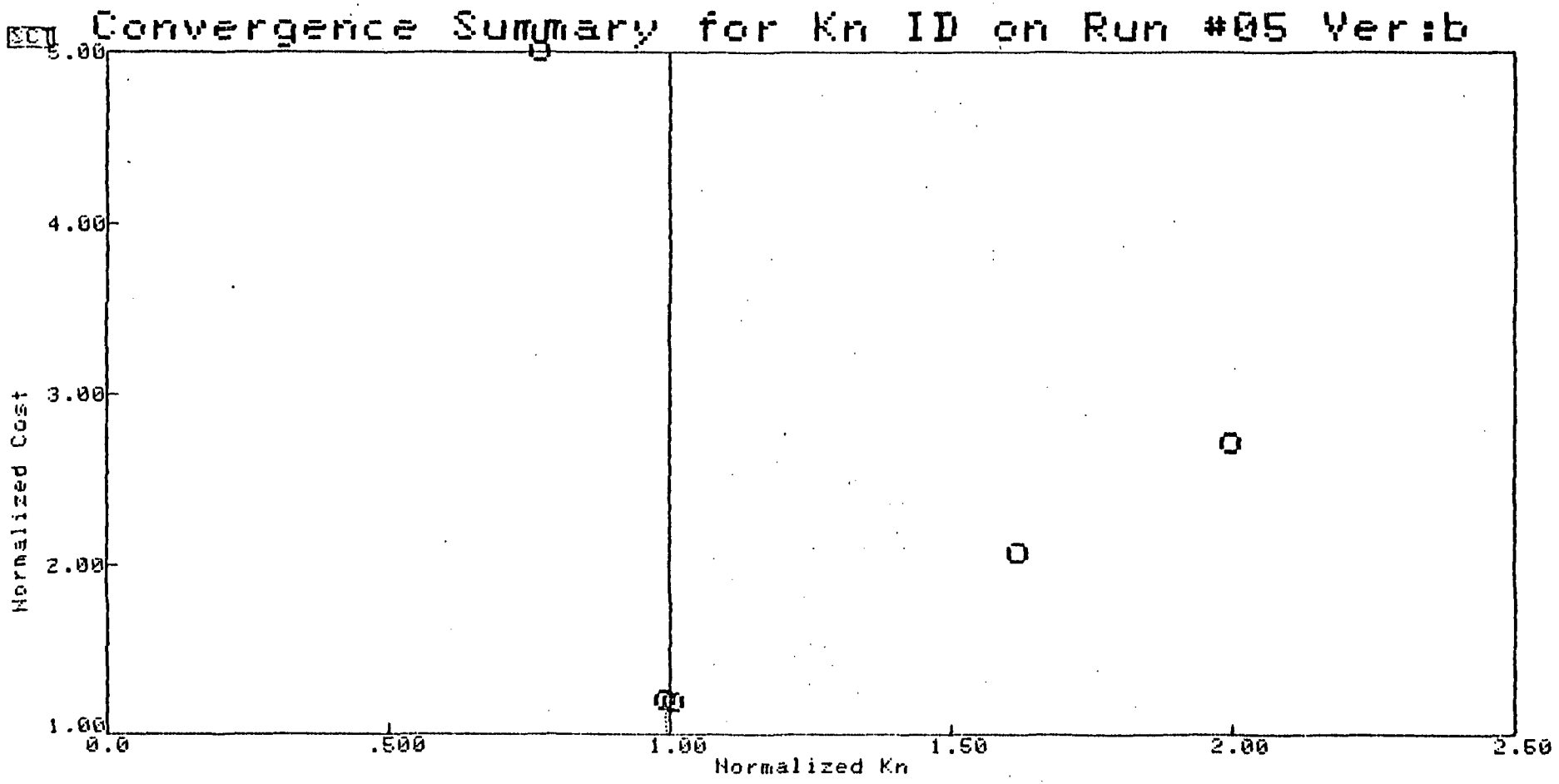

Figure 4.28 Run 5 K_p Convergence (1 kHz data)

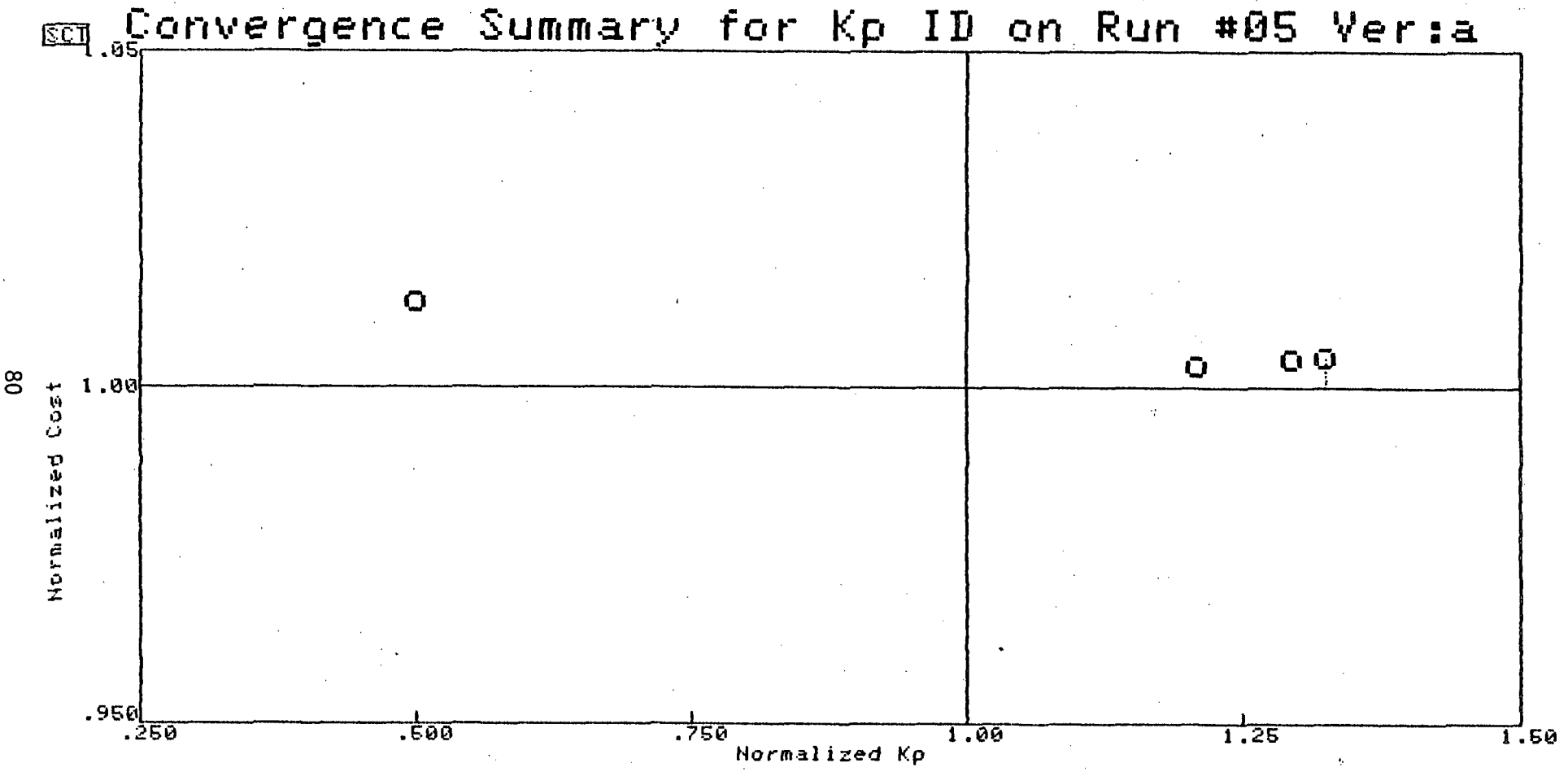

Figure 4.29 Run 5 Kn Convergence (5 kHz data)

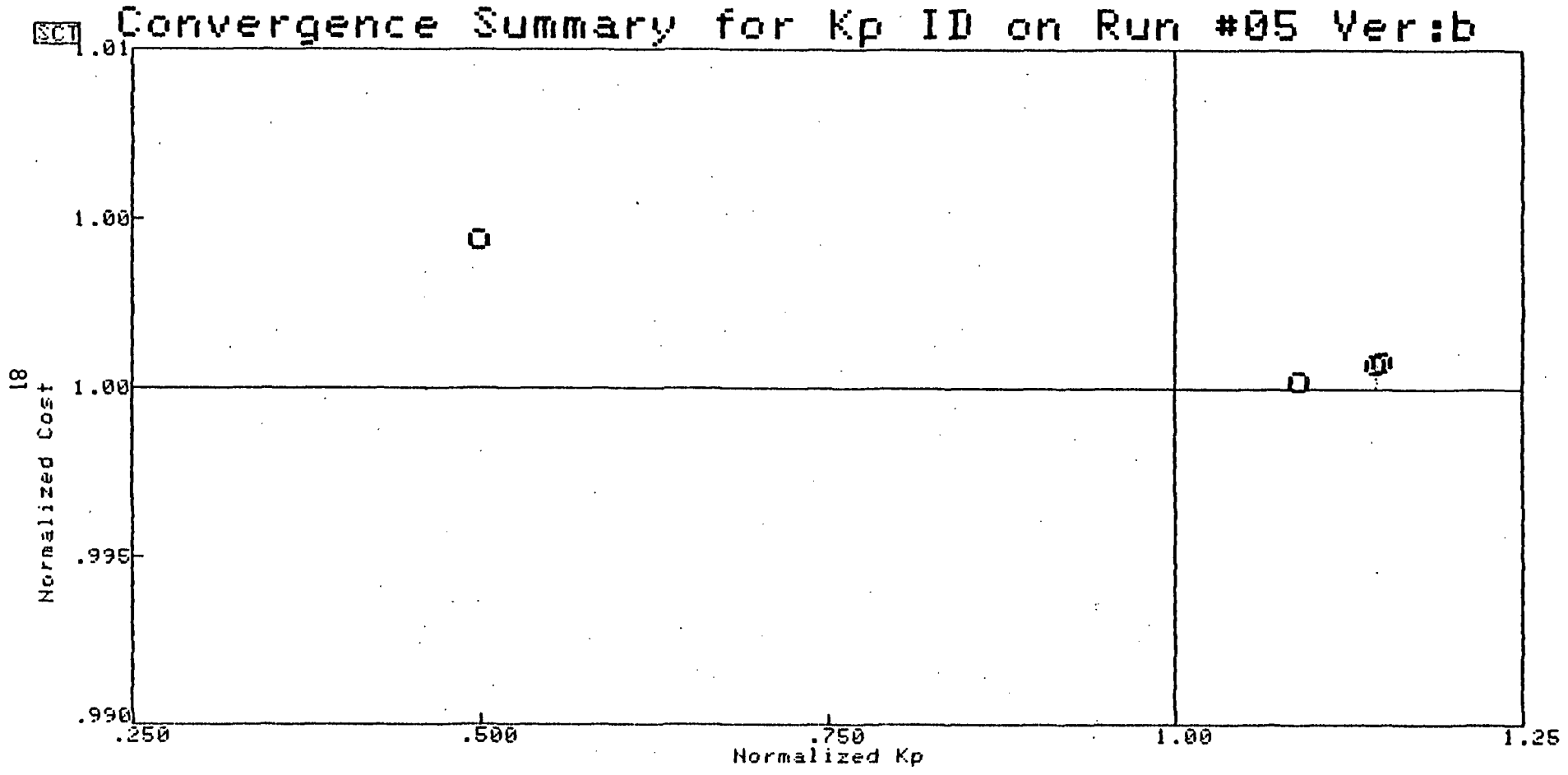

Figure 4.30 Run 5 K_p Convergence (5 kHz data)

Table 4.6
K-Parameter Identification for Run 5

Run	Initial Kn	Final Knf	Actual Kn	Initial Kp	Final Kp	Actual Kp	Comments
n05b	16.0	7.94	8.00	0.05		0.10	5 kHz
p05b		7.94	8.00	0.05	0.115	0.10	5 kHz

Run 5 Observations: Kp typically has a small effect on model response, and as a result has poorly conditioned information matrices resulting in poor convergence. Increasing precision should aid the situation, increasing the sampling frequency surely does.

4.6.1.2 Run 7 (Figures 4.31 and 4.32)

Run 7 parameters are similar to those of Run 5 except that a Kp was chosen to produce a recoverable stall. Kn and AT were identified successfully as shown in Tables 4.3 and 4.7; difficulties arose when Kp was identified. The difficulty with Kp was due to the amount of time spent in positive stalled flow. Because the stall is recoverable, the compressor spends approximately 15 milliseconds in positive flow, about 4 percent that of the non-recoverable Run 5. When this is coupled with the fact that the Kp gradient is very small, the indication is that there is not enough Kp information for identification.

This conclusion is illustrated in Figure 4.33. Two Kp identifications were attempted; one at 4 times actual value and one at twice the actual values. Both identifications failed to converge satisfactorily, mainly because the gradients were just too small, as demonstrated by the small scale of the cost function in the figure.

The experiences of Run 5 lead to two approaches to attempt to solve this problem: (1) a double-precision algorithm to improve the parameter step size calculation and (2) use of a 5-kHz signal or additional versions of the same run to add more information and help reject signal noise. This second (5-kHz) approach was used in Run 5 and was also used in Run 7. The 5-kHz results show limited improvement (see Figure 4.34).

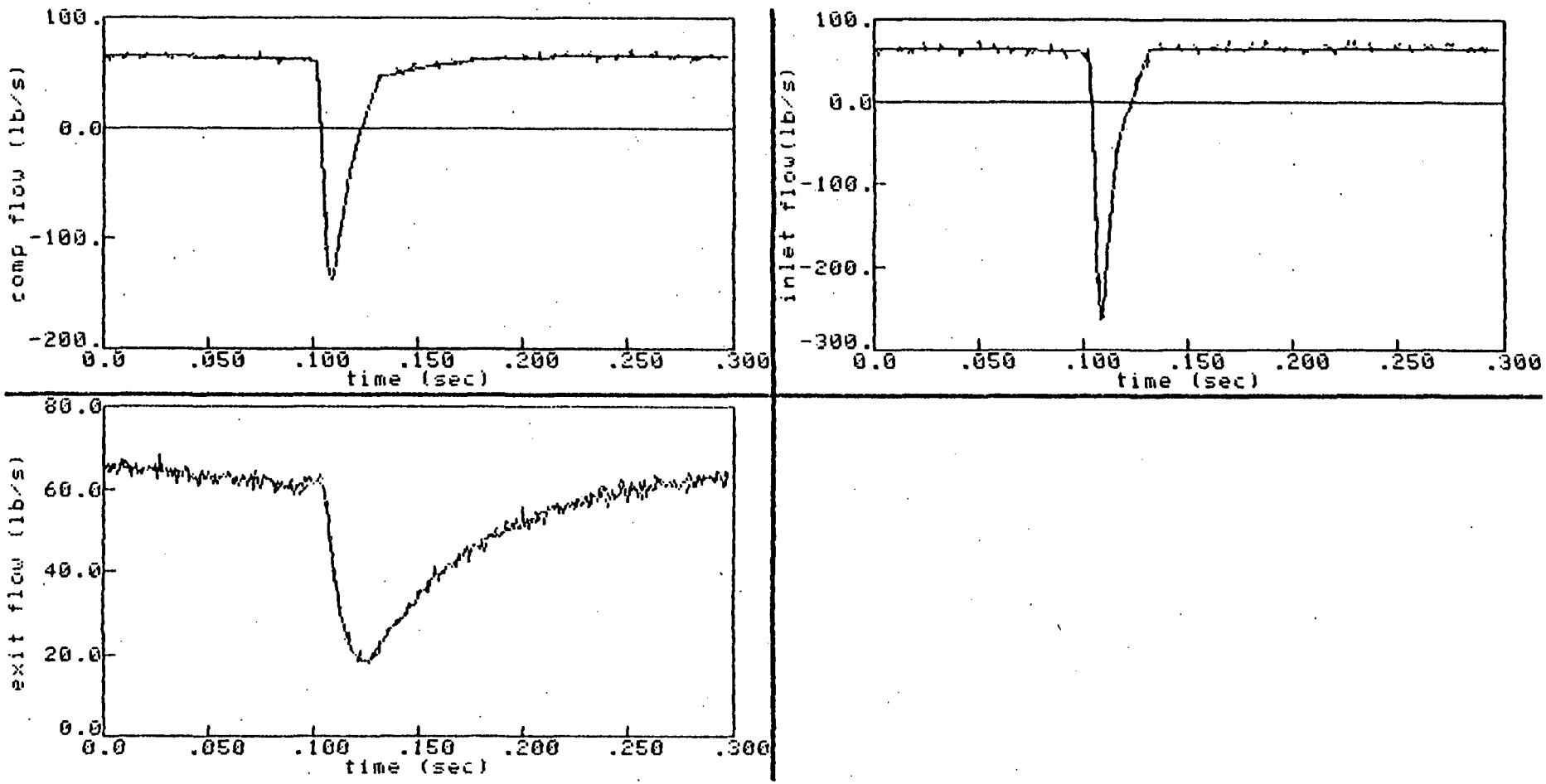

Figure 4.31 Run 7 Identification
(SCT, solid line; NASA, dashed line)

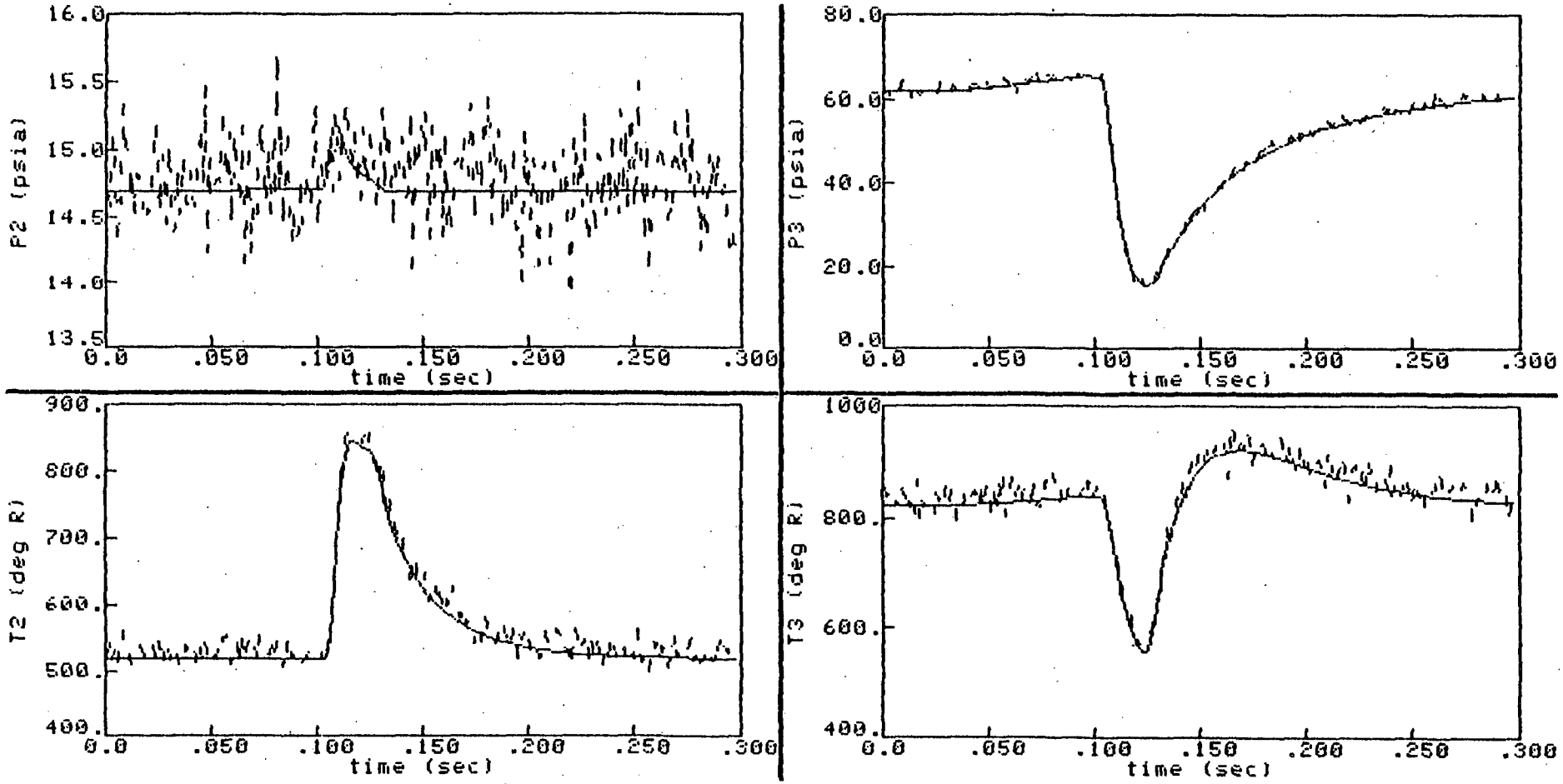

Figure4.32 Run 7 Identification
(SCT, solid line; NASA, dashed line)

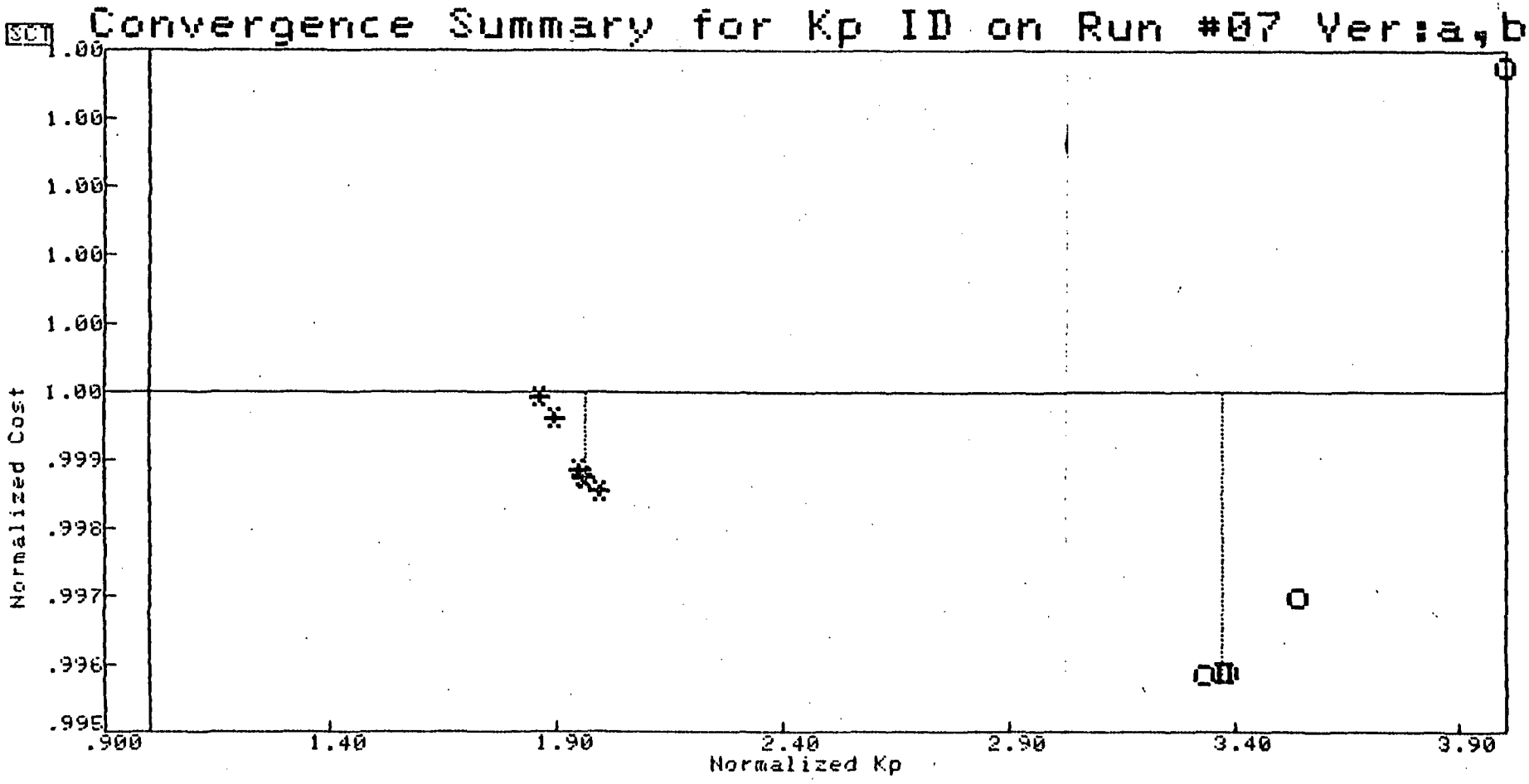

Figure 4.33 Run 7 k_p Convergence for cases a = o and b = *

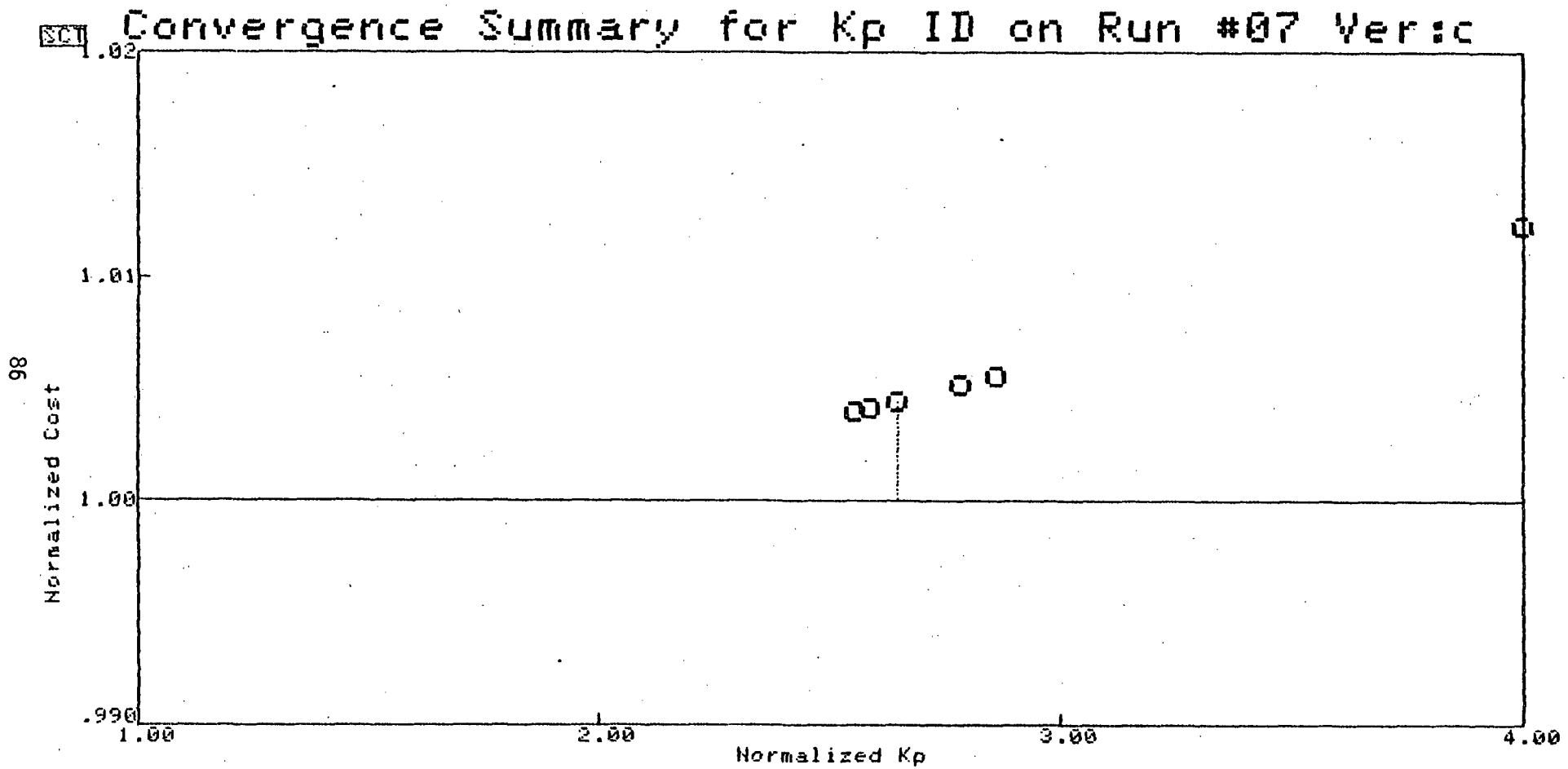

Figure 4.34 Run 7 k_p Convergence (5 kHz data)

Table 4.7
K-Parameter Identification for Run 7

Run	Initial Kn	Final Knf	Actual Kn	Initial Kp	Final Kp	Actual Kp	Comments
n07a	4.0	8.22	8.00	2.00		0.50	
p07a		8.22	8.00	2.00	1.688	0.50	min at 1.7
p07b		8.22	8.00	1.00	.9833	0.50	
p07c		8.22	8.00	2.00	1.321	0.50	5 kHz

4.6.1.3 Run 9 (Figures 4.35 and 4.36)

Run 9 is a non-recoverable stall with light damping exhibited in the positive stalled flow oscillations. Two Kn identifications were made for Run 9 in order to test qualitatively the effects of Kp errors on Kn. The first identification was obtained using an initial Kp value that made the identification model recover even though the data indicated a non-recoverable stall. The results of this identification showed moderate success, with Kn approaching 34 percent of actual value. The use of this Kp guess produced stall characteristics significantly different from those of the data and served to test the previous sensitivity and physical analysis results which indicated Kp values should have minimal impact upon Kn identifications (see Section 4.5.2.2).

This theory was verified by the second Kn identification which used a Kp that produced a non-recoverable stall effect (model and data agree.) The results of this second case were nearly identical to the first and supported the no-effect theory. This is an important result, because it indicates that Kn can be identified regardless of the value of Kp. Kp could be grossly misguessed and still not affect the identification of Kn.

After Kn was identified, Kp was identified with the new Kn as the best-guess value. The convergence was significantly improved over those of the two previous cases (see Figure 4.37). Again, the reason seems to lie with information content. Because the run is a lightly damped non-recoverable stall, the model spends a large amount of time in positive flow and also

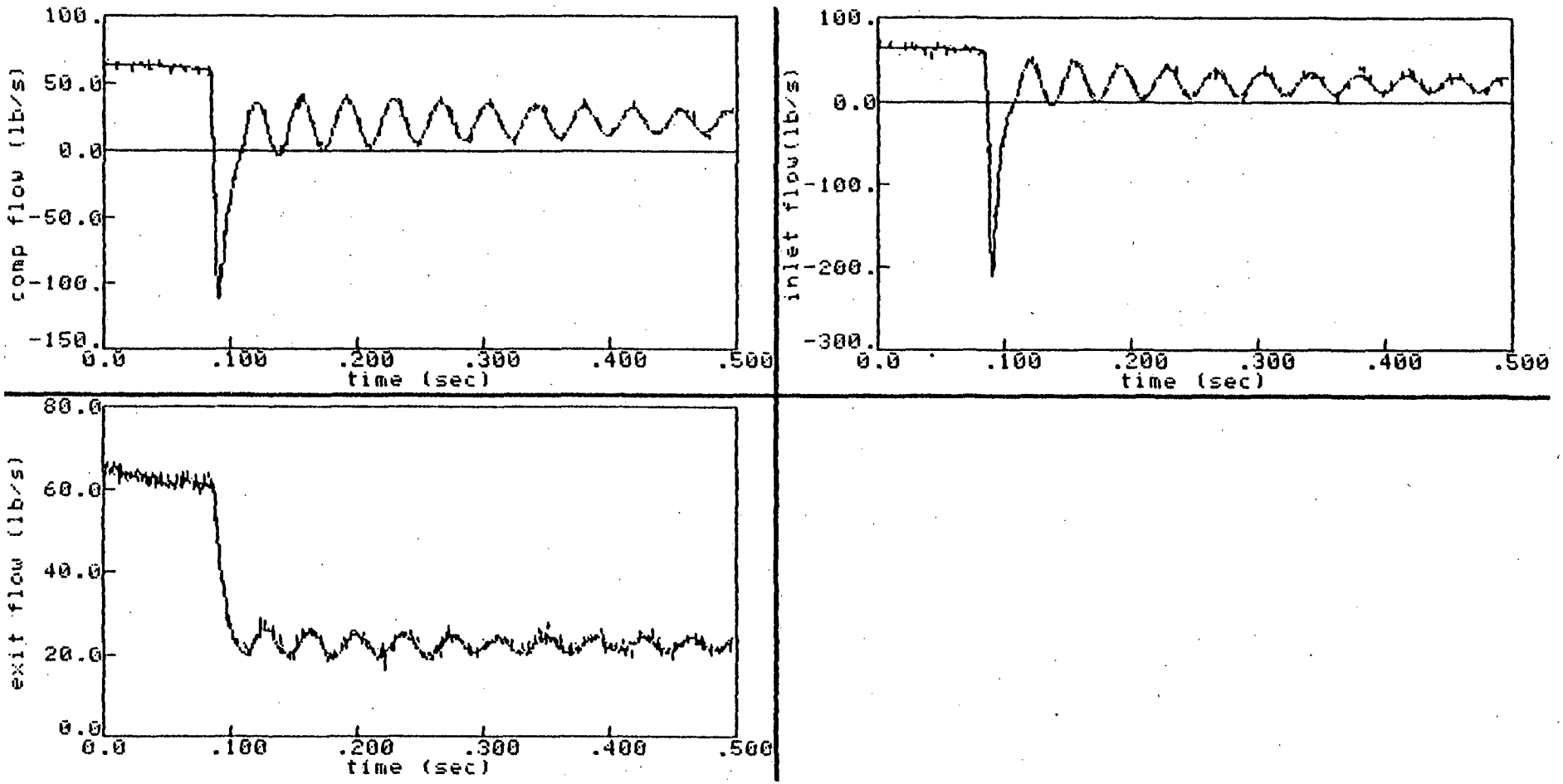

Figure 4.35 Run 9 Identification
(SCT, solid line; NASA, dashed line)

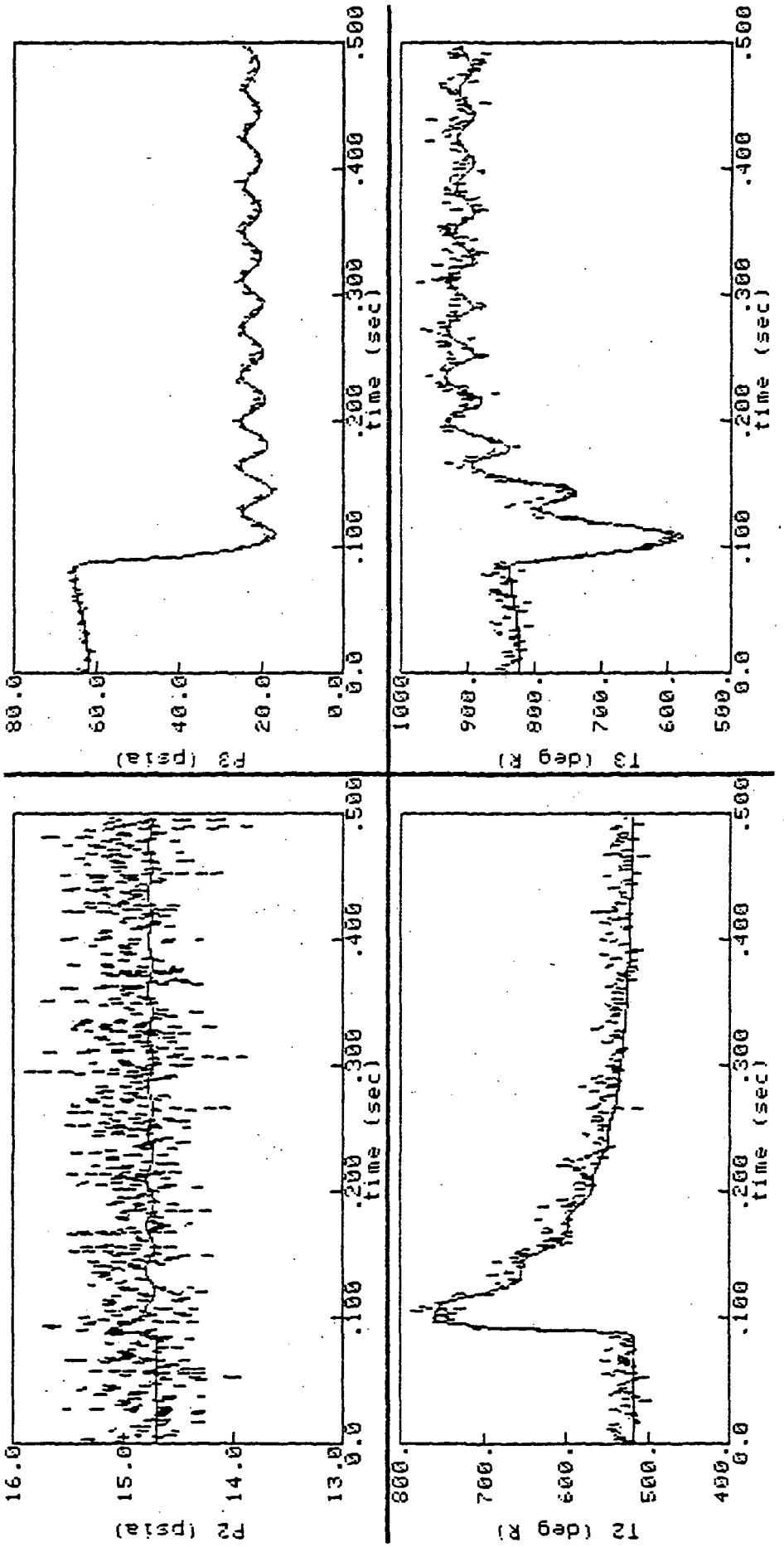

Figure 4.36 Run 9 Identification
(SCT, solid line; NASA, dashed line)

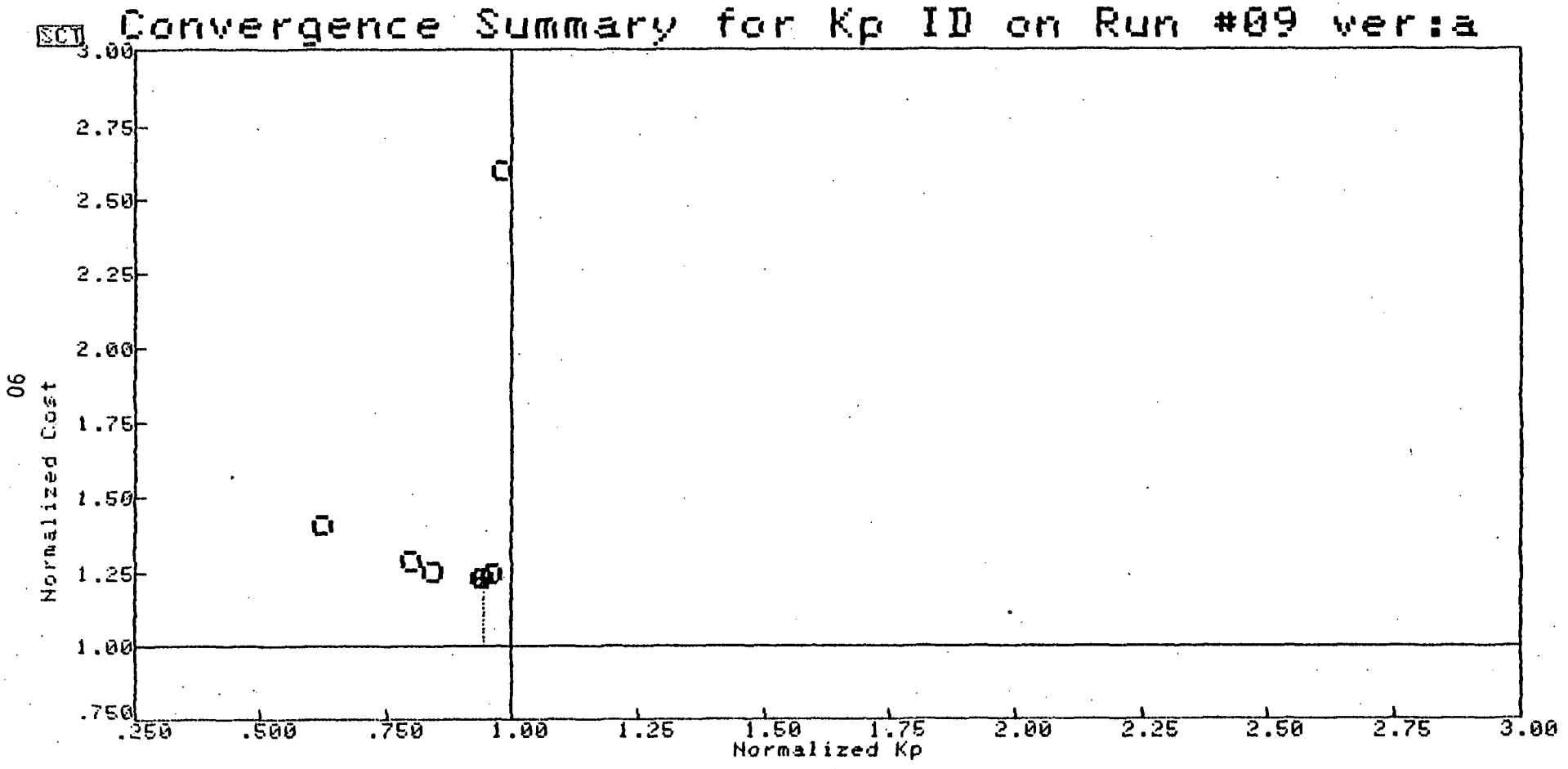

Figure 4.37 Run 9 K_p Convergence

provides a large amount of unique information. More data points on the stalled compressor map are provided which contribute to improved identification. Note the gradients are much larger than those from runs 5 and 7. Also note that the lowest cost is not at the actual value, but is slightly less. The maximum likelihood value of Kp has been biased by the biased Kn.

Run 9 Observations: Kn is oblivious to initial Kp values. Manuevers with a great deal of movement increase identification ability. Kp is biased by inaccurate Kn values.

Table 4.8
K-Parameter Identification for Run 9

Run	Initial Kn	Final Knf	Actual Kn	Initial Kp	Final Kp	Actual Kp	Comments
n09a	14.0	17.9	20.0	1.50		0.80	(recover/stall)
n09b	14.0	17.9	20.0	0.50		0.80	(stall/stall)
p09a		17.9	20.0	0.50	0.755	0.80	

4.6.1.4 Run 10 (Figures 4.38 and 4.39)

Run 10 is a stall that cycles 5 times before recovery. The Run 10 results support the information identifiability relationship and provide experience with marginally recoverable stalls.

Two identifications were made for Kn. The first identification used the entire 0.5 seconds of data in determining the gradient relationship between measurement errors and the Kn parameter. The second run used only 0.2 seconds of data. A hypothesis was being tested that said that the excess information in case a, which contains no negative stalled flow information, would only increase gradient uncertainty. Therefore, if less extraneous information were used, the gradient would be more accurate and the convergence properties would improve. That is indeed what happened (see Table 4.9).

A similar test was preformed for the identification of Kp. All 0.5 seconds were used in the first Kp identification while only the first 0.26

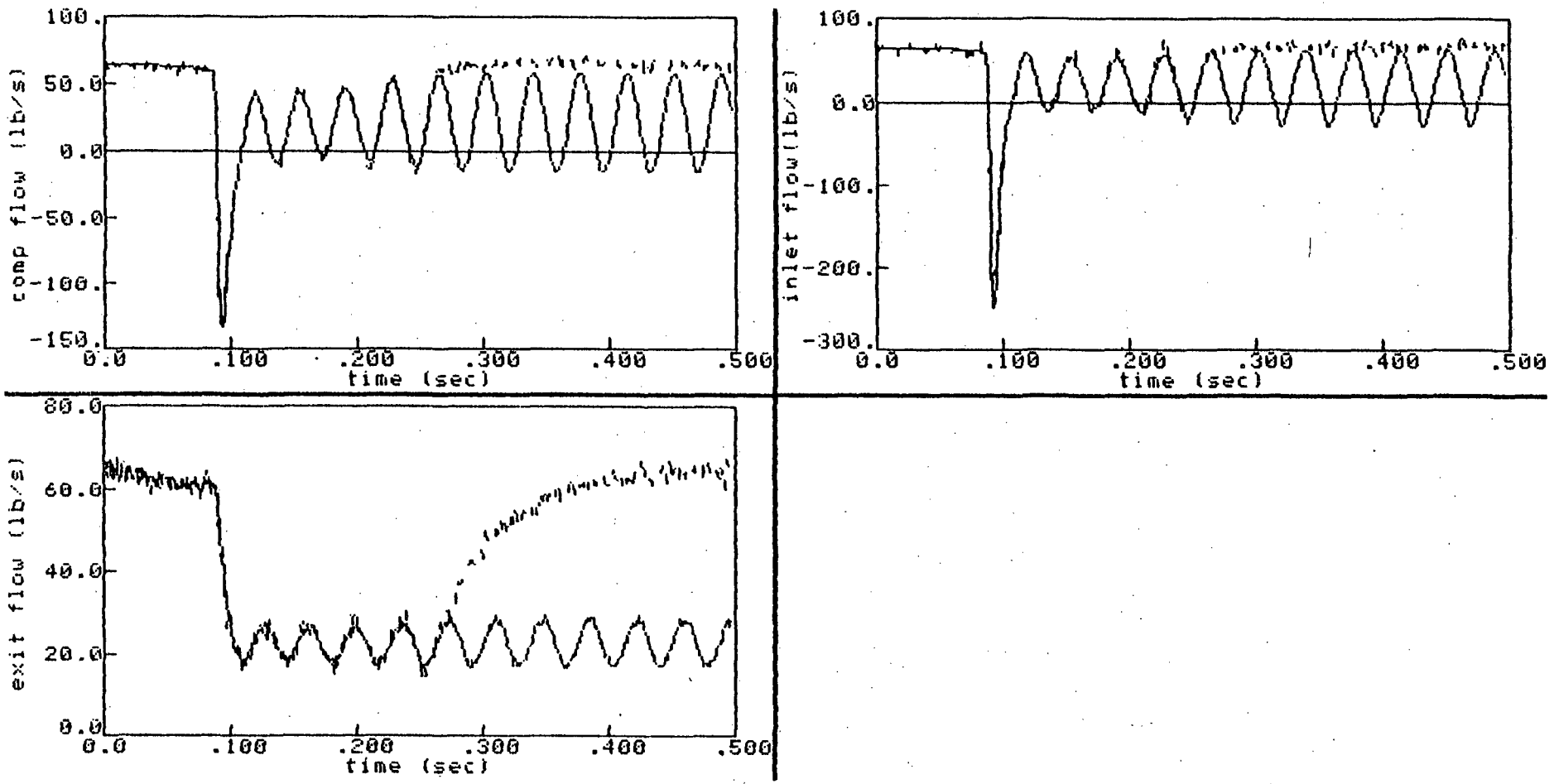

Figure 4.38 Run 10 Identification
(SCT, solid line; NASA, dashed line)

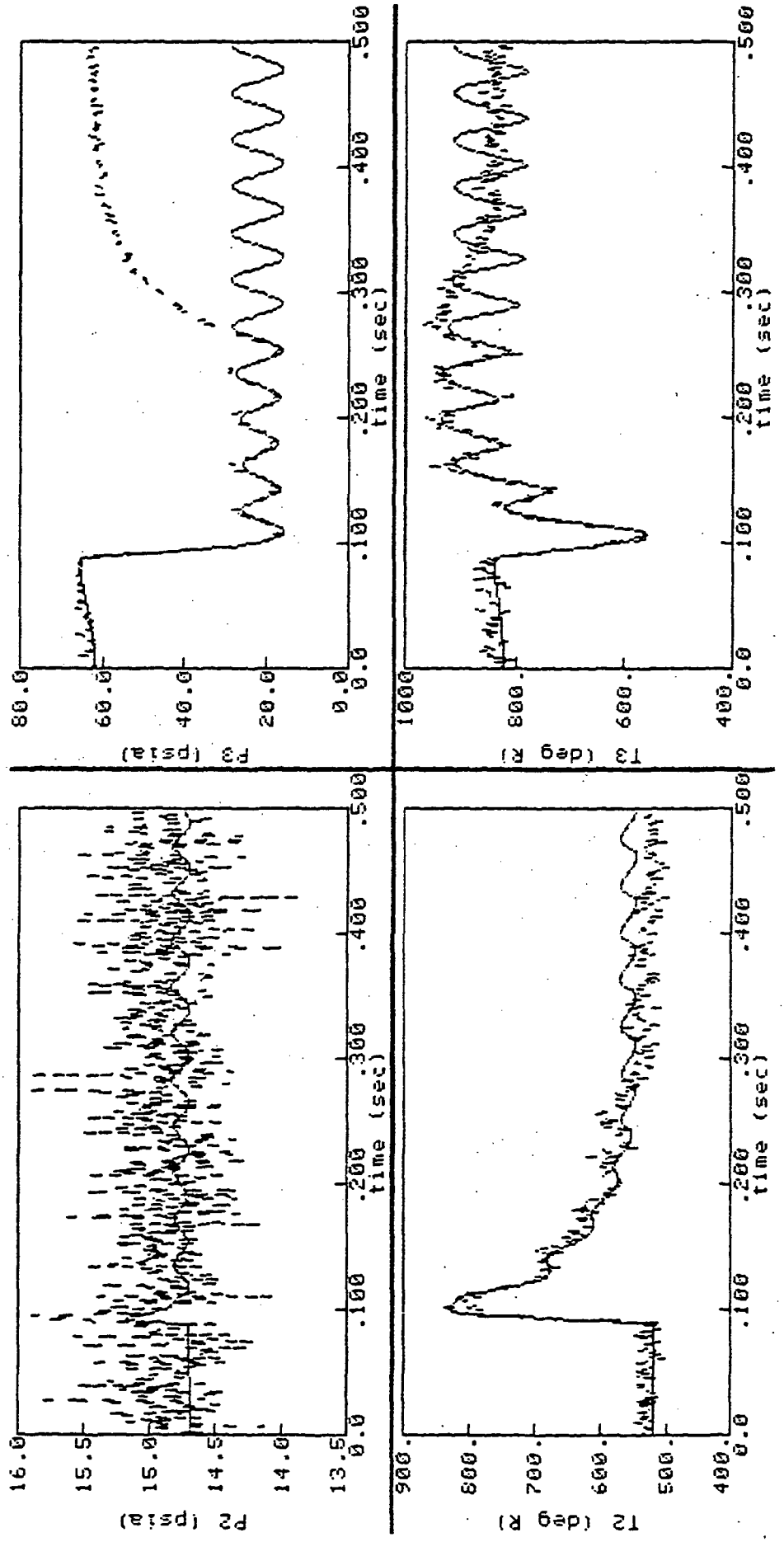

Figure 4.39 Run 10 Identification
(SCT, solid line; NASA, dashed line)

seconds in the second identification. (0.26 seconds is the time it takes the compressor to recover.) The results of these two identifications were inconclusive. The second Kp identified was further away from actual than the first, but there several outside factors could be influencing the second's convergence: 1) the Kp values may be biased by the identified Kn, 2) the 0.26 seconds of data does not contain all of the Kp information available. Examination of the exit flow and P3 responses in Figures 4.38 and 4.39 reveals that there is still unstalled initial condition information in the signals after recovery. The results of this Kp test were inconclusive.

The Kp identification provided an excellent opportunity to test identification of parameters that are around a nonrecoverable/ recoverable boundary. At this boundary (Figure 4.40), slight Kp changes around the nominal value can drastically change the character of the compressor response. For example, if the actual Kp value used in generating the data were changed 10 percent, the response would change to a non-recoverable stall or a single cycle recoverable stall. This presents a difficulty to SCIDNT because Kp gradients around this Kp boundary are likely to be rather erratic.

In run 10, both identified Kp's were within 20 percent of the actual value, but both produced nonrecoverable stalls in the model response. Even though the data showed recovery after 5 stalled cycles, the identified model did not. Examination of the overlayed responses in Figures 4.38 and 4.39 reveals the identified model response follows the data quite well but only until the data recovers. It is likely that the Kp which would produce a 5 cycle stall for Kn= 9.32 would likely be less than 0.8 (see Figure 4.40); how much less is not known.

This all leads to the question of how to identify a better Kp, a Kp that would produce a 5-cycle stall. All of the methods mentioned so far (higher frequency signals or additional data sets) would likely help the identification, but how much cannot be predicted with the given data. Further refinement of the recovery model might create a model structure that is more amenable to identification of the parameters or values which determine recovery.

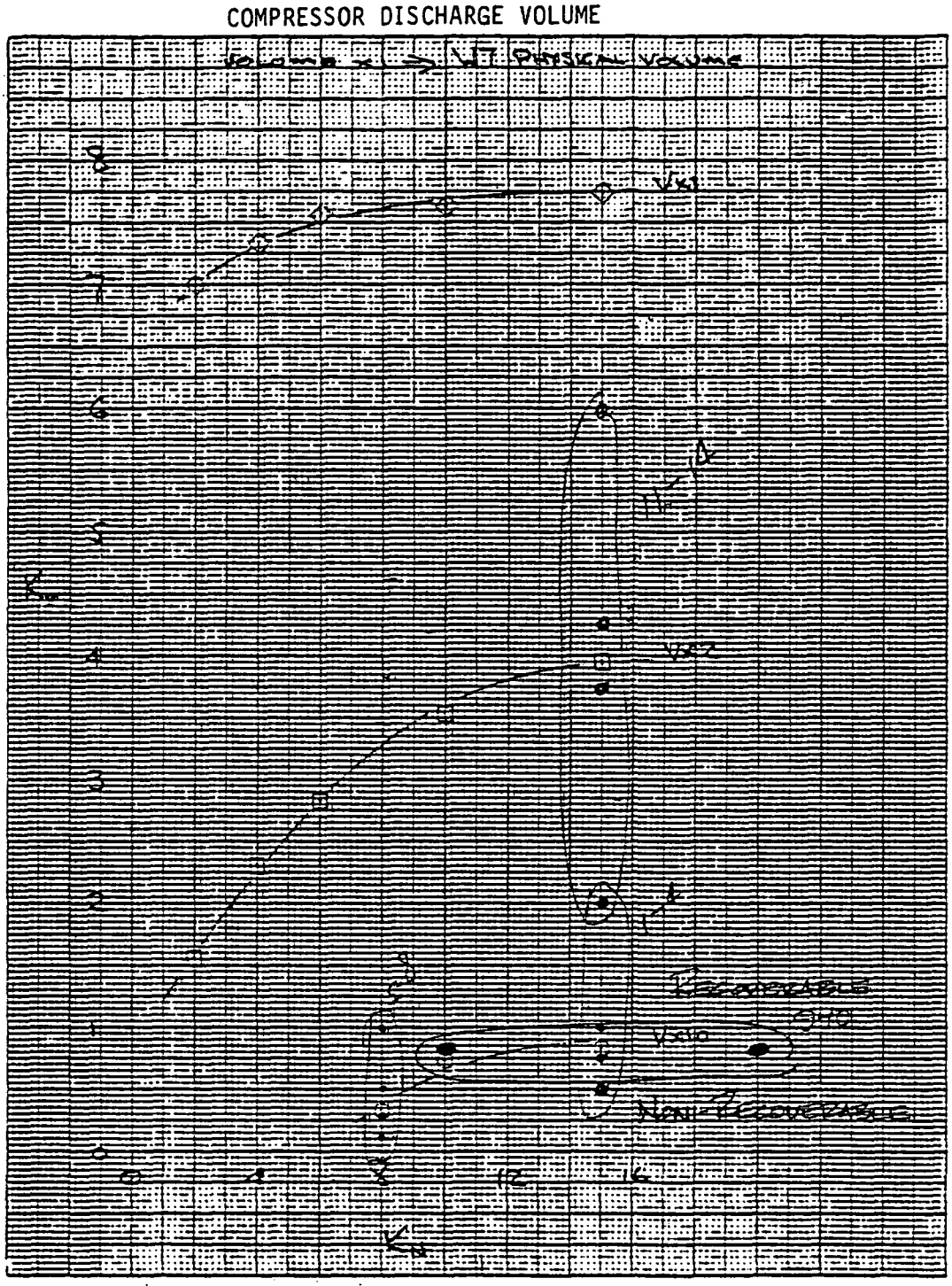

Figure 4.40 Recovery/Non-Recovery Boundary

Run 10 Observation: Use only the data that contains information pertaining to the parameter being identified.

Table 4.9
K-Parameter Identification for Run 10

Run	Initial Kn	Final Kn	Actual Kn	Initial Kp	Final Kp	Actual Kp	Comments
n10a	16.0	9.13	10.0	0.50		0.80	(stall/rec:5)
n10b	16.0	9.32	10.0	0.50		0.80	t<.2 sec
p10a		9.32	10.0	0.50	0.688	0.80	(stall/rec:5)
p10b		9.32	10.0	0.50	0.669	0.80	t<.26 sec

4.6.1.5 Run 11 (Figures 4.41 and 4.42)

Run 11 is a non-recoverable stall run with high frequency (60 Hz) stall oscillations and medium damping. The identification results were satisfactory considering the difficulties enocuntered in synchronizing the data and model.

Normally, an AT is identified, and the identified value causes data and model to synchronize, however in this case, the identified value did not produce synchronization.

AT was identified as usual with the initial (incorrect) K-parameter values. When this identification failed to produce favorable results, AT was identified again using the actual K-parameter values, but again the results were unfavorable. The problem appears to be in the initial guess of AT. The initial guess produced a negative gradient, indicating that the maximum-likelihood value is greater than the initial guess value. This is in fact true. But when SCIDNT stepped AT to a larger value, the model-data errors increased, and SCIDNT halted the identification process. It is possible that the effects of time shifts on a periodic function (such as a nonrecoverable stall) have produced a cost function with several local minima, thus causing convergence difficulties.

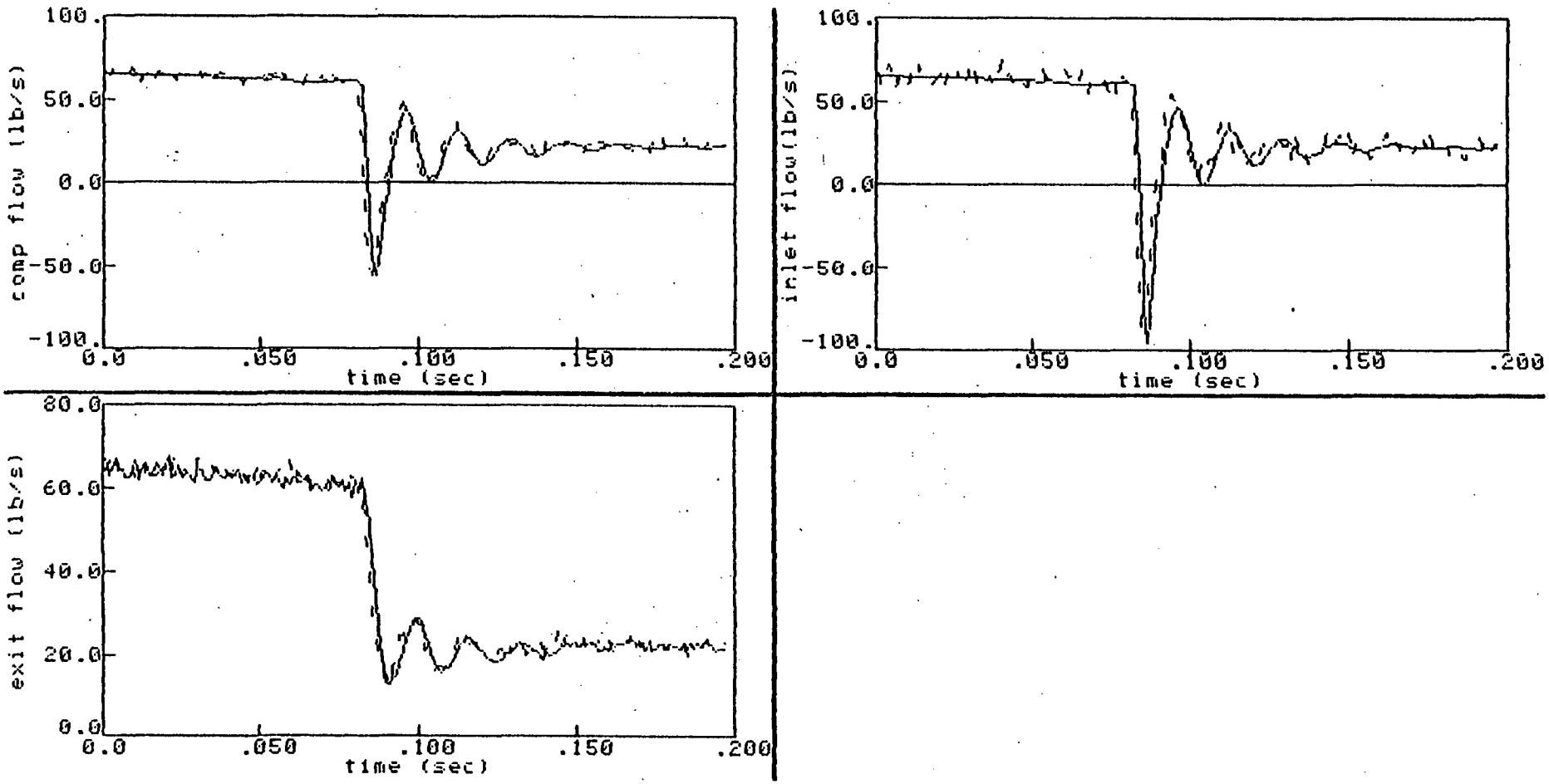

Figure4.41 Run 11 Identification
(SCT, solid line; NASA, dashed line)

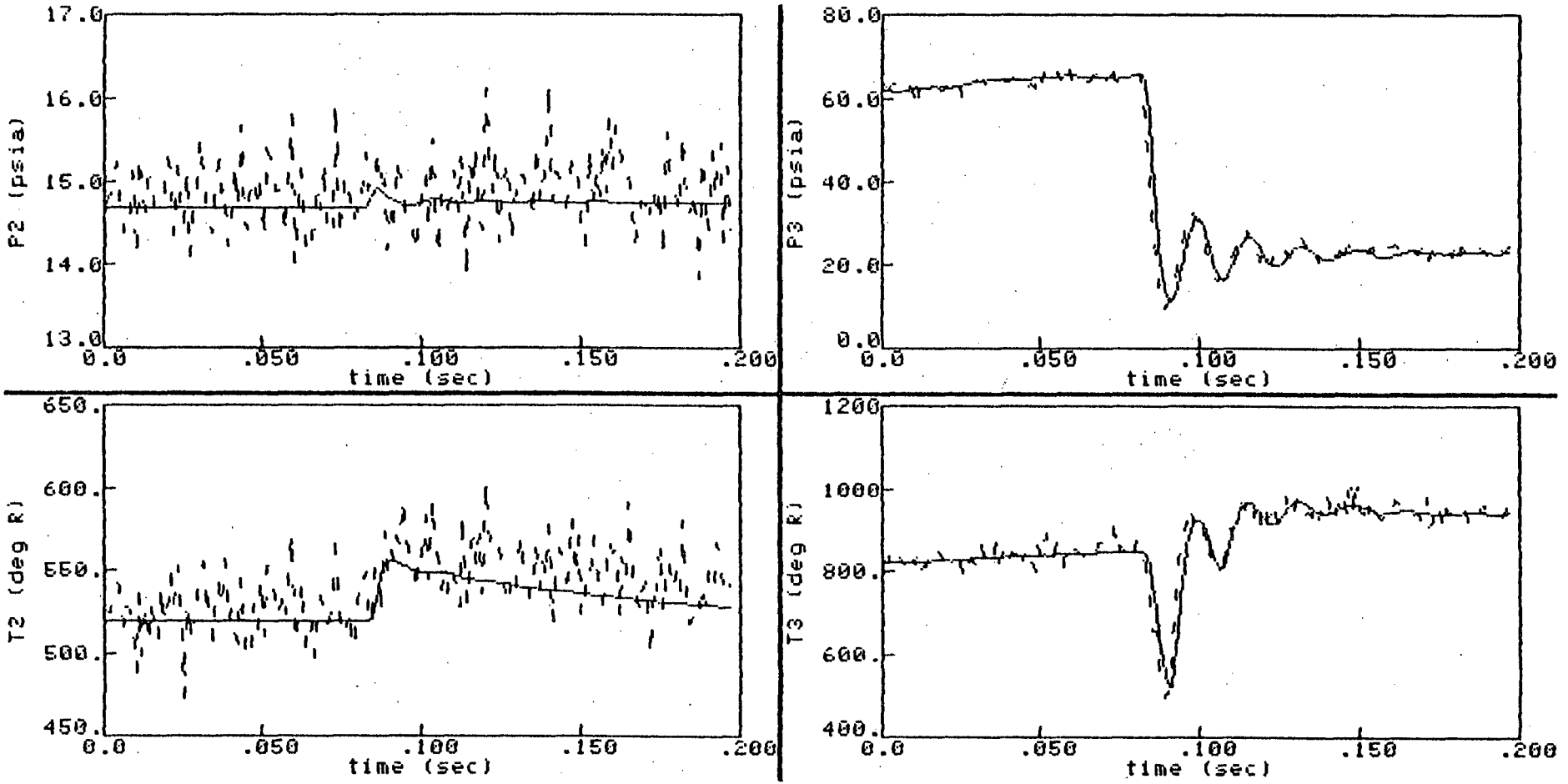

Figure 4.42 Run 11 Identification
(SCT, solid line; NASA, dashed line)

Figure 4.43 is an example plot of the RMS error resulting from two phase shifted sinusoids. Notice that at each multiple of 2π there is a local minimum. Since the stall model and data are similar to phase shifted sinusoids, it may be that the initial guess of AT puts the cost function near one of these local minima's. And since SCIDNT converges to minima, either absolute or local, the progression would stop right there.

Further analysis would be needed to ascertain if local minima is the difficulty. The "egg-crate" type pattern in Figure 4.43 is, however, a reasonable cost function pattern that must be considered when preforming identification. It should always be considered that an initial parameter guess may produce convergence into a non-absolute minima.

Kn and Kp were identified with asynchronous model plant measurements, and despite these asynchronisms, the identifications were fairly successful. Kn converged in the correct direction and stopped at 35 percent above actual value. Figure 4.41 shows that the model and data were poorly synchronized in negative stall flow, yet even under these conditions, the identification was reasonable. The success of the Kp parameter identification is even more surprising. Kp was identified within 3 percent of actual with the given asynchronism. This result is a positive indication that SCIDNT can identify reasonably well in the face of significant model-data asynchronisms although the general desire is to avoid them.

Run 11 Observation: SCIDNT demonstrates some robustness towards asynchronous model-data.

Table 4.10
K-Parameter Identification for Run 11

Run	Initial Kn	Final Kn	Actual Kn	Initial Kp	Final Kp	Actual Kp	Comments
n11a	8.0	8.001	15.0	3.00		2.00	AT is off
n11b	8.0	20.174	15.0	3.00		2.00	still off t<.2 sec
p11a		20.174	15.0	3.00	3.00	2.00	still off
p11b				3.00	2.055	2.00	do not ID AT

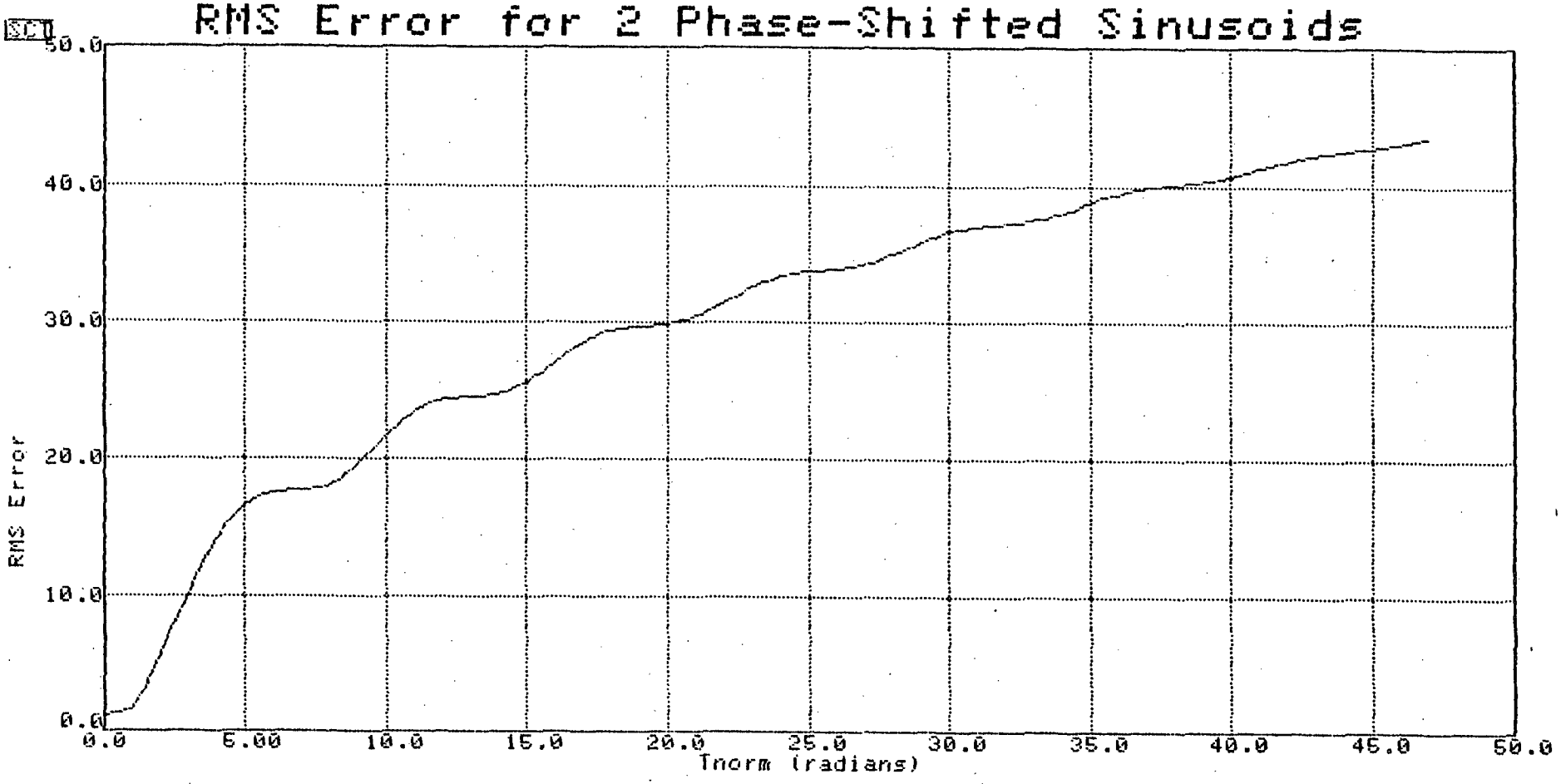

Figure 4.43 Cost Function For Phase-Shifted Sinusoids

4.6.1.6 Run 13 (Figures 4.44 and 4.45)

Run 13 is similar to Run 11 in its fast response time, except that it is a recoverable stall. The entire stall lasts for about 10 milliseconds, only 2 percent of the 500 millisecond data frame. Multiple identifications were made for the run in an effort to improve SCIDNT convergence, but final results were marginally successful.

Three identifications were made for Kn. In the first identification, a Kp value was used that caused the model to enter a non-recoverable stall. The Kn identified from this run is considerably below the actual value. To determine if Kp had induced the error, another run was made with a recovering Kp value. In this case, the identified Kn moved in the opposite direction from actual Kn. The two results are inconclusive if not perplexing. There appears to be a lack of information problem here (only 5 milliseconds of negative stall flow data is available.) Improving information content would probably improve this identification.

A final Kn run was made without identifying AT during the identification. This was done to test the hypothesis that AT was influencing the convergence of Kn. The results indicate there is some influence of AT, but not significant enough to improve the identified Kn. (It still is in the direction opposite of the actual value.)

So the Kp identification began with a rather suspect value of Kn (20.88). In the first run, an initial Kp value of 5.5 was used. SCIDNT calculated a small, albeit negative gradient for the cost of Kp, which indicated that the most-likely value was greater than 5.5. SCIDNT followed the gradient and eventually converged at a value of 5.51, indicating a local minima in the cost curve around Kp = 5.51. To investigate the situation further, a new Kp identification was made with an initial value beyond the local minima, out at 10. This time the gradient pointed towards the actual value and SCIDNT converged towards it. However, this time convergence was marked at Kp = 6.057.

Both of these Kp identifications are summarized in Figure 4.46. There is indeed a minimum in the cost curve around Kp= 6. In fact, this minima is lower than the nominal cost. The interpretation is that SCIDNT has operated

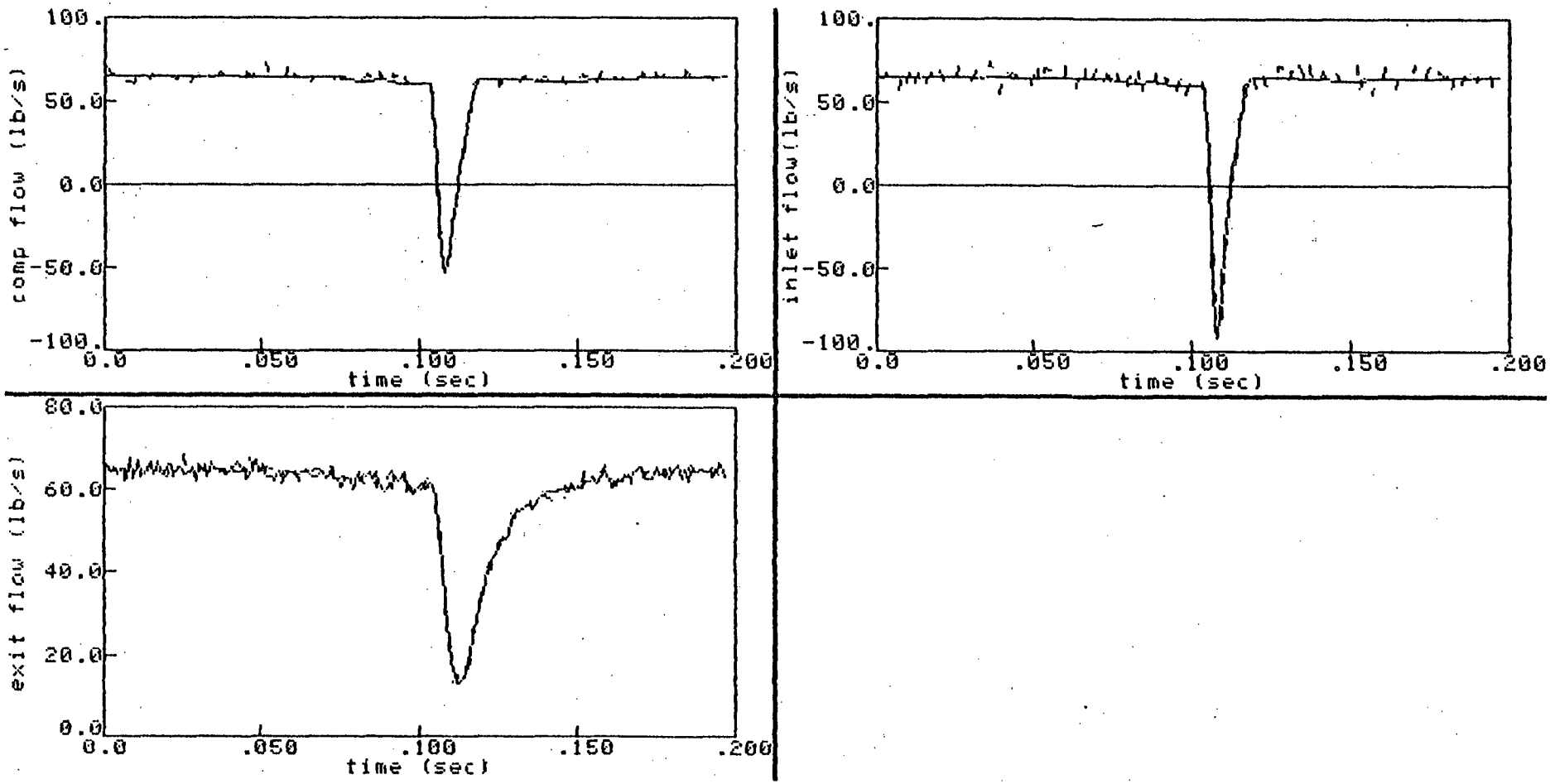

Figure 4.44 Run 13 Identification
(SCT, solid line; NASA, dashed line)

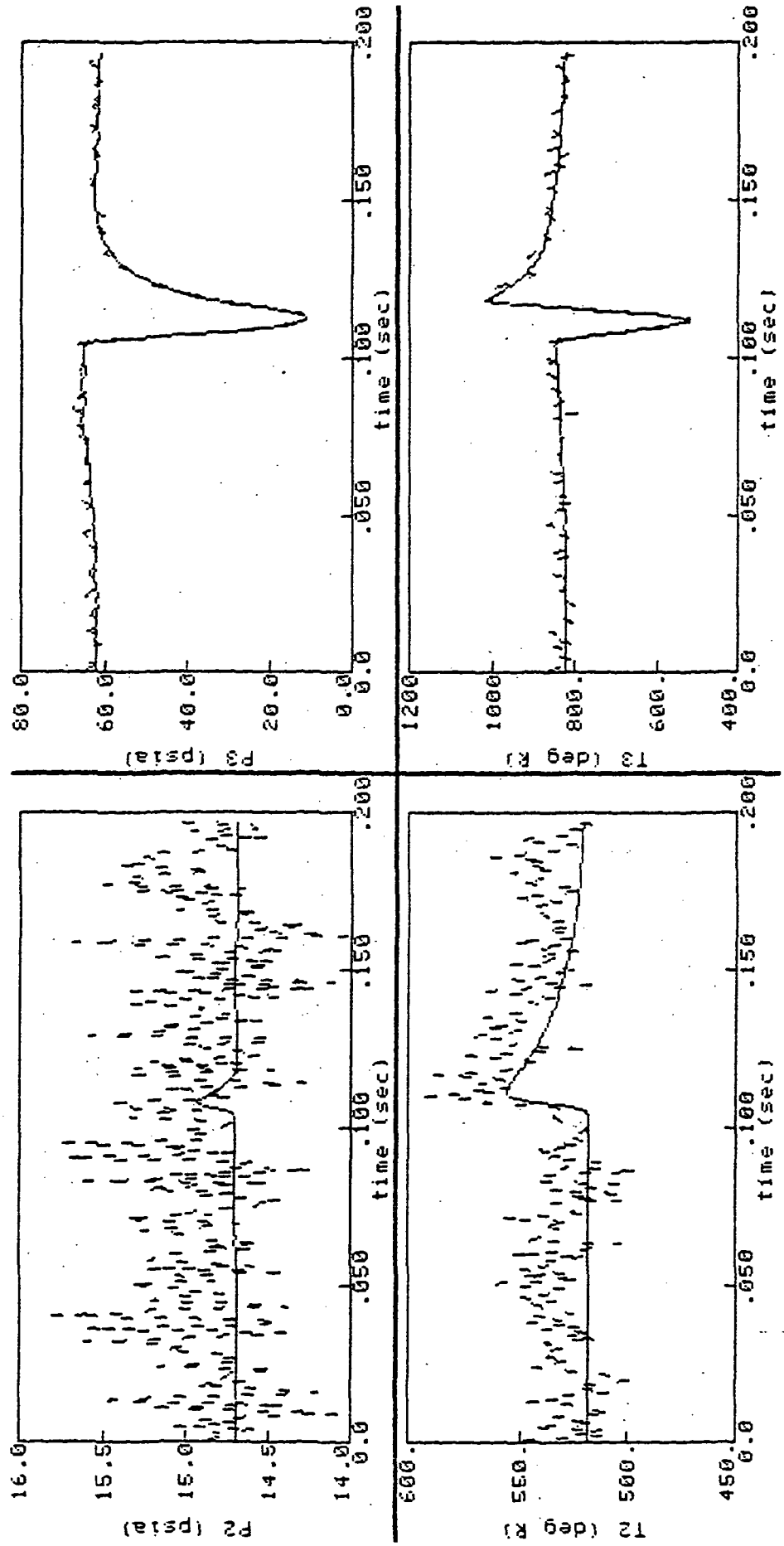

Figure 4.45 Run 13 Identification
(SCT, solid line; NASA, dashed line)

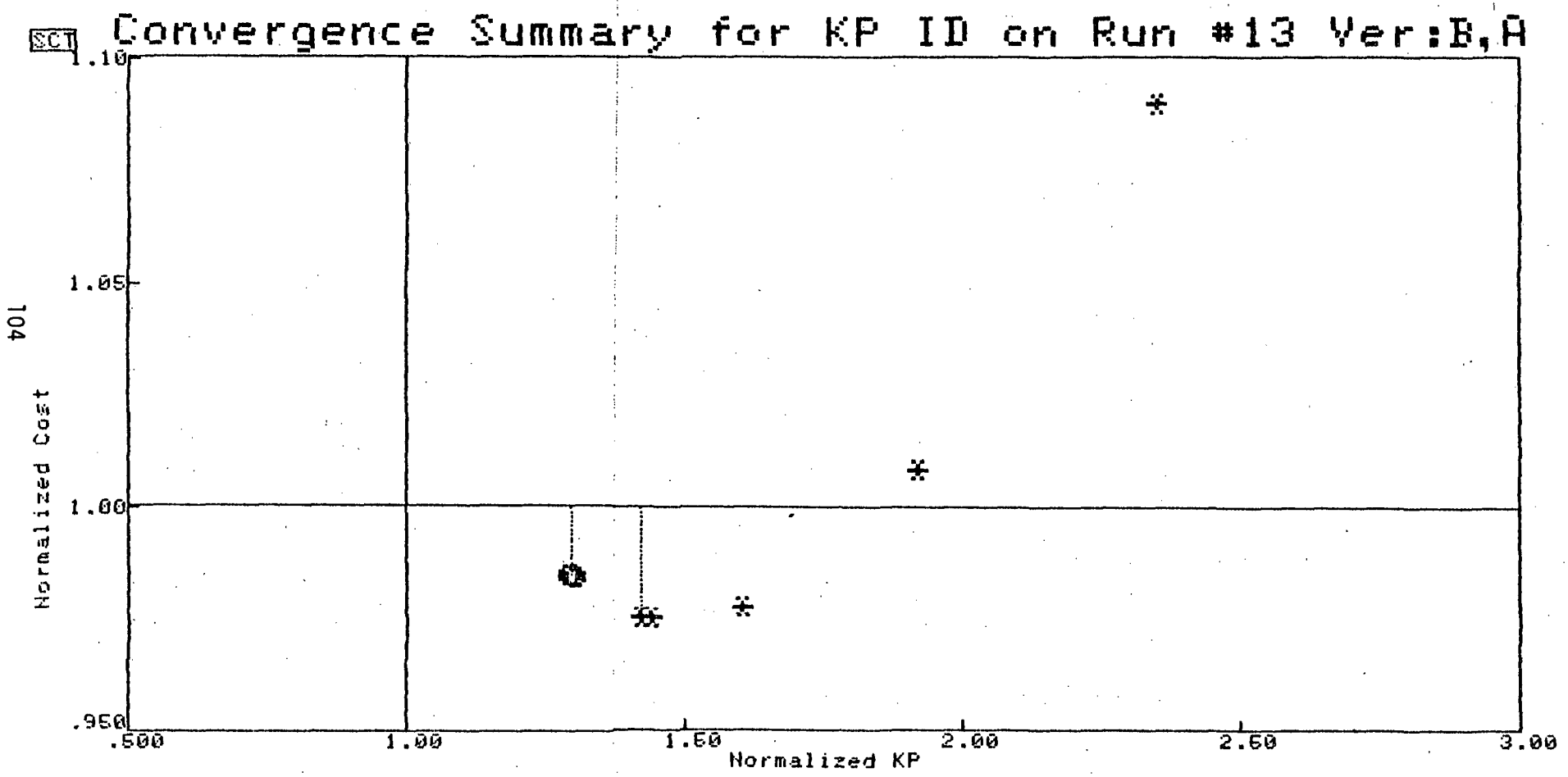

Figure 4.46Run 13 K_p Convergence cases A = o and B = *

just as expected: it found the minimum-cost parameter set. It just happens that the identified set is not the actual parameter set. The shifted local minimum is due to signal biases or aliases, or biases from the inaccurate Kn.

To see if additional information would reduce the alias or bias, a third run was made using a 5-kHz measurement signal. In this case the convergence is better and moves closer to the actual value. Not only did the increase in information improve the convergence, apparently it also reduced noise effects so that the shape of the cost curve no longer had a minima near 5.5.

Run 13 Observation: Demonstration of insufficient information effects.

Table 4.11
K-Parameter Identification for Run 13

Run	Initial Kn	Final Kn	Actual Kn	Initial Kp	Final Kp	Actual Kp	Comments
n13a	16.0	9.81	15.0	4.00		4.25	(stall/rec)
n13b	16.0	20.88	15.0	5.50		4.25	(rec/rec)
n13c	16.0	19.76	15.0	5.50		4.25	do not ID AT
p13a		20.88	15.0	5.50	5.51	4.25	gradient wrong
p13b		20.88	15.0	10.0	6.057	4.25	
p13c		20.88	15.0	5.00	4.807	4.25	5 kHz data

4.6.1.7 Run 15 (Figures 4.47 and 4.48)

Run 15 is a non-recoverable stall with medium-light damping in the stall oscillations. A standard identification procedure was followed, i.e., a Kn identification followed by a Kp identification. The indentifications were successful and no procedural revisions were required. Tabular results are shown below; graphical results are shown in Figures 4.47 and 4.48.

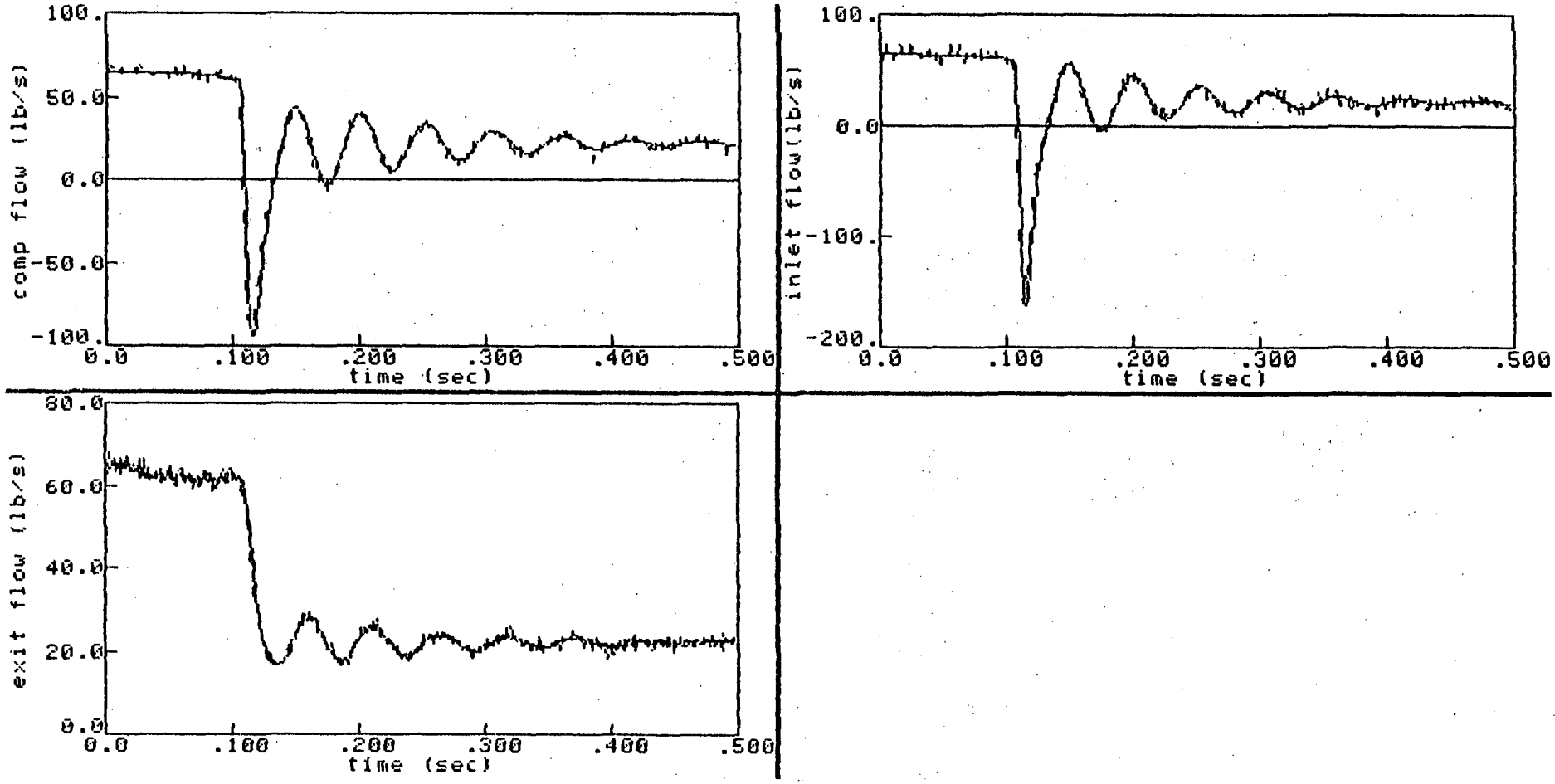

Figure 4.47 Run 15 Identification
(SCT, solid line; NASA, dashed line)

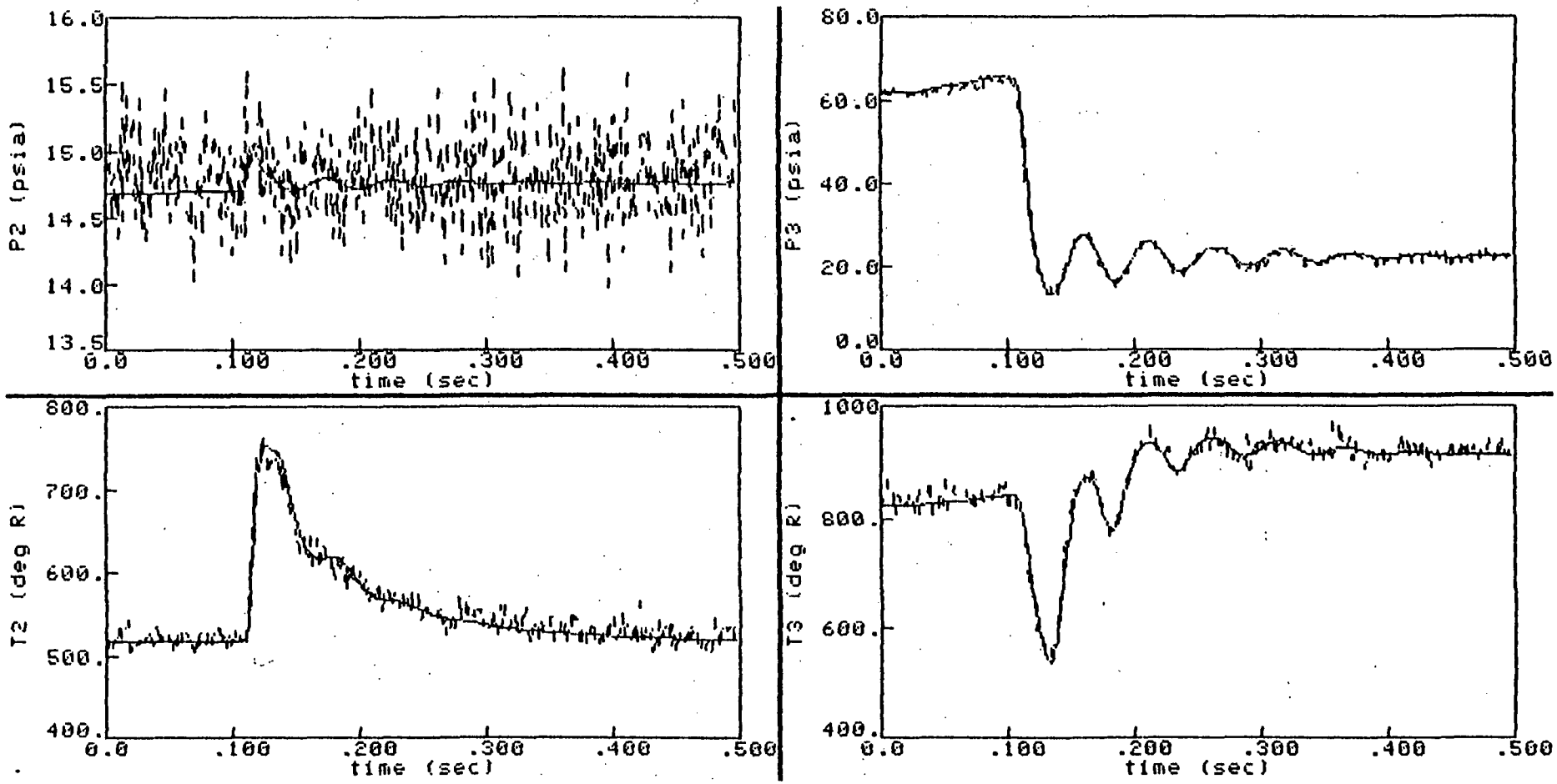

Figure 4.48 Run 15 Identification
(SCT, solid line; NASA, dashed line)

Table 4.12
K-Parameter Identification for Run 15

Run	Initial Kn	Final Kn	Actual Kn	Initial Kp	Final Kp	Actual Kp	Comments
n15a	30.0	12.78	15.0	0.50		1.00	
p15a		12.78	15.0	0.50	0.899	1.00	

4.6.1.8 Run 17 (Figures 4.49 and 4.50)

Run 17 is a recoverable stall run with response time similar to Run 15. The identification for Run 17 was standard except for one special test. The test was to see if SCIDNT could identify Kp by beginning with a Kp value that produced the wrong stall characteristic. The initial Kp was chosen to produce a non-recoverable stall in the model while the data indicated a recoverable stall. The idea was to test the robustness of SCIDNT: could it identify a Kp and cross the recoverable/non-recoverable stall boundary? The answer for this run is no. The results may have improved if the data set were limited to the first 0.2 seconds. The Kp identification was successful when the initial value was switched to a Kp value with a recovery characteristic.

Run 17 Observation: SCIDNT unable to cross recovery/non-recovery boundary.

Table 4.13
K-Parameter Identification for Run 17

Run	Initial Kn	Final Kn	Actual Kn	Initial Kp	Final Kp	Actual Kp	Comments
n17a	30.0	15.6	15.0	0.50		2.00	(stall/rec)
p17a		15.6	15.0	0.50	0.458	2.00	(stall/rec)
p17b		15.6	15.0	3.00	2.026	2.00	(rec/rec)

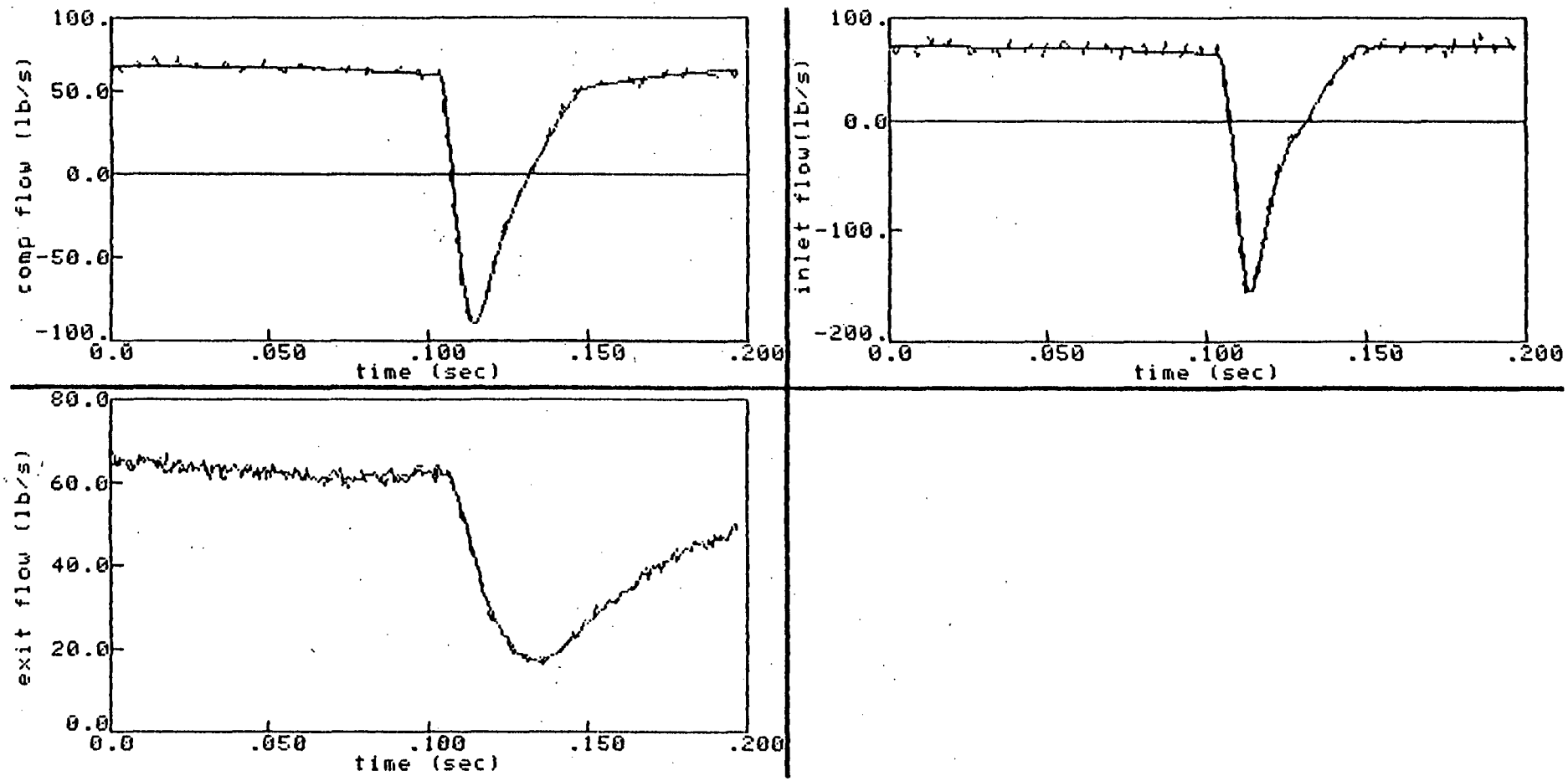

Figure 4.49 Run 17 Identification
(SCT, solid line; NASA, dashed line)

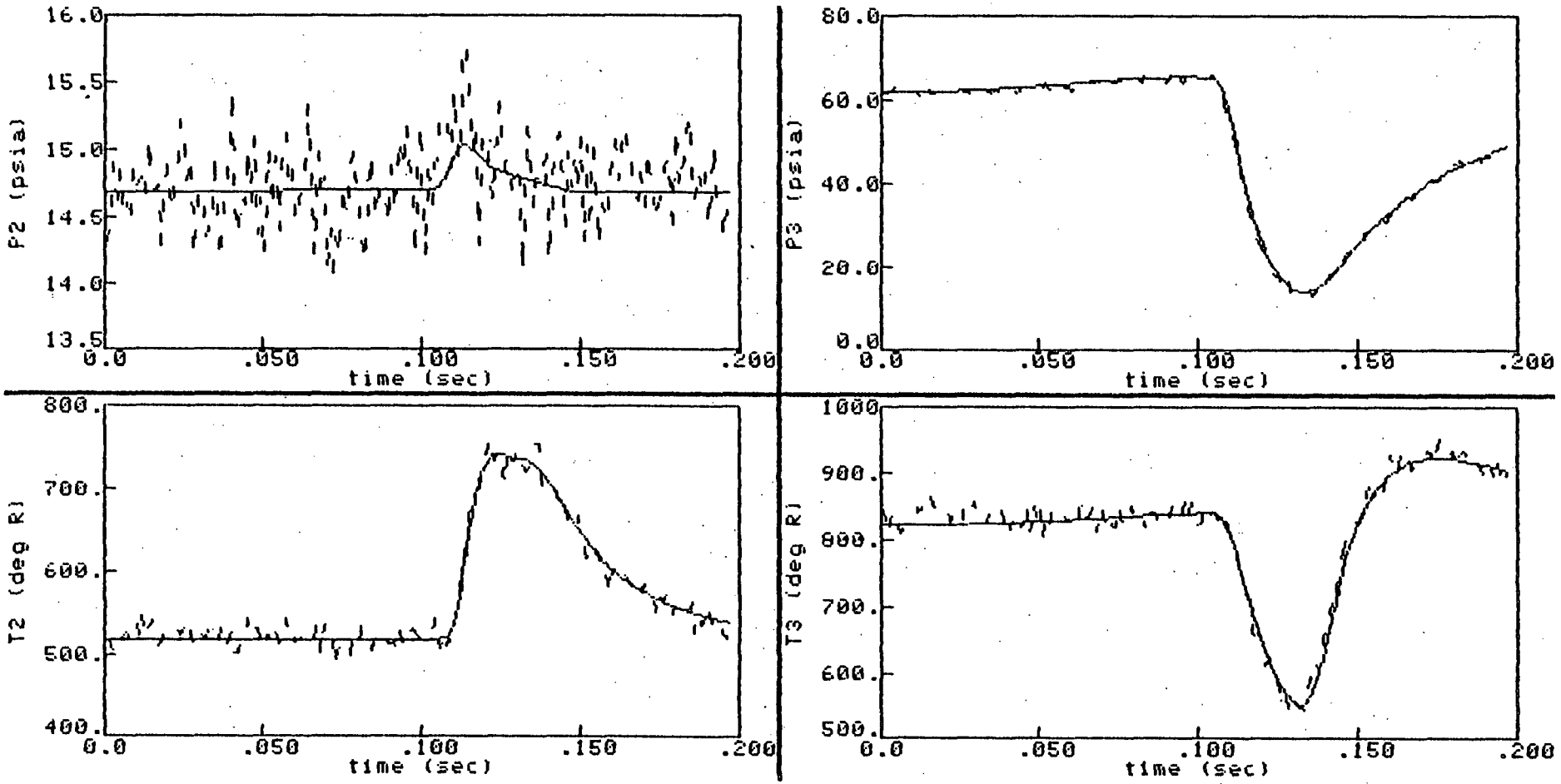

Figure 4.50 Run 17 Identification
(SCT, solid line; NASA, dashed line)

4.7 IDENTIFICATION EXPERIENCES

The compressor rig identifications successfully identified compressor map parameters. Some identifications were more successful than others and these were studied so that identification procedures could be improved and refined. A variety of experiences also were gained which spawned much of the work done in Task B.

The following is a summary of experiences drawn from the compressor model parameter identifications. The experiences give an indication of what could be done in the future to maximize compressor identification accuracy and were studied even further in the I/S study (Task B) to predict the effects of noise, sample rate, asynchronizations, reduced measurement sets, etc. The results of Task B form a foundation of identification requirements and guidelines that were used to maximize identification accuracy in the turbofan demonstration.

4.7.1 Model-Plant Differences: Time Skews

Observation: Due to slight differences between the model and plant, the SCT digital model stalls slightly later than the NASA hybrid model when given the same input. This delay introduces a time skew into the identification and can bias compressor parameter estimates.

Response: An input scaling factor, AT, was introduced to the SCT compressor model so the input could be artificially increased to hasten the onset of stall. The parameter was identified using SCIDNT until it produced synchronization between model and plant. This procedure worked fairly well but was troublesome and in some cases unsuccessful.

4.7.2 Initialization

Observation: The initial state values of the dynamic compressor rig model were supplied to SCT by NASA Lewis. In a normal identification situation, these values would not be available and would have to be estimated

or identified from the data. Incorrect initial values produce steady state errors between the plant and model that could bias parameter estimates.

Response: Future identifications should make provisions for parameterization of initial condition values, i.e., the initial conditions should be model parameters (under the SCIDNT definition of model parameters) and be accessible for identification.

4.7.3 Estimate Parameter Biasing

Observation: If a parameter is poorly identified, that is, if it is inaccurate, then it is able to affect the estimate of other parameters. This can be understood physically in the Kn and Kp identifications. If Kn is in error, then the model and plant will be in disagreement from the inception of negative stall flow till the end of the maneuver. Since most of the positive stall flow (determined by Kp) follows negative stall flow, the Kn errors produce model-plant mismatches that affect the Kp identification.

Response: The quantitative effects of this and other modeling "errors" is worth pursuing. Certainly, other errors in parameter values, lumped parameter assumptions, sensor time lags, etc., could have significant impact upon compressor map parameter identifications as well. The problem of estimation "sensitivities" is addressed in Task B (Chapter V).

4.7.4 Information Content

Observation: Identifications improved with more information. Most of the compressor rig work was done using only one out every five data points. When all data points were used, identification accuracy improved.

Observation: Noisier data decreases identification accuracy for all parameters.

Observation: Compressor parameter identifications seem to have a predictable relationship tied to available information. For example, in recoverable stalls, there is less time spent in positive stalled flow, and correspondingly, Kp identifications in recoverable stalls are marginal to poor. Kn identifications on the other hand seem to be impervious to the type of stall and are satisfactory, regardless of stall type.

Observation: Specific sensors can be eliminated from the identification process. Through elimination of certain sensors it was found that P2 (under the present noise levels) contributes little to Kn or Kp identification.

Response: The precise effects of sampling frequency, noise levels, type of stall and sensor set configurations require further investigation. A greater understanding of these effects will help define instrumentation requirements and help in streamlining identification procedures. This is done in Chapter V.

4.7.5 Separate Kn and Kp Identifications

Observation: Kn and Kp must be identified separately because of dramatic differences in the amount of information available for each parameter. If identified together, Kn dominates the identification convergence and the Kp estimate is left unimproved.

Response: Simultaneous identifications may be possible if the accuracy of the algorithm is improved. Conversion of the SCIDNT code from single (32-bit) precision to double (64 bit) precision may produce the desired accuracy.

4.7.6 Fixed-Step Integration

Observation: Unreliable results have been obtained when using the variable step SCIDNT integration routine. Specifically, the calculation of Kp

gradients loses fidelity under variable-step integration. Loss of fidelity is tied the fact that the Kp gradients are very small in recoverable stalls (meaning that Kp has very little effect on changing the stall trajectory when the stall is recoverable.) Thus, when minor gradient errors are introduced via the variable-step integration, Kp gradient values are distorted and identification is disrupted.

Response: SCIDNT is capable of integrating the compressor rig model using an efficient, variable-step integration package. Use of this package could produce considerable computer cost savings; however, the package cannot be used because of the accuracy problems.

Because of the discontinuous nature of the stall-capable model, very small integration steps are needed at times. Adjusting the variable-step integration parameters of the package is not sufficient to produce an accurate integration. Therefore, a fixed-time step is required. (First-order Euler integration is used.)

V. TASK B: IDENTIFIABILITY AND SENSITIVITY STUDY

The success of any parameter identification algorithm is dependent upon both the form of the system model and the condition of the measurement signals. This fact was highlighted by the results of the compressor model identifications in Chapter IV, where it was was noted that Kn and Kp parameter identifications varied from one type of model to another (e.g. non-recoverable to recoverable stall models) and from one sample rate to another (e.g., 1 kHz to 5 kHz).

In response to these results, a series of studies was conducted to quantify relationships between identification success and model form and measurement conditions. These identifiability and sensitivity study results not only accurately predict identifiability, they also provide an analytical tool for specifying instrumentation arrangements and predicting performance.

The concept of identifiability is based upon a measure of uncertainty in estimated parameters; uncertainty being a measure of the likely proximity of the actual parameter value to the estimated value. If an estimated parameter has a "large uncertainty," then the range in which the actual value is likely to be is fairly large. Typically, uncertainty is expressed as a standard deviation.

The uncertainty in a parameter estimate can be predicted before the estimate is made, based upon an assumption of appropriate noise levels, sample rates, etc. Knowing the uncertainty before identification provides a measure of what is termed "identifiability". One purpose of this study is to investigate how identifiability changes under various model and measurement conditions. The validity of the identifiability concept will be verified by comparing actual identifications with predicted identifiability.

Another benefit of uncertainty measures is that they provide a means for evaluating parameter identifications. When a parameter is estimated, it is desirable to know just how good the estimate is, i.e. how close to actual the estimate is likely to be. One way to quantify this is with uncertainty.

It is mentioned above that uncertainty relationships provide a means to predict the likely proximity of estimate and actual. Uncertainty is used

before identification (a priori) to predict how accurate the identification will be. Yet uncertainty can also be used after identification (post de facto) to measure the likelihood that the actual parameter value is nearby. These two uncertainty values are very similar, but in the a priori case, the original parameter guess is likely to be far from the actual value and thereby gives an imprecise estimate of accuracy (the estimate is always better than actual). After identification, however, the estimated parameter is closer to actual, and the post de facto uncertainty value gives a better idea of how close the estimate is to the real value.

To summarize, the identifiability portion of study indicates there are direct relationships between identifiability and number of data points, sample rate and noise levels. The study also demonstrates that identifiability changes under varied sensor set conditions including sensor lags, no flow sensors, and multiple sensor sets. These results can be used to make trade offs between various sensor arrangements, sensor noise levels, sample rates, etc., in determining instrumentation specifications in follow-on work. This is anticipated to be one of the major benefits arising from this study. Test results and past identification runs for the compressor rig were also explained in the study.

The sensitivity portion of the study demonstrates how parameter identification is sensitive to various types of modeling errors. Errors considered include errors in compressor map parameters, sensor lag time constants, and dimensional (volumes, resistance levels, etc). Sensitivity bias matrices are fundamental tools which can explain why identified parameters are biased away from actual values. The bias sources examined in this chapter showed that bias effects were potentially a much larger source of identification error than the uncertainties due to noise and sample rate effects in the compress rig study in Task A.

5.1 IDENTIFIABILITY

Recall from Chapter III that the Hessian provides a measure of estimate parameter uncertainty. This discussion focuses upon the use of the Hessian for developing identification relationships, later it is used for studying

sensitivity. Development of identifiability relationships is based upon results found in Section 3.4.1 and on other aspects of parameter estimation theory.

Identifiability is "a measure of the likelihood that any estimated parameter is within a specific range of the actual parameter value." It can also be thought of as a measure of confidence (or uncertainty) in a parameter estimate. This is a more quantitative way of viewing identifiability. Mathematically, uncertainty is expressed as a standard deviation.

To understand what affects M (and uncertainty), consider M written in another form. The information matrix relationship in Eq. (3.8) in Chapter III equates M to a sum of partial innovation vector products normalized by the measurement noise covariance matrix, R. If R is considered to be diagonal, then Eq. (3.8) can be expanded to a scalar relation where each measurement (or innovation) contribution is seen separately.

$$M = \sum_{j=1}^{M} \frac{1}{\sigma(y_j)^2} \left\{ \sum_{i=1}^{N} \left(\frac{\partial \nu_j}{\partial \theta} \right)^2 \right\} \tag{5.1}$$

In this form, it is possible to see clearly the relationships between parameter uncertainty and number of data points (N), number of measurements (m), and measurement noise level ($\sigma(y)$). Generally speaking, as the number of data points increases, parameter uncertainty decreases with $1/\sqrt{(N)}$, i.e. the ability of the parameter algorithm to identify a parameter will improve with the square root of N. One simple way to increase the number of data points is to use a higher sample rate. Another way is to make several runs under the same conditions. In the latter approach, even though sample rate has not increased, the number of data points for the same type of information is increased. Other conditions do impinge upon the selection of sample rate minimums, but generally, identification can be improved without increasing sample rates by using multiple identification runs.

Equation (5.1) also indicates that as the number of outputs is increased, uncertainty decreases -- not a very surprising result. Equally predictable is the fact that uncertainty increases as measurement noise increases. In fact, uncertainty increases in direct proportion to overall increases in measurement noise levels.

The term within the highest level brackets in Eq. (5.1) has a unique characteristic. From Eq. (3.9) of Chapter III and Eq. (5.1), it is apparent that this term is only dependent on the model output and the number of data points. Thus, if θ is near the actual θ, then the values for each output j are relatively constant. This is illustrated by rewriting Eq. (5.1):

$$\sigma(\theta) = \left[\sum_{m=1}^{M} \frac{m(\nu, \theta)}{\sigma(y)^2} \right]^{-1/2} \tag{5.2}$$

where

$m(\nu, \theta)$ is the contribution of the jth innovation over the entire measurement period (N points.)

and

$\sigma(y)$ is the noise level associated with the jth measurement

Since $m(v,\theta)$ is constant near θ actual, it is possible to relate uncertainty changes to various combinations of sensor noise levels. In fact by making any $\sigma(y)$ very large, it is possible to see how uncertainty will change without the contributions of a sensor, i.e., what happens to uncertainty under limited sensor sets.

This completes the development of identifiability formulae. Many of these results are used in later sections to explain how uncertainty changes under various instrumentation conditions.

5.2 SENSITIVITIES

Consider the problem: Given parameters to be identified, what identification errors will result if other model parameters are biased or incorrect? For in-stall compressor parameters, the effects of biased parameters are substantial.

The effect of one parameter on the identification of another is called parameter "sensitivity." Parameters being identified (affected) are customarily called "estimate parameters" (θ); remaining (affecting) parameters

are called "nuisance parameters" (ϕ). As with identifiability, the answers to this sensitivity problem are found within the Fisher information matrix.

The information matrix defined in Eq. (3.8) of Chapter III is an np x np matrix, for np model parameters. If only ne parameters are being estimated, M can be rearranged and partitioned as follows:

$$M = \begin{array}{c} \\ ne \\ nn \end{array} \begin{array}{c} \begin{array}{cc} ne & nn \end{array} \\ \left[\begin{array}{c|c} M_{11} & M_{12} \\ \hline M_{21} & M_{22} \end{array}\right] \end{array} \tag{5.3}$$

where

ne = number of estimate parameters
nn = number of nuisance parameters
np = ne + nn

M_{11} is the Fisher information matrix that relates the changes in J due to changes in only the estimate parameters, θ. During parameter identification, only the M_{11} portion of the information matrix is used, the portion which pertains to the parameters being identified. (So actually only M_{11} is used in the parameter stepping algorithm, Eq. (3.5).)

A relationship between θ and ϕ can be found by using other portions of the information matrix, namely, M_{12}, in conjunction with M_{11}. M_{12} can be expressed as

$$M_{12} = E\left\{ \frac{\partial J}{\partial \theta} \frac{\partial J}{\partial \phi} \Big|_{\theta,\ \phi\ =\ \theta_i,\ \phi_i} \right\} \tag{5.4}$$

Combining the information in M_{11} and M12 yields,

$$X_b = M_{11}^{-1} M_{12} = E\left\{ \frac{\partial \theta'}{\partial J} \frac{\partial \theta}{\partial J} \frac{\partial J}{\partial \theta} \frac{\partial J}{\partial \phi} \right\} \tag{5.5}$$

where

X_b = bias matrix

The bias matrix indicates how much the estimate parameters change for a unit change in the nuisance parameters. Equation (5.5) is the exact solution for the scalar case (J, θ, and ϕ scalars) and has similar interpretations in the general matrix case. Equation (5.5) can be used to estimate the effects of biased parameters on the estimation of other parameters. For the worst case results, the absolute value of each element in the $X_b \Delta\phi$ product is taken. The worst-case estimate parameter (θ) errors are,

$$\text{worst error} = |M_{11}^{-1}M_{12}||\Delta\phi| \tag{5.6}$$

where

$\Delta\phi$ is the change in ϕ off nominal.

Equation (5.6) is the primary means used in analyzing potential effects of nuisance parameter errors in Section 5.3.2. A typical application would be the effect of a change in a sensor time constant. For example, assume T3 has a modeled time lag constant of 100 milliseconds, and the actual sensor constant is 120 milliseconds. The question would be, how might this nuisance parameter error bias an estimate of Kn or Kp.

5.3 STUDY RESULTS

Presented here are practical results observed by applying the theoretical identifiability and sensitivity formulas derived in Sections 5.1 and 5.2. Results have been split into two major areas 1) instrumentation effects on identifiability (e.g. sample rate, sensor noise, sensor lags, etc.) and model and error effects on sensitivity (nuisance parameters and model structural errors). In general, the results support both of the theories discussed above; they also demonstrate practical methods for improving future identifications and specifying instrumentation requirements.

5.3.1 Instrumentation Effects

5.3.1.1 Sample Rates and Multiple Maneuvers

The basic uncertainty relationship for sample rates is found in Eq. (5.1). The relationship is simply: if N is increased by some factor kN, then uncertainty decreases by a factor $1/\sqrt{(kN)}$. N can be increased by three distinct ways:

(1) the sample rate can be increased;

(2) the number of measurement runs can be increased (e.g. make two tests on a stalling compressor under identical conditions and use both measurement sets for identification: "multiple maneuver approach,"); or

(3) use redundant sensors.

All methods theoretically produce the same results. Consider the effect of increasing N in Eq. (5.2):

$$\sigma(\theta) = \left[\sum_{j=1}^{m} \frac{m(J, \theta)}{\sigma(y)^2} \right]^{-1/2} \tag{5.7}$$

Here, $\sigma(\theta)$ is expressed as a function of $m(\nu, \theta)$ and $\sigma(y)$ for N data points. From Eqs. (5.1) and (5.2), if N changes by a factor of kN, then uncertainty $(\sigma(\theta))$ changes by a factor of $1/\sqrt{(kN)}$. Rewriting Eq. (5.2) to express this relationship yields:

$$\sigma(\theta) = \left[kN \sum_{j=1}^{m} \frac{m(\nu, \theta)}{\sigma(y)^2} \right]^{-1/2} \tag{5.8}$$

where

$m(\nu, \theta)$ is the contribution of the jth innovation over the entire measurement period (Nstd points);

$\sigma(y)$ is the noise level associated with the jth measurement measurement;

and

kN is the actual number of data points divided by some standard number

The theoretical relationship between sample rates and uncertainty is illustrated in Figures 5.1 and 5.2 for four different cases: Kp and Kn uncertainties for Runs 5 and 7 (non-recoverable and recoverable) under conditions of 5 percent noise. The 5 percent noise level represents Gaussian noise with a standard deviation equal to 5 percent of the steady-state, unstalled, output levels. Noise level values along with the four cases are summarized below:

Table 5.1
Noise Levels (Standard Deviations)
for Study of Sample Rate Effects

	$\dot{W}1$	$\dot{W}2$	$\dot{W}3$	P2	P3	T2	T3
S.S.	65.	65.	65.	14.7	62.2	519.	823.
5 percent	3.25	3.25	3.25	.735	3.11	25.95	41.15

Figure 5.1 illustrates the inverse square-root relationship between uncertainty and sample rate (or number of points.) The same results are shown in Figure 5.2 for 1 percent noise in a log-log plot. Here the relationship between log sample rate and log uncertainty is linear (slope=-1/2.)

SCIDNT is capable of statistically analyzing measurement noise and determining the uncertainty of a model's being representative of the measurement data (a primary way of determining parameter estimate confidence.) Twelve test cases were studied using SCIDNT to see how uncertainty changed with the sample frequency using simulated noisy data. These twelve measured uncertainties are plotted in Figure 5.2. Of these cases, three uncertainties were measured for each test case at three different sample rates using the simulated data. The lines in Figure 5.2 result from using Eq. (5.8) in conjunction with $m(\nu, \theta)$ contributions determined at 1 kHz and 1 percent noise levels. The measured uncertainties follow theory very well. Uncertainty

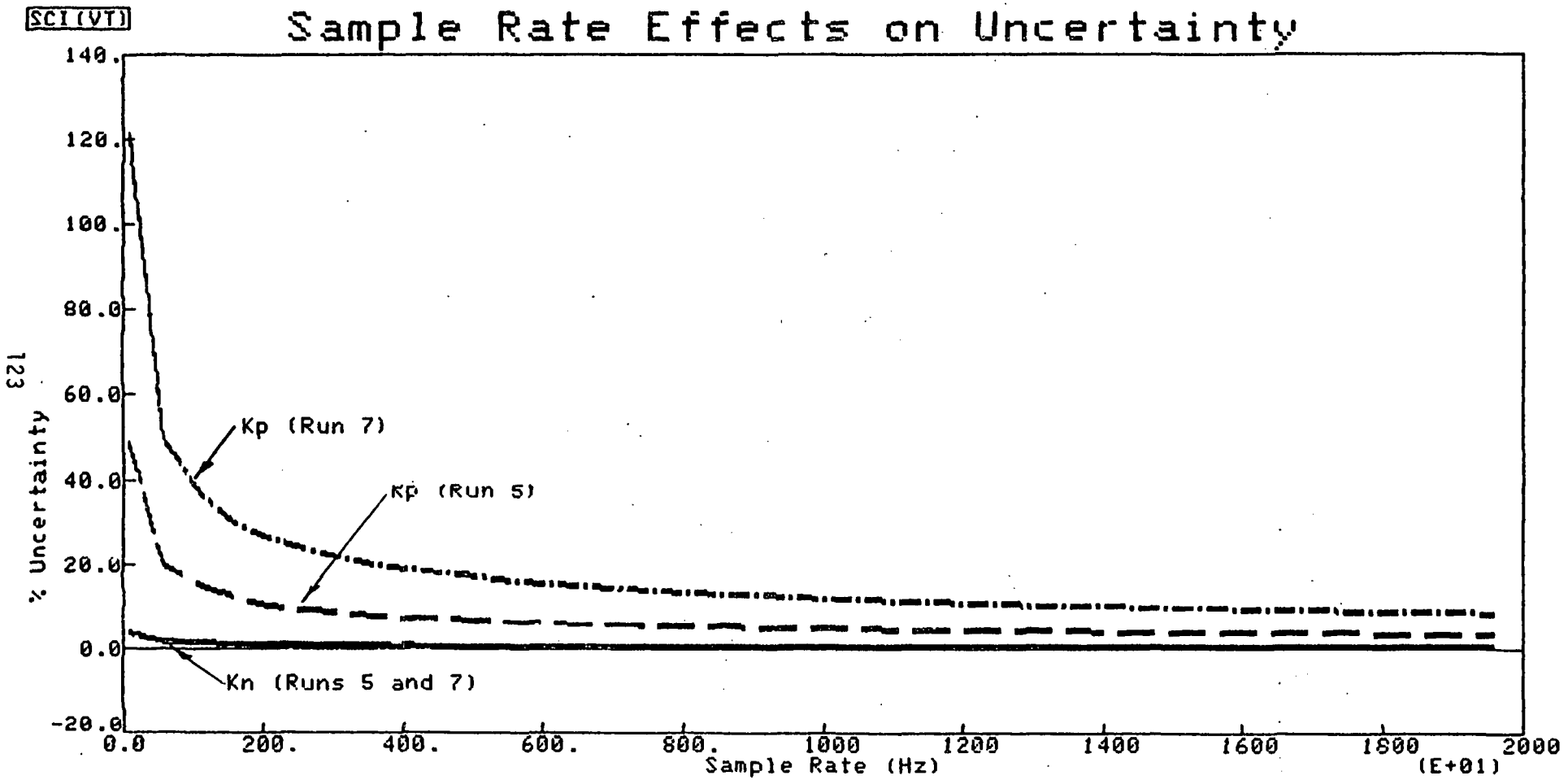

Figure 5.1 Sample Rate Effects (5 Percent Noise)

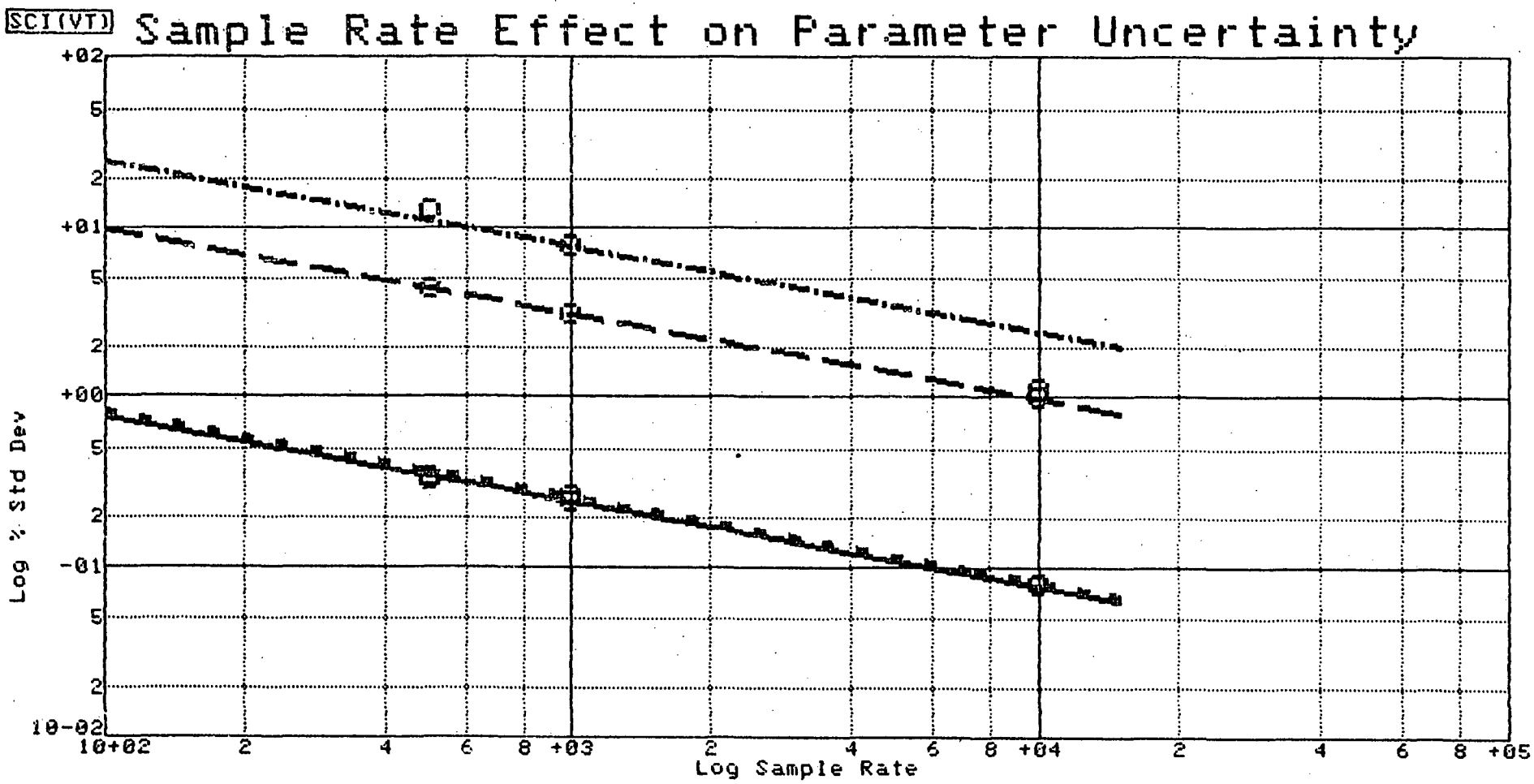

Figure 5.2 Sample Rate Effects (Log-Log) (1 Percent Noise)

for the stalling compressor model does indeed follow an inverse square relationship with sampling rate.

These results also highlight the basic identifiability differences between Kp and Kn for non-recoverable and recoverable stall cases. In general, Kn is more identifiable than Kp and is relatively independent of the type of stall. Kp is much less identifiable than Kn and does not fare as well in recoverable stallsas in non-recoverable stalls (not surprising since there is less Kp information in a recoverable stall.) The differences in identifiability are fairly dramatic.

Consider the example where the noise levels are the same for all four identifications and the user seeks a 1 percent confidence level in estimates. It would require 1 measurement set at 100 Hz and 1 percent noise to achieve a 1 percent confidence level with a Kn identification. It would take 100 measurement sets at 100 Hz to achieve the same accuracy with Kp in an non-recoverable stall model. And it would take 400 measurement sets at 100 Hz to achieve the same accuracy with Kp in a recoverable stall model. From a sample rate point of view, sample rates of 0.1 kHz, 10 kHz and 40 kHz would be needed to achieve the same accuracies in all three cases. The concept is the same for all cases. It takes 100 to 400 times more data to identify Kp as well as Kn (for Runs 5 and 7).

Figure 5.2 can be used in two ways. First, if a Run 5 identification has been made at some arbitrary frequency, then Figure 5.2 could be used to assign some confidence to that estimate, e.g., the actual value is likely to be within 2σ values. Secondly, Figure 5.2 can be used to determine instrumentation requirements. If a minimal confidence level is established before an engine test, then sample rates, number of probes and number of test runs can be traded off to achieve the desired accuracy for all parameters of interest. (Note: The compressor model can only be used for identification down to near 100 Hz. Rates much lower than this miss too much data and the stall may be missed altogether).

An important assumption made in these discussions is that noise is always white and unbiased. This is why uncertainty improvements can theoretically be had even as sample rates approach the continuous case. In actuality, noise is not white and there are definite points beyond which an increase in the sample rate would not improve estimate uncertainty or identifiability.

Future identifications should determine fundamental parameter uncertainties before identification by using typical noise levels and sample rates. From these uncertainties (and Eq. 5.8), it can be determined what sample rates or number of manuevers would be necessary to obtain a desired accuracy.

5.3.1.2 Sensor Noise

From Eq. (5.8), estimated uncertainty is proportional to the sensor noise (assuming that relative noise levels between sensors is constant). Thus, if base noise levels change by some $k\sigma$ percent, then uncertainty will also change by $k\sigma$ percent. A graphical example of this relationship is shown in Figures 5.3 and 5.4. The noise levels used in this example are in the same proportions as those in Table 5.1, and the $m(\nu, \theta)$ values are based upon a 1-kHz sample rate. Figures 5.3 and 5.4 examine the relationships between four cases -- the same four mentioned above (Kp and Kn for Runs 5 and 7).

The graphs indicate that as noise approaches zero, uncertainty disappears and identifiability is maximized. The differences in identifiability between Kn, Kp in a non-recoverable stall, and Kp in a recoverable stall are indicated by the different slopes of the curves.

The next phase in the study considers a slightly more complicated situation. In Figures 5.5 through 5.7 are three sets of graphs indicating how Kn uncertainty changes in Run 5 when noise on just a single sensor is increased. Each line represents Kn uncertainty for 5 percent noise on all sensors except one, and that one noise level is allowed to vary from 0 to 25 percent.

The graphs point out several important relationships. For example, all of the pressure and temperature sensors have little effect on decreasing uncertainty past about a 2 percent noise level. Decreasing noise on any one of these sensors will increase identifiability only if their noise level is less than 2 percent.

The same is not true for flow measurements. Figure 5.5 indicates that identifiability is fairly strongly associated with the flow measurement noise levels, particularly for inlet flow. A large amount of information is being

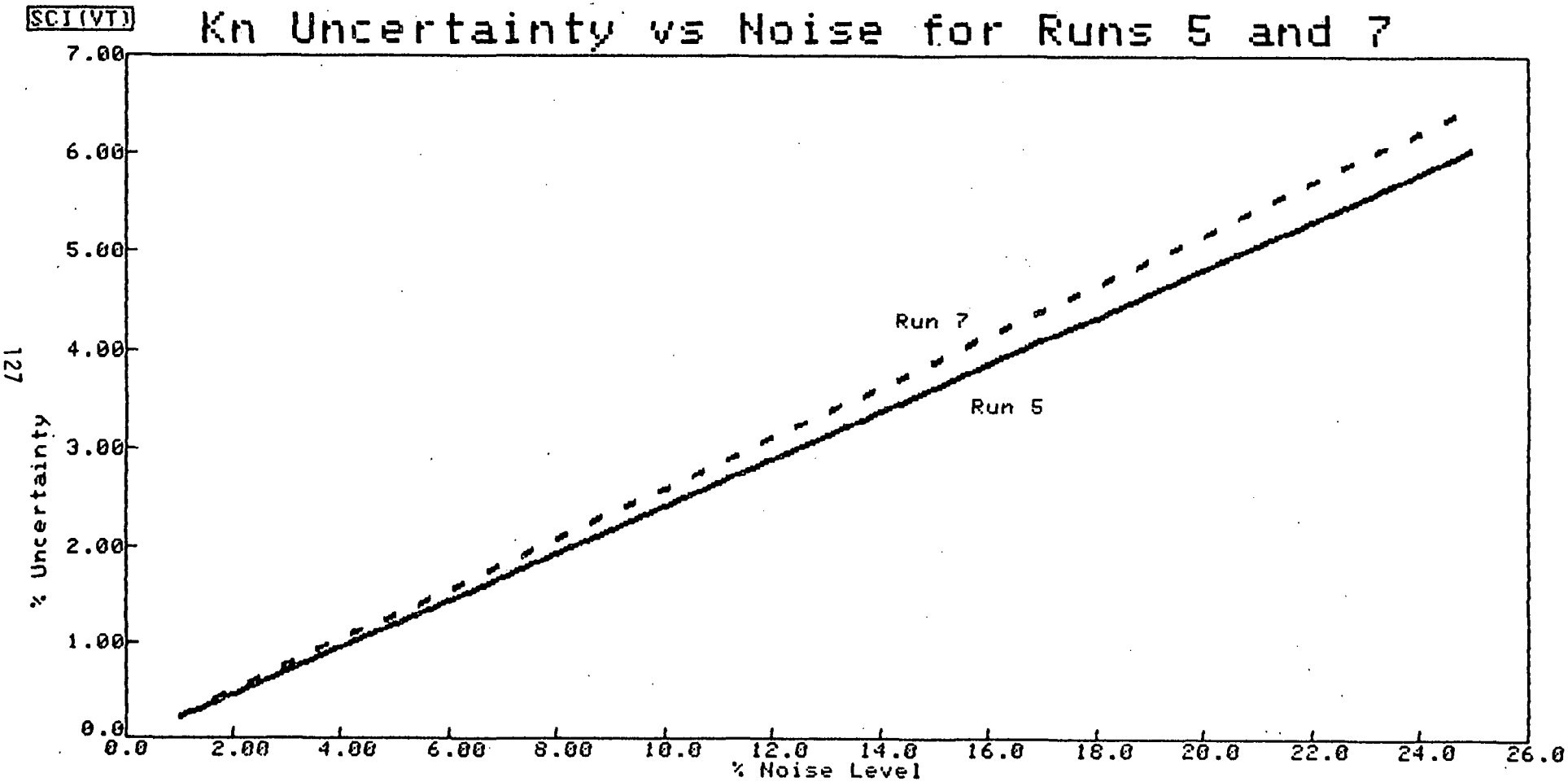

Figure 5.3 Noise Effects on Kn

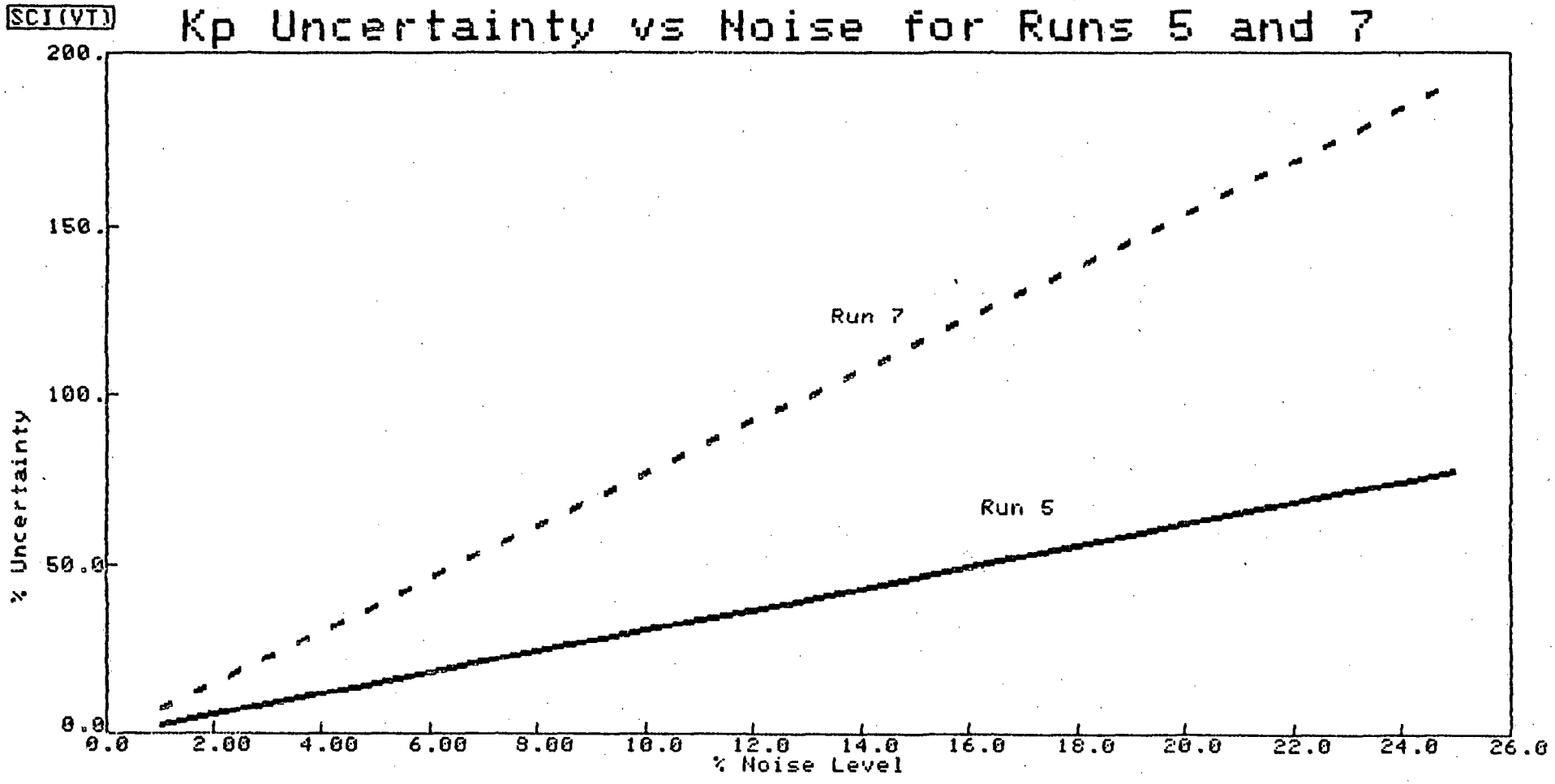

Figure 5.4 Noise Effects on Kp

contributed by flow measurements in the $m(\nu, \theta)$ term — enough information to make the flow contributions significant even at a 5 percent noise level. Inlet flow is a good example of this. Decreasing noise in the inlet flow measurement, even at the 15 percent level, causes uncertainty decrease. No other sensor has this great an impact. This is an indication that the inlet flow sensor is quite important to identification of Kn as will be seen in Section 5.3.1.4.

Figures 5.5 through 5.7 show that some measurements, flows in particular, tend to be large contributors of information. They demonstrate in a subtle way the different value of each type of measurement, i.e., the different information contributions from each measurement. Understanding which sensor contributes what becomes important knowledge when sensor configurations are determined. Section 5.3.1.4 shows how the ratio of $m(\nu, \theta)$ to $\sigma(y)$ can be used as a measure of these contributions.

5.3.1.3 Sensor Lags

Sensor lags, particularly in temperature sensors, are an inevitable nuisance to be confronted in parameter identification. To this point, the compressor model has not included models for sensor lags. In this section the compressor rig model is expanded to include lags to consider identifiability effects induced by lagging or dynamic sensors.

The focus in this section is on temperature sensor lags (later examples consider pressure and flow measurement dynamics as well). A first order lag was chosen to model temperature sensor dynamics and the lag time constants are listed below:

Table 5.2
Temperature Sensor Time Constants

Sensor	Time Constant (msec)
T2	170.
T3	170.

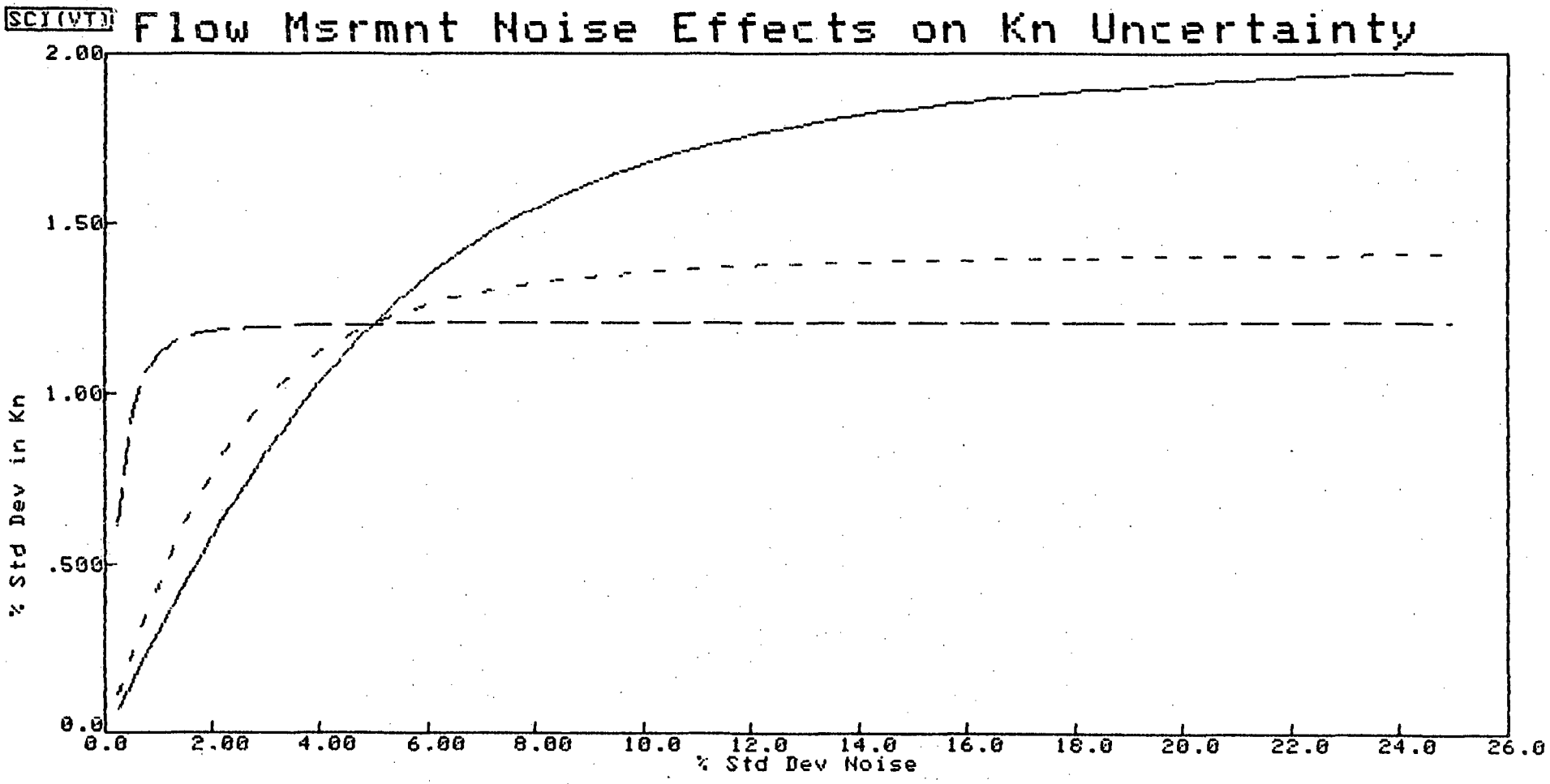

Figure 5.5 Flow Measurement Noise Effects

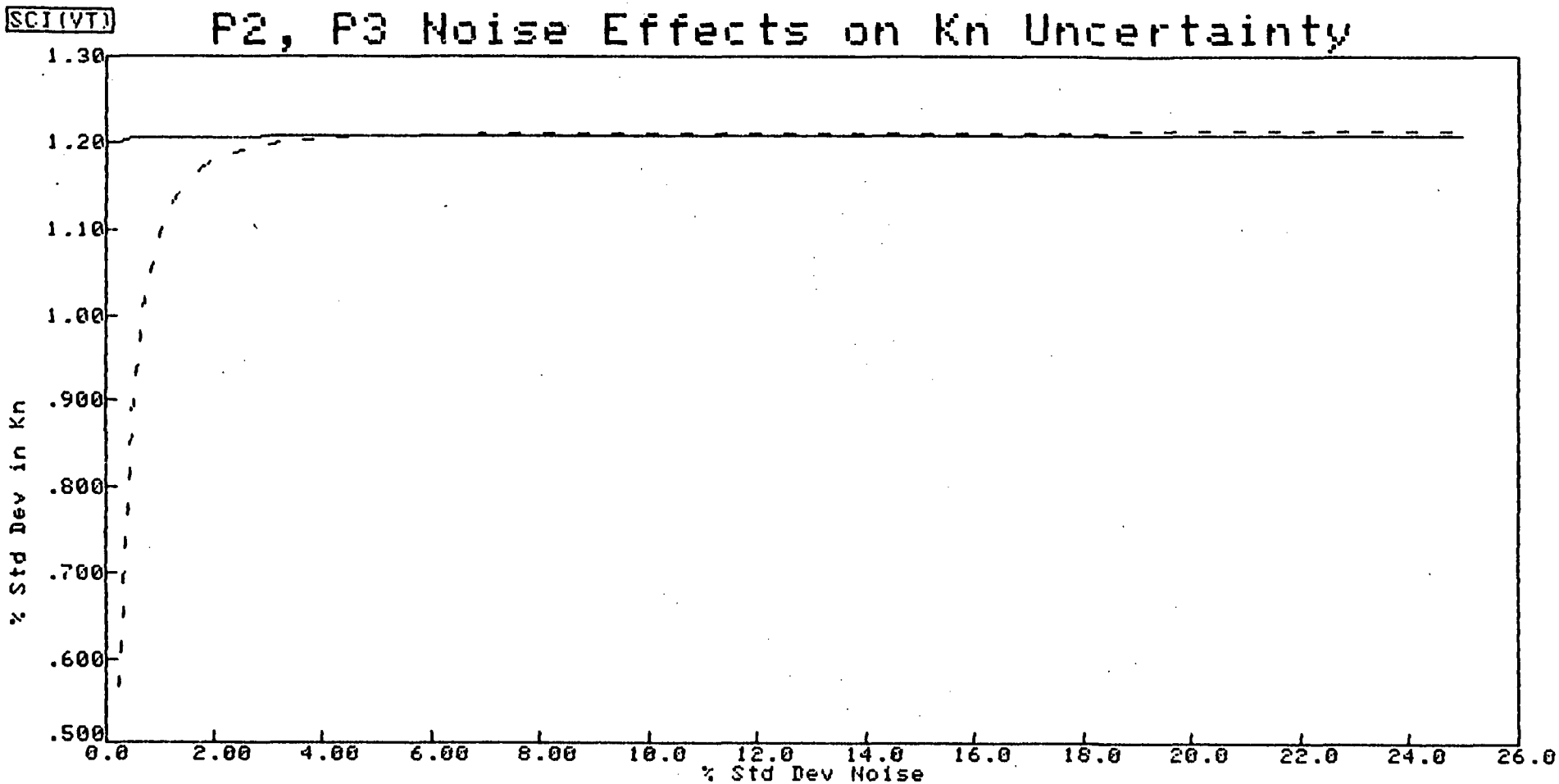

Figure 5.6 Pressure Measurement Noise Effects

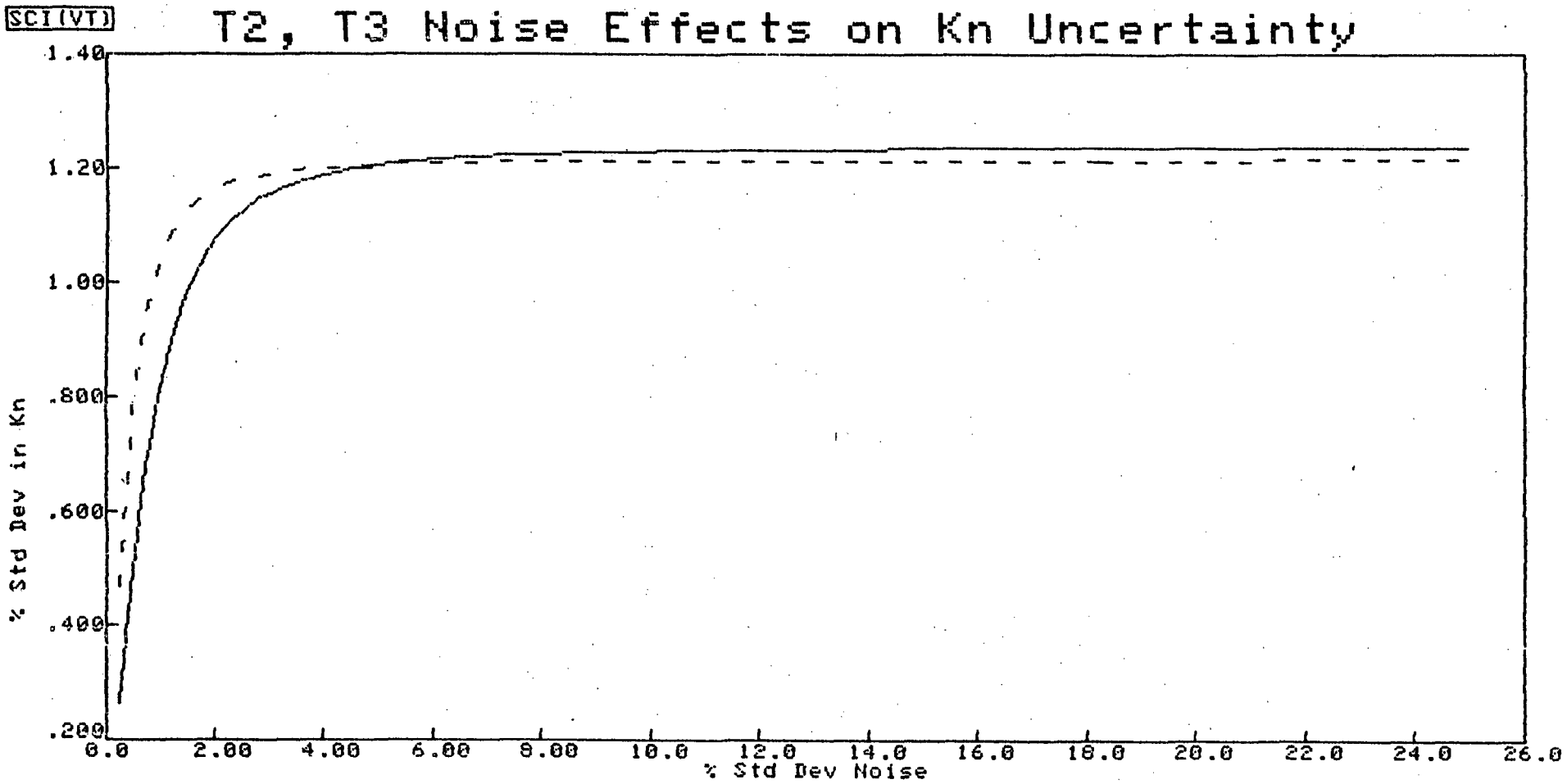

Figure 5.7 Temperature Measurement Noise Effects

Several sample cases were examined to study how temperature lags alter identifiability. Eight identification cases were examined in all. Four of the cases are identical to those discussed in Section 5.3.1.1; the remaining four differ only in that lags are added to the temperature measurements.

Results are shown in Figures 5.8 and 5.9. In general, the difference between temperature sensors with lags and without lags is minimal after the contributions of all the other sensors. This is because temperature sensors with or without lags contribute little by way of $m(\nu, \theta)$ to the information matrix and uncertainty values.

Although temperature lags have little effect on decreasing uncertainty in a full sensor set, they can still be a major source of identification error. The influences of temperature lags go beyond simply reducing the amount of information in M. For example, if the estimated time constants in the sensor model differ from the actual sensor dynamics, the result is a plant-model disagreement or modeling error. This modeling error can induce biases on estimated Kn and Kp parameters. These and other model error-related topics fall under the sensitivity study discussed in Section 5.3.2.

5.3.1.4 Sensor Contributions

The previous two sections brought up a concept of "sensor contributions." In theory and practice, each sensor contributes a specific portion of the parameter information contained in M. This section explores Eq. (5.2) to show how contributions from each measurement can be quantified and compared. Results show how sensor sets can be chosen for maximum identifiability and how sensor constraints can limit that identifiability.

Measurement contributions can best be understood by re-examining Eq. (5.2). In that relationship the elements of the information matrix are expressed as sums of contributions from each measurement taken over time, N. The measurement contributions $m(\nu, \theta)$ are normalized by a noise level so that their contributions are weighted according to both the scale and "believability" of the measurement signal. Thus, when the contributions from each measurement are summed, they are compatible and comparable. The contribution concept uses this "compatible and comparable" idea to allow comparative evaluations of the contributions.

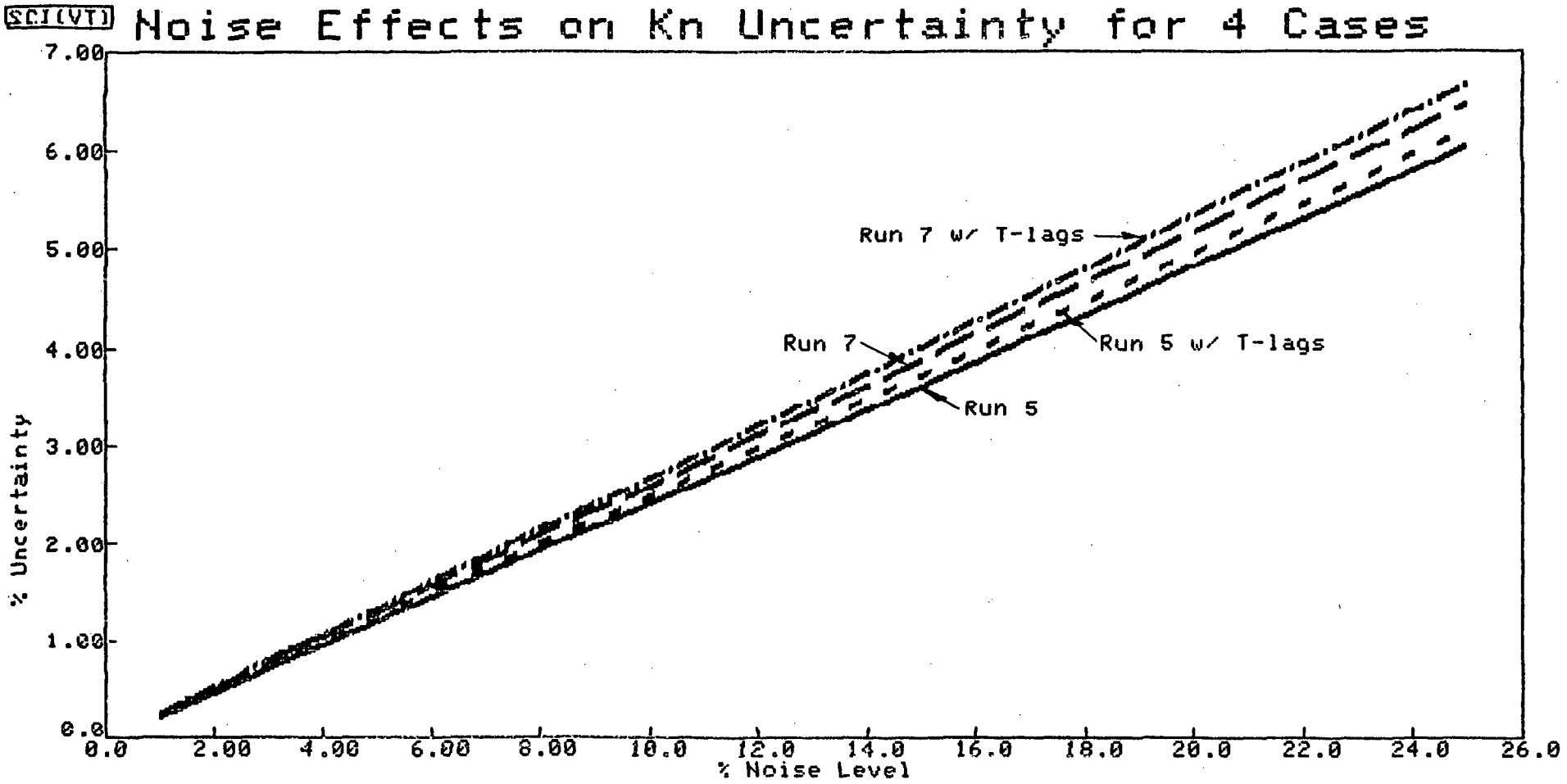

Figure 5.8 Noise Effects with Temperature Lags

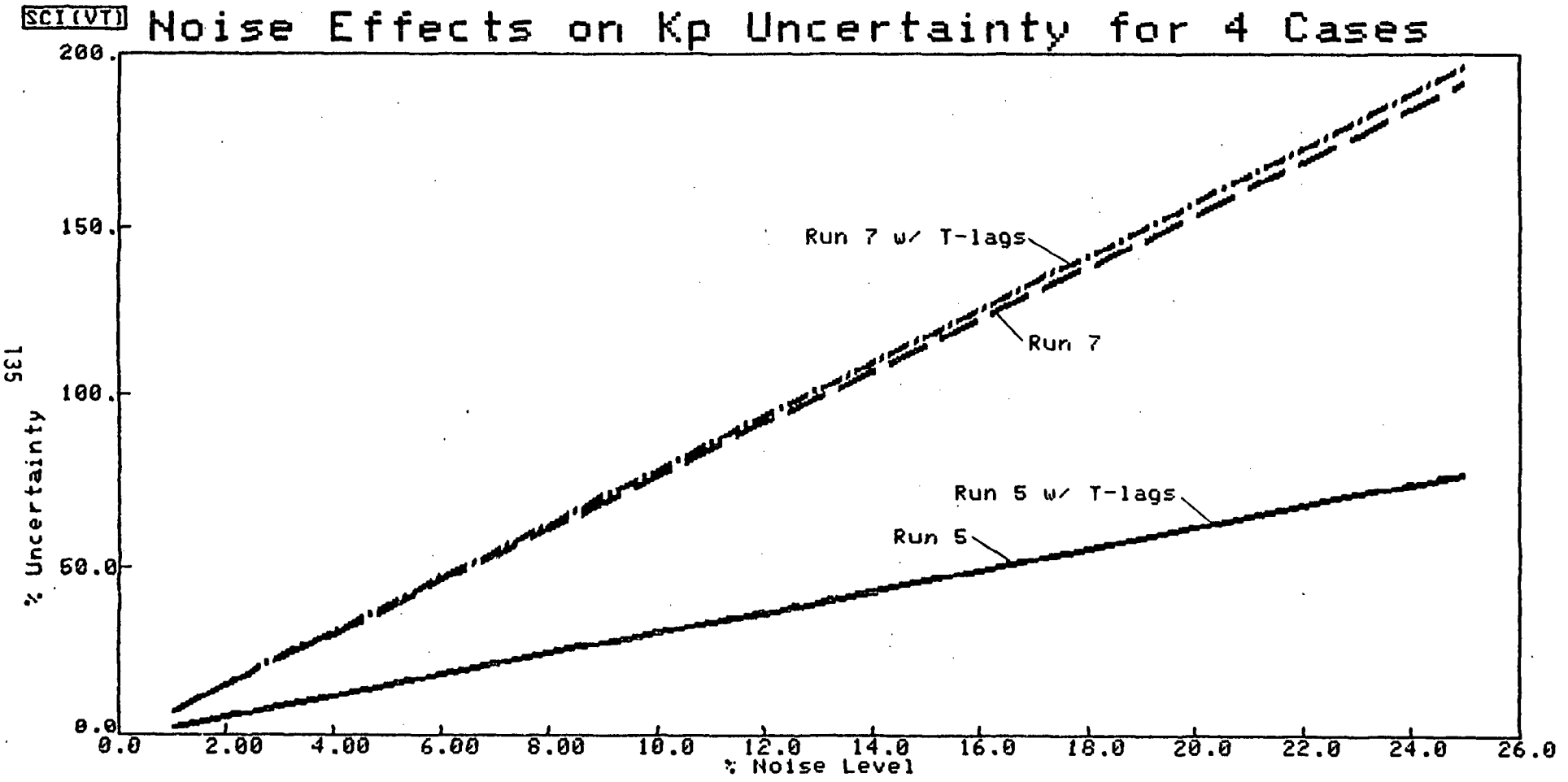

Figure 5.9 Noise Effects with Temperature Lags

For example, consider where Kn is the sole estimate parameter and M is a scalar. Dividing each summed element in Eq. (5.2) by M, the resulting values indicate what percent of M is contributed by each measurement. (Keep in mind that the contributions will vary according to the sensors present and the level of noise on each sensor.) Although it is not possible to show any direct relationship between individual measurement contributions and uncertainty, the percentage results do provide an excellent comparative measure of effectiveness for each sensor.

Figure 5.10 is an example result. It shows the contribution of each sensor to the Kn information matrix for Run 5. Noise levels at 5 percent of initial values were used. In general, the flow sensors, inlet flow in particular, show the greatest contribution of Kn information. P3 and T2 provide smaller amounts of information than P2 and T3. It is worth stressing that all of these relationships could change with different noise levels. The measurement contribution tool can be used to great advantage in several ways. First, if sensors and their noise levels are already known, it can be determined which sensors contribute the most information and should be used in the identification process. Second, if sensors are being chosen, their contribution relationships can be used to determine what noise levels on what sensors would be acceptable.

Sixteen examples of measurement contributions are shown in Figures 5.10 through 5.25. The examples examine contributions to Kn and Kp for recoverable stall and non-recoverable stall, for sensor configurations with temperature lags and without, and for where flow measurements are not available. (Scenarios with unavailable flow measurements are studied by simply omitting the flow measurement contributions from the sum in Eq. 5.2.) The changes are generally predictable. Flow measurements are of primary import throughout all scenarios; temperature contributions decline when lags are present (the information is being filtered out); and pressure and temperature contributions increase when flow measurements are unavailable.

Flow measurements are not critical to identifying in-stall compressor map parameters, but are valuable. Much of the valuable information in the flow measurements could be extracted from other measurements under the proper conditions. This can be seen by examining the compressor rig equations.

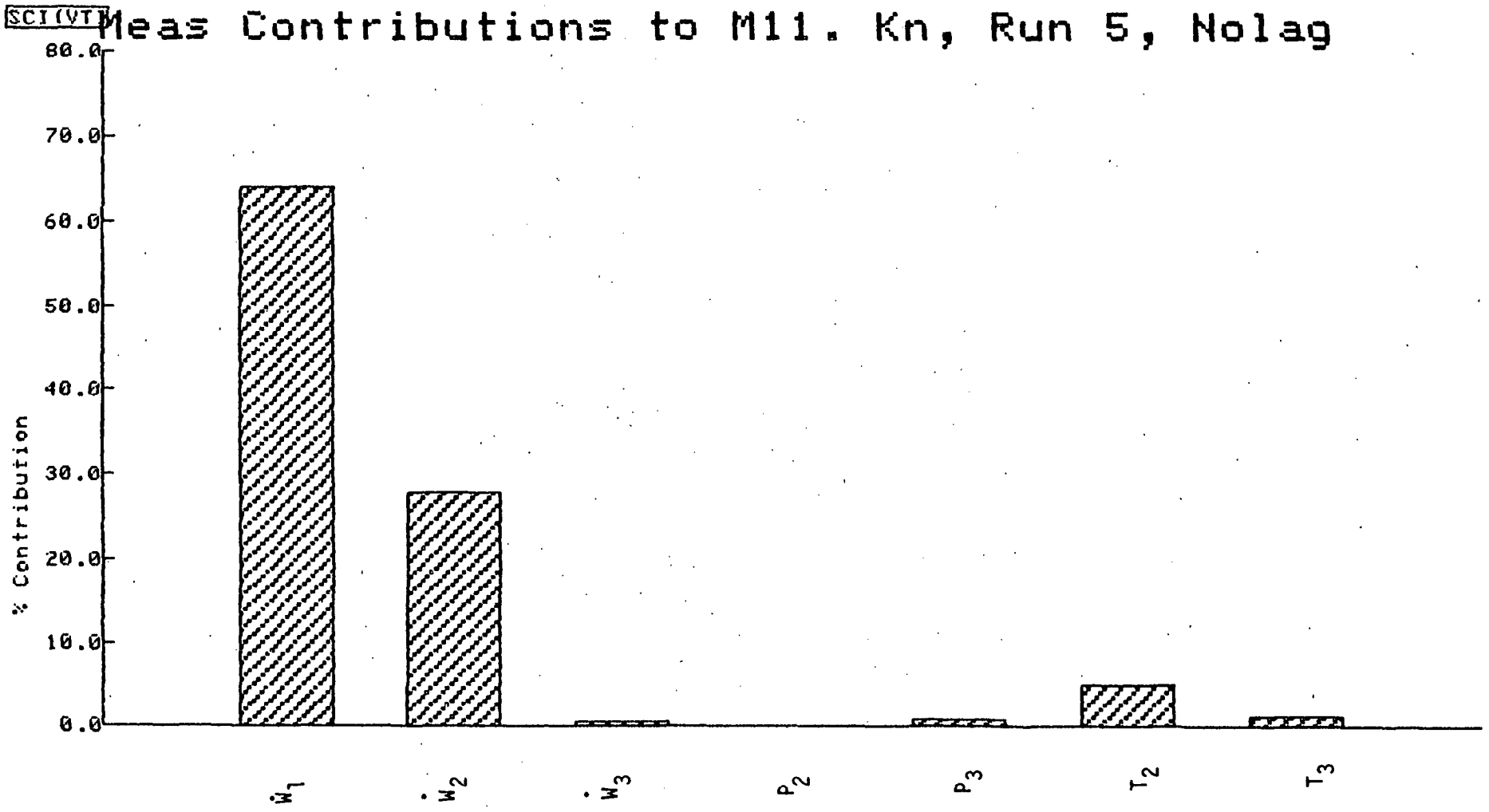

Figure 5.10 Kn, Run 5, No Lags, Contributions

Inlet flow can be replaced by P2 since inlet flow is a simple resistive function of the pressure drop across stages 1 and 2, and in this model, P1 is constant. Thus, inlet flow is directly related to P2, and therefore P2 contains the same information. In the measurement contribution figures, inlet flow contributes more information because its noise levels are small in comparison to its sensitivity to the Kp and Kn parameters. If P2 had a sufficiently small noise level, it would show the same contribution as the inlet signal.

Assume an inlet flow measurement is not available and is to be synthesized using the P2 signal. The maximum allowable noise level on P2 to achieve the same contribution level as $\dot{W}1$ with 1 percent (3 lb/sec) noise would be:

$$\dot{W}1 + \sigma(\dot{W}1) = [P1 - (P2 + \sigma(P2))] / R0$$

where

$R0 = 0.00158$ psi/(lb/sec)

To have the same apparent noise on the synthesized inlet flow, the P2 noise level would have to be:

$$\sigma(P2) = \sigma(\dot{W}1) * R0$$

if

$$\sigma(\dot{W}1) = 3 \text{ lb/sec}$$

then

$$\sigma(P2) = .00474 \text{ psia}$$

So a $\dot{W}1$ with 1 percent noise (1 percent of initial value) can be replaced with a P2 measurement only if the pressure noise is less than .00474 psia or 0.03 percent. Even though P2 and inlet flow contain the exact same information, P2 is outweighed by inlet flow because it has a comparatively high noise level. Figures 5.10 through 5.17 provide good examples of this.

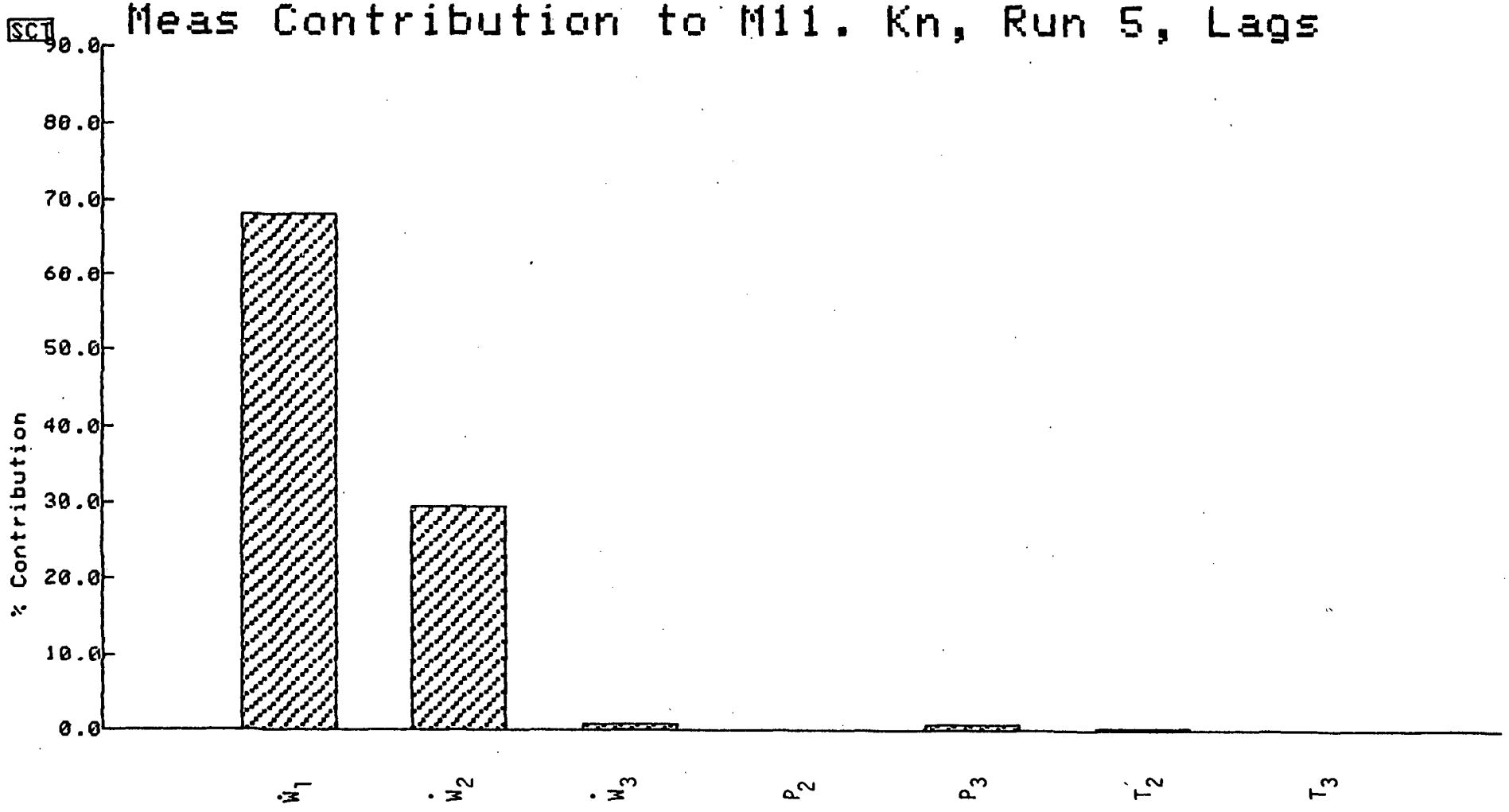

Figure 5.11 Contributions

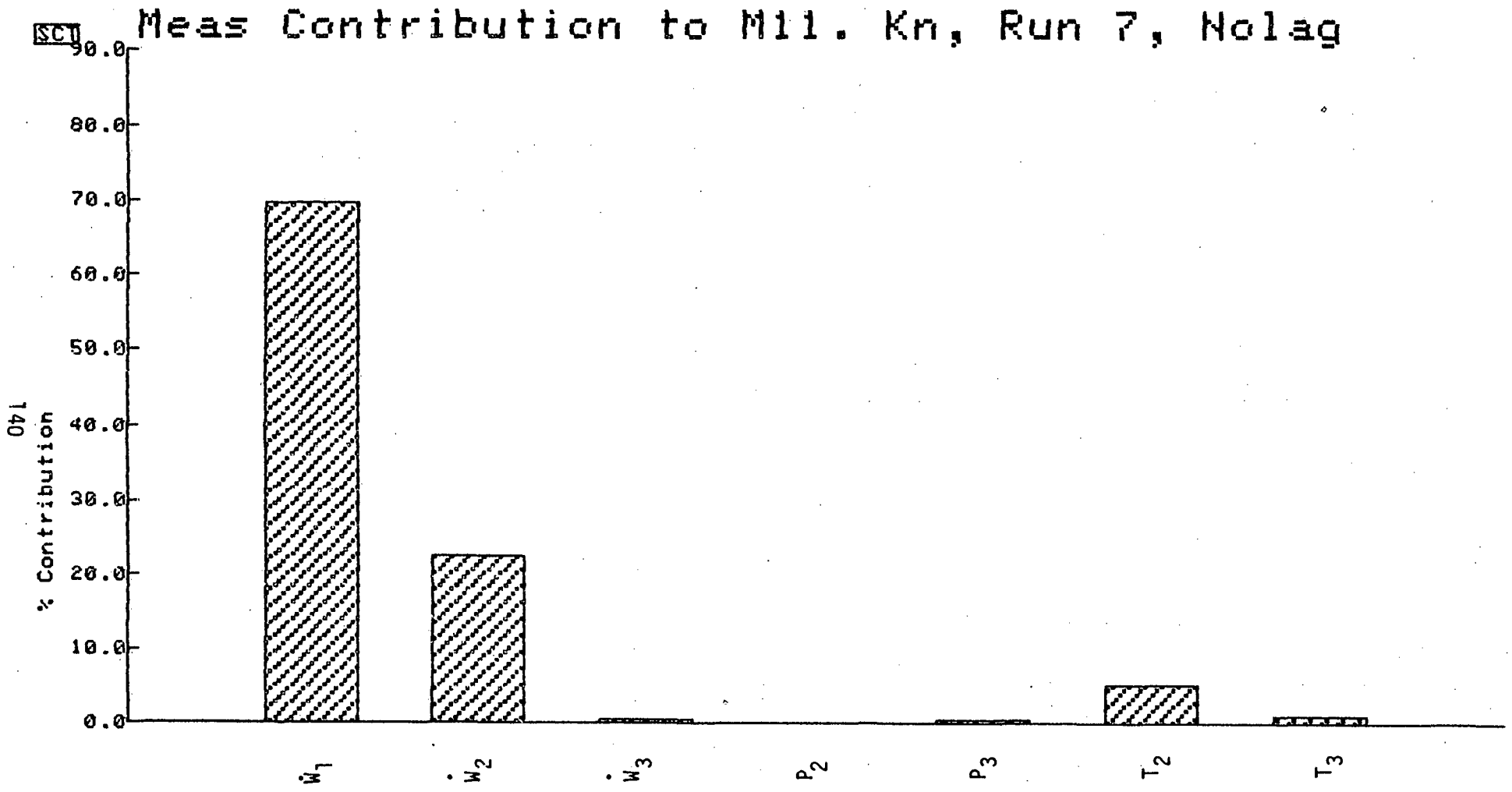

Figure 5.12 Contributions

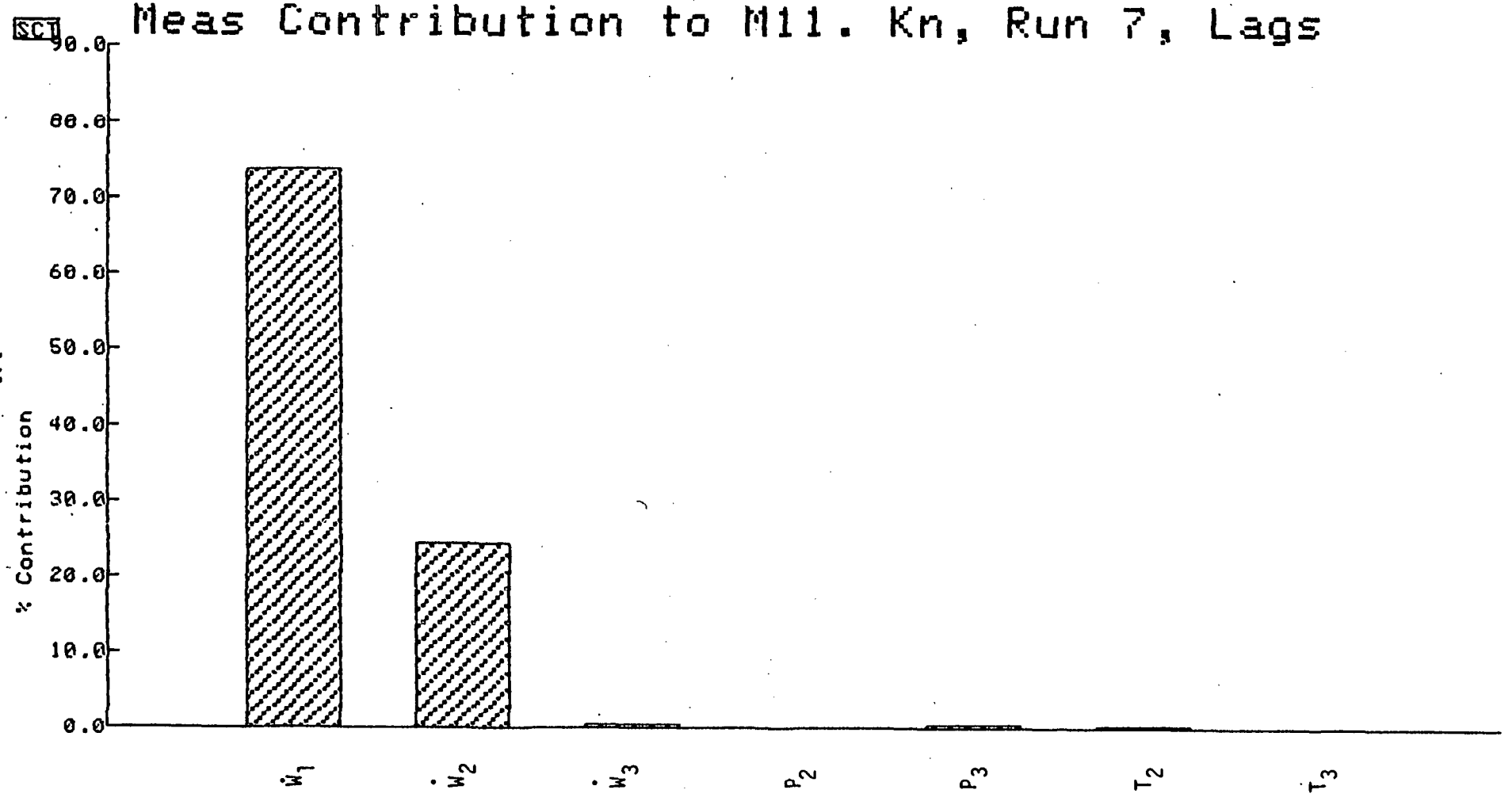

Figure 5.13 Contributions

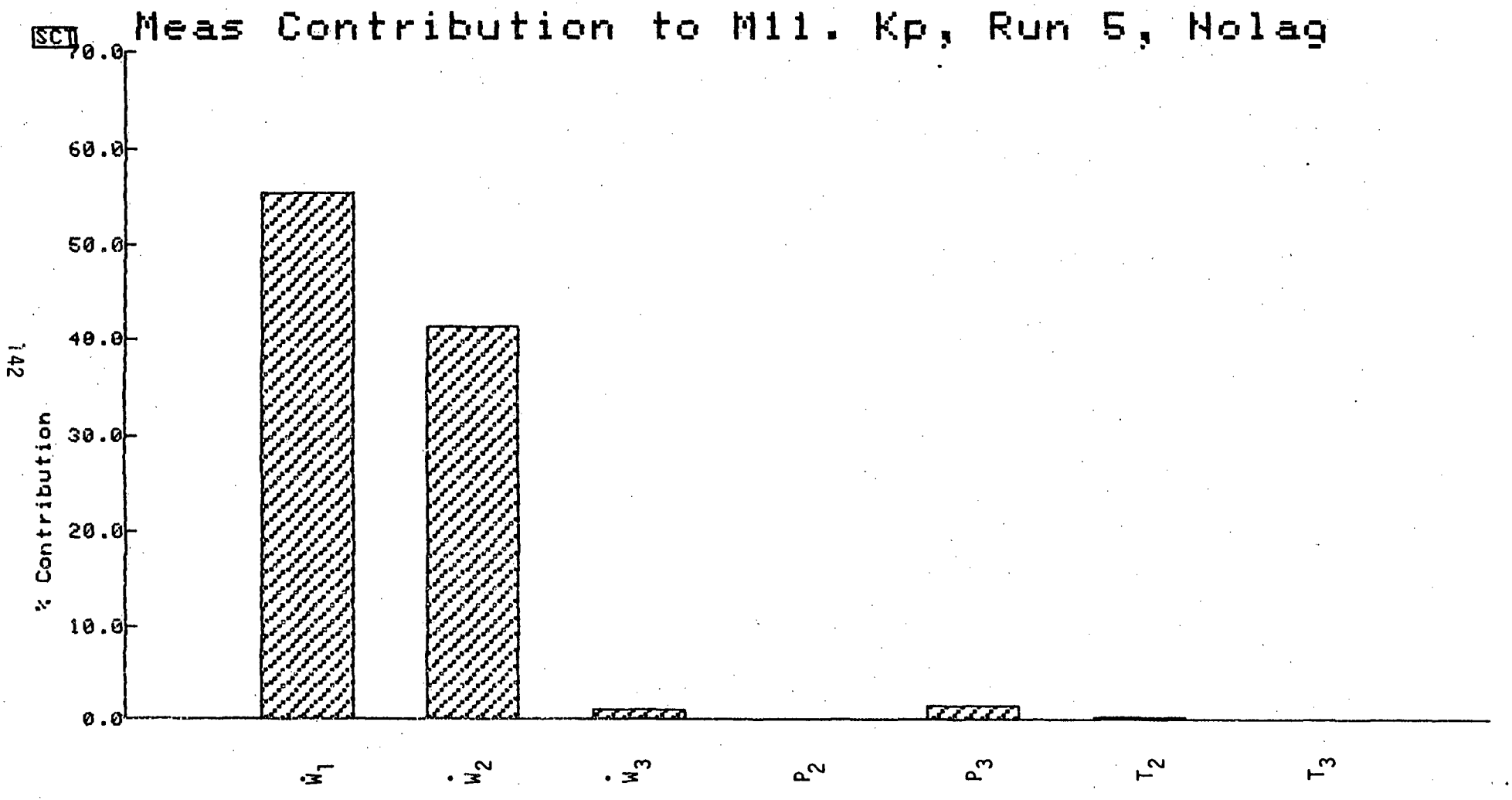

Figure 5.14 Contributions

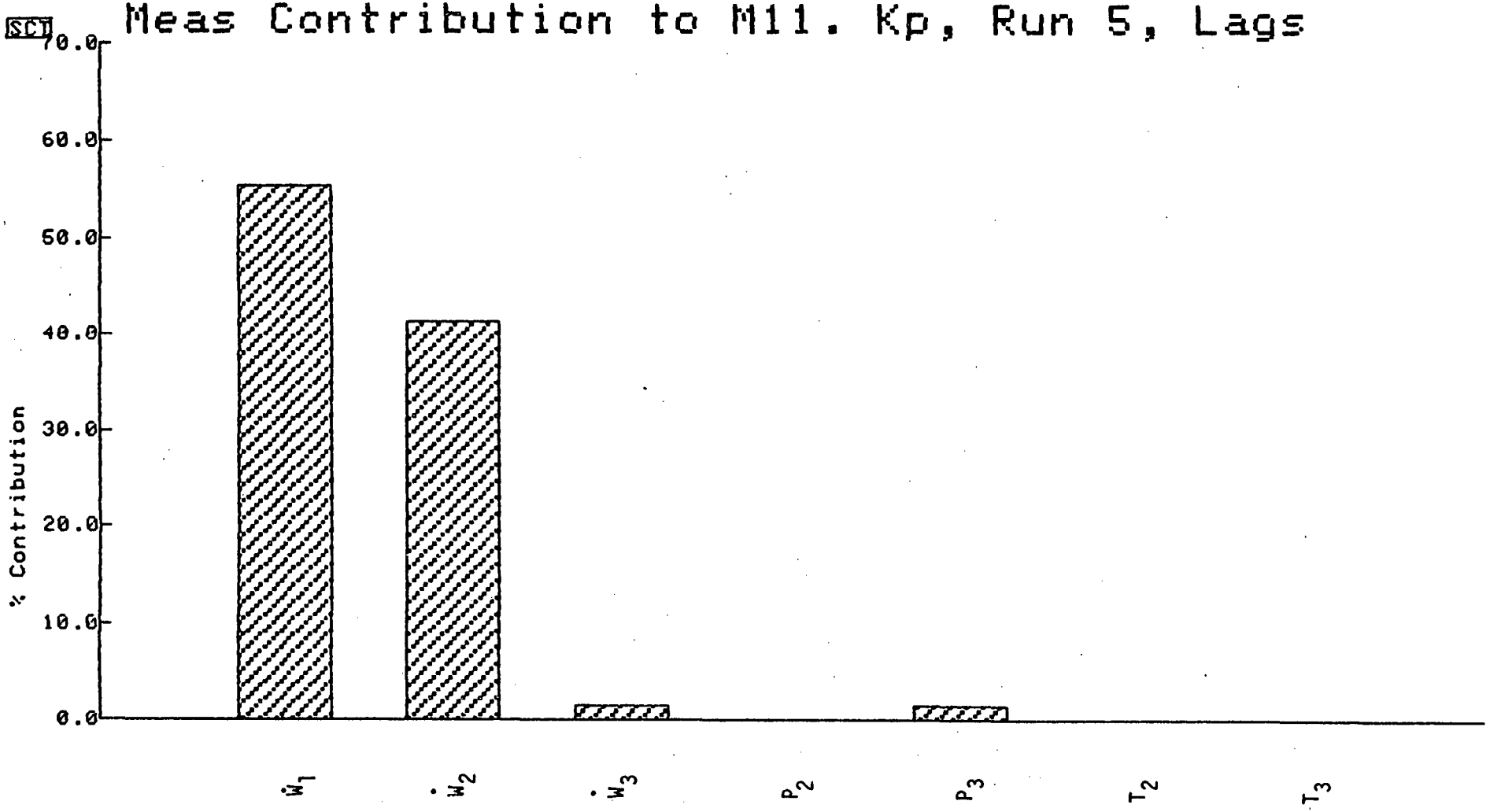

Figure 5.15 Contributions

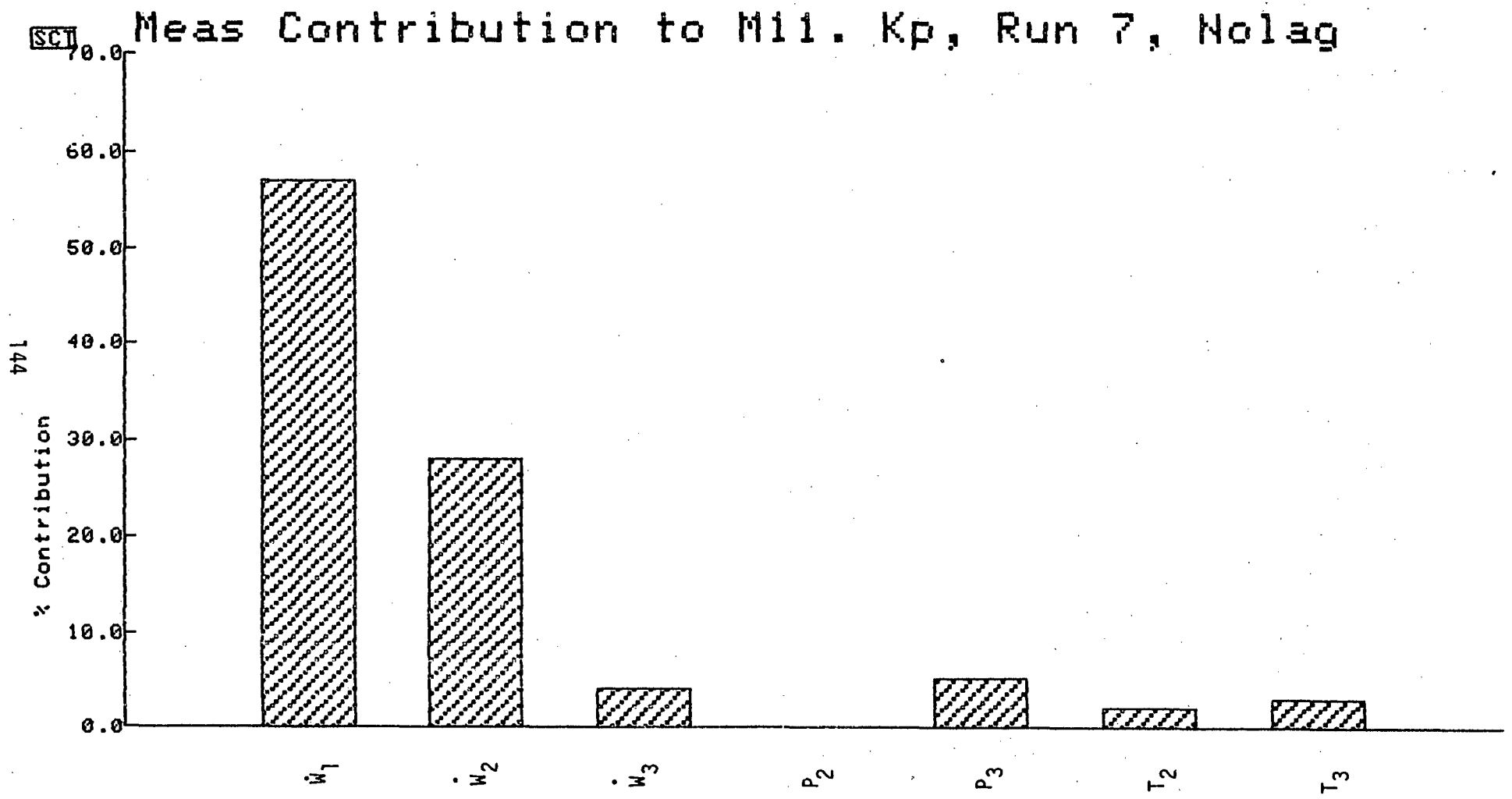

Figure 5.16 Contributions

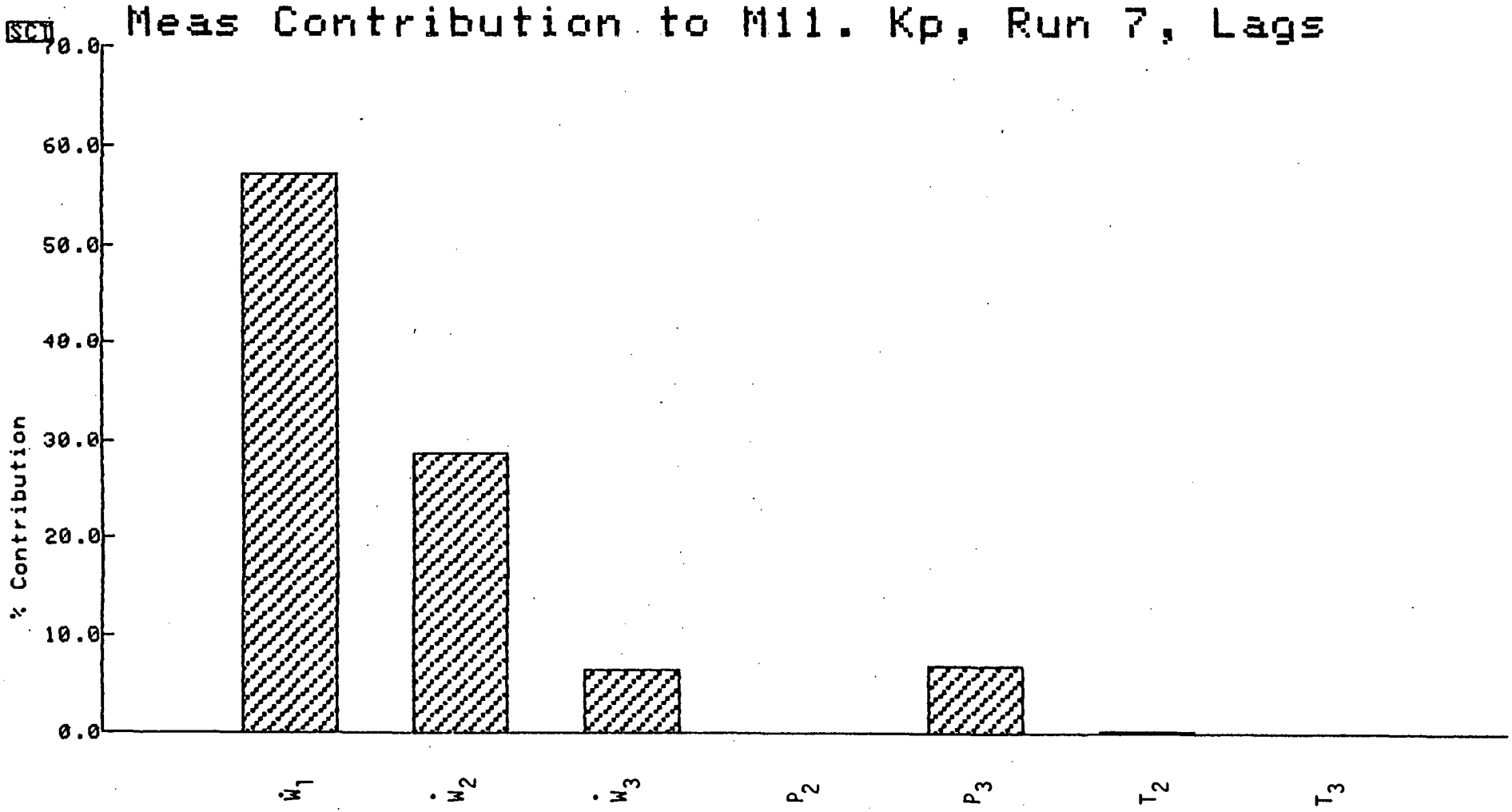

Figure 5.17 Contributions

Similar relationships can be found between exit flow and P3 and T3. Theoretically, P3 alone could identify in-stall compressor maps, but it would have to be a very clean, unbiased sensor.

The measurement contribution software developed at SCT is capable of determining exactly which sensors are most valuable under various noise (and drift) levels. Such an analysis requires a definite model and good estimates of noise and drift levels. If it is known that flow measurements will not be available, it can be determined what kind of accuracy is needed on other parameters (e.g. RO in the above example) and what kind of noise can be tolerated on other sensors so that they can be used as substitutes.

5.3.1.5 Combined Identifiability Results

In the above subsections, identifiability was related to a number of variables: sample rates, number of maneuvers, overall noise levels, sensor-specific noise levels, presence of sensor lags, absence of flow measurements, etc. In this section, these identifiability relationships are unified to illustrate how identifiability and uncertainty can be predicted for almost any measurement system, for both recoverable and non-recoverable stalls.

At a very basic level, one in which the $m(\nu, \theta)$ values for each sensor are known, it becomes possible to predict parameter estimate uncertainties for almost any possible measurement configuration. Table 5.3 lists $m(\nu, \theta)$ values for eight different identification cases considered at 1 kHz. Using the $m(\nu, \theta)$ values as basic building blocks, parameter uncertainties can be obtained for any expected noise level and sampling conditions, for systems with lags and for systems without certain sensors.

Table 5.3
Measurement Contributions (m's)

Case	$\dot{W}1$	$\dot{W}2$	$\dot{W}3$	P2	P3	T2	T3
1	727.	316.	8.16	.00172	9.21	3550.	2560.
2	43.3	18.5	1.65	.000101	1.10	370.	101.
3	684.	221.	5.49	.00162	6.42	3330.	1810.
4	38.9	14.4	.976	.000093	.963	221.	123.
5	24500.	18300.	491.	.0579	627.	7996.	14300.
6	1203.	909.	85.4	.00316	102.	1587.	7234.
7	164.	80.6	12.2	.000389	13.8	431.	1399.
8	37.6	27.3	13.7	.000085	14.5	73.5	89.5

Case	Theta	Run	Conditions
1	Kn	5	Normal
2	Kn	5	Lags
3	Kn	7	Normal
4	Kn	7	Lags
5	Kp	5	Normal
6	Kp	5	Lags
7	Kp	7	Normal
8	Kp	7	Lags

Signal	Sensor Time Constant
$\dot{W}1$, $\dot{W}2$, $\dot{W}3$	27 msec
P2, P3	27 msec
T2, T3	170 msec

Equation (5.8) is the fundamental relationship that allows these $m(\nu, \theta)$ values to be used in conjunction with various kN and $\sigma(y)$ values. Recall that each $m(\nu, \theta)$ value is a function only of the model outputs and the θ values. If a $m(\nu, \theta)$ value is omitted from the sum, the effect is equivalent to omitting a sensor from the measurement system. If a sensor has a lag placed upon it, it does not affect the other $m(\nu, \theta)$ values, so a $m(\nu, \theta)$ value for a lagged sensor can be "swapped" with an unlagged $m(\nu, \theta)$ value. The following is a demonstration of these principles.

Noise Levels (Standard Deviations)

$\dot{W}1$	$\dot{W}2$	$\dot{W}3$	P2	P3	T2	T3
—	—	—	.1470	1.866	2.595	40.33

Sample rate : 5.7 kHZ, 3 maneuvers

Noise Levels : P2 - 1 percent, P3 - 3 percent, T2 - .5 percent, T3 - 4.9 percent

Sensor Set : $\dot{W}$'s omitted, lags on P2 and P3

Run : 5

$$M(Kp) = 3*5.7 * \left[\frac{.00316}{.0216} + \frac{102.}{3.482} + \frac{7996.}{6.734} + \frac{14300.}{1626.} \right]$$

$$\sigma(Kp) = 1 / \sqrt{(M(Kp))}$$

$$= .00691 = 6.91 \text{ percent}$$

Thus, in a scenario with no flow sensors, lags on the pressure sensors, lag-free temperature sensors, a 5.7-kHz sample rate, and three distinct maneuvers, Kp can be identified with 95 percent confidence to within 14 percent. A similar exercise is done for a case that was identified using synthesized data (see Section 5.4.2).

(In doing this example without flow measurements, it is apparent that T2 is the overwhelming contributor of information. In fact, under these noise conditions, the other three sensors could be omitted from the instrumentation with little consequence.)

Several likely sensor scenarios have been considered using the above data. The results are shown below in Table 5.4 and are used to draw a few general conclusion about compressor map parameter identifiabilities and uncertainties.

Table 5.4
Summary of Kn and Kp Uncertainties Under Eight Different Run and Sensor Conditions

Theta	Run	Conditions	sigma	percent chg
Kn	5	Normal	0.2414	—
Kn	5	Temperature Lags	0.2486	2.98
Kn	5	No Flow Meas.	0.8985	272.
Kn	5	T-Lags and No Flows	1.999	728.
Kn	7	Normal	0.2594	—
Kn	7	Temperature Lags	0.2609	0.57
Kn	7	No Flow Meas.	0.9670	273.
Kn	7	T-Lags and No Flows	2.418	832.
Kp	5	Normal	3.092	—
Kp	5	Temperature Lags	3.095	0.10
Kp	5	No Flow Meas.	21.65	600.
Kp	5	T-Lags and No Flows	23.63	664.
Kp	7	Normal	7.668	—
Kp	7	Temperature Lags	7.063	-7.89
Kp	7	No Flow Meas.	23.51	207.
Kp	7	T-Lags and No Flows	25.72	236.

Sigma is the uncertainty at 1-kHz sample rate and 1 percent noise. Uncertainties can be determined at other conditions, sigma need only be multiplied by the kN or $k\sigma$ factors discussed in Sections 5.3.1.1 and 5.3.1.2.

Table 5.4 shows mostly familiar results about uncertainty under various measurement conditions. Temperature lags do little to change uncertainty except when Kn is being identified without flow measurements. (Figures 5.18

through 5.25 indicate this is because P2 and P3 contain little Kn information.) The absence of flow measurements has a profound impact on all identifications; most significantly perhaps in the Kp uncertainties where uncertainty is rather large anyway. Kn is much more identifiable than Kp, and Kp loses about 50 percent of its identifiability if the measured stall is recoverable. (These generalizations are specific to Runs 5 and 7 and may differ in other models.)

Together, Tables 5.3 and 5.4, and Eq. (5.8) combine to produce a valuable tool for not only predicting identifiability but evaluating the quality of identified parameters. They provide a means for evaluating compressor identification runs and can be used to evaluate various sensor set configurations.

5.3.2 Model and Error Effects

Modeling errors can have a large effect on parameter identifications, namely by biasing the estimates. The types of errors considered in this section are grouped into three categories:

(1) estimate parameter biases (the effect of one estimated parameter (in error) upon the estimate of another);

(2) nuisance parameter biases (the effect of an error in a non-estimated parameter such as V2 or RO on an estimated parameter); and

(3) measurement-induced biases errors in estimated parameters (primarily induced by time skews in the data).

Study results show that in-stall compressor map parameters are quite sensitive to a variety of model errors and precautions should be taken in identification to avoid negative identification influences. Specifically, Kp is very sensitive to Kn errors, and both Kn and Kp are sensitive to errors in Ro, V2, V3, and L, errors in sensor time constants, and input time skews.

The primary means for studying these modeling errors is with the use of the bias matrix defined in Section 5.2. Recall the matrix has the form:

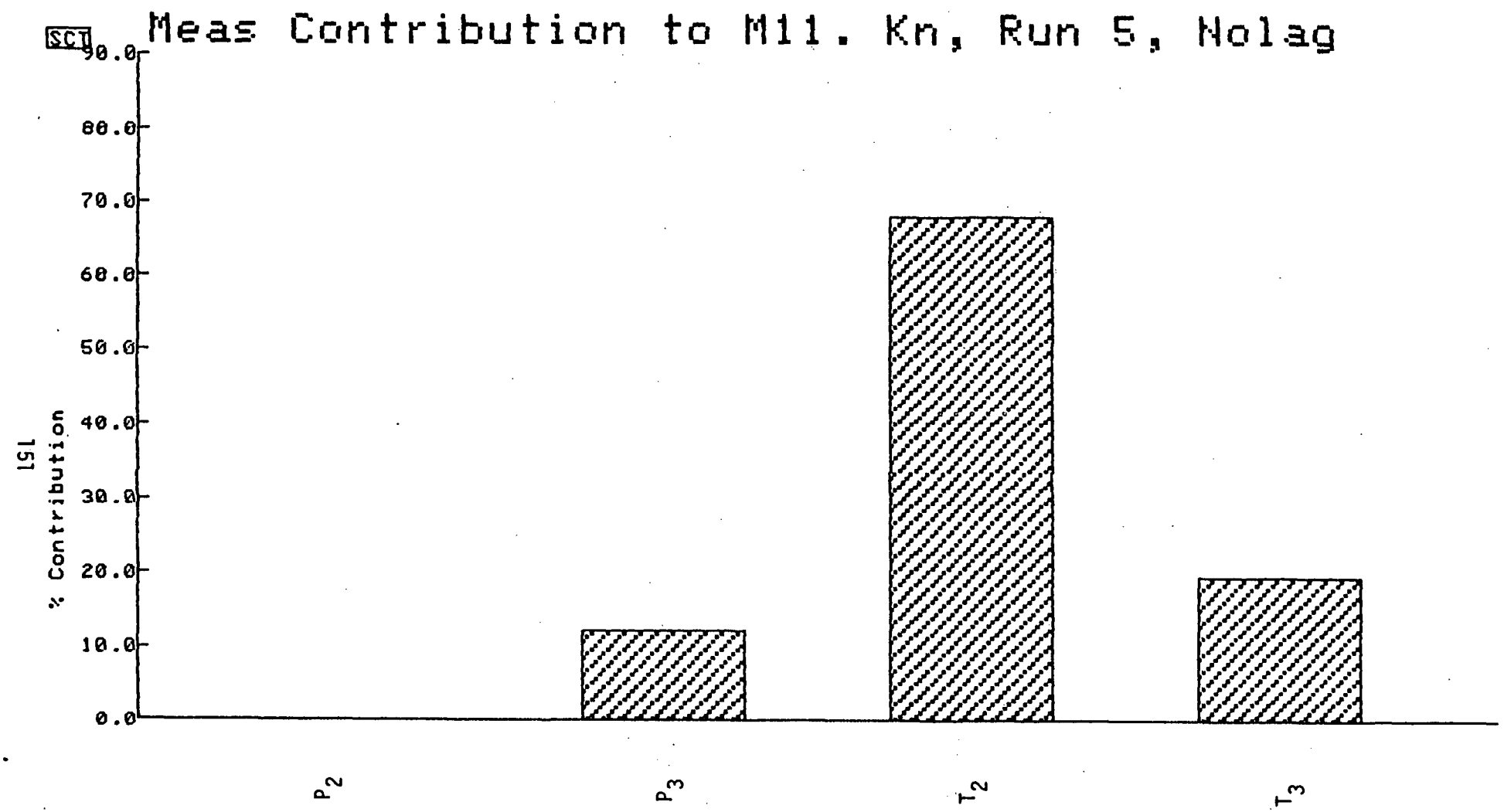

Figure 5.18 Contributions Assuming No Flow Measurements

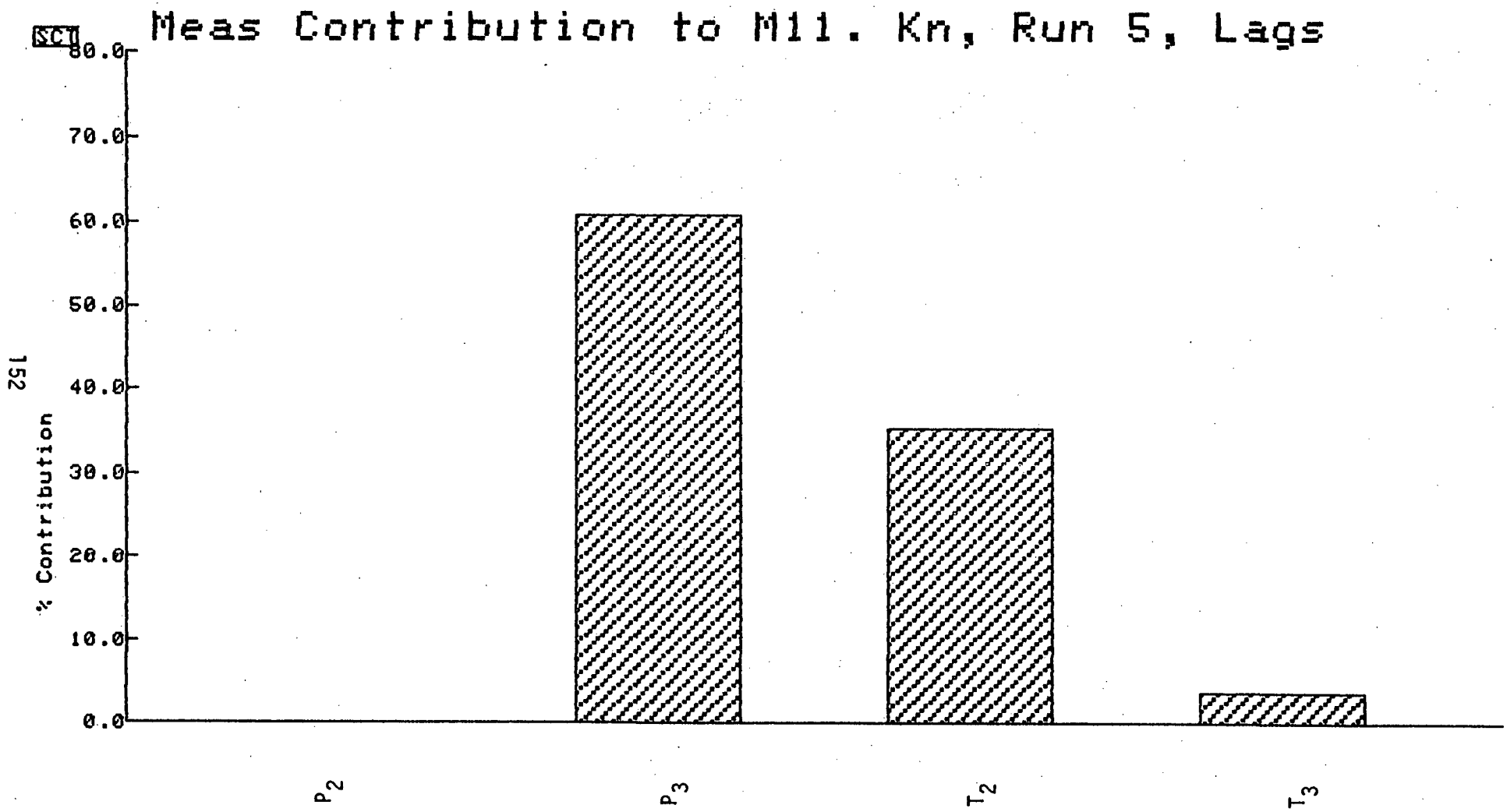

Figure 5.19 Contributions

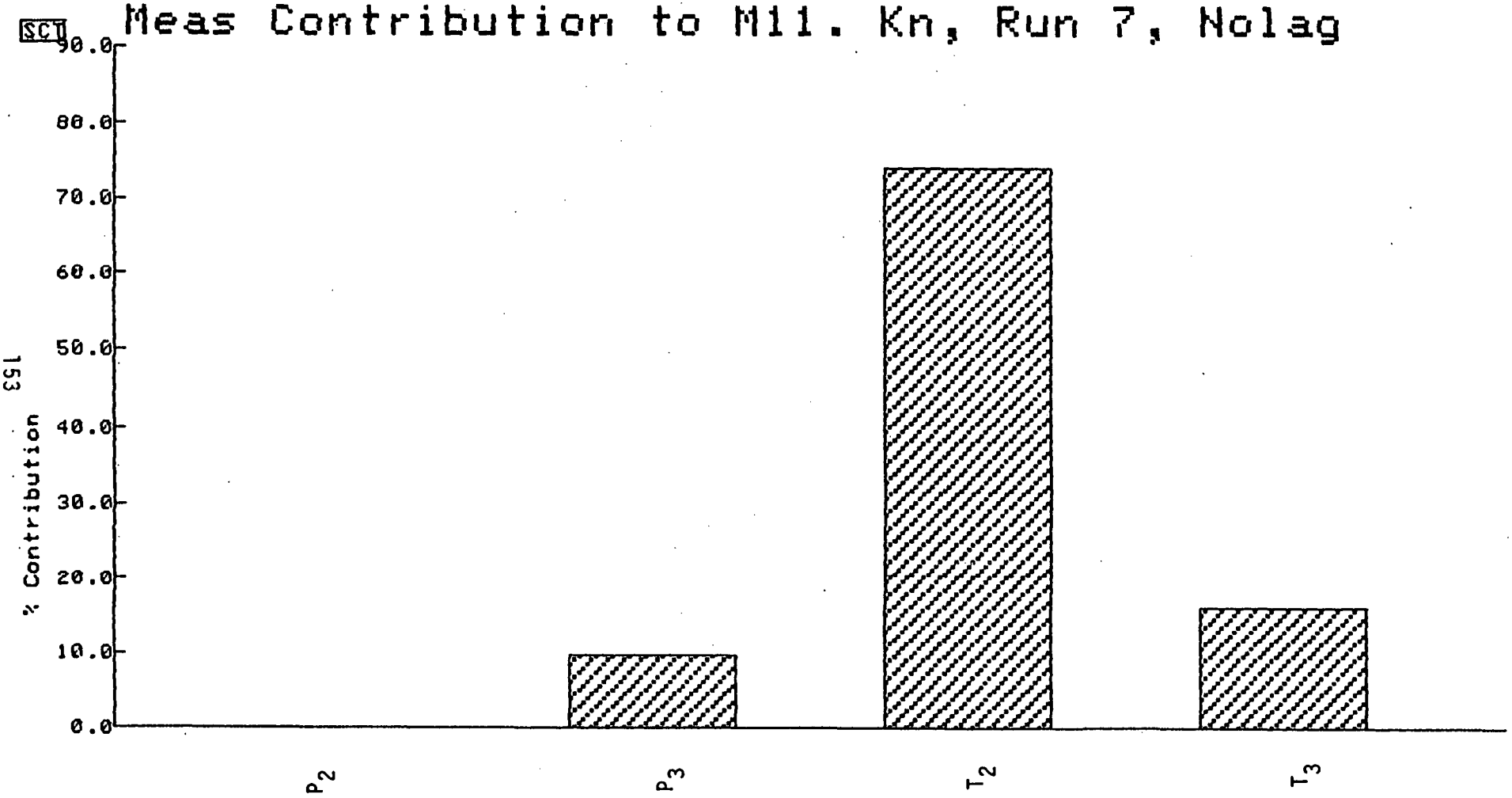

Figure 5.20 Contributions

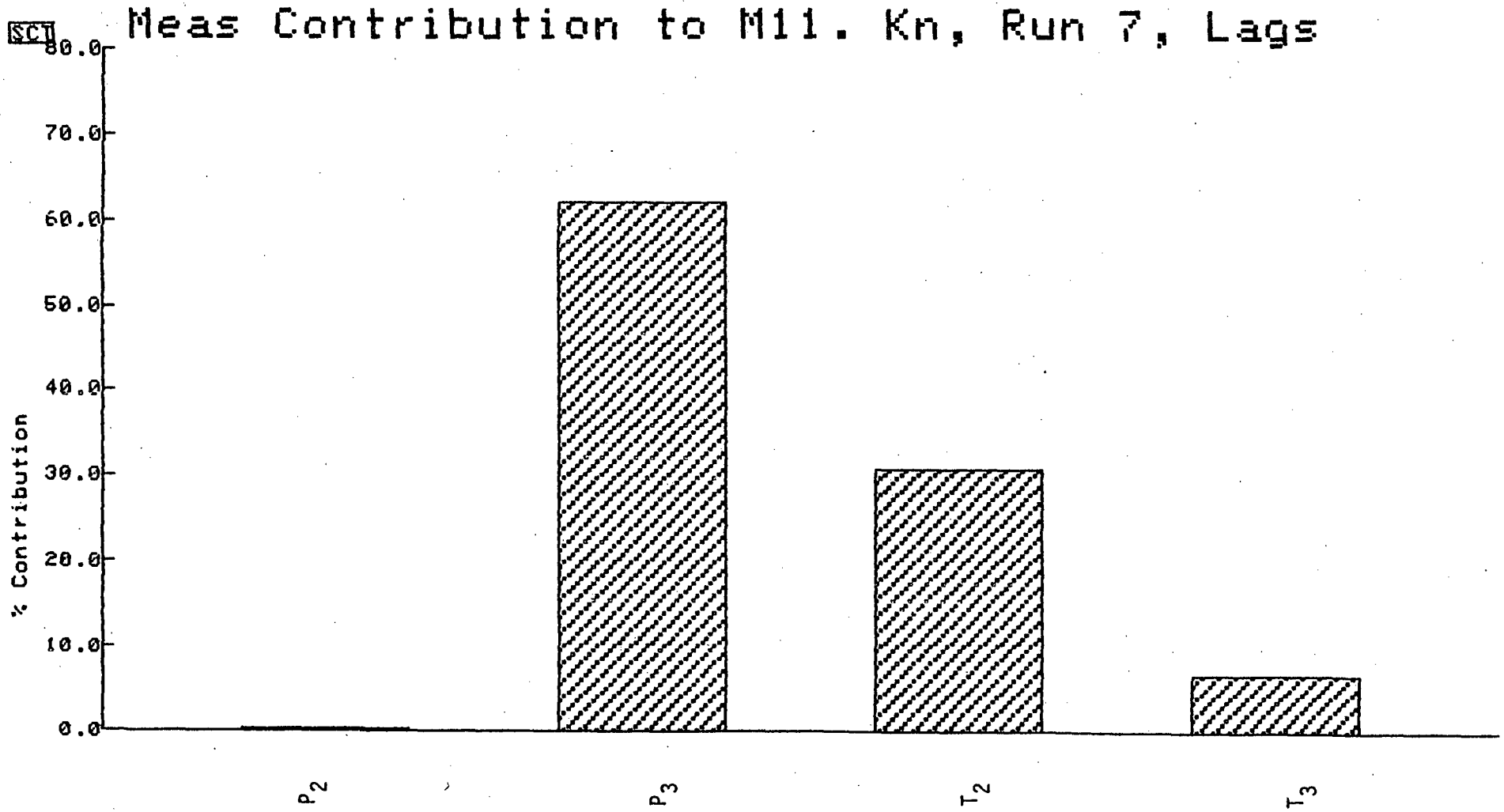

Figure 5.21 Contributions

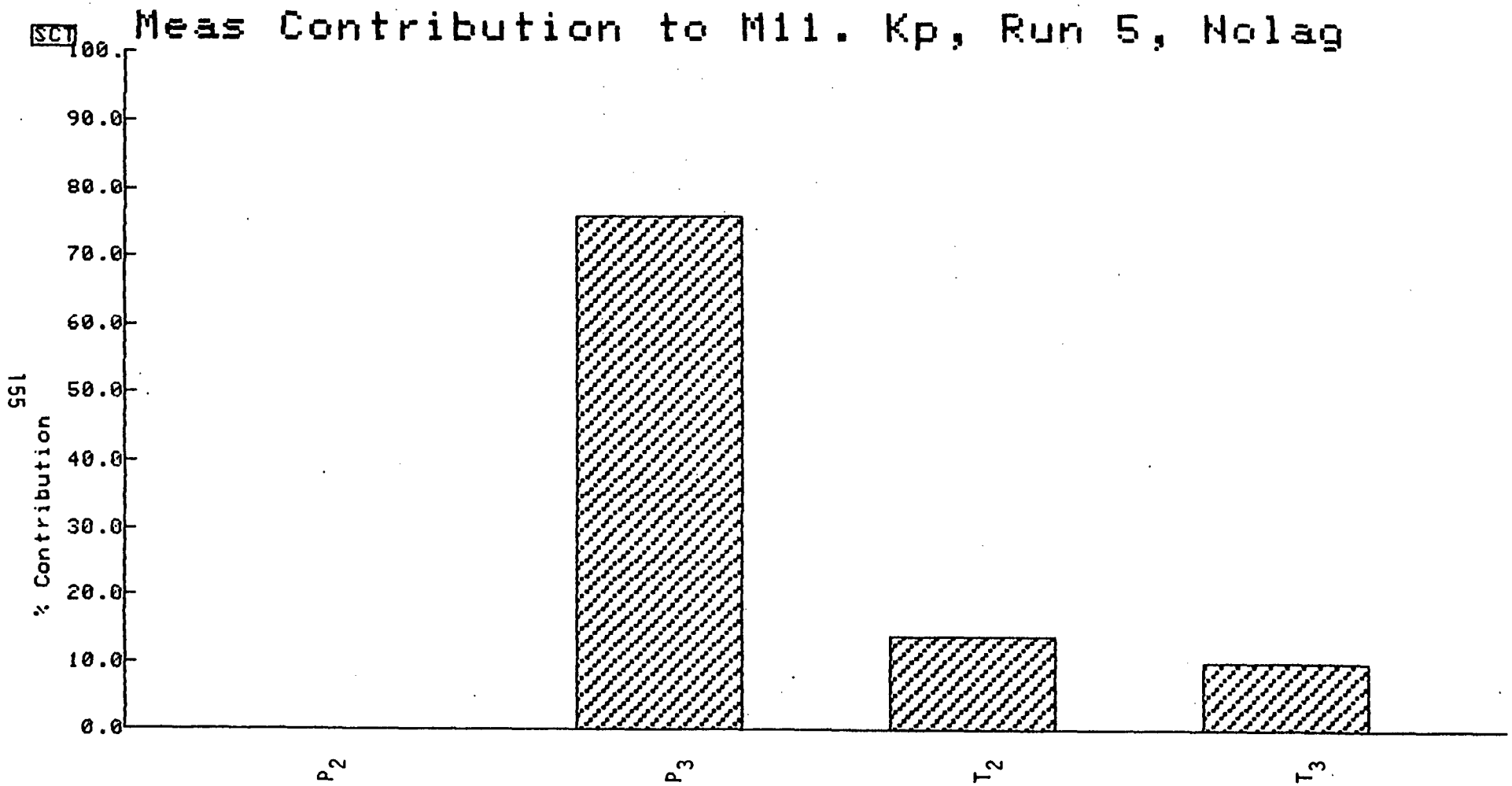

Figure 5.22 Contributions

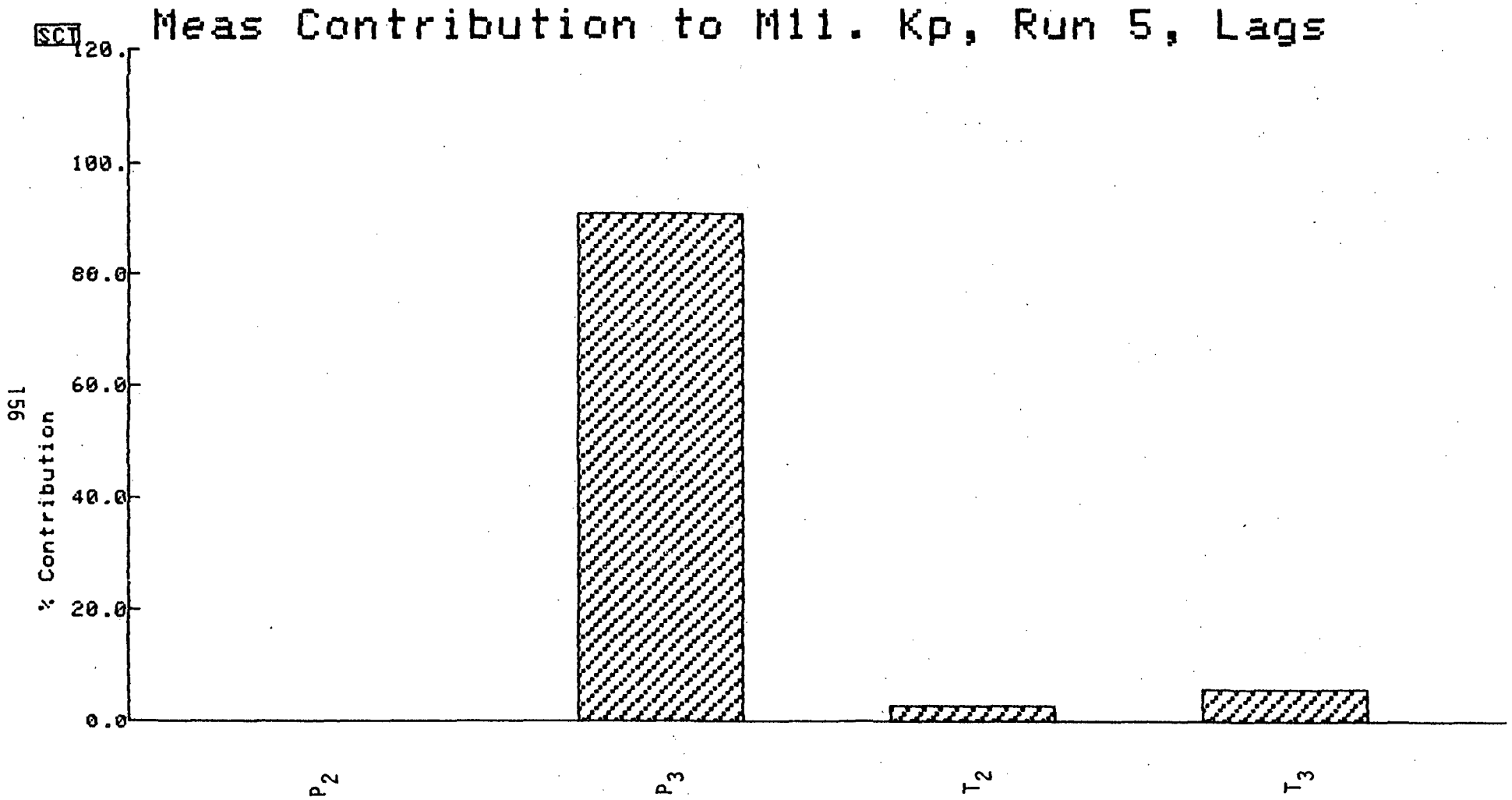

Figure 5.23 Contributions

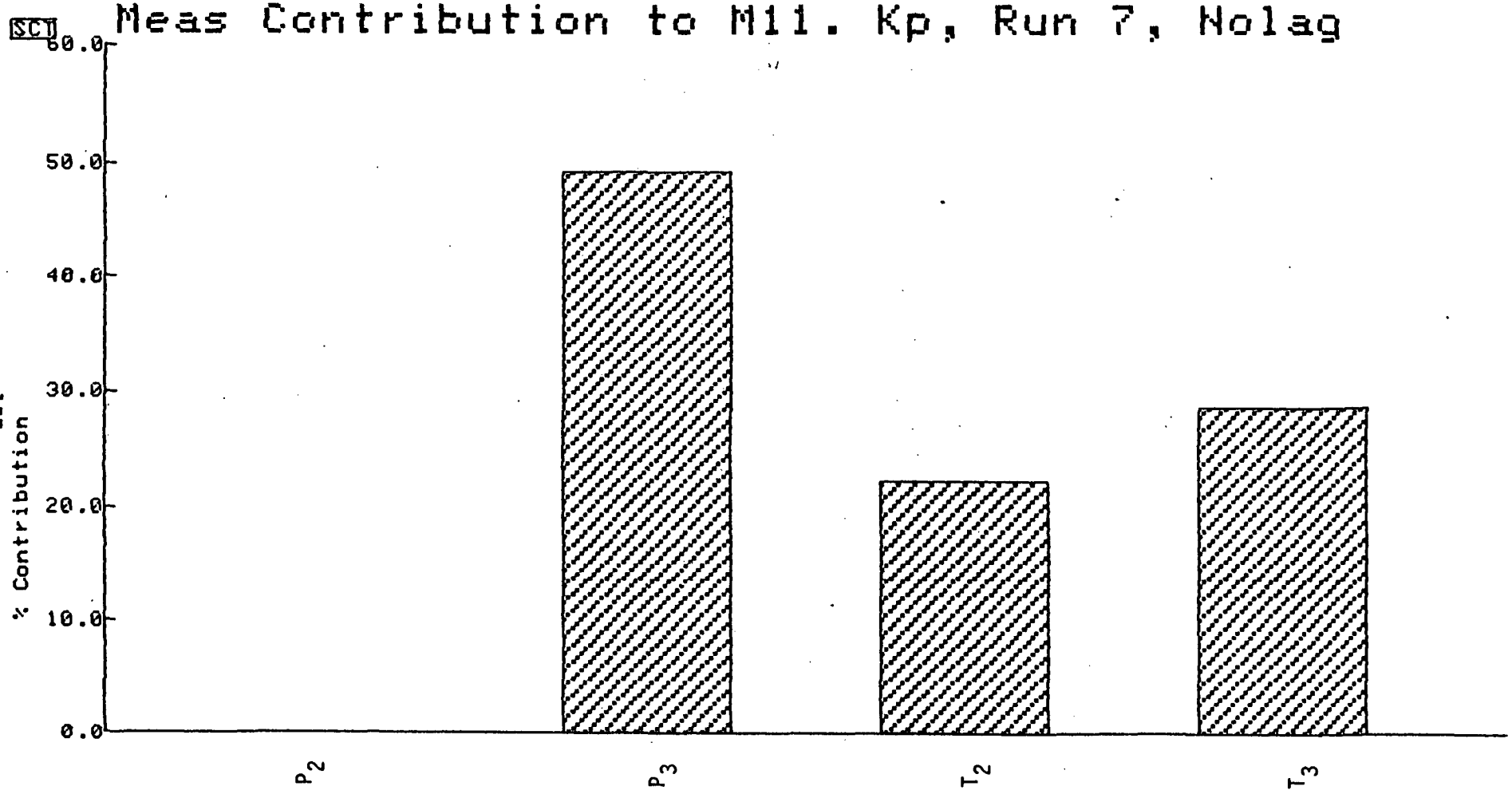

Figure 5.24 Contributions

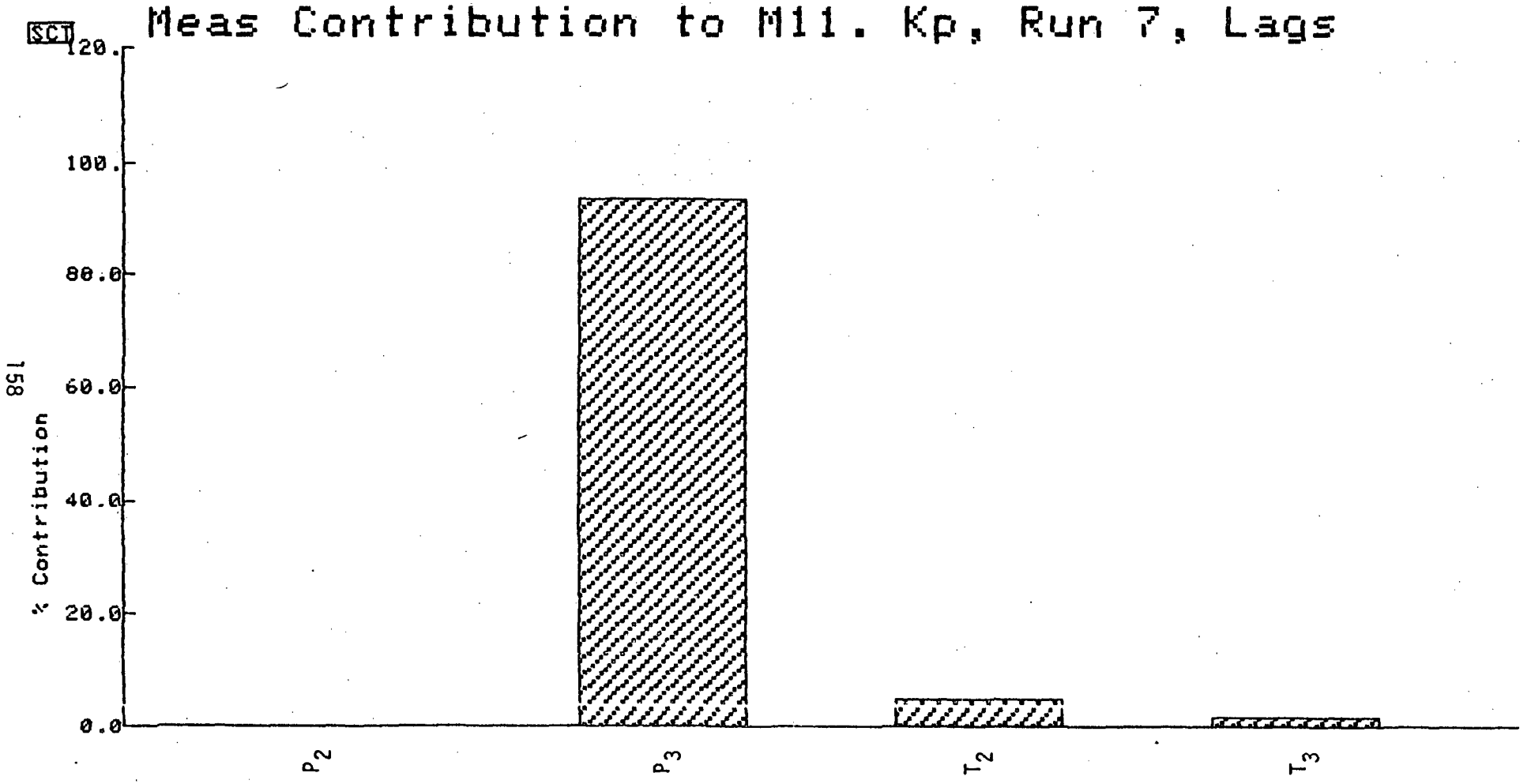

Figure 5.25 Contributions

$$X_b = M_{11}^{-1} M_{12} = E\left\{ \frac{\partial \theta'}{\partial J} \frac{\partial \theta}{\partial J} \frac{\partial J}{\partial \theta} \frac{\partial J'}{\partial \phi} \right\}$$

$$= E\left\{ \frac{\partial \theta}{\partial \phi} \right\} \qquad (5.9)$$

where

X_b = bias matrix

The matrix measures estimate parameter "sensitivity" (a measure of how much an estimate parameter is biased by a nuisance parameter error). X_b depends upon sensor noise levels which are a part of J, therefore, biases are expected to vary under different noise conditions.

5.3.2.1 Estimate Parameter Biases

Noise effects can affect parameter estimate biases by adding uncertainty. However, study of the noise levels observed in the compressor rig indicated that noise was not responsible for the more significant estimate errors. The most probable source of estimate parameter errors eminates from within the estimate parameters themselves. In Chapter IV it was discussed how the Kn and Kp parameters must be identified separately because of the two-stage nature of the stalled model. It was also explained that because Kp is highly sensitive to Kn, Kn must be as near its actual value as possible before Kp is identified. The conclusion in Chapter IV was that Kn must be identified before Kp so that any error in Kn will have a minimal effect on Kp. This section quantifies this effect and demonstrates that even slight Kn errors can cause significant Kp errors and may have strongly affected the Kp identifications.

Table 5.5 contains the normalized bias matrix (scalars) relating Kp to Kn (and vice versa) for Runs 5 and 7 at 1 percent noise levels. The normalized bias matrices, or sensitivities, indicate what percent bias will be induced in the estimated parameter (Kp or Kn) given a bias in the other parameter. Generally, Kn has a greater effect on Kp than vice versa. The magnitude of the Kp sensitivity is quite significant considering that Kn is likely to be in error considering identifiability limitations (uncertanties).

Table 5.5
Kn and Kp Normalized Bias Matrices (Scalars)

Kp Bias due to Kn (Run 5) :	4.968
Kp Bias due to Kn (Run 7) :	17.98
Kn Bias due to Kp (Run 5) :	.0308
Kn Bias due to Kp (Run 7) :	.0117

The sensitivity values provide a good indication of relative sensitivities, yet it is important to know just how well they can predict actual biases considering the nonlinear nature of the compressor model. A study was made by identifying Kn with biases in Kp (and vice versa) for Runs 5 and 7. The identifications were made with noise free measurement data so that the uncertainties in the final identified values would be minimal.

Results of the study are shown in Figures 5.26 through 5.29. Generally, the results indicate that the bias matrix and a first order prediction are well able to predict estimate parameter-induced biases. Thus, the sensitivities in Table 5.5 can be used with reasonable confidence to predict Kp and Kn biases in model runs 5 and 7, and can be used to guestimate biases in other non-recoverable and recoverable models.

The value of this result cannot be understated. It is likely that this estimate parameter bias effect is one of the primary sources of parameter estimate error encountered in the identifications documented in Chapter IV.

5.3.2.2 Dimensional Parameters

This section examines the effects of "fixed" compressor model parameters on the identification of KP and KN. The parameters studied are RO, V2, V3 and L, inlet resistance, stage 2 volume, stage 3 volume, and compressor flow inductance, respectively. The study differs slightly from the previous study in that it uses Run 4 instead of Runs 5 and 7 for a base model.

A normalized bias matrix for dimensional parameter sensitivities is shown below. (The matrix is normalized to nominal values of KP, KN, RO, V2, V3, and L.)

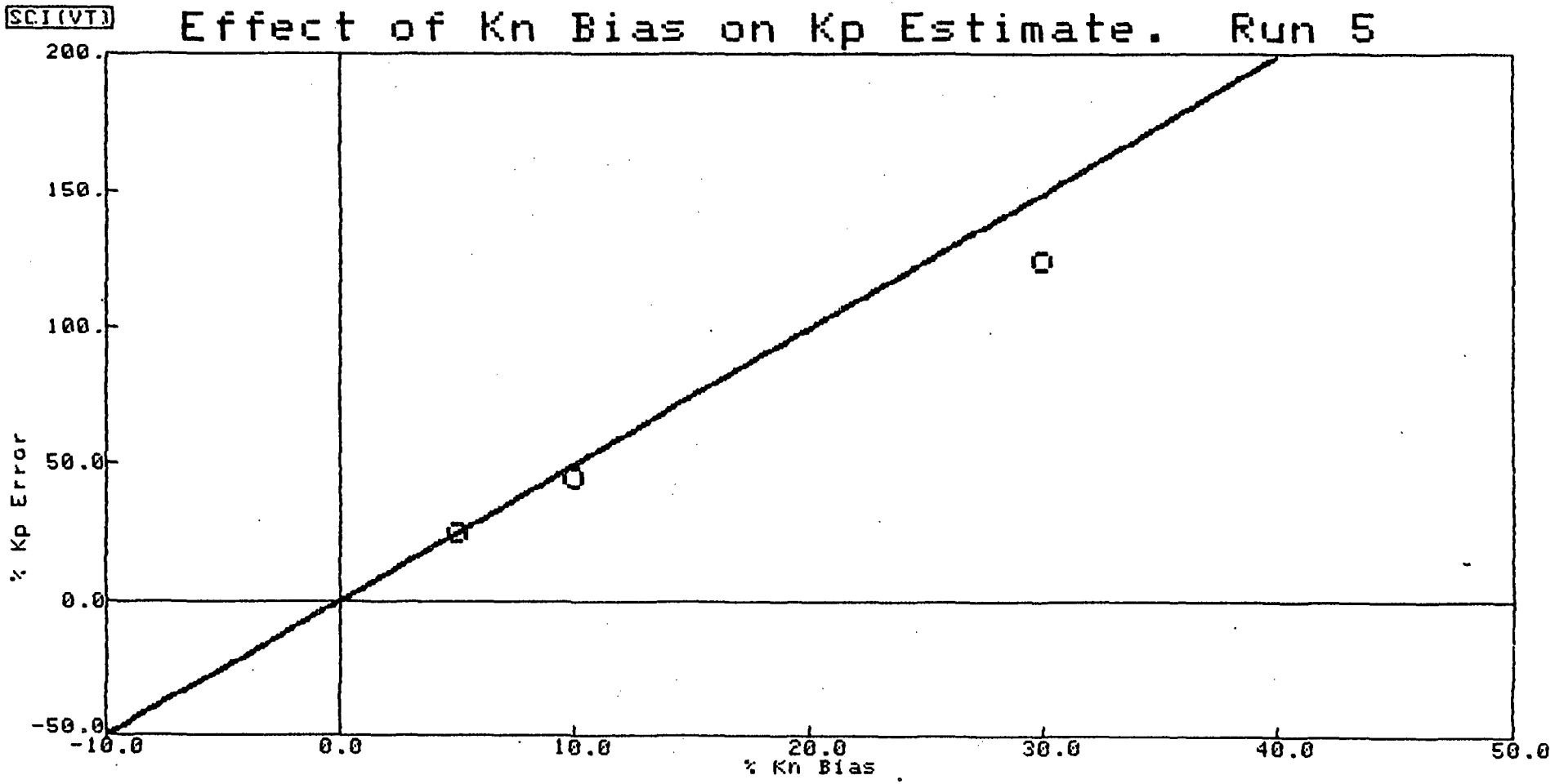

Figure 5.26 Kn as a Nuisance Parameter, Theory and Three Test Results

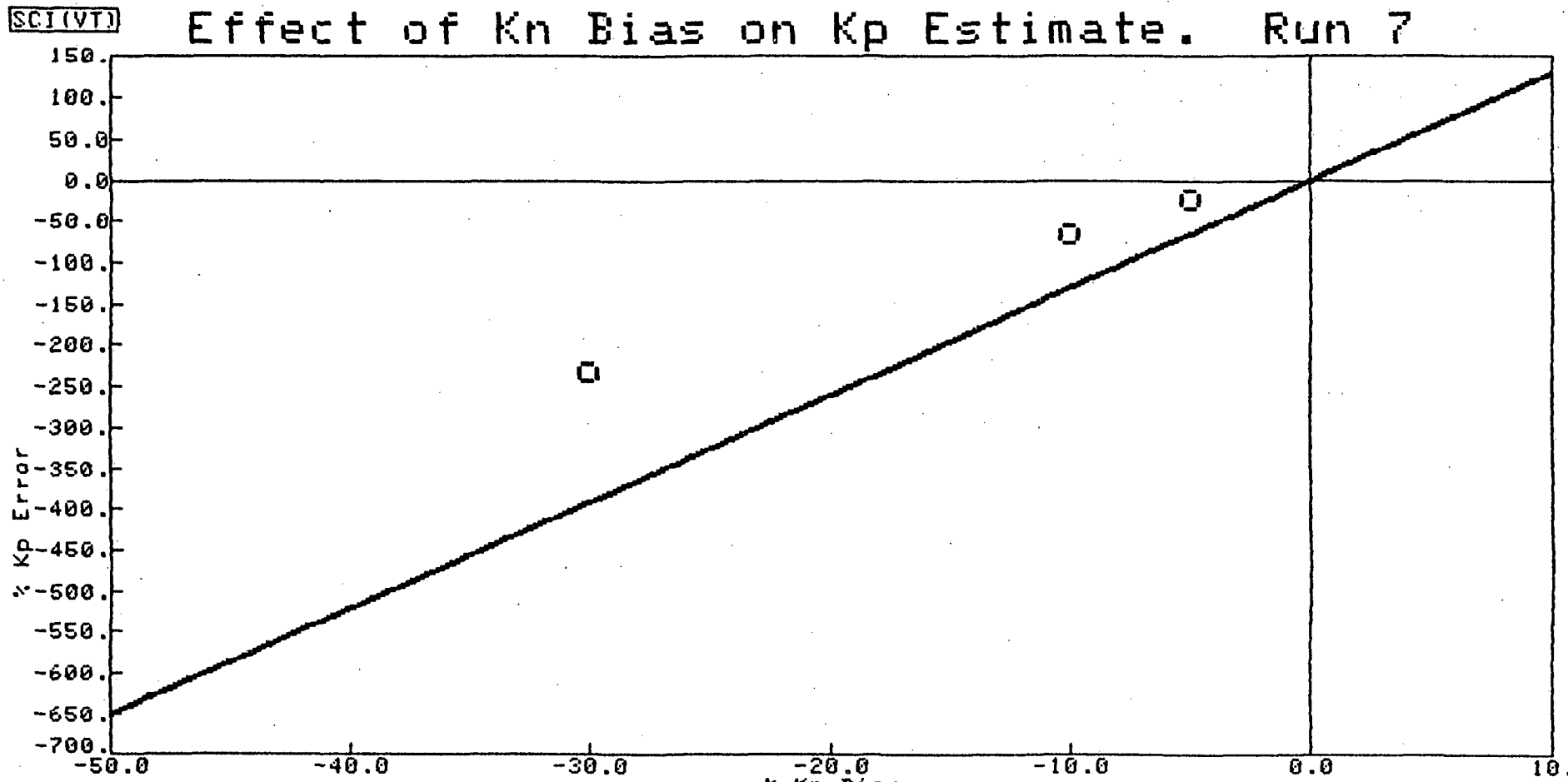

Figure 5.27 Kn as a Nuisance Parameter, Theory and Three Test Results

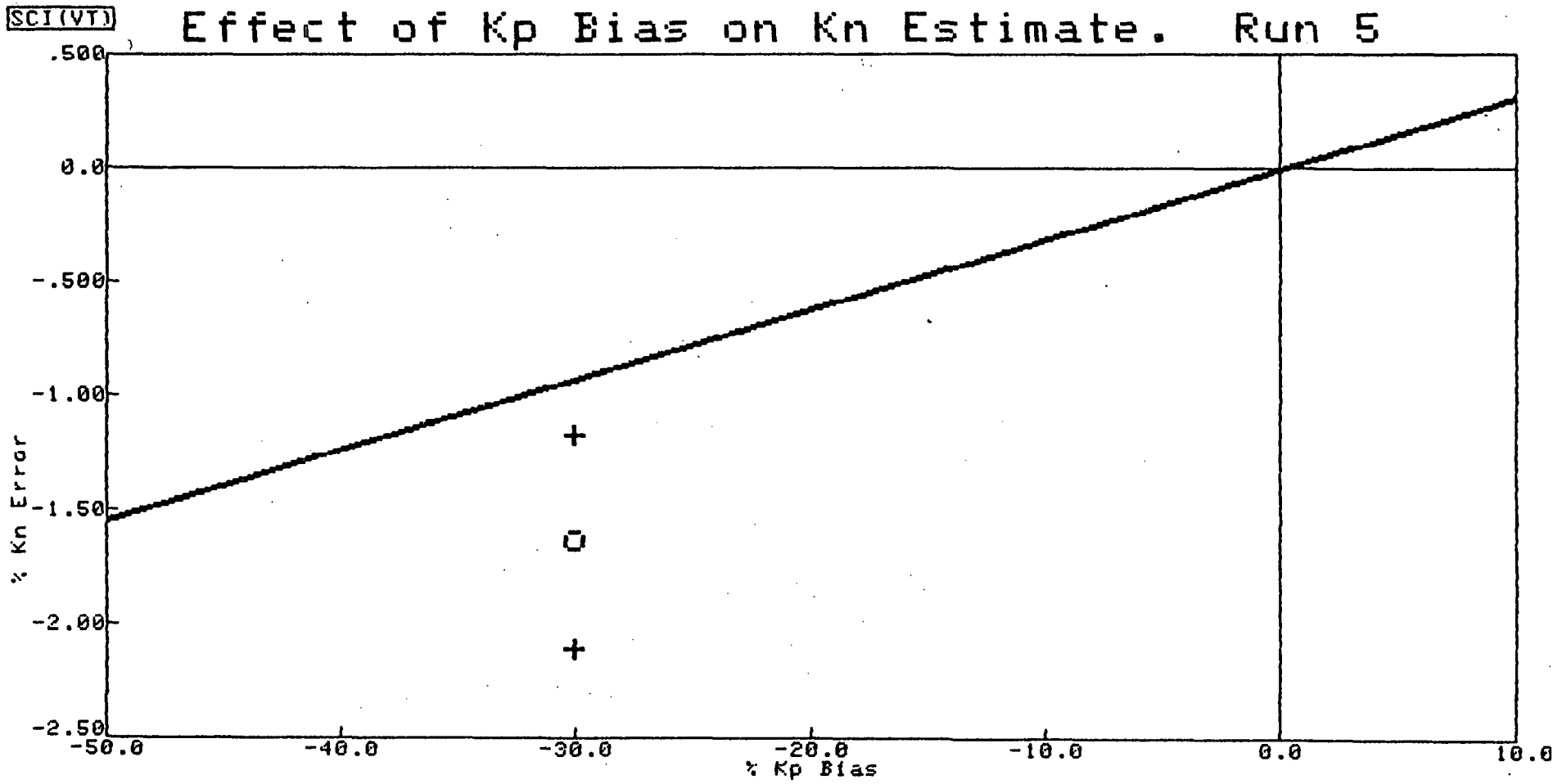

Figure 5.28 Kp as a Nuisance Parameter, Theory and One Test Point with a 2σ Bound

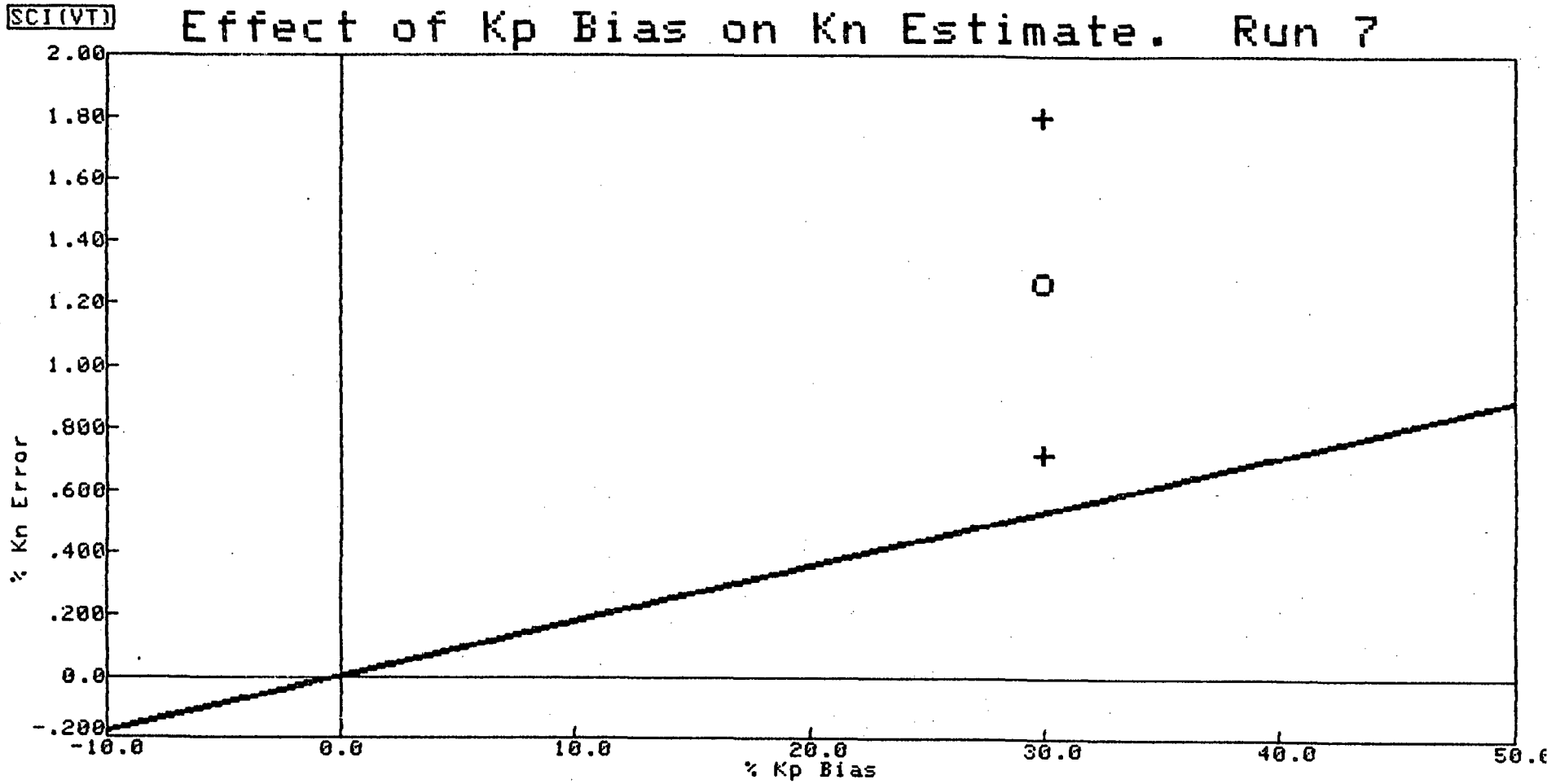

Figure 5.29 Kp as a Nuisance Parameter, Theory and One Test Point with a 2σ Bound

	RO	V2	V3	L
KP	-0.06199	0.5542	-2.6920	-0.5018
KN	0.8562	-0.1758	-0.3890	-0.08378

The normalized matrix indicates that a 1 percent error in V3 would produce a -2.692 percent error in the Kp estimate, a 5 percent error would produce a -13.45 percent error. Other example effects of five percent errors in the "fixed" dimensional parameters are summarized Table 5.6.

Table 5.6
Percent Bias Expected in Estimate Parameters Due to 5 Percent Errors in "Fixed" Dimensional Parameters

in	due to	RO	V2	V3	L
KP		-0.3099	2.771	-13.46	-2.510
KN		4.28	0.879	1.945	0.419

Kp and Kn are quite sensitive to the value of V3. In fact, Kp and Kn are fairly sensitive to all of the dimensional parameters considered, indicating that stalled compressor map parameters are highly dependent upon the compressor model structure and its parameters.

5.3.2.3 Sensor Lags

Parameter identifications can also be influenced by errors in estimated time lag constants. In this analysis, all sensors are assumed to have first order sensor lag characteristics, and the modeled sensor lags have time constant errors. The results show that time constant errors can significantly bias K-parameter estimates and should be given worthy attention in the identification process.

The time constants chosen for each sensor are characteristic of what can be expected in a test-cell.

Table 5.7
Sensor Time Constants

Signal	Sensor Time Constant
$\dot{W1}$, $\dot{W2}$, $\dot{W3}$	27 msec
P2, P3	27 msec
T2, T3	170 msec

Two bias matrices were determined for Runs 5 and 7. The results are listed in Table 5.8.

Table 5.8
Normalized K-Parameter Sensitivities Errors
in Modeled Time Constants

Run 5:

	$\dot{W1}$	$\dot{W2}$	$\dot{W3}$	P2	P3	T2	T3
Kn	2.585	1.265	.0281	.0001	.2220	.2710	.0198
Kp	8.335	4.489	2.769	.0004	2.649	1.850	-.2060

Run 7:

	$\dot{W1}$	$\dot{W2}$	$\dot{W3}$	P2	P3	T2	T3
Kn	3.110	1.359	.1567	.0001	.1610	.1670	.0158
Kp	6.502	3.420	1.199	.0002	2.240	5.814	.3138

The normalized bias matrix indicates that a 5 percent error in any of several time constants could produce at least a 15 percent error in Kn or Kp estimates. It appears that, given that so much information is already lost with the sensor lags, any corruption of the information resulting from improper sensor models has a severe effect upon the identification process. The normalized bias matrices also follow the same proprtions as the measurement contributions. This is expected since an error in a "valuable" signal would likely have a large impact on the identification process.

Significant efforts must be made in future identifications to understand the effects of sensor time constant errors and to devise procedures (e.g., identification) to minimize the errors and their effects.

5.3.2.4 Time Skews

Timing skews in measurement data also effect the identification of Kp and Kn. Results indicate that timing skews may have a large effect upon the identification of Kp and Kn.

Using the same procedure as above with Run 4 as a model basis, a bias matrix was produced to relate the estimate parameters to the nuisance parameters. In this case, the nuisance parameters are now, dlayU1, dlayY1, dlayY2,... dlayY7, and the estimate parameters remain Kp and Kn. DlayU1 is a time quantity representing the amount of time U(1), or Knoz, is skewed from the rest of the measurement data. dlayY1 is a similar quantity for the Y(1) measurement, W1dot. Each signal was perturbed by 0.1 milliseconds to produce the bias matrix shown below:

Normalizing the bias matrix to nominal values of Kp and Kn and millisecond delay values yields:

	Knoz	$\dot{W}1$	$\dot{W}2$	$\dot{W}3$
KP	6.997E-01	1.359E-04	1.639E-06	-8.290E-07
KN	5.340E-02	-2.318E-04	-7.713E-07	3.987E-07

	P2	P3	T2	T3
KP	5.155E-09	-1.190E-06	-5.570E-06	-1.436E-07
KN	-8.767E-09	5.724E-07	2.681E-08	6.900E-08

A value of 0.2 msec was chosen to represent a possible time skew value. Skews of this size in the output values have minimal impact on the identification of Kp and Kn, and yet a 0.2 msec skew between output values and the input signal would produce a 1 percent error in Kn and a 14 percent error in Kp. A skew in this area could cause substantial identification problems.

It is not necessary that time skews appear in the recording process for them to appear during identification. Other influences may produce the same effects. Recall from Chapter IV that special action (identification of a new throttling coefficient) had to be taken in order to synchronize the onset of stall between measured data and the SCT model. Despite this action, a time skew remained (see Run 11). This is one way in which an apparent time skew can appear in the identification process. It is likely that such skews, in smaller magnitudes, contributed to the errors in the compressor model identifications.

5.4 EXAMPLE RESULTS

Section 5.3 demonstrated the usefulness of uncertainty (identifiability) and sensitivity tools. In demonstrating these tools, a few theoretical examples were given, most notably in the effect of sample rates and estimate parameter biases. This section illustrates how these tools can be successfully applied to actual identification problems.

5.4.1 Six Example Cases

Six example identification cases were chosen to study the accuracy of the uncertainty theories. The cases are all based upon Run 5 but consider various noise level, sensor lag, and limited sensor set configurations. The measurements used in the identification were generated by SCT and are shown in Figures 5.30 through 5.35. The uncertainty predictions of the study were extremely accurate, and the formulae developed in Section 5.3.1 successfully predicted identifiability.

A description of the six example cases is given below in Table 5.9. Also listed are the uncertainties predicted with the given noise levels, sensor lags and sensor sets applied to the formulae of Eq. (5.8). Sensor time constants are found in Table 5.7, sample rate is 1 kHz, and "no W's" means no flow measurements were used in identification. The estimated noise levels are shown in Table 5.10. (These values may be higher than actual values because a slightly different process was used to add the noise.)

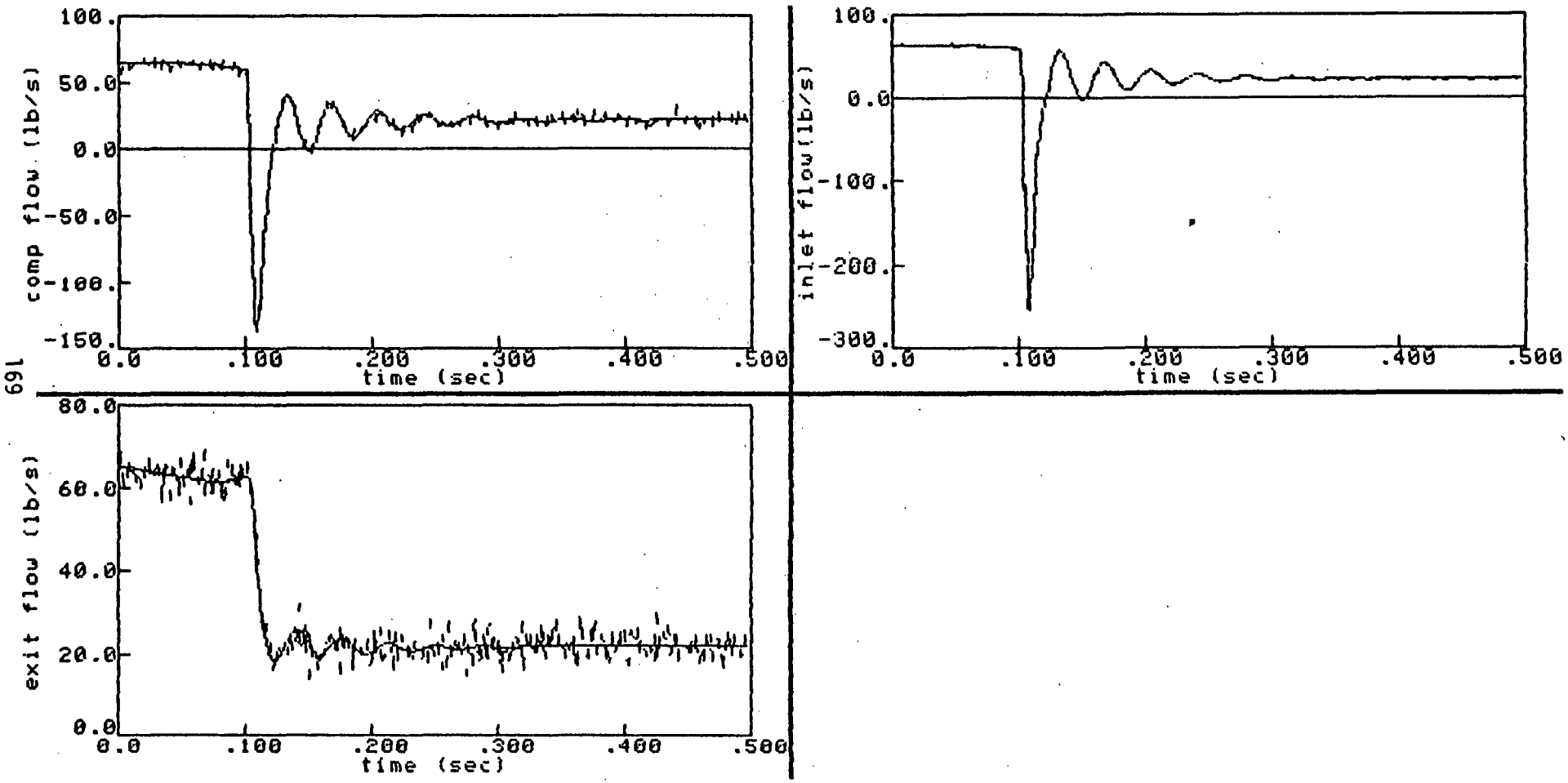

Figure 5.30 Run 5 Test Case with Noise (Identified, solid line; Measured, dashed line)

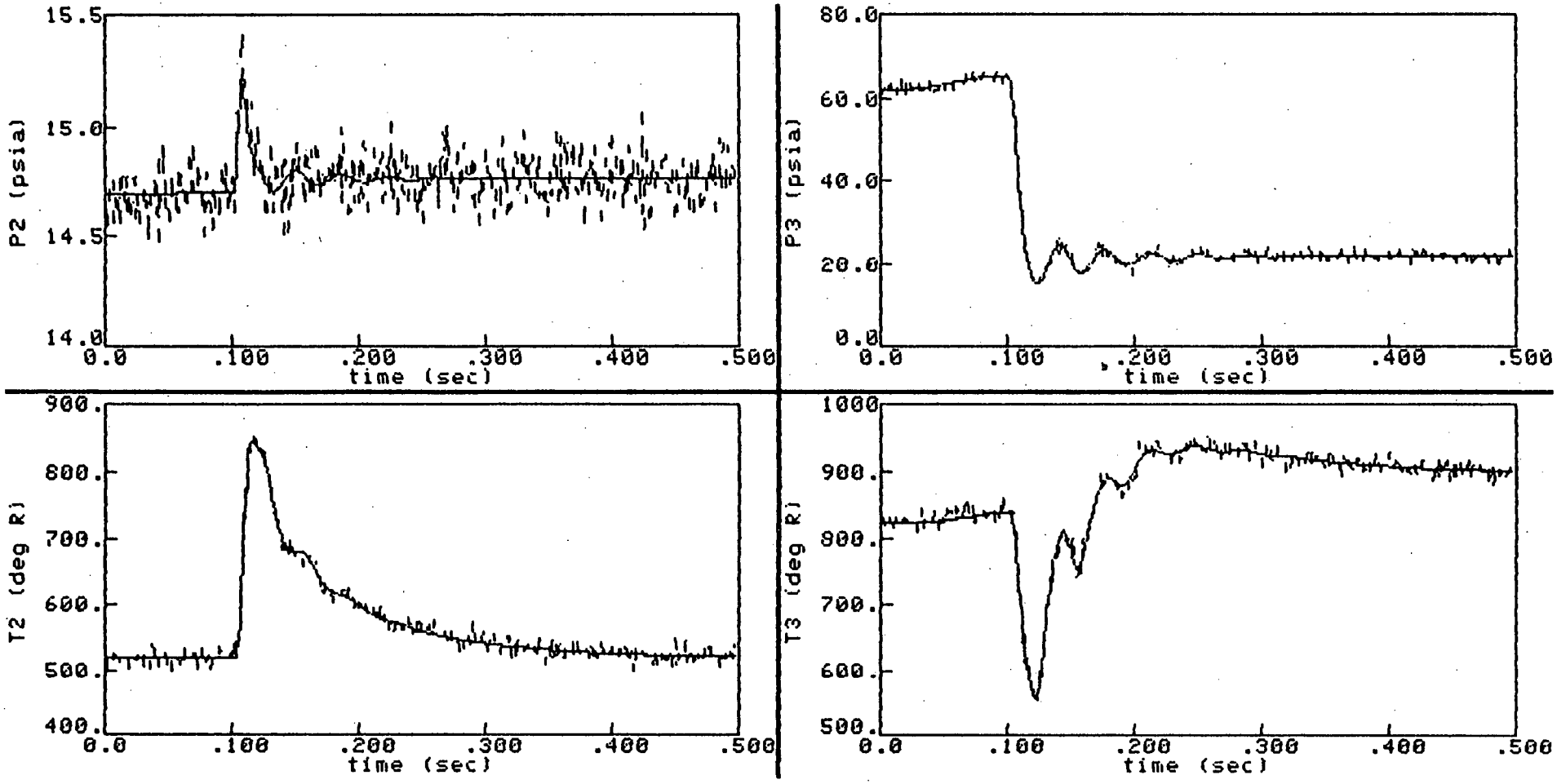

Figure 5.31 Run 5 Test Case with Noise (Identified, solid line; Measured, dashed line)

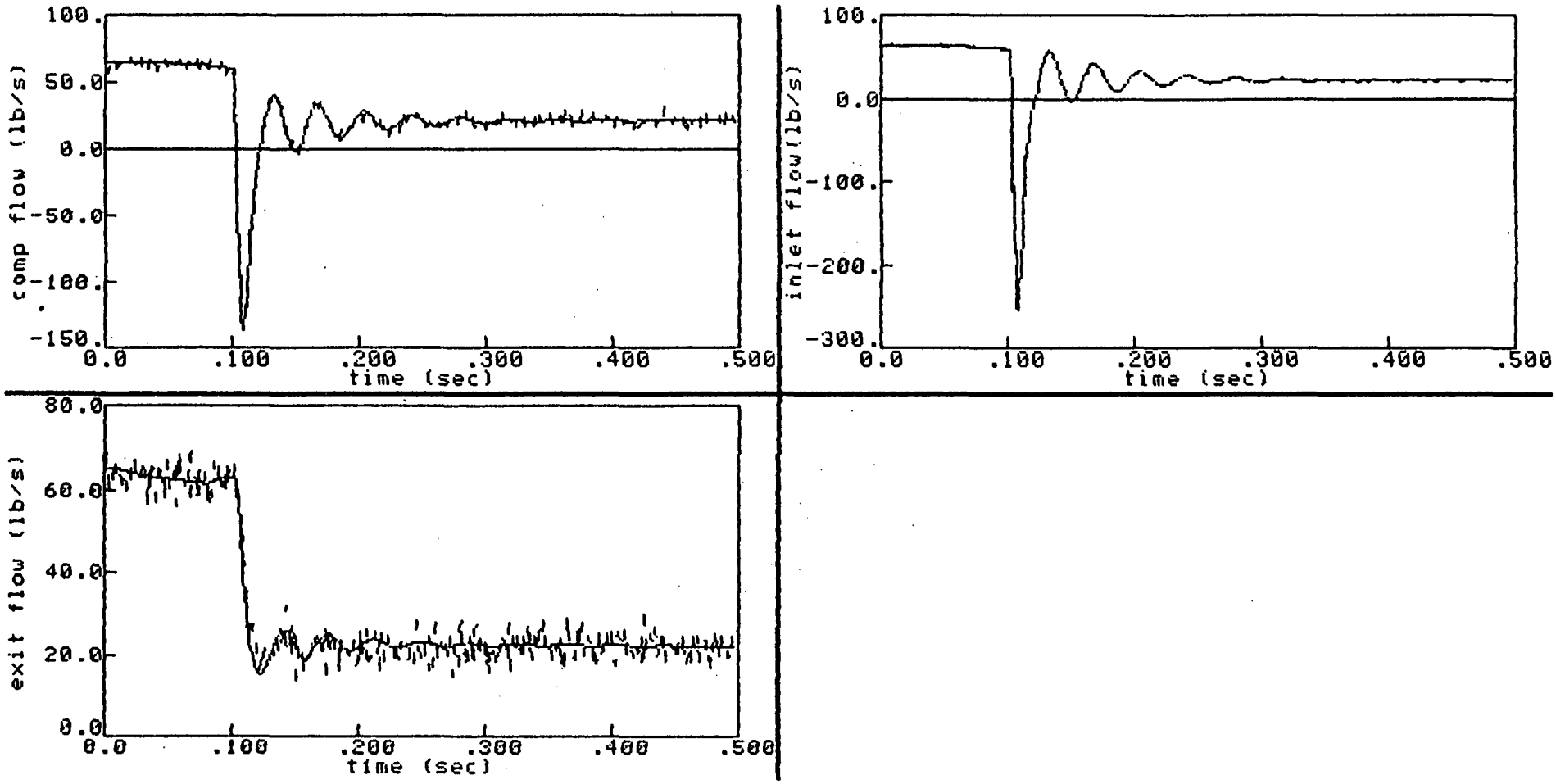

Figure 5.32 Run 5 Test Case with Noise and Temperature Lags (Identified, solid line; Measured, dashed line)

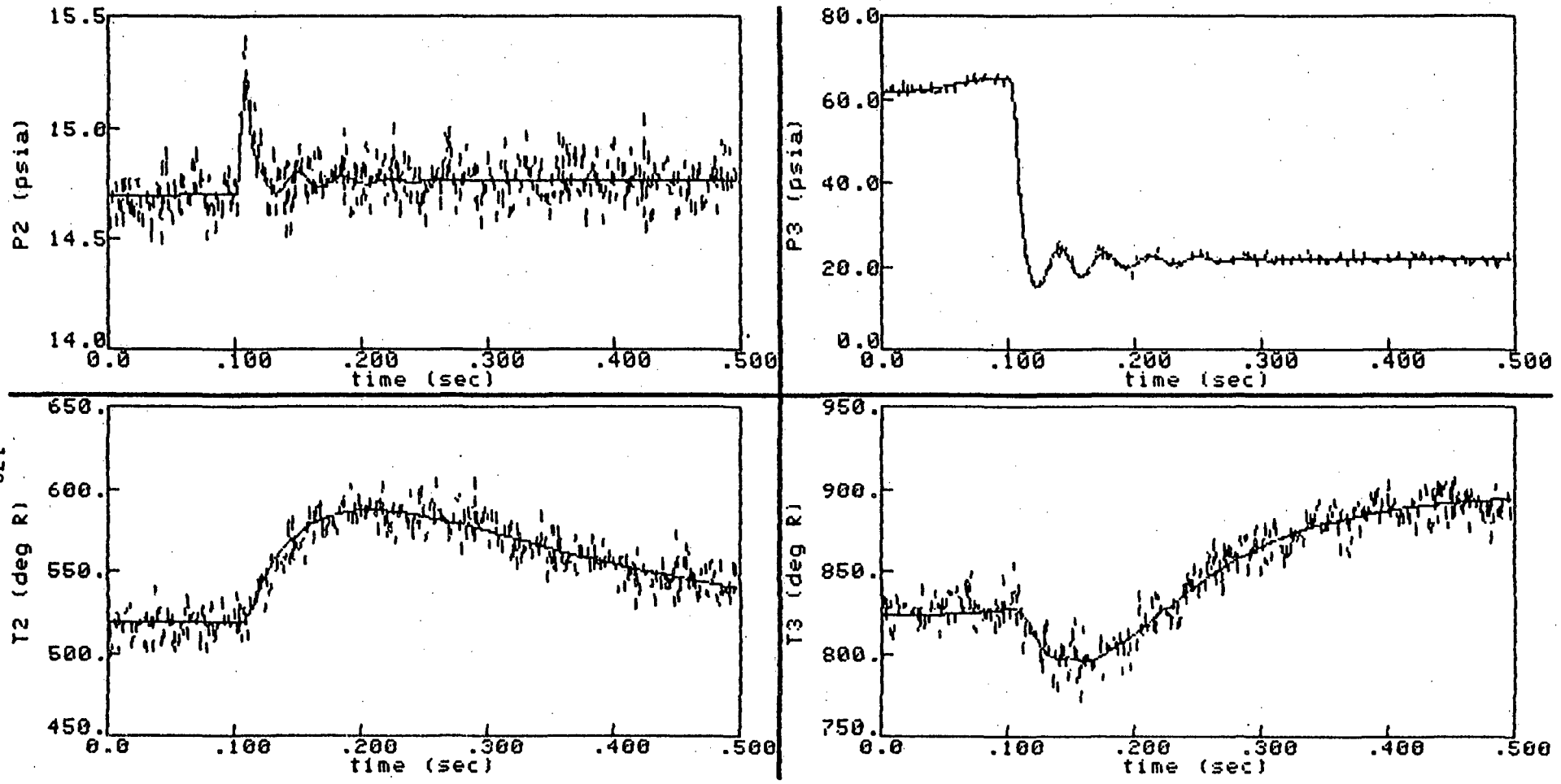

Figure 5.33 Run 5 Test Case with Noise and Temperature Lags (Identified, solid line; Measured, dashed line)

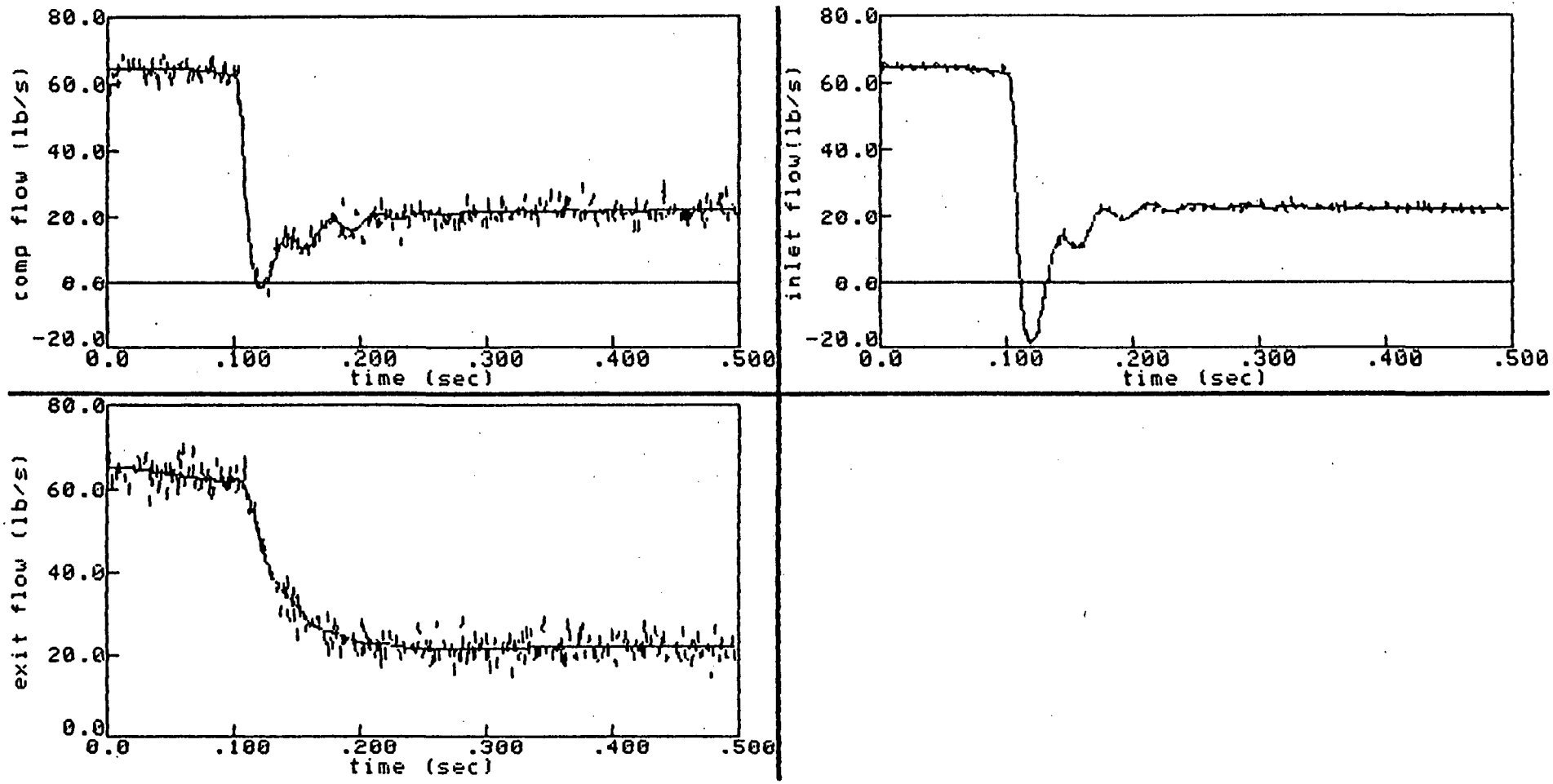

Figure 5.34 Run 5 Test Case with Noise and Lags on All Sensors (Identified, solid line; Measured, dashed line)

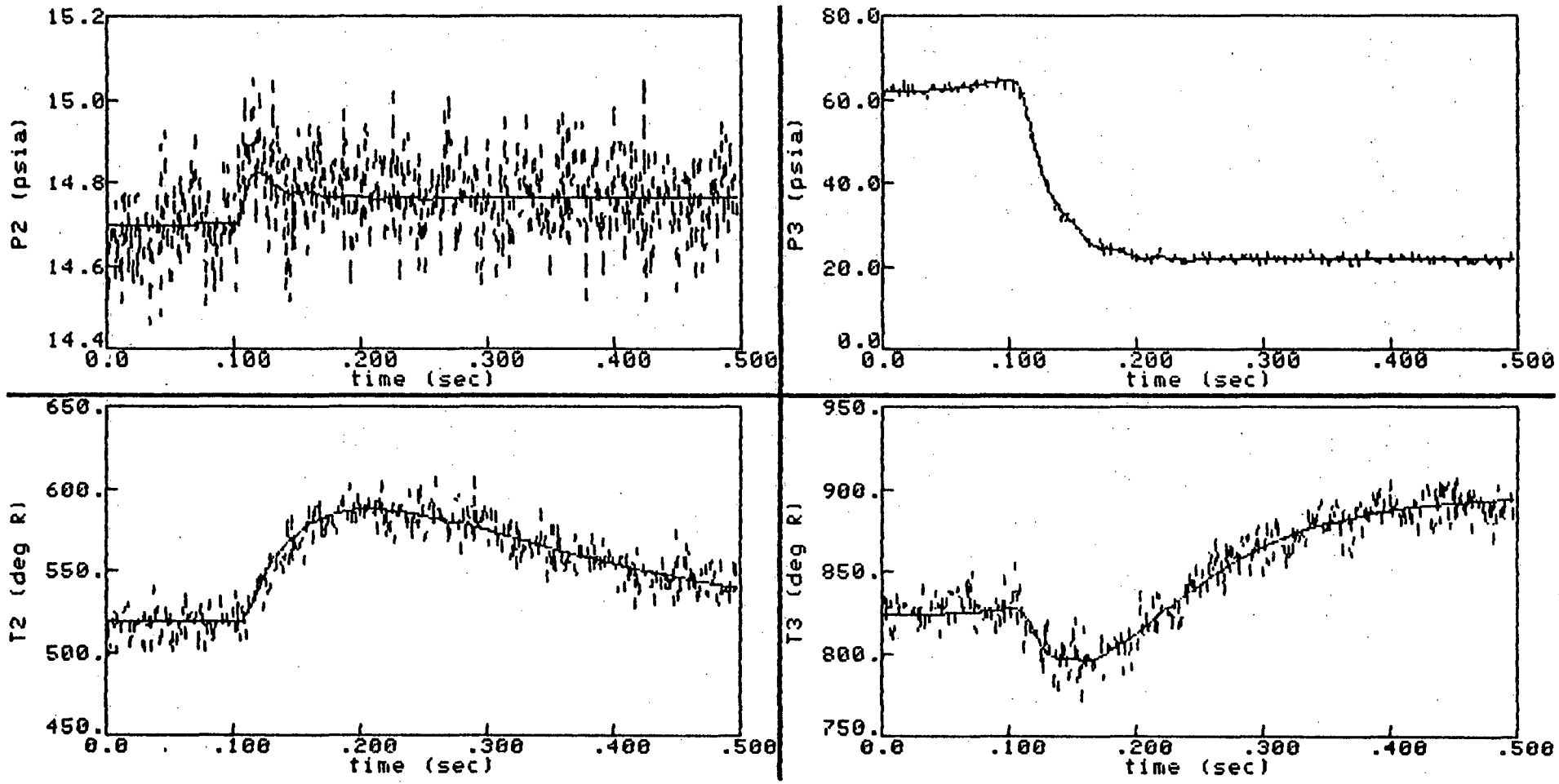

Figure 5.35 Run 5 Test Case with Noise and Lags on All Sensors (Identified, solid line; Measured, dashed line)

Table 5.9
Description of Six Example Cases

Cases	Theta	Noise	Sensor Lags: Temp	P and $\dot{W}$	no $\dot{W}$'s	Sigma (%)
1	Kn					0
2	Kn	X				0.54
3	Kn	X			X	1.50
4	Kn	X	X			0.57
5	Kn	X	X	X		2.15
6	Kn	X	X	X	X	5.20
1	Kp					0
2	Kp	X				7.58
3	Kp	X			X	34.7
4	Kp	X	X			7.61
5	Kp	X	X	X		31.5
6	Kp	X	X	X	X	73.6

Table 5.10
Noise Levels (%)

$\dot{W}1$	$\dot{W}2$	$\dot{W}3$	P2	P3	T2	T3
1.298	3.081	2.948	0.1023	1.015	9.884	10.24

The results of the six cases are summarized in Table 5.11. None of the resulting identification errors was due to biasing since there were no nuisance parameter errors (including Kn and Kp). Two different sigma values are given in Table 5.11. The first value is the a priori uncertainty estimate and is calculated when the model is already at the actual parameter value; thus, it is a low estimate of uncertainty. The second sigma value is calculated by SCIDNT at the identified parameter values (not necessarily the actual value). This second value generally is larger because of error terms introduced by model-plant measurement mismatches. It also is a better

estimate of the true uncertainty of the estimated parameter (parameter confidence).

Table 5.11
Six Example Case Results

Case	Theta	Actual	Ident	percent error	percent cent σ [a]	percent cent σ [b]
1	Kn	8.0	8.000	0.000	0.0002	0.00
2	Kn		7.939	-0.764	0.519	0.54
3	Kn		8.023	0.293	1.490	1.50
4	Kn		7.931	-0.863	0.545	0.57
5	Kn		8.163	2.040	1.710	2.15
6	Kn		8.370	4.630	5.270	5.20
1	Kp	0.1	.1000	0.000	0.003	0.00
2	Kp		.1053	5.350	6.160	7.58
3	Kp		.1370	37.00	15.70	34.7
4	Kp		.1014	1.400	6.830	7.61
5	Kp		.0831	-16.90	28.90	31.5
6	Kp		.0600	-40.00	106.0	73.6

[a] denotes post de facto estimate uncertainty

[b] denotes a priori uncertainty

The results in Table 5.11 provide a good opportunity to test the validity of the uncertainty and identifiability concepts. By dividing the percent error by sigma values, the result is a standardized error. Statistical theory predicts that if the sigma's are correct, i.e., if the identifiability and uncertainty ranges are correct, then the standardized errors will follow a Gaussian distribution.

The normalized values are summarized in a histogram in Figures 5.36 and 5.37. The results indicate that a priori uncertainty calculations well predict identifiability, and the post de facto parameter uncertainties provide an excellent measure of confidence. Both sets of uncertainties show that the

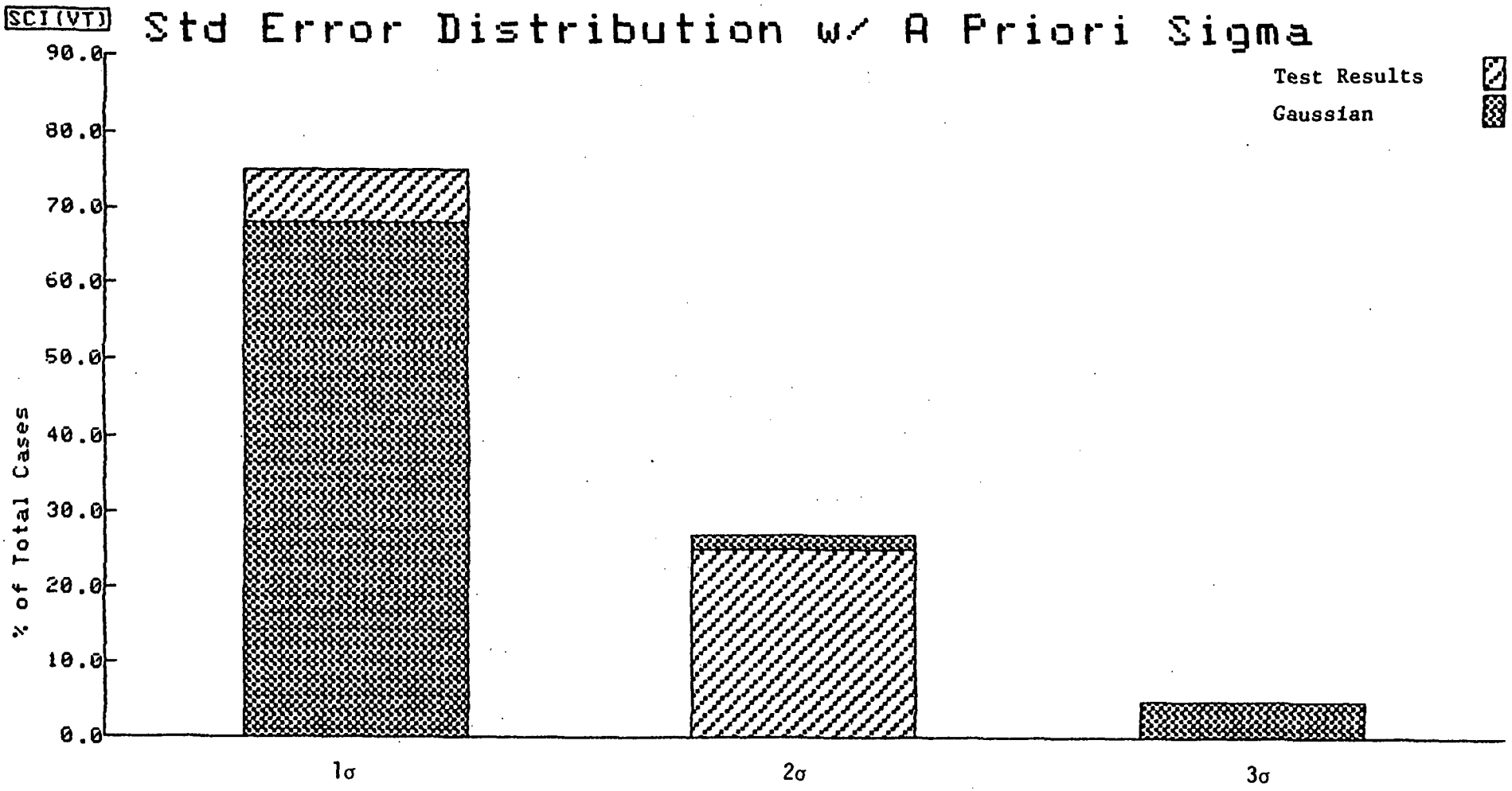

Figure 5.36 Standardized Test Results Compared to Gaussian Predictions (Standardized to Sigma b)

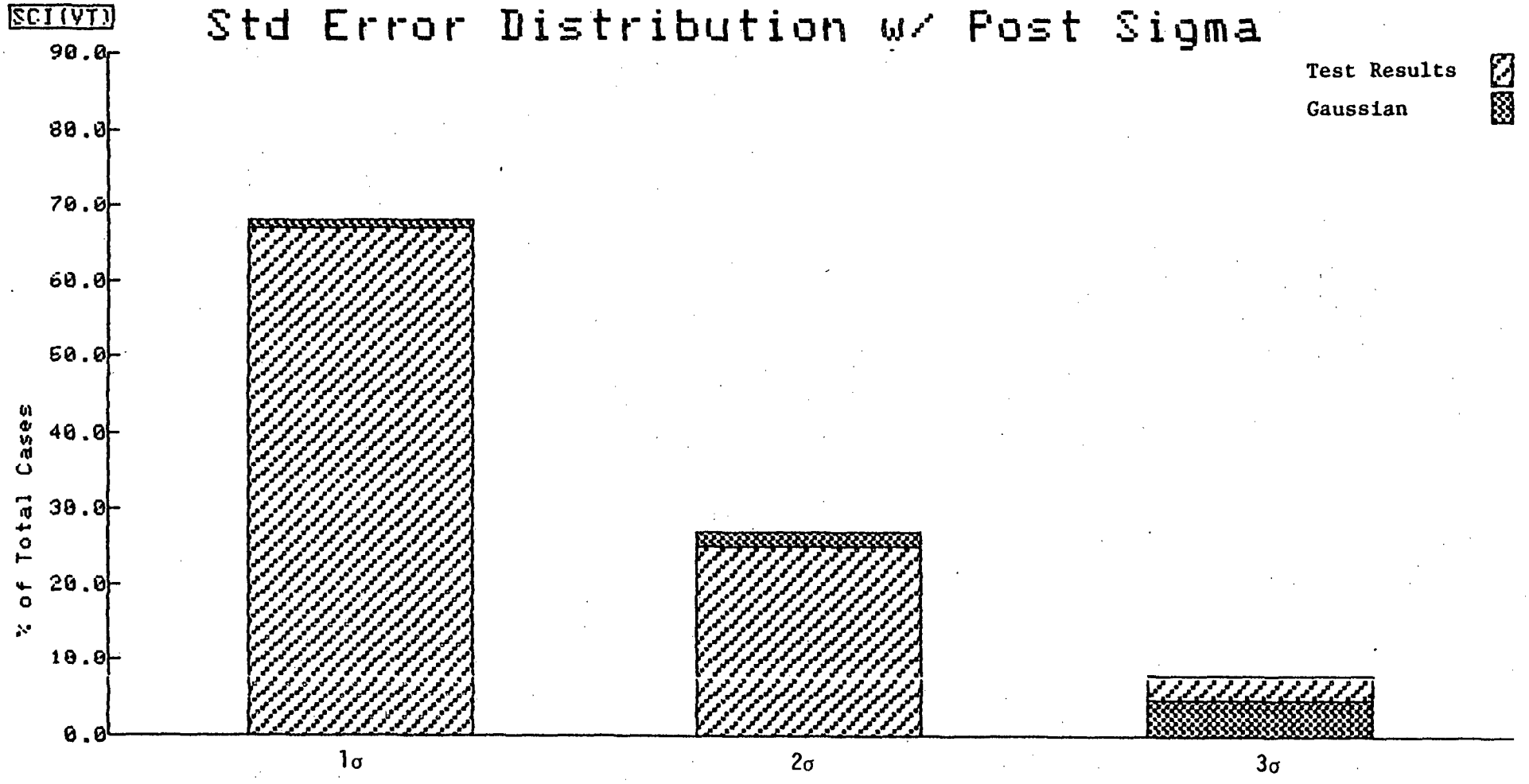

Figure 5.37 Standardized Test Results Compared to Gaussian Predictions (Standardized to Sigma a)

identification errors are indeed gaussian and are well predicted by standard deviations. The six example cases provide strong evidence of the validity of the uncertainty principles. (The a priori uncertainties are sometimes more pessimistic than they should be because of the high original noise levels chosen. Post de facto uncertainties are more realistic since they use noise levels estimated by SCIDNT using the actual measurements.)

5.4.2 Test Case

A test identification was made to evaluate both sensitivity and identifiability concepts at the same time. Unlike the six example cases given above, nuisance parameter errors are present in the test case and lead to biases in the identified parameters.

Following the outline of a normal identification run, Kn was identified first with an inaccurate guess of Kp (because the actual value is assumed unknown). This inaccurate Kp causes the Kn estimate to be biased from actual. Kn is not expected to be the actual value anyway since sensor noise limits its identifiability. Kp, in turn, is expected to be biased because of errors in the identified Kn. Sensitivity and identifiability relationships can both be used explain these results.

The test case is described by the following:

Table 5.12
Noise Levels (Standard Deviations)

$\dot{W}1$	$\dot{W}2$	$\dot{W}3$	P2	P3	T2	T3
—	4.55	4.55	1.029	4.35	36.33	57.54

Sample rate: 2 kHZ

Noise Levels: P2 - 7 percent, P3 - 7 percent, T2 - 7 percent, T3 - 7 percent

Sensor Set : $\dot{W}1$ omitted, No lags

Run : 5

The results of the identifications, along with a priori uncertainties, estimated bias levels and post de facto uncertainties (confidences), are all summarized below.

Table 5.13
Test Case Identification Results

Theta	Ident	e(θ) (%)	e(ϕ) (%)	bias (%)	e(θ) - bias (%)	sigma[a] (%)	sigma[b] (%)
Kn	7.628	-4.65	-50.0	-1.80	-2.85	2.000	1.997
Kp	.0964	-3.60	-4.65	-21.2	17.6	22.6	22.5

[a] denotes post de facto estimate uncertainty
[b] denotes a prior uncertainty

Both parameters were identified to within 5 percent of actual values, although the confidence in Kp (22.6 percent uncertainty) is much less than that for Kn (only 2 percent uncertainty.) An expected identification bias was calculated for each parameter given the known errors. In the case of Kn, the initial value of Kp was 50 percent below the actual value. This, in theory, would cause the identified Kn to be biased 1.8 percent below the actual value. After correcting the observed error in Kn for this bias, the resulting error is well within 2 standard deviations of uncertainty. Kp then was identified with the identified Kn (which was off by -4.65 percent). The same procedure indicates the corrected error (17.6 percent) to be within 1 standard deviation of uncertainty. Although this error is greater than the uncorrected error, the uncertainty range suggests that both values are reasonable.

5.5 APPLICATION TO NASA DATA IDENTIFICATION

Efforts were made using identifiability and sensitivity tools to determine what factors may have influenced the compressor results. These

efforts, however, were limited by of the size of the job involved. Results did indicate that noise and sample rate effects could only have played a minor role in biasing the compressor rig estimates. Sensitivity effects, particularly from estimate parameter biases and time skew biases, were likely responsible for some of the larger errors. Precautions were taken in the turbofan study to minimize their effects after recognizing the potentials of these biasing influences.

Aside from the effects of noise and sample rates on uncertainty, the following influences are believed to be the major sources of error in the compressor model identification study:

(1) input and outputs time skewing (model lags or leads data);

(2) biases in several of the measurements; and

(3) excessive noise on the input.

Knowledge gained in the compressor identifications and this sensitivity analysis were used to avoid many of these bias inducing contributors in the turbofan identifications. The general approach was simply to identify and minimize these errors within the identification process itself. This was the approach taken earlier with the synchronization of the model and data in the compressor identifications. For the turbofan, the synchronization effort was fortified by identifying an input time skew parameter in place of AT. Similarly, measurement bias level parameters were to be identified if necessary so that they could be incorporated into the identification model and their biasing effects, minimized.

The actions taken to avoid error effects with the turbofan provide valuable experience for future identifications, particularly since these types of influences are typical of those encountered in "real world" identifications.

5.6 SUMMARY

The following is a brief summary of the results and conclusions of the identification and sensitivity study.

5.6.1 Uncertainty

(1) Identifiability of estimate parameters (in the form of uncertainty) can be predicted before identification.

(2) Uncertainty can be used as a measure of confidence for identified parameters.

(3) Uncertainty is directly linked to and can be estimated using sample rates, number of manuevers, noise levels, sensor time constants and limited sensor sets.

(4) Uncertainty relationships can be used to determine instrumentation requirements.

5.6.2 Sensitivity

(1) Sensitivity is a measure of predicted biases in estimate parameters due to unmodeled errors (in other parameters, time constants, time skews, etc.).

(2) In-stall compressor map parameters are highly sensitive to estimate parameter errors, dimensional parameter errors, time constant errors, and especially input-output time skews.

5.6.3 Verification

(1) Identifiability and sensitivity results were verified using synthetic data.

5.6.4 Application

(1) Sensitivity results in particular seem to explain a large amount of the errors seen in the compressor model identifications. No effort was made to verify this quantitatively because of the level of effort involved.

(2) Identifications with the turbofan model used sensitivity results to identify outside error influences and compensate their effects in identification.

VI. FINAL DEMONSTRATION WITH TURBOFAN MODEL

6.1 BACKGROUND

The turbofan identifications are the second and last phase of the compressor map parameter identification demonstration. This second phase concentrates upon developing advanced procedures for stall parameter identifications. The experiences and tools gained from Tasks A and B were instrumental in developing a more streamlined and comprehensive approach to turbofan parameter identification. These improved procedures resulted in excellent identification accuracies achieved for the stall and engine parameters. Those areas where identification was not entirely successful were correctly predicted and explained by I/S tools. I/S tools also predict that nonrecoverable stall data (as opposed to recoverable stall data) will be necessary to identify Kp in future identifications, and that flow measurements probably will not be required for any of the stall and engine parameter identifications considered in this program.

The procedures used regarding the recording and transferral of data for the turbofan were identical to those used for the compressor rig study (see Section 4.1).

6.2 TURBOFAN MODEL DEVELOPMENT

Like the compressor rig model, the turbofan model was also developed from the NASA Lewis TF-34 lumped-parameter model [1]. the turbofan is a twelfth-order model with the following features:

(1) adiabatic volume effects;
(2) resistive inlet, duct and crossflows;
(3) inductive flow through fan and compressor;
(4) quasi-steady compressor and fan maps;
(5) choked turbine flow;
(6) fixed absolute speed, variable correct speed;
(7) fixed variable geometry;
(8) capable of reverse flow.

A schematic diagram of the turbofan model is shown in Figure 6.1, and an example stall response of the model is given in Figures 6.2 through 6.5.

6.3 SPECIAL CONSIDERATIONS

6.3.1 Initial Conditions in the Parameter Vector

The parameters used in the turbofan model were extended to include initial condition values (IC's) as parameters. Including IC's as parameters made it possible to identify plant initial conditions using measured plant outputs. This is a significant improvement in the identification approach in that it allows IC's to be identified from real data rather than taken as givens from NASA Lewis specifications. There are two important benefits in using this approach: (1) identifying IC's from measured data is a more real world approach to initializing the model and (2) there is a greater certainty that the NASA and SCT models were operating under the same conditions. The following briefly discusses how initial conditions were made into model parameters and how they were identified.

The turbofan model is represented in three major subroutines according to the conventions and requirements of SCIDNT. The three subroutines are: (1) STATE, which calculates 12 state derivatives of the turbofan given present state, input conditions and model parameters, (2) MEAS, which calculates model outputs (flows, temperatures, pressures) based upon the current states, inputs and measurement conditions, and (3) STATIC, which determines initial state conditions based upon model parameters and user specifications (in this case, steady state operation at a specified operating point.) The new feature added to the turbofan model is a special implementation in the STATIC routine.

STATIC was redesigned to allow determination of turbofan initial conditions from three major conditions: (1) inlet pressure and temperature, TO and PO, (2) fan operating point (uncorrected flow and speed), and (3) compressor operating point (uncorrected flow and speed). Once these three conditions are determined, STATIC calculates all 12 turbofan states in steady state, and they become state IC's for the STATE and MEAS routines attached to SCIDNT.

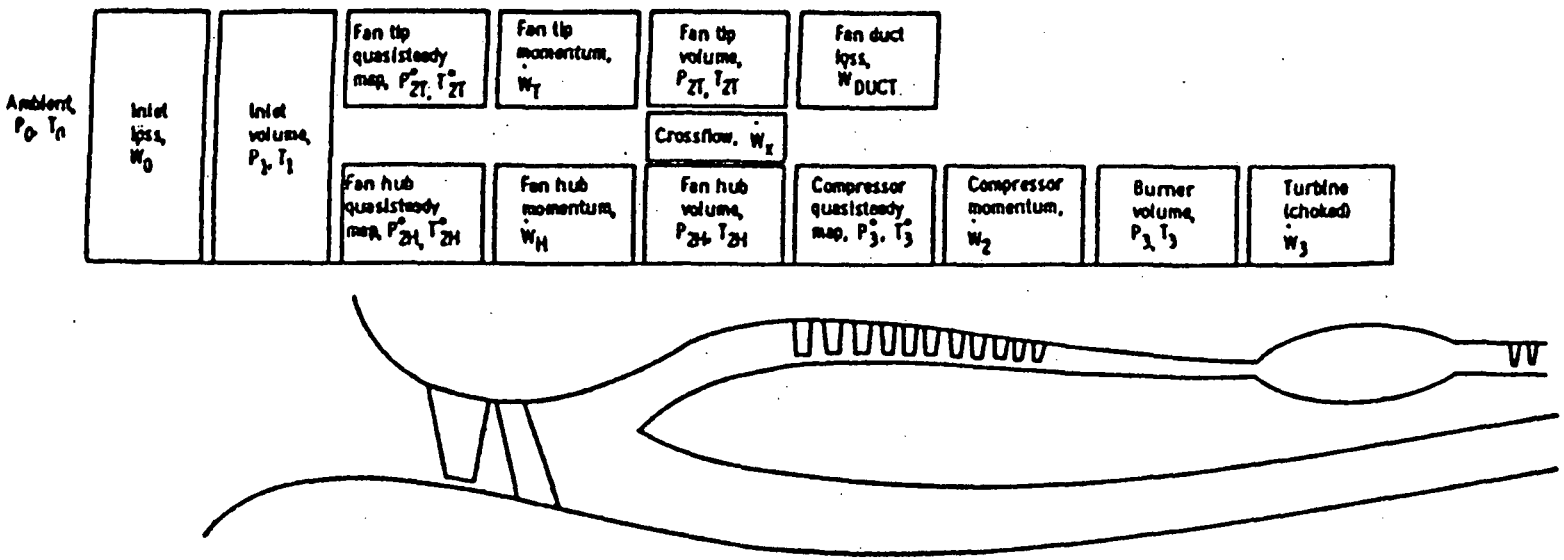

Figure 6.1 Schematic Diagram of the Turbofan Model
(from Reference 1)

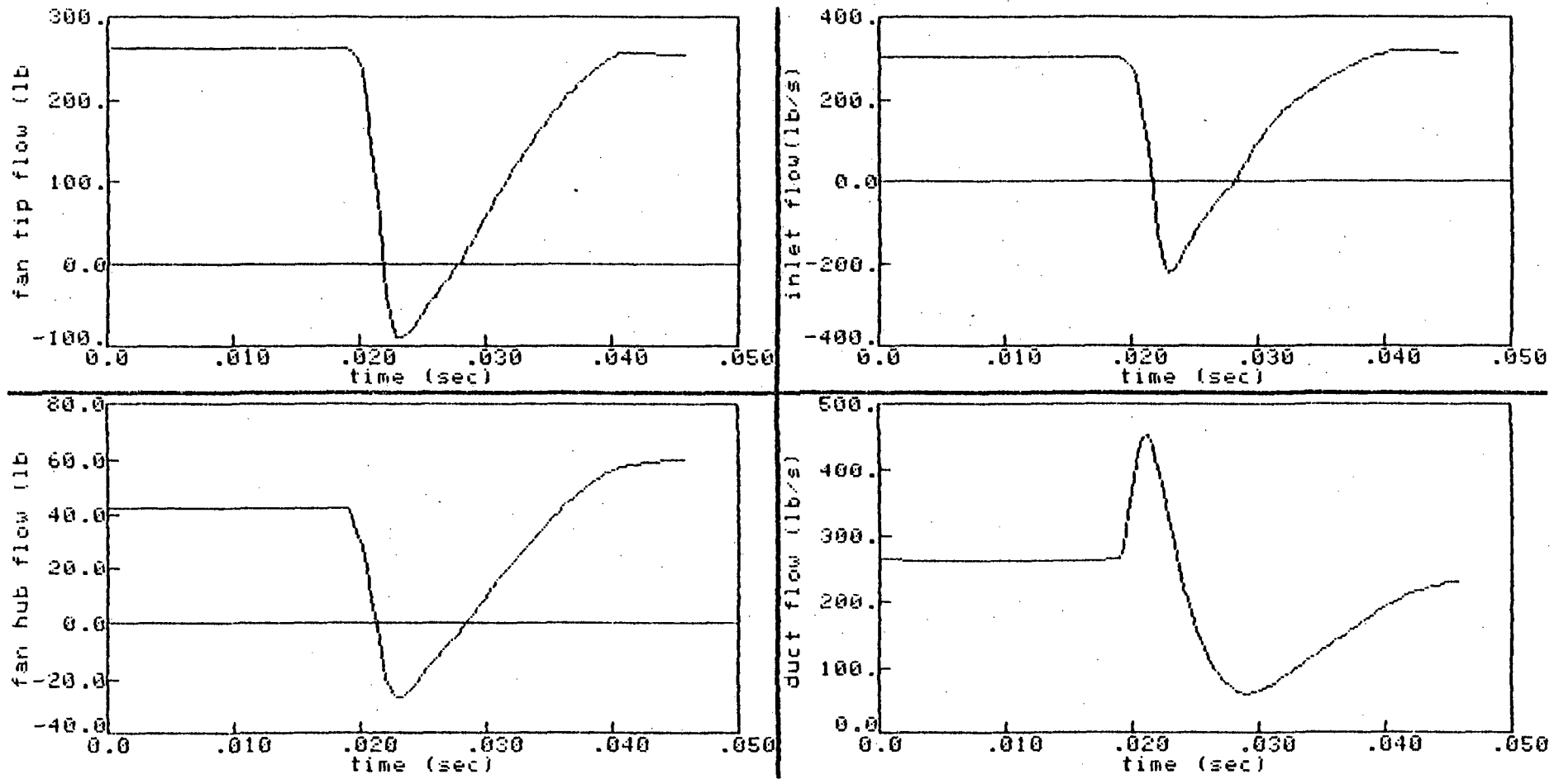

Figure 6.2 Turbofan Model Response -- Recoverable Stall

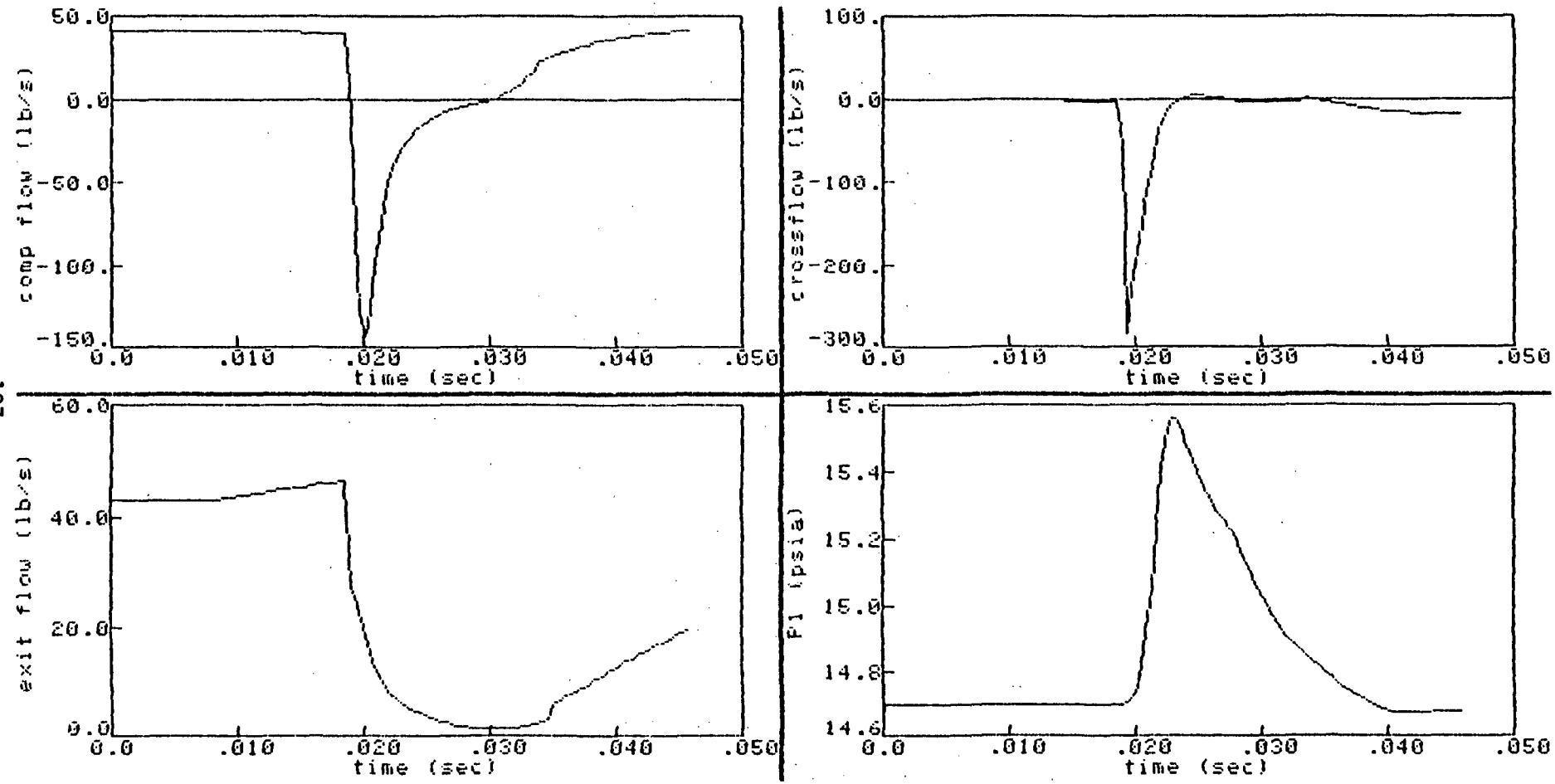

Figure 6.3 Turbofan Model Response -- Recoverable Stall

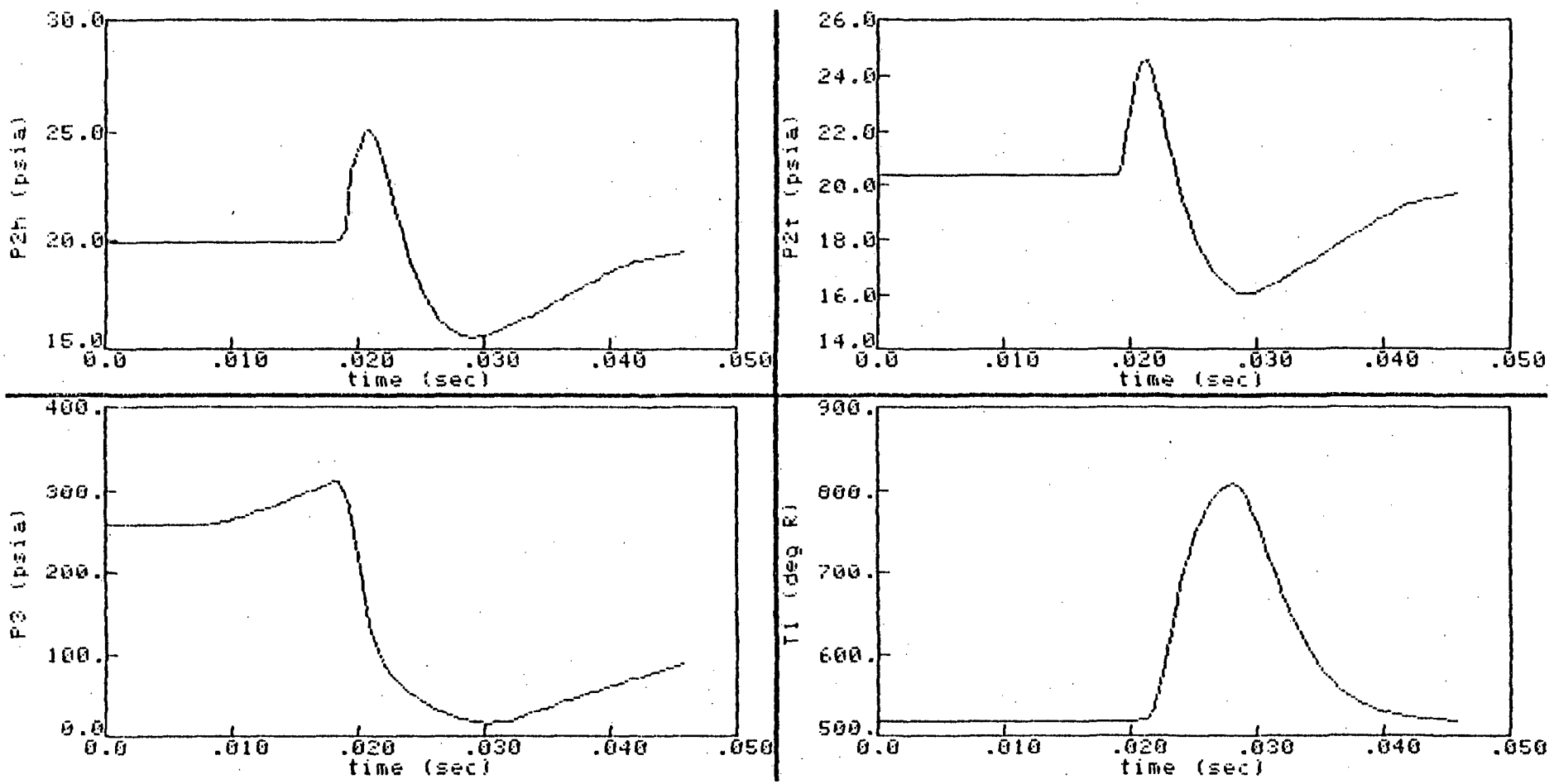

Figure 6.4 Turbofan Model Response -- Recoverable Stall

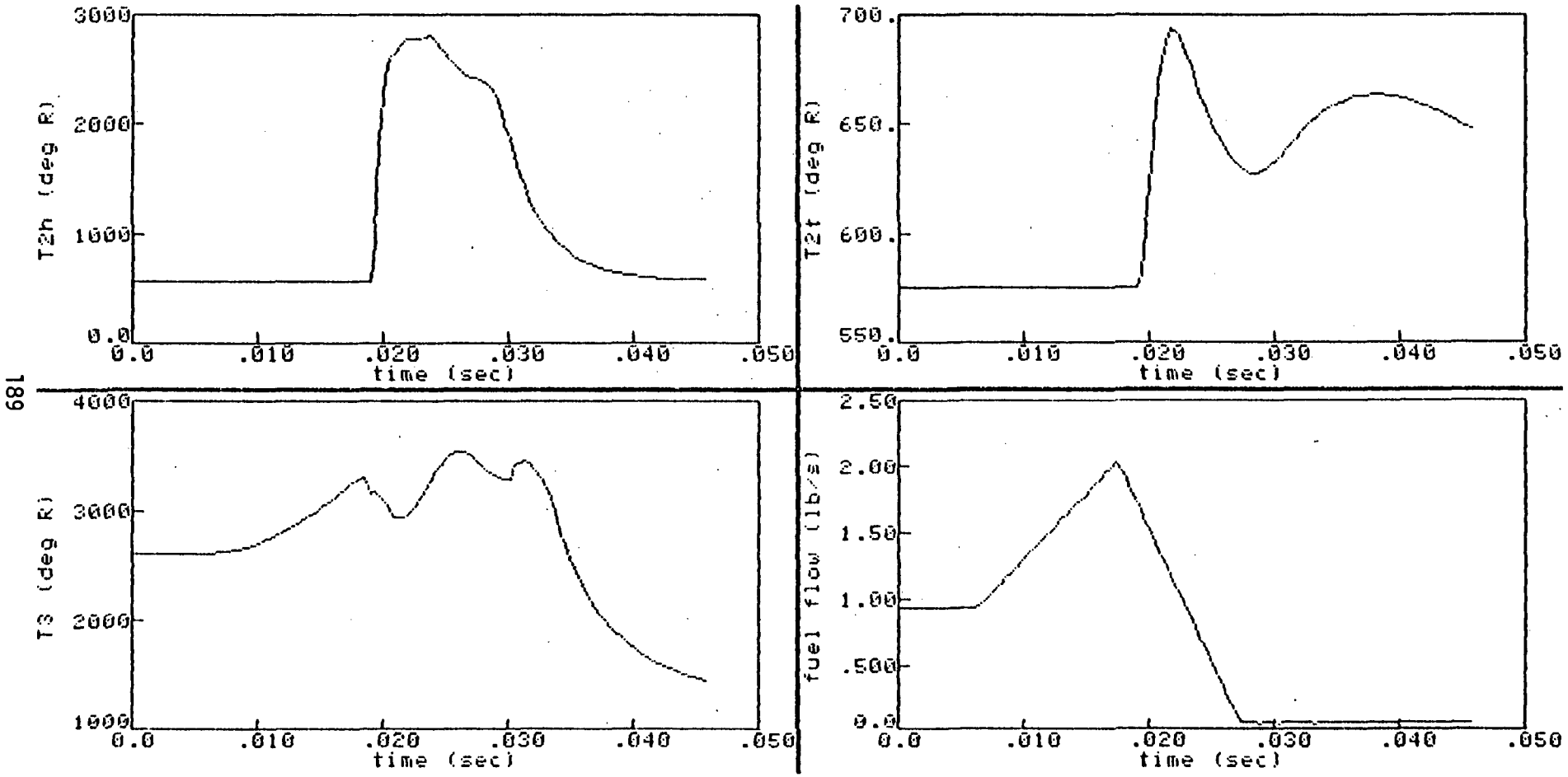

Figure 6.5 Turbofan Model Response -- Recoverable Stall

The critical part of this implementation is the way in which operating conditions are specified. The model parameter vector is extended beyond normal model parameters (resistance, volume, compressor map parameters, etc.) to include 6 flow, speed, temperature, and pressure values. Unlike the other parameters, these special IC parameters are used only once to calculate model initial conditions. Since they still are considered model parameters, they can be treated like any other model parameter and can therefore be identified. This is the critical aspect. Once measured steady-state outputs are known (pressures, temperatures, etc.), then the initial conditions of the plant can be identified as parameters.

Initial conditions of the turbofan were identified to demonstrate the technique and verify the NASA-supplied values. The results are shown below for the operating points. In general, the identified conditions are quite close to those reported by NASA Lewis. Values identified from run 1 were used in the turbofan identifications. (Note: speed values are an absolute fraction; they do not include theta correction.)

Table 6.1
Identified Initial Conditions

Parameter	NASA	Run 1	Run 2
PNFoper	.9000	9.0070100E-01	9.0034527E-01
PNCoper	1.055	1.0504104E+00	1.0494944E+00
WFdotIC	303.7	3.0329800E+02	3.0336107E+02
W2dotIC	41.8	4.1984400E+01	4.1923758E+01

6.3.2 Double Precision

Turbofan identifications used a double-precision version of SCIDNT instead of the single-precision version used for the compressor rig. The move to double precision was prompted by two considerations: (1) the ability to invert the Hessian, M, and (2) the accuracy of the gradient calculation, g. Both processes involve the parameter stepping (gradient search) algorithm in

Eq. (3.5) in Chapter III. The move to double precision helped to alleviate some of the earlier problems encountered with (1) and (2) and helped improve overall convergence properties.

$$\theta_{i+1} = \theta_i - pM^{-1} * g \qquad (6.1)$$

where

θ = np x 1 parameter vector

g = gradient of J

M = gradient of g

= 2nd partial of J

p = a user defined scalar (< 1.) used to control rate of convergence.

Note that the gradient search algorithm requires that the second partial of the cost function, the Hessian, be inverted. While this presents no obvious difficulties as long as M is well conditioned, problems may arise when M is nearly singular.

In the compressor rig study, an effort was made to identify Kp and Kn simultaneously. Problems arose however when the two parameters produced a 2x2 Hessian that was poorly conditioned and difficult to invert. The solution at that time was to identify the two parameters separately (inverting the 1x1 M being trivial). The approach did have drawbacks, though. Separate identifications meant that estimate parameters could be biased and influenced by other estimate parameters. In fact, it was found that Kp could be significantly biased by Kn (see Chapters IV and V).

By converting to a double precision SCIDNT, the poorly conditioned Hessian became more invertable. This allowed simultaneous identifications to be made in some cases and helped to eliminate the parameter biases associated with separate identifications.

The second reason why double precision was implemented revolves around the accuracy of the gradient calculation. In the Kp parameter identifications (compressor rig study), the gradient of Kp was much flatter than that of Kn. Interpreted physically, a flat gradient means that the parameter has a small

effect of the response on the model. Precision errors can significantly affect the gradient value and identification convergence properties when the gradient is small. This problem was mentioned in the compressor rig identifications in Sections 4.5.4 and 4.6.1.2.

The double-precision SCIDNT is more effective in the calculation of small gradients such as the one associated with Kp. This has been translated into increased identification accuracy.

The benefits of double-precision code are two-fold. First, the increased precision allows for simultaneous parameter estimations, thereby reducing parameter biases; and second, overall parameter convergence and identification accuracy are improved as gradient calculations are improved.

6.3.3 Limited Sensor Sets

The are two rounds of turbofan identifications. The first round used noise-free data with all turbofan measurements. The second round used noisy data with only pressure and temperature measurements (no flow measurements.) This second round of identification more closely mimics the instrumentation conditions that would be encountered with real engine data.

6.3.4 Stall Detection

In the compressor rig identifications, one of the major obstacles was getting the SCT model to stall at the same time as the NASA data. Out of that experience, a new approach was developed to synchronize stall between the plant and model. This section presents a new method developed for the turbofan identification. Results of the technique's effectiveness are presented.

In the identification process, a plant and plant model are fed the same inputs. If the plant and model are identical, the outputs of the two will be identical. If the plant and model outputs do not agree, the model must be revised to produce better agreement (the job of SCIDNT). In the stall parameter studies, the inputs are designed to initiate stall. If the model and plant differ even slightly, their responses will differ and they may stall

at different times producing stall asynchronism. This was seen in the compressor rig and is also a matter of concern with the turbofan, since the model usually does differ from the plant (at least slightly). The solution presented here is to work with a stall time parameter.

The approach is to first make a rough estimate of the time that stall begins in the data. For the turbofan fan, this is accomplished by examining the data before identification and detecting rapid drops in P3dot. Once the stall time is estimated, the SCT turbofan model is forced to stall only at that specified stall time. This specified time (TSTART), like the initial conditions, is a model parameter and therefore can be identified to minimize the stall time differences. Through this method, stall synchronization can easily be achieved.

This stall detection technique worked well for the turbofan identifications. Unlike the compressor rig identifications, there were no observable skews between stall onset in the model and plant. A preliminary table of identified stall times is shown below.

Table 6.2
Identified Stall Times

Run No.	Stall Time
5	.01875
10	.01785
15	.01846
20	.01818

6.3.5 Recovery Detection

The TSTART parameter was created and integrated into the SCT model so that the model and data could be synchronized. In the same vein, a TSTOP parameter was created to see if such a parameter could be used to ensure simultaneous recovery of the model and plant.

The idea behind the TSTOP parameter identification is analogous to the TSTART parameter identification; that is, to get the model and plant to

recover (or stall) at the same time. As with the stall time, it was felt that an incorrect recovery point could bias the estimate of the KPC parameter by introducing extraneous model-plant errors. However, unlike the stall time issue, the attempt to identify a TSTOP parameter was a failure and actually detrimental. The failure was beneficial in another sense though, because it leads to further insight about the role of KPC in recoverable stalls.

From the TSTOP investigations, it was found that KPC affects the stalling turbofan in two ways: (1) whether or not the compressor will recover, and (2) when the compressor will recover. Other than the time of recovery, KPC appears to have little effect on measured responses. This means that by altering the position of the recovery line (by changing KPC), the primary result is to change the time of recovery. The shape of the positive stalled flow map seems to have little direct effect on engine responses in recoverable stalls. It also means that KPC and TSTOP seem to be very similar in their effect on engine responses. Thus, when trying to identify KPC and TSTOP simultaneously, the result is analogous to identifying the same parameter twice: one parameter is identified accurately and the other parameter is misidentified. In the KPC and TSTOP case, the TSTOP parameter was usually identified very accurately while the KPC parameter was misidentfied as being a value near zero.

TSTOP was introduced to the model but then was later removed when this above effect was discovered. Once TSTOP was removed, KPC identifications improved significantly.

The conclusion is that TSTOP defines some of the engine characteristics normally reserved for KPC, and when TSTOP is used in the model, it can alter the meaning of KPC. Furthermore, since TSTOP and KPC are nearly interchangeable, it is implied that KPC's primary effect on recoverable stalls is in the determination of the time of recovery. This means that, for recoverable stalls, KPC has little effect on the shape of the response curve during positive stalled flow; its greatest effect is on the time of recovery.

6.4 TURBOFAN IDENTIFICATION PROCEDURES

The special considerations and techniques used in the turbofan parameter identifications are summarized below. The special techniques are as a result of experience gained in the compressor rig and identifiability/sensitivity studies and reflect the special consideration outlined in Section 6.3.

(1) Identify initial conditions. This includes the ambient conditions (TO and PO) as well as the two operating points (fan and compressor flows and speeds.)

(2) Detect time of stall. This step utilizes a test which searches for rapid drops in P3dot. A similar procedure could be used on actual test data.

(3) Identify measurement biases (optional).

(4) Incorporate preliminary identified conditions into turbofan model.

(5) Identify parameters with noise-free data.

  (a) Identify Rx, V3, KNC, and TSTART with only unstalled and negative stalled flow data. (KPC is not identified in this step because of its sensitivity to errors in KNC and TSTART. The idea is to identify the parameters that KPC is sensitive to before KPC is identified. This may reduce biases induced in the KPC estimate.)

  (b) Incorporate the identified parameters from the previous step into the model and identify Rx, V3, KNC and KPC with the entire stall maneuver.

(6) Repeat set 5 for second round using noise-supplemented data.

(7) Evaluate.

6.5 TURBOFAN IDENTIFICATIONS USING NOISE-FREE DATA

The first round of turbofan parameter identifications is summarized below in Table 6.3. The identifications are for four engine parameters, Rx, V3, KNC and KPC, and a fifth temporal parameter, TSTART. In general, the

identifications using the noise-free data were quite successful, particularly the Rx, V3 and KNC identifications. The identified models are compared to the measured data in Figures 6.6 through 6.13.

Table 6.3
Turbofan Identifications Using Noise-free, Recoverable Stall Data

Run	TSTART (sec/100)	Rx (x1/100)	V3	KNC	KPC
5	1.8720	1.004	3337.	51.86	6.427*
6	1.7305	.9902	3347.	50.47	4.127*
9	1.7777	.9639	3328.	95.25*	3.406
10	1.7820	.9758	3324.	99.53*	4.160
13	2.2698	1.054	2637.*	48.63	3.960
14	1.7730	1.045	2647.*	47.72	5.026
17	1.9227	2.039*	3288.	48.74	4.982
18	2.1387	2.041*	3279.	50.67	4.431
Average		1.005	3317.	49.68	4.327
Actual		1.000	3319.	50.00	5.000
percent error		0.5	-.06	-.64	-13.5
Average*		2.04	2642.	97.42	5.277

*identified unknown values. Not included in first average.

The original parameter estimates are summarized in Table 6.4. A total of 15 measurements were used in the identifications; they are summarized in Table 6.5. (T3star and P3star, although provided by NASA Lewis, were omitted since they represent quantities that cannot actually be measured in a turbofan. The variables are intermediate variables which are unique to the lumped parameter turbofan model and have no analogous quantities in a turbofan engine.)

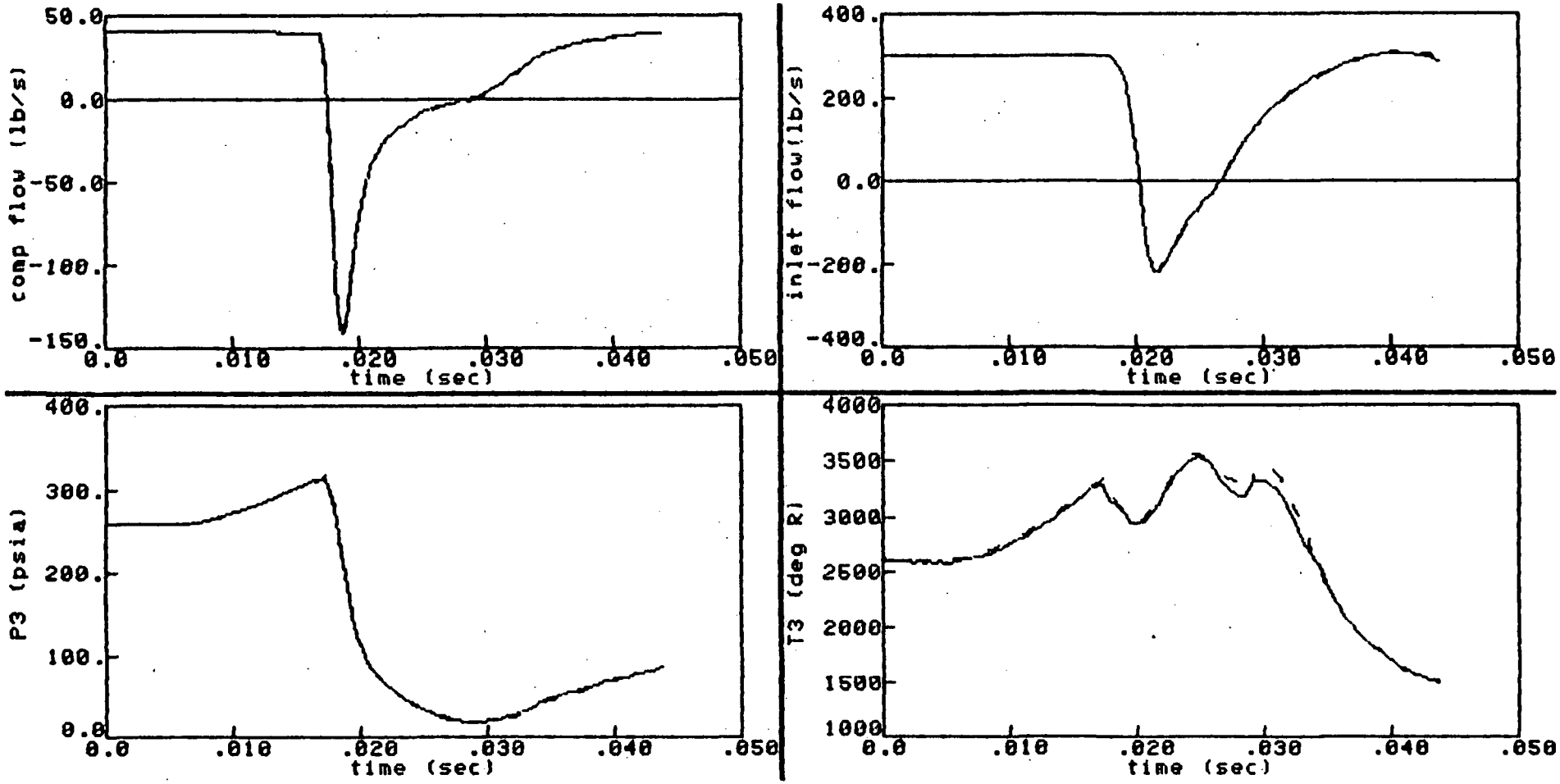

Figure 6.6 Turbofan Identification with Noise-Free Data, Run 5 (SCT, dashed line; NASA, solid line)

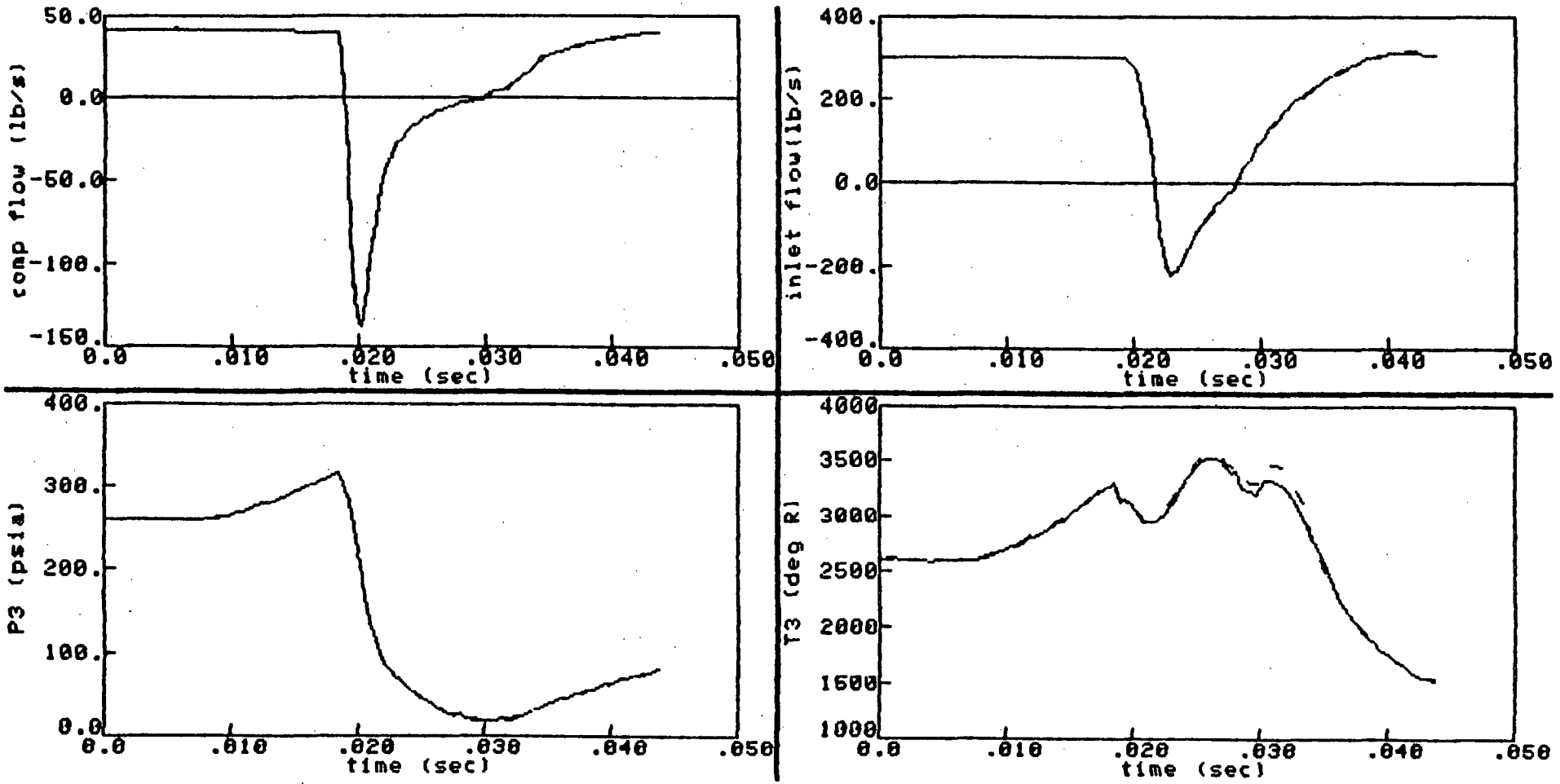

Figure 6.7 Turbofan Identification with Noise-Free Data, Run 6 (SCT, dashed line; NASA, solid line)

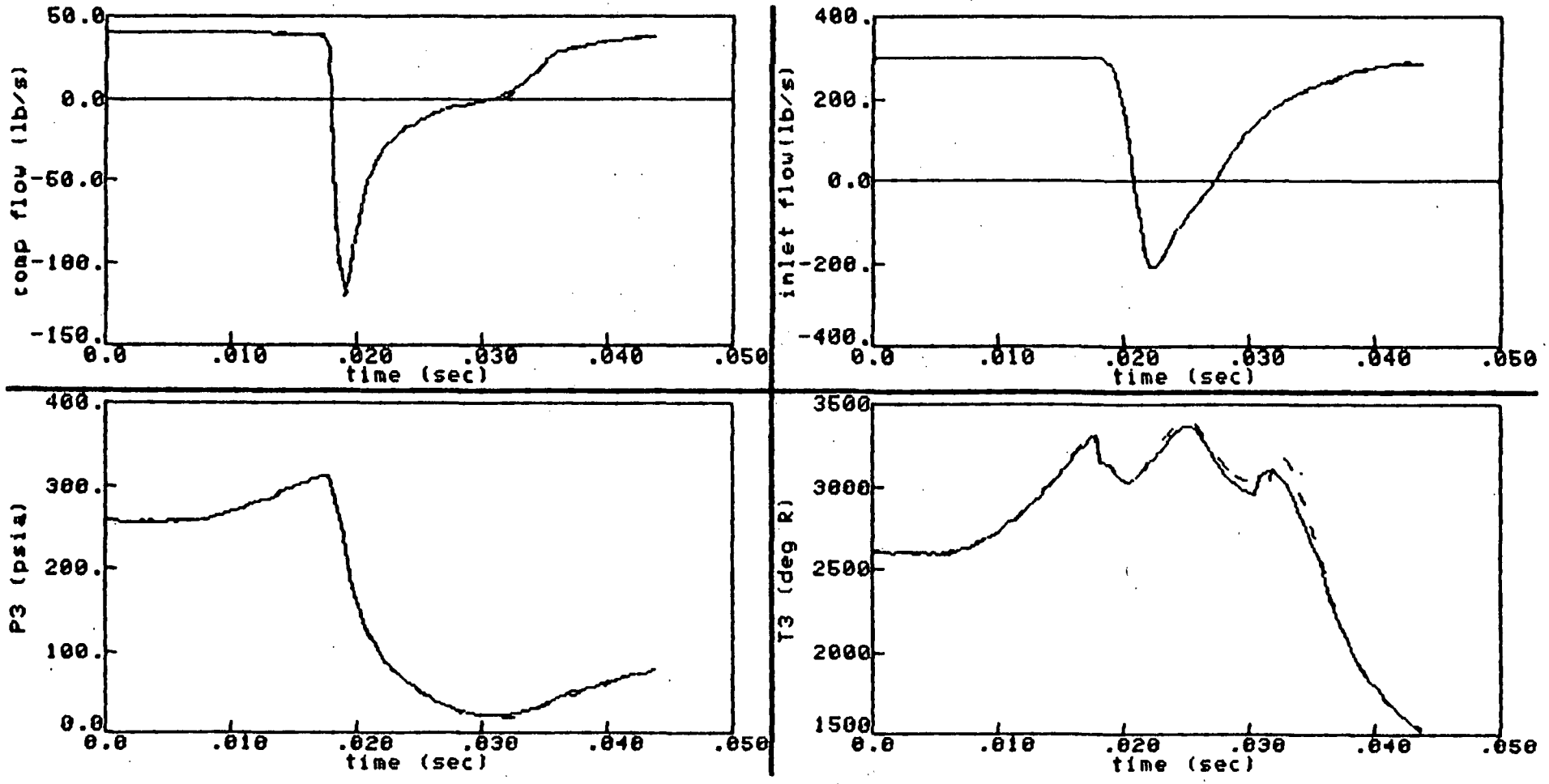

Figure 6.8 Turbofan Identification with Noise-Free Data, Run 9 (SCT, dashed line; NASA, solid line)

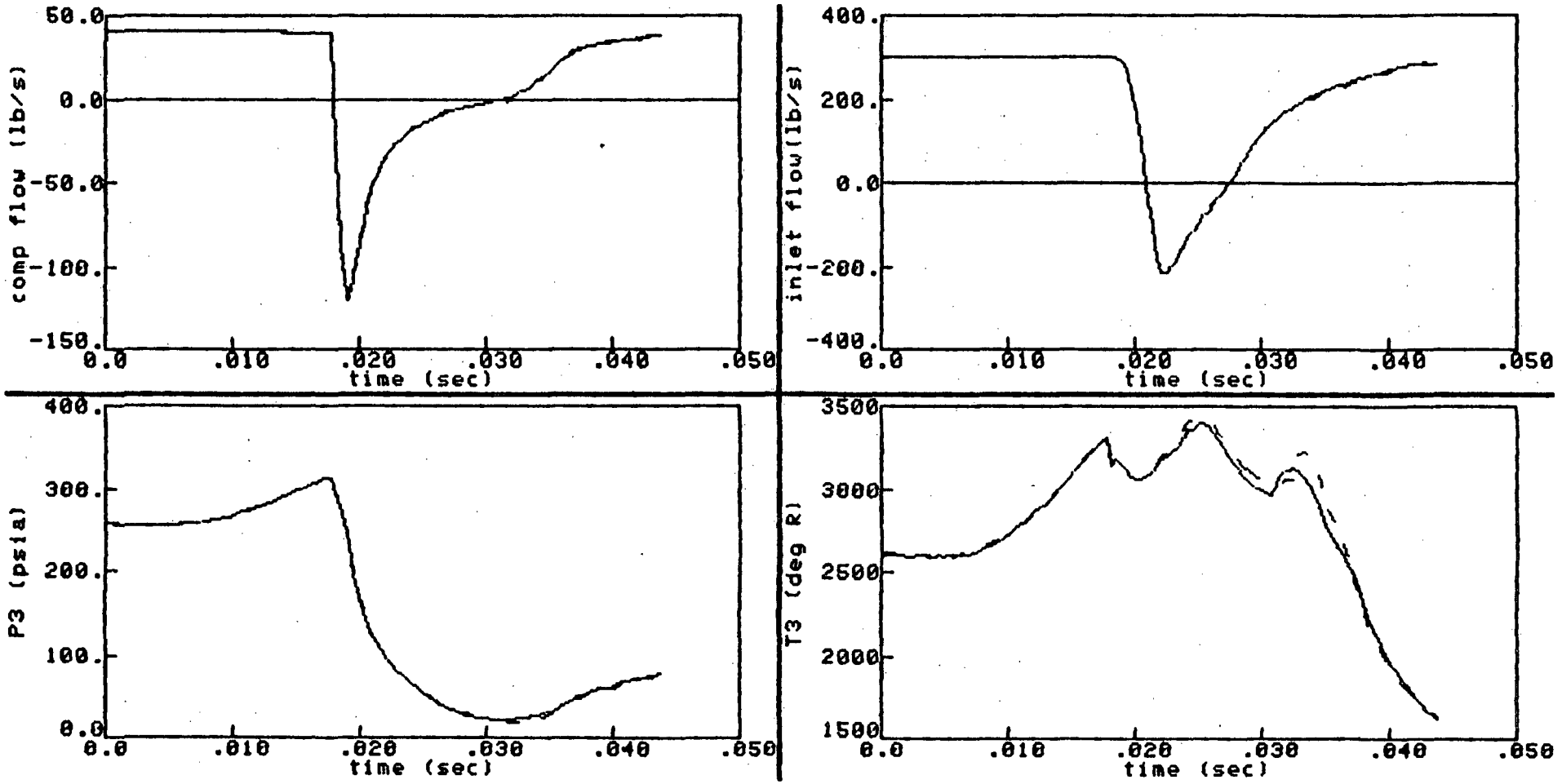

Figure 6.9 Turbofan Identification with Noise-Free Data, Run 10 (SCT, dashed line; NASA, solid line)

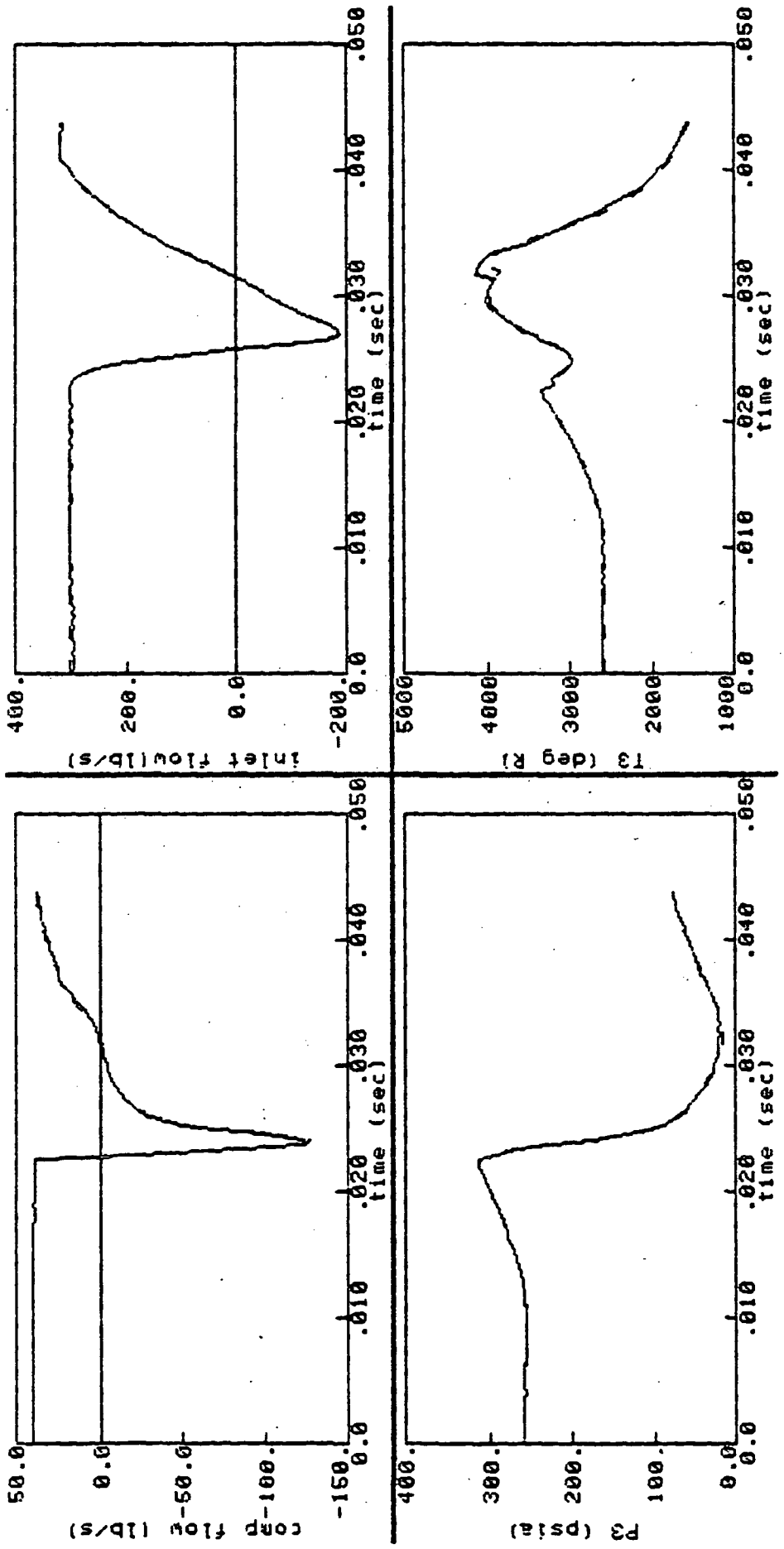

Figure 6.10 Turbofan Identification with Noise-Free Data, Run 13 (SCT, dashed line; NASA, solid line)

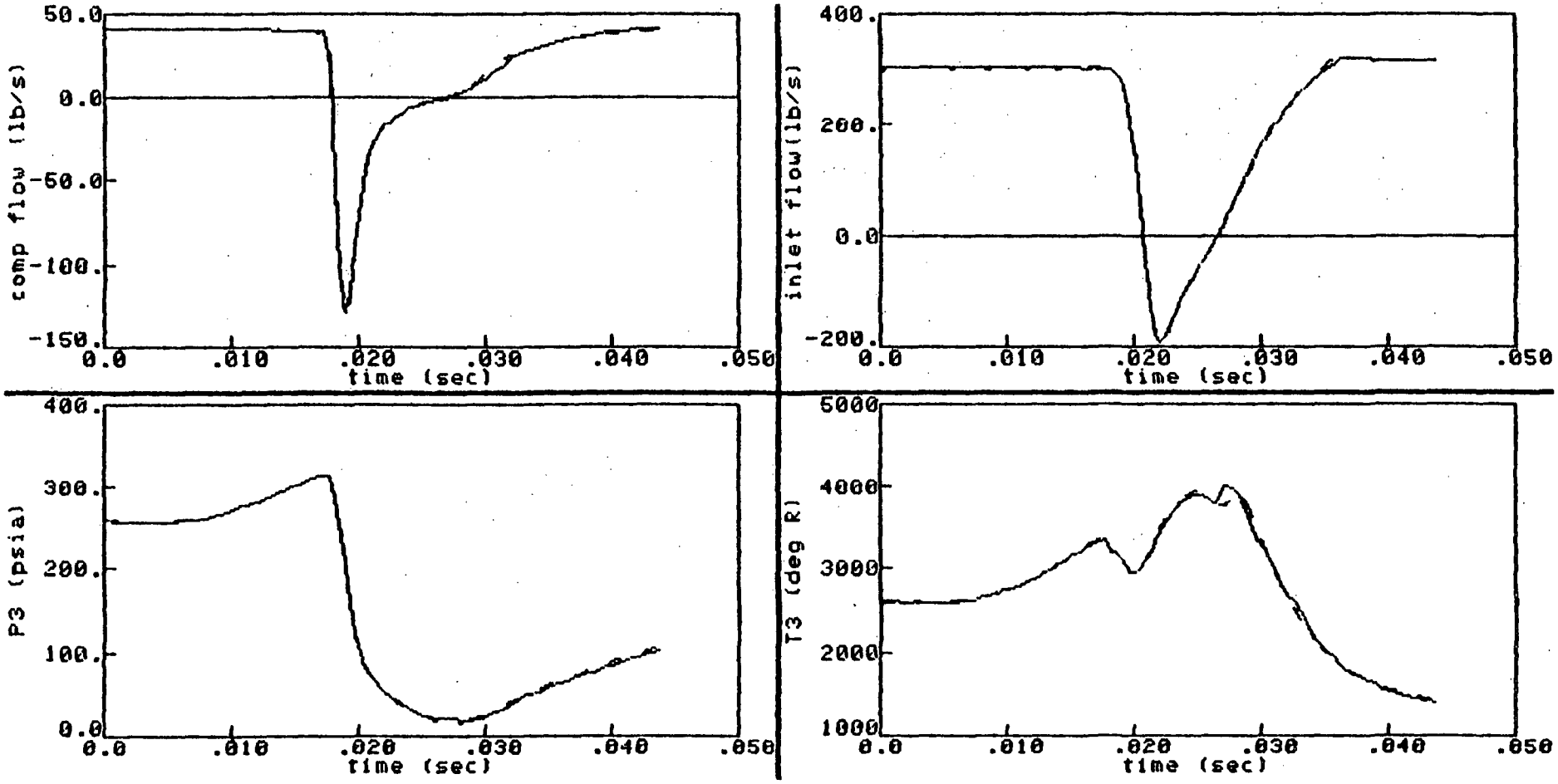

Figure 6.11 Turbofan Identification with Noise-Free Data, Run 14 (SCT, dashed line; NASA, solid line)

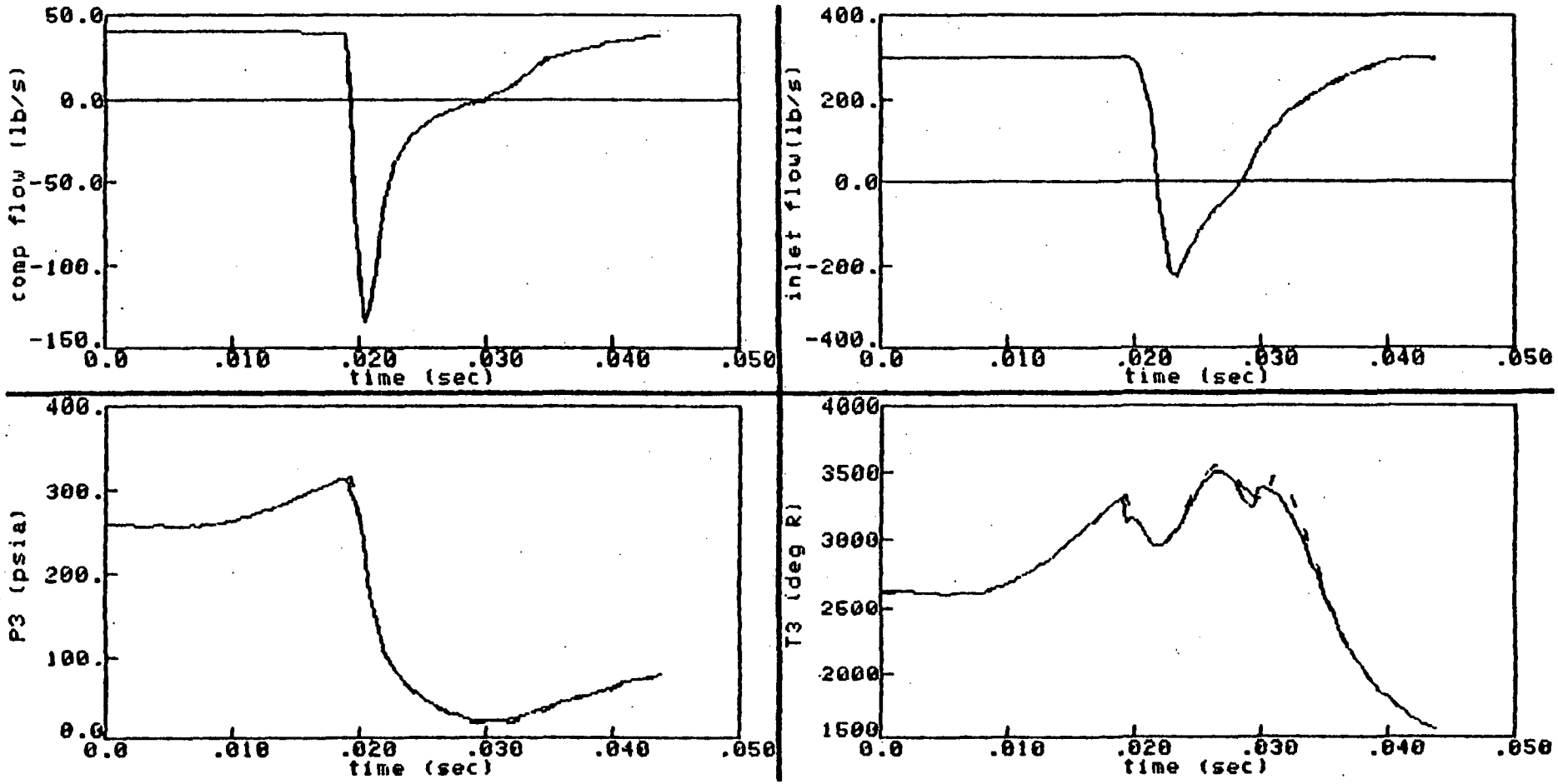

Figure 6.12 Turbofan Identification with Noise-Free Data, Run 17 (SCT, dashed line; NASA, solid line)

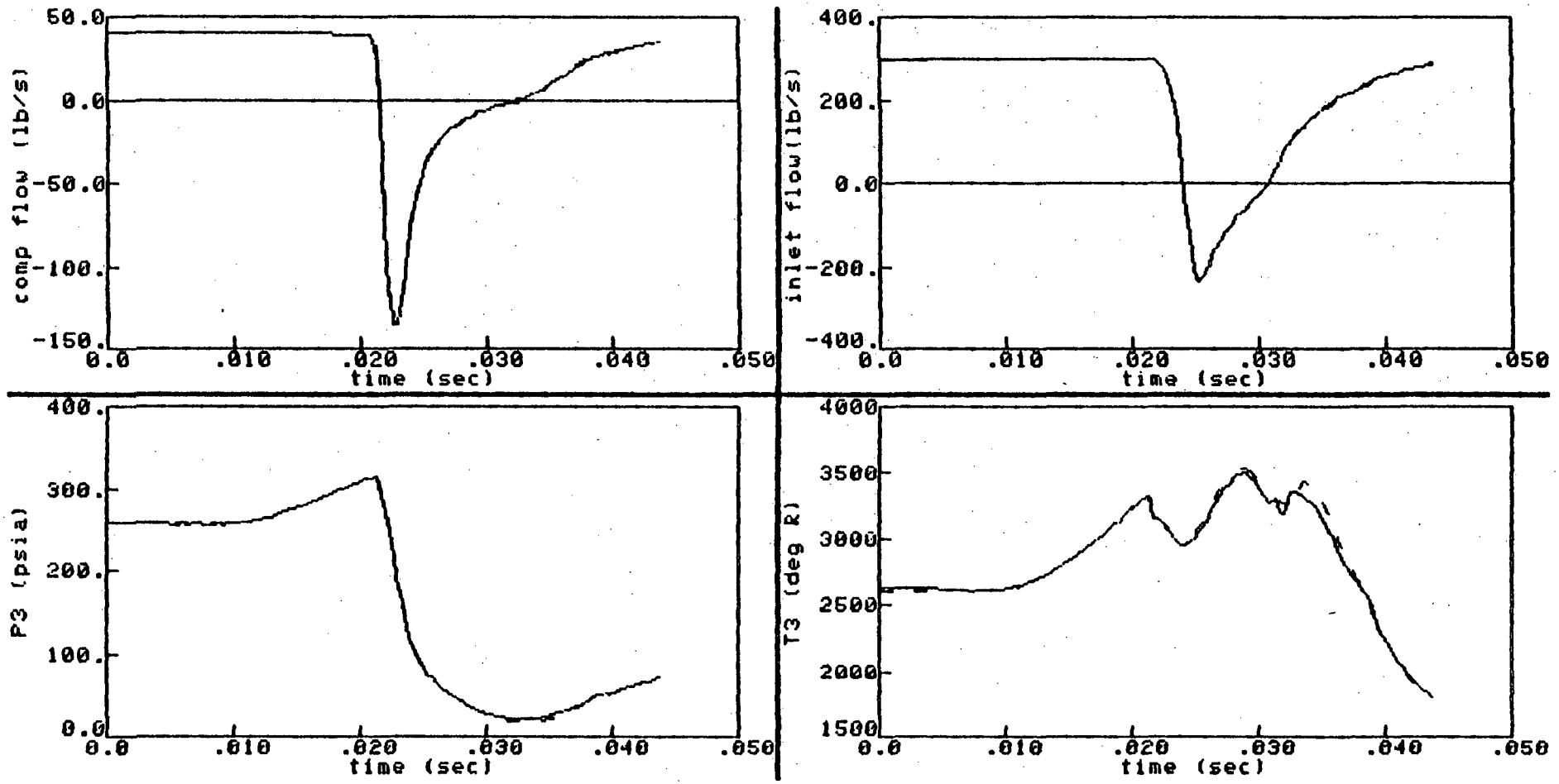

Figure 6.13 Turbofan Identification with Noise-Free Data, Run 18 (SCT, dashed line; NASA, solid line)

Table 6.4
Turbofan Identifications Original Parameter Estimates
(Before Identification)

Run	TSTART (sec/100)	Rx (x1/100)	V3	KNC	KPC
5	1.9000	1.500	3019.	25.00	10.00
6	1.7500	1.500	3019.	25.00	10.00
9	1.8000	.5000	4319.	25.00	7.500
10	1.8100	.5000	4319.	25.00	7.500
13	2.2900	1.500	2319.	25.00	7.500
14	1.7900	1.500	2319.	25.00	7.500
17	1.9400	1.500	2319.	25.00	7.500
18	2.1600	1.500	2319.	25.00	7.500

Table 6.5
Measurements Used in Noise-free Data Identifications

WOdot	inlet flow
WTdot	fan tip flow
WHdot	fan hub flow
WDdot	duct flow
WXdot	crossflow
W2dot	compressor flow
W3dot	exit flow
P1	pressure, stage 1
P2t	pressure, stage 2 tip
P2h	pressure, stage 2 hub
P3	pressure, stage 3
T1	temperature, stage 1
T2t	temperature, stage 2 tip
T2h	temperature, stage 2 hub
T3	temperature, stage 3

Three of the four engine parameters, Rx, V3 and KNC, were identified with great accuracy (to within 1 percent of actual) in the first round of identifications. This is not surprising, considering the model and plant are

identical and the data were noise free. Yet the KPC identifications, averaging around a 13 percent identification error, were less successful than might be expected (under perfect, noise-free conditions, exact identification is predicted by theory.) It will be shown later that KPC is practically unidentifiable in recoverable stall even with low noise levels. And, given that there was some small amount of noise in the "noise-free" data (see T2h for example), imperfect KPC identifications are not unreasonable.

Several alterations to the identification procedures were made in an effort to improve the KPC identifications. Although no technique proved to be successful, the revised alterations are summarized and discussed below for documentation and reference.

6.5.1 New Procedures for Improving KPC Identifications

(1) The above identifications used two steps in identifying the engine parameters. First, Rx, V3, and KNC were identified; then these three were identified along with KPC. In an effort to improve the KPC values identified in this second step, a third step was added to identify KPC by itself, without the influence of the other parameters. Since KPC and KNC were being identifed simultaneously, it was suspected that the KNC identification may be influencing the KPC results, as had happened in the compressor rig identifications. However, this added third step did little, if anything, to improve the KPC identifications.

(2) Another technique investigated involved reducing the number of sensors used. Only the compressor flow measurement was used in a few identifications in an effort to improve the KPC results. If some of the other measurements were biased or in some way inaccurate, they might influence the identification. Using a single measurement source would eliminate these negative influences if they did exist as long as the single measurement itself was unbiased. The technique again showed no improvement in the KPC identifications and was not pursued further.

(3) By definition, KPC only affects the turbofan model when the model is in a positive, stalled flow mode. Thus, KPC identification is mainly dependent upon data representing positive stalled flow (note: KPC can influence state variables after recovery and thus still affect the model when not in a positive stalled flow regime).

Using this knowledge, a technique was employed whereby only positive stalled flow data were used in the identification. The procedure called for the twelve turbofan states to be known at the onset of positive stalled flow so that the model could be initialized. The states were determined by propagating the turbofan model using the previously identified engine parameters until the end of negative stalled flow and the states were noted. Once the model was initialized and the measurement data edited to include only the data of interest, the identification followed the normal identification procedure. However, the KPC identifications failed to improve.

The theory being tested was that the timing of the model switching (from negative stalled flow to positive stalled flow) may be hampering the KPC identifications. Even if KNC is fixed (not identified), the point at which the model switches into positive stalled flow may vary because a small part of the trajectory moves through positive stalled flow just at the onset of stall. If the switching point is allowed to vary, then in theory, the cost function gradients may exhibit unusual characteristics because of what "appears" to be a time skew problem. This concept was discussed for the compressor rig in Section 4.5.2.3.

(4) A final technique used, and already mentioned above, involved the creation of a "stall end" time parameter, TSTOP. Again, the TSTOP parameter was intended to eliminate differences in the time of recovery between model and plant produced by slight model-plant differences (similar in concept to the TSTART problem.) The difficulty with the technique is that TSTOP, the time of recovery, is in large part determined by KPC. Thus when TSTOP is used, the value of KPC is practically eliminated, i.e., KPC has little if no effect on the model. The when TSTOP is used, KPC identifications suffer rather than improve.

The reason these techniques were unsuccessful, or marginally successful, was primarily due to the limited identifiability of KPC. As will be discussed later, different KPC values have very little effect on the engine response in recoverable stalls. Consequently, there is very little "KPC information" to be found in the measurements. Most of the above techniques were aimed at isolating the information or eliminating unwanted background information. The techniques were unsuccessful primarily because the amount of KPC information was just too small, even with the use of special technical enhancements.

6.6 TURBOFAN IDENTIFICATIONS USING NOISY DATA

The results of the second round of turbofan identifications are summarized in Table 6.6. In this round, random white noise was added to the data and the measurement set used in identification was reduced significantly (see Table 6.7). Flow measurements were entirely eliminated from the measurement set so that the importance of their presence in stall parameter identification could be determined.

Identification of three of the four engine parameters was very good, especially considering the added presence of noise. The fourth engine parameter, KPC, did not fare so well. Its identification was much impeded by the lack of flow measurement information and the added noise. The identified models are compared to the measured data in Figures 6.14 through 6.21.

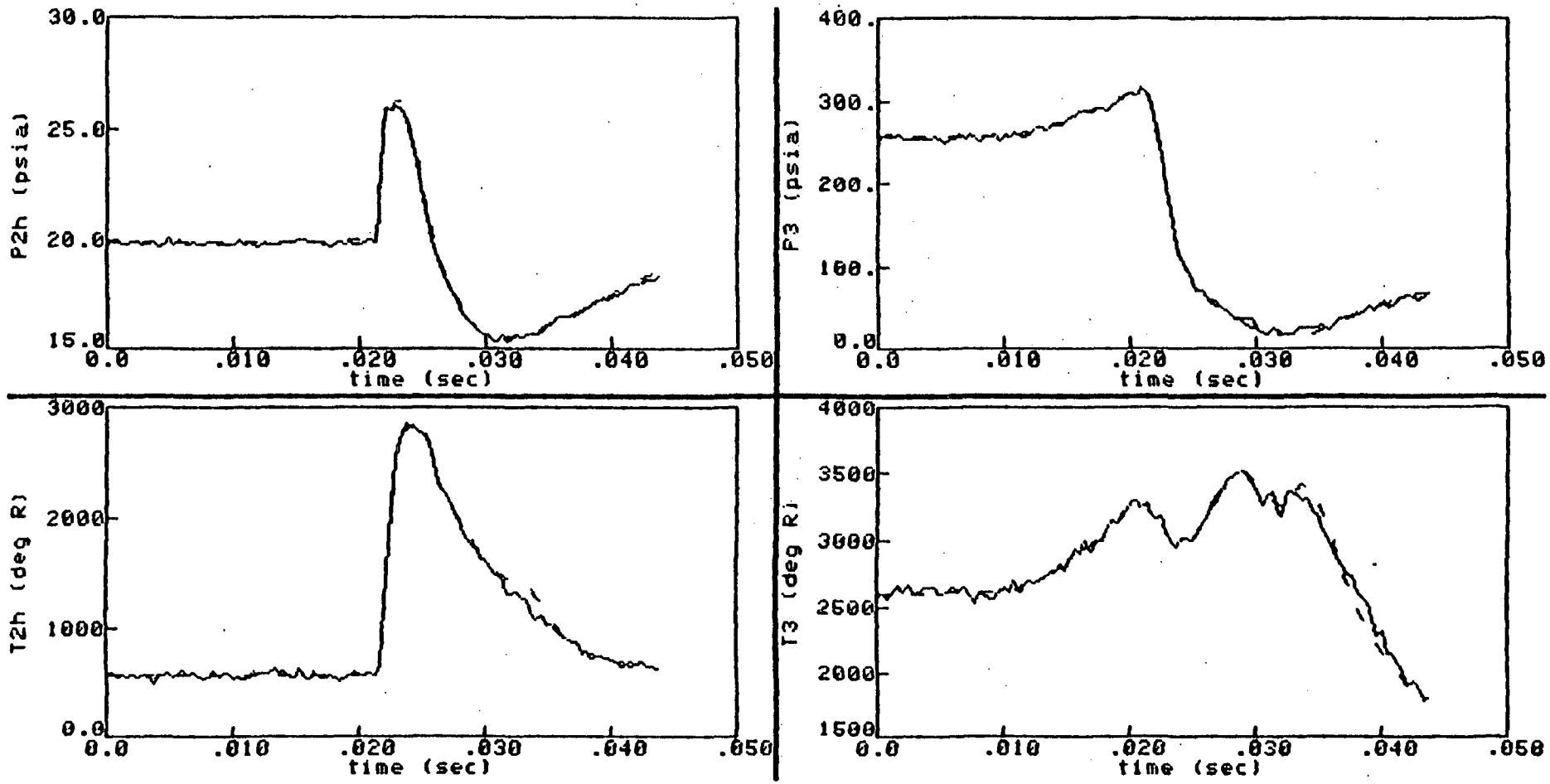

Figure 6.14 Turbofan Identification with Noisy Data, Run 5 (SCT, dashed line; NASA, solid line)

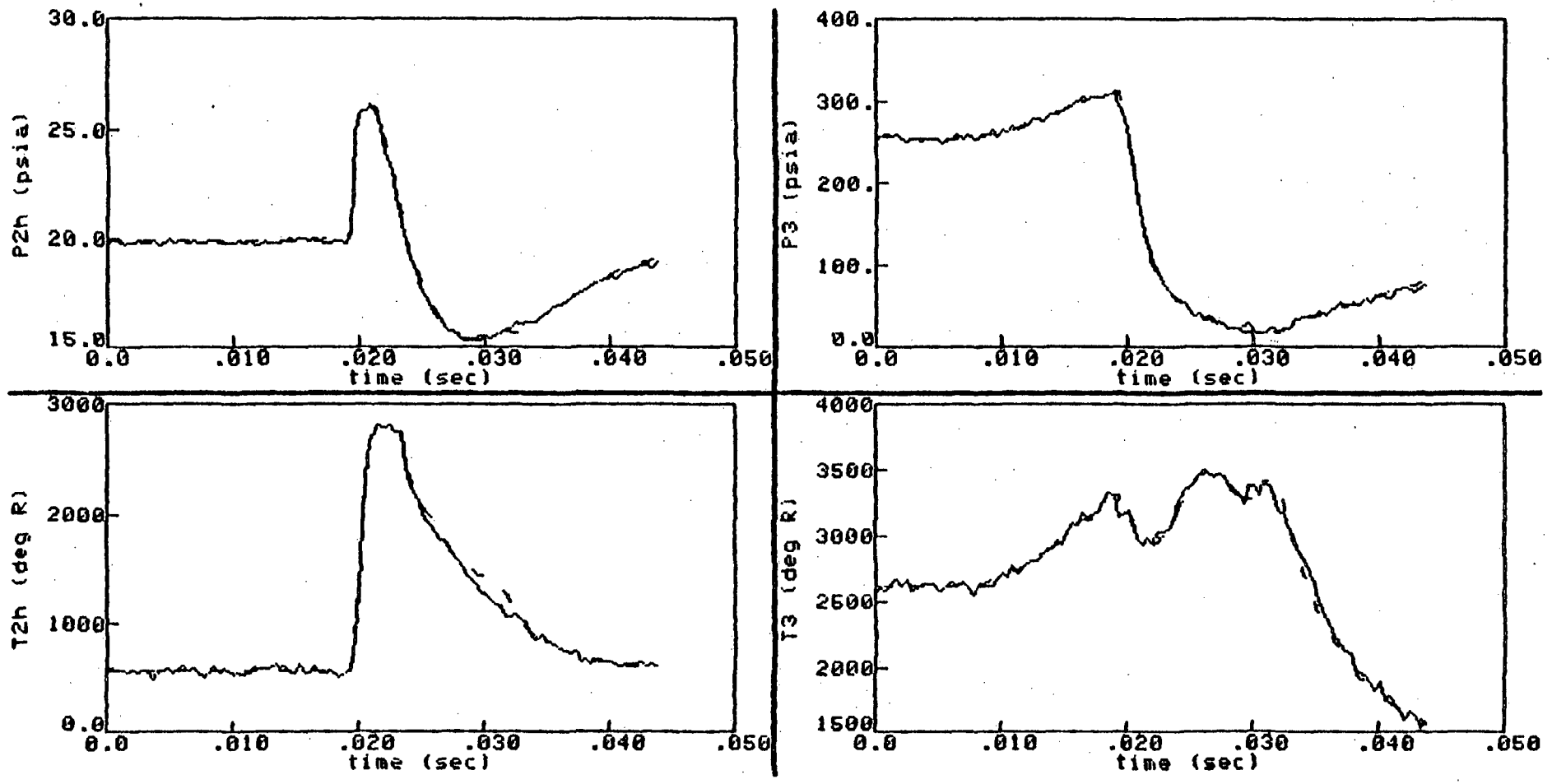

Figure 6.15 Turbofan Identification with Noisy Data, Run 6 (SCT, dashed line; NASA, solid line)

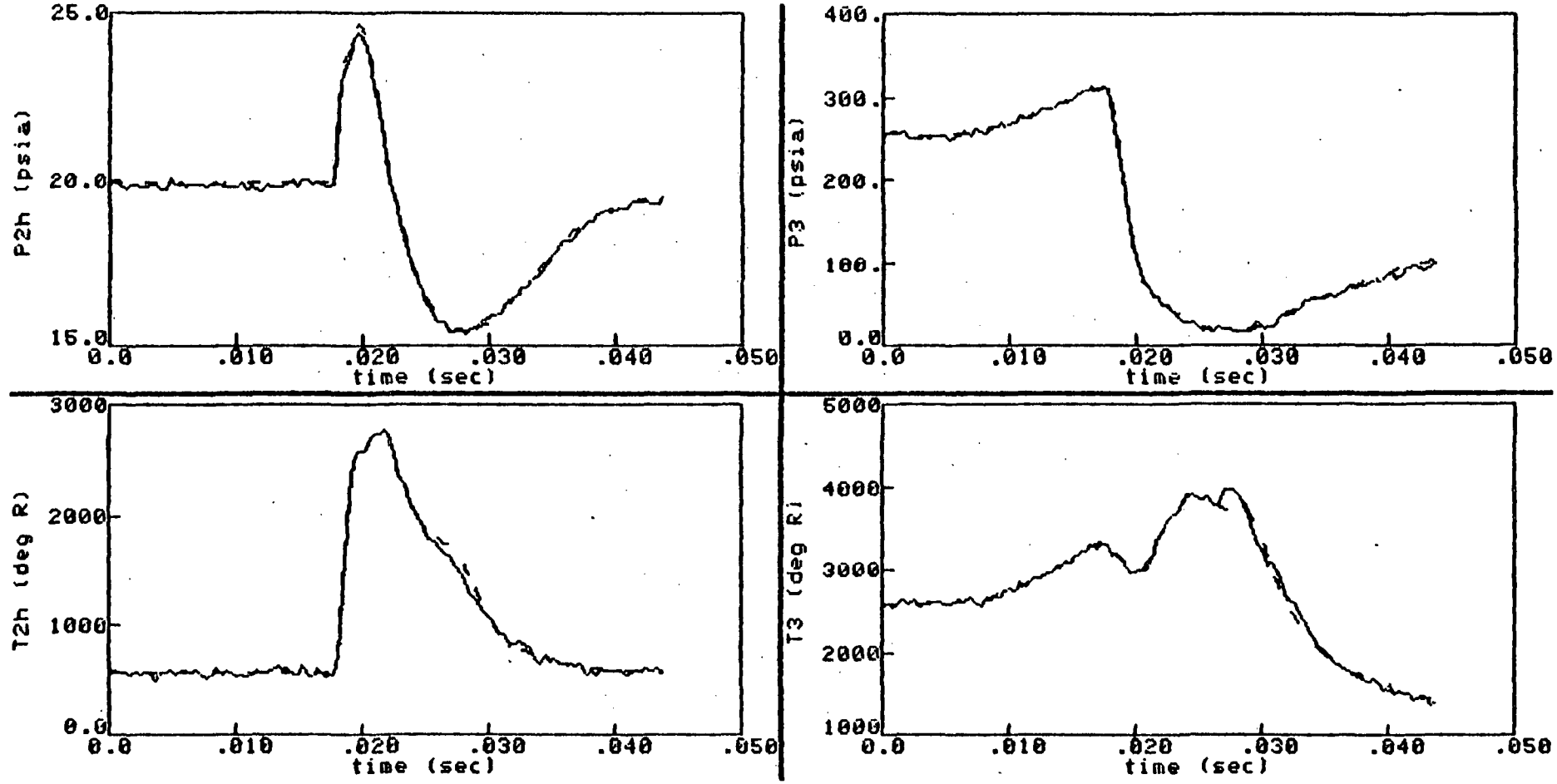

Figure 6.16 Turbofan Identification with Noisy Data, Run 9 (SCT, dashed line; NASA, solid line)

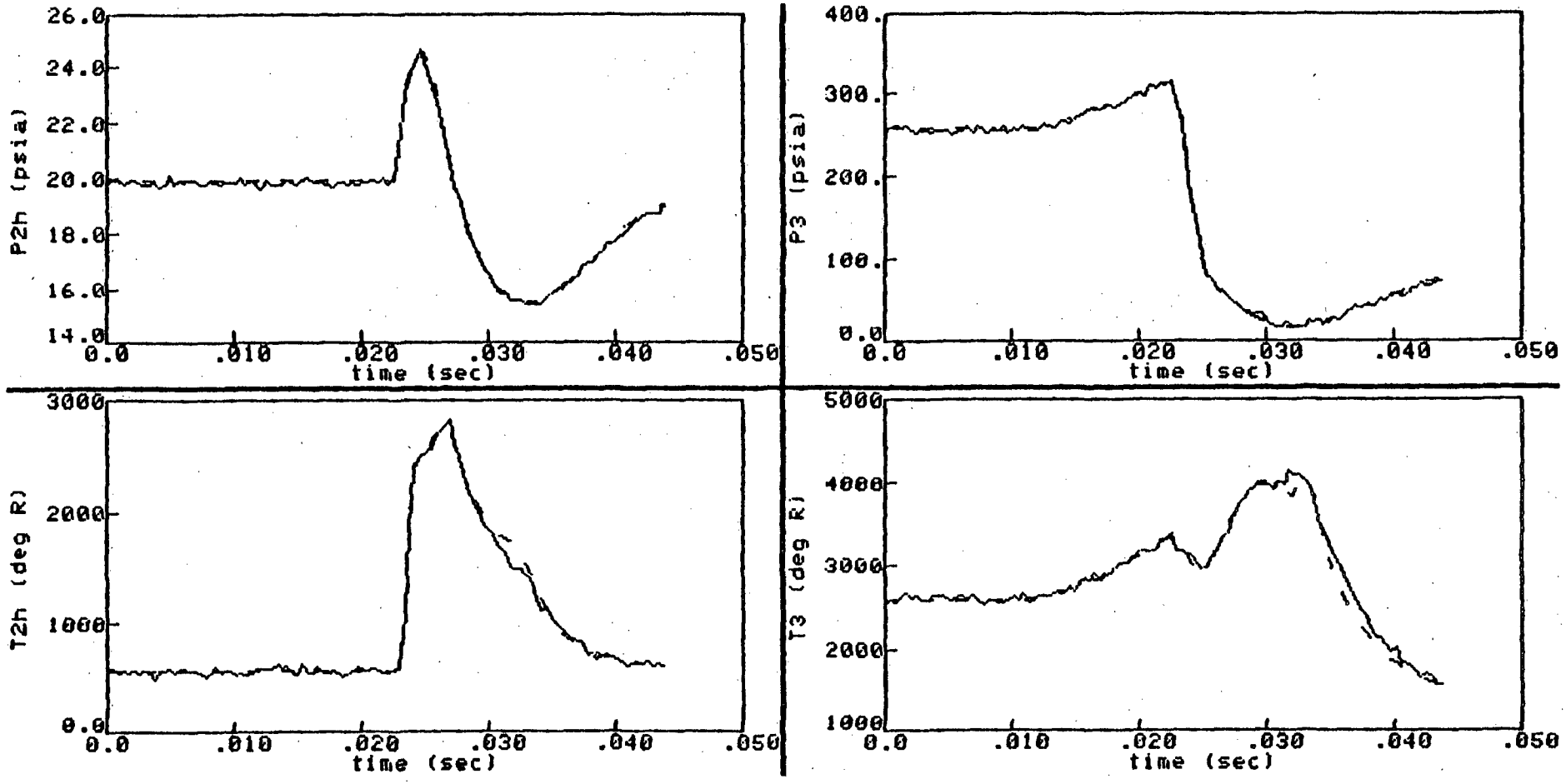

Figure 6.17 Turbofan Identification with Noisy Data, Run 10 (SCT, dashed line; NASA, solid line)

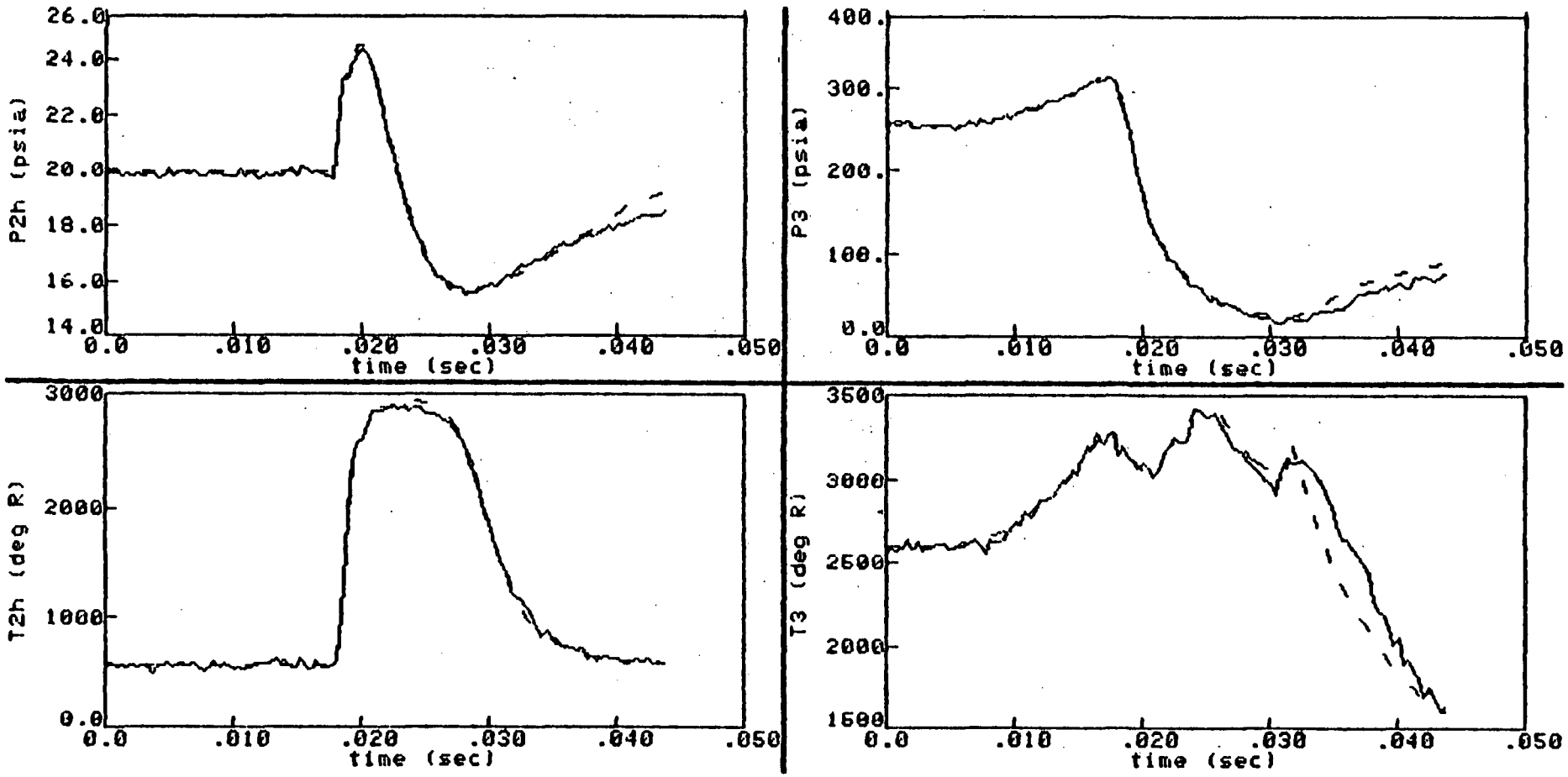

Figure 6.18 Turbofan Identification with Noisy Data, Run 13 (SCT, dashed line; NASA, solid line)

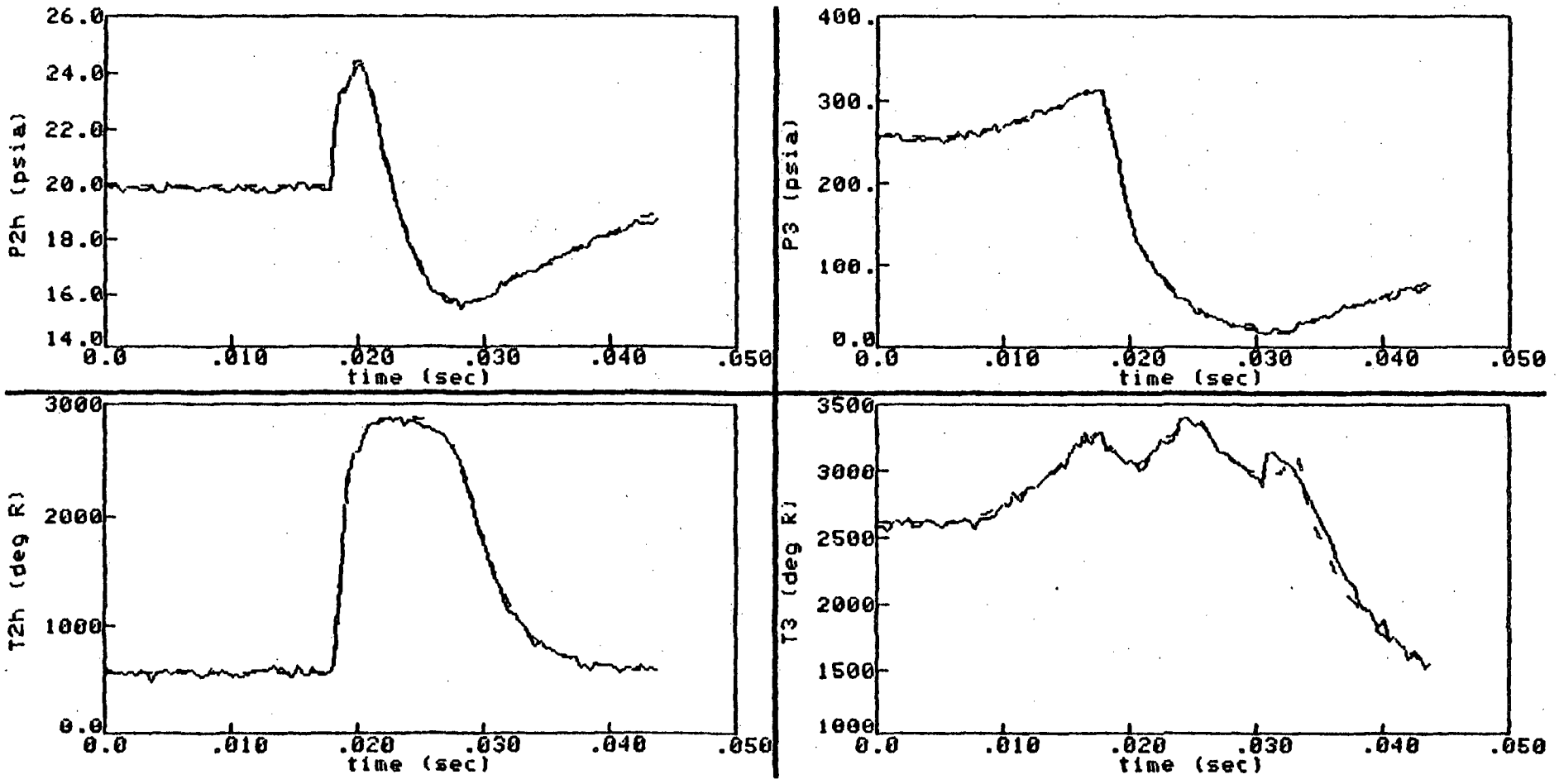

Figure 6.19 Turbofan Identification with Noisy Data, Run 14 (SCT, dashed line; NASA, solid line)

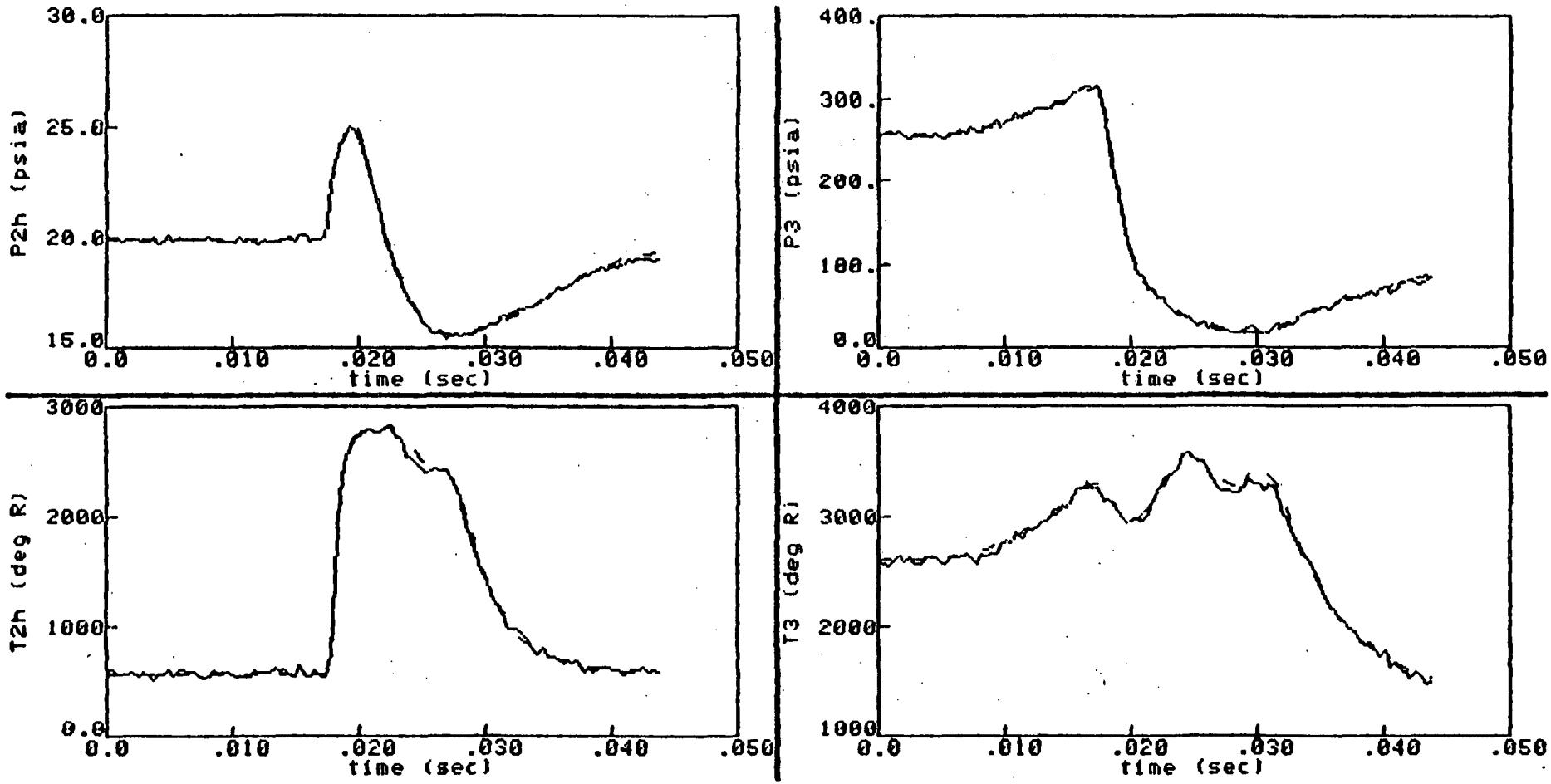

Figure 6.20 Turbofan Identification with Noisy Data, Run 17 (SCT, dashed line; NASA, solid line)

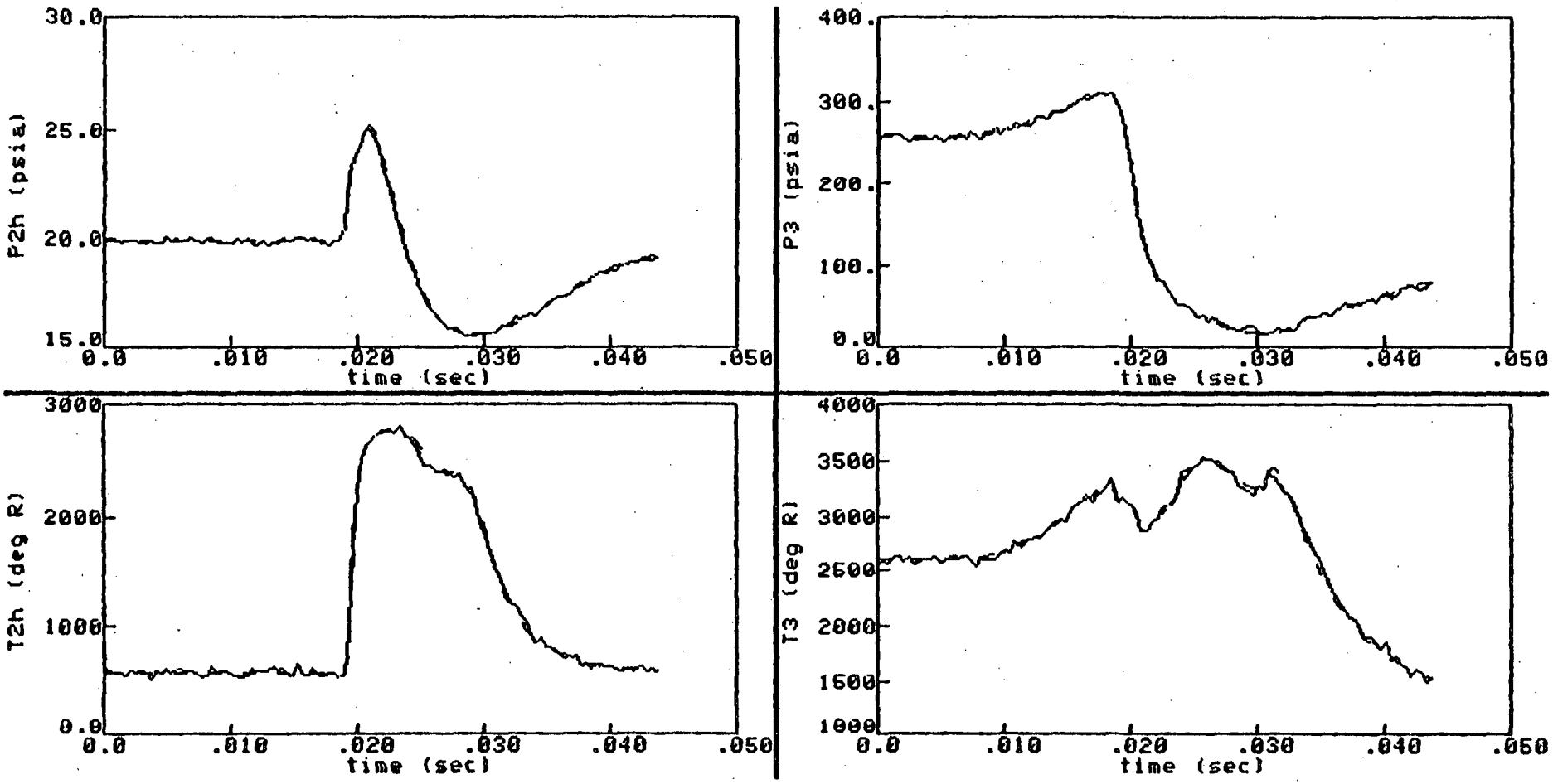

Figure 6.21 Turbofan Identification with Noisy Data, Run 18 (SCT, dashed line; NASA, solid line)

Table 6.6
Turbofan Identifications Using Noisy Recoverable Stall Data

Run	TSTART (sec/100)	Rx (x1/100)	V3	KNC	KPC
5	1.8729	.9781	3403.	47.28	N/C
6	1.7307	.9817	3389.	47.24	N/C
9	1.7755	.9453	3483.	99.29*	N/C
10	1.7820	.9662	3398.	98.66*	N/C
13	2.2689	1.0245	2644.*	48.21	N/C
14	1.7750	1.1225	2572.*	52.22	N/C
17	1.9214	1.9356*	3387.	47.45	N/C
18	2.1367	1.9225*	3406.	45.82	N/C
Average		1.003	3411.	48.03	N/A
percent error		0.3	2.77	-3.93	N/A
Average*		1.9291	2608.	98.98	

*identified unknown values. Not included in first average.
N/C no change
N/A not applicable

Table 6.7
Turbofan Identifications Sensor Set and Standard Deviation of Added Noise Levels

P1	0.08 psia
P2t	0.08 psia
P2h	0.08 psia
P3	3.0 psia
T1	3.0 deg R
T2t	3.0 deg R
T2h	30.0 deg R
T3	30.0 deg R

6.7 TURBOFAN IDENTIFICATION EVALUATION

The successes and failures in the turbofan identifications can be explained by examining the identifiabilities, or uncertainties associated with each parameter. Using Run 10 as a standard for the recoverable runs, the identifiability for each parameter given the sensors and noise levels in Table 6.7 are the following:

Table 6.8
Parameter Identifiabilities in Percent Standard Deviation

	1T	2T
Rx	0.1602	0.3204
V3	0.0830	0.1660
KNC	0.5143	1.0286
KPC	31.81	63.62

Table 6.8 simply says that for any single recoverable run, Rx can be identified to within 0.32 percent and KPC to within 63 percent, 95 percent of the time. Both of these examples are best-case examples (perfect model-plant agreement) and are therefore somewhat over-optimistic. They do indicate that while Rx, V3 and KNC are quite easily identified, KPC is rather difficult to identify with recoverable stall data. In fact KPC could not be identified at all in the second round of turbofan identifications.

To get a greater physical understanding of why KPC identifications are so difficult, two propagations of the Run 10 model were made. The first propagation consisted of the nominal parameter set (see Figure 6.22), the second consisted of identified Rx, V3, KNC and KPC parameters (see Figure 6.17).

Even though the KPC value in the second set was off by 100 percent (10 vs. 5), the measurement cost errors were practically identical to the values produced in the nominal case. In fact, the identified model errors were about 1/10 percent less than the nominal cost errors. This indicates that the differences in the stall trajectory produced by changing KPC are being overshadowed by sensor noise. The other parameters are identifiable because their differences are still significant in the presence of noise.

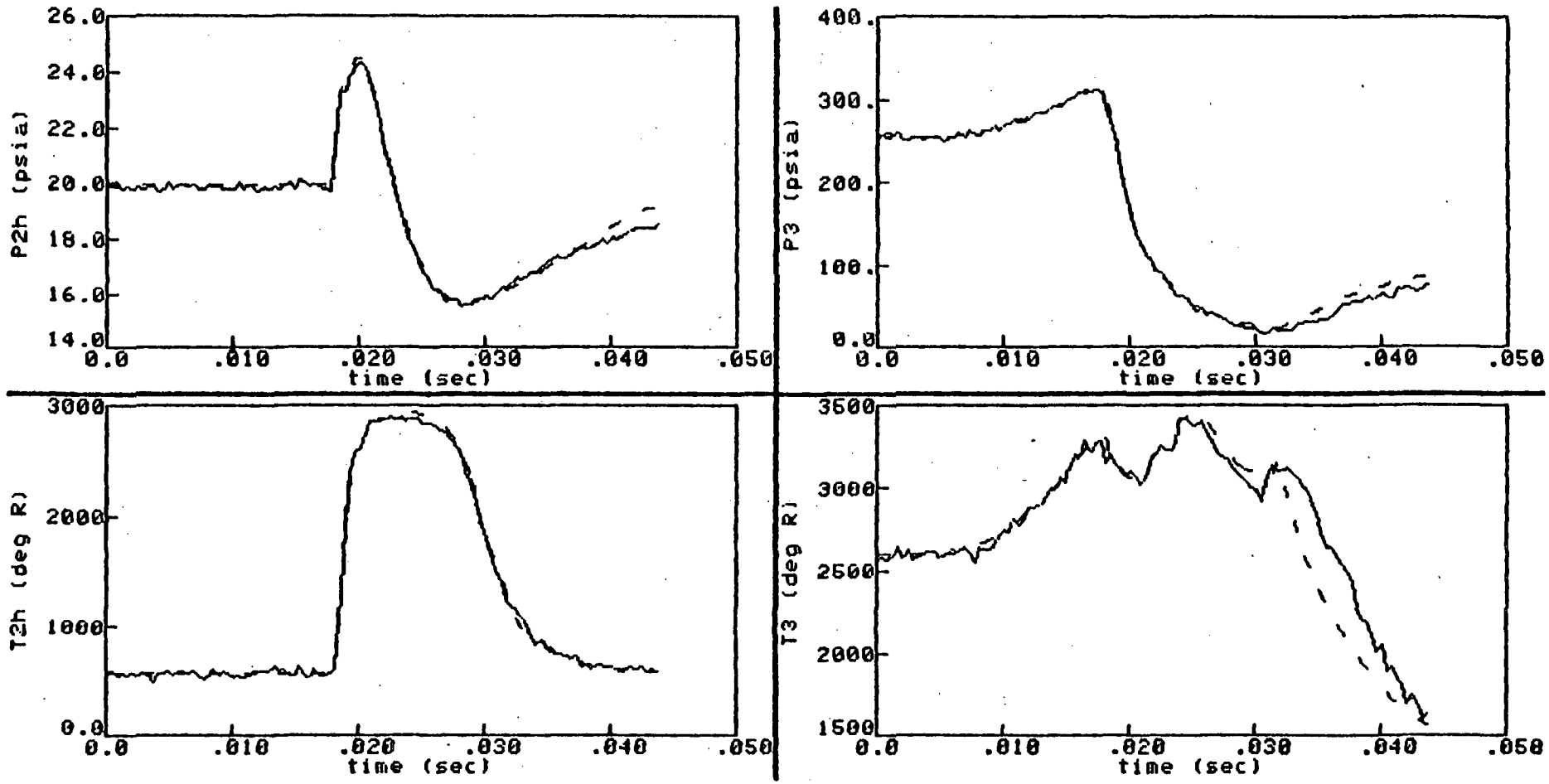

Figure 6.22 Turbofan Nominal Propagation, Run 10 (SCT, dashed line; NASA, solid line)

Simply stated, the model trajectory cannot be significantly improved by changing KPC in recoverable stall identifications. The changes in trajectory produced by KPC parameter changes are insignificant in comparison to uncertainties introduced by noise. To SCIDNT, the result is that a proper gradient cannot be determined.

KPC recoverable stall identification might be improved under better sensor set and noise conditions (could be studied by using the measurement contributions in Appendix A and methods outlined in Chapter IV). But for this particular scenario, KPC is unidentifiable.

6.7.1 Measurement Contributions

The informational contributions of each measurement to the engine parameters have been summarized graphically in Figures 6.23 through 6.30. The contribution levels are dependent upon the noise assumed on each sensor; the noise levels are shown in Table 6.9.

Table 6.9
Measurement Noise Levels Used in Calculating Contribution Levels

WOdot	3.0 lb/sec
WTdot	3.0 lb/sec
WHdot	3.0 lb/sec
WDdot	3.0 lb/sec
WXdot	3.0 lb/sec
W2dot	3.0 lb/sec
W3dot	3.0 lb/sec
P1	0.08 psia
P2t	0.08 psia
P2h	0.08 psia
P3	3.0 psia
T1	3.0 deg R
T2t	3.0 deg R
T2h	30.0 deg R
T3	30.0 deg R

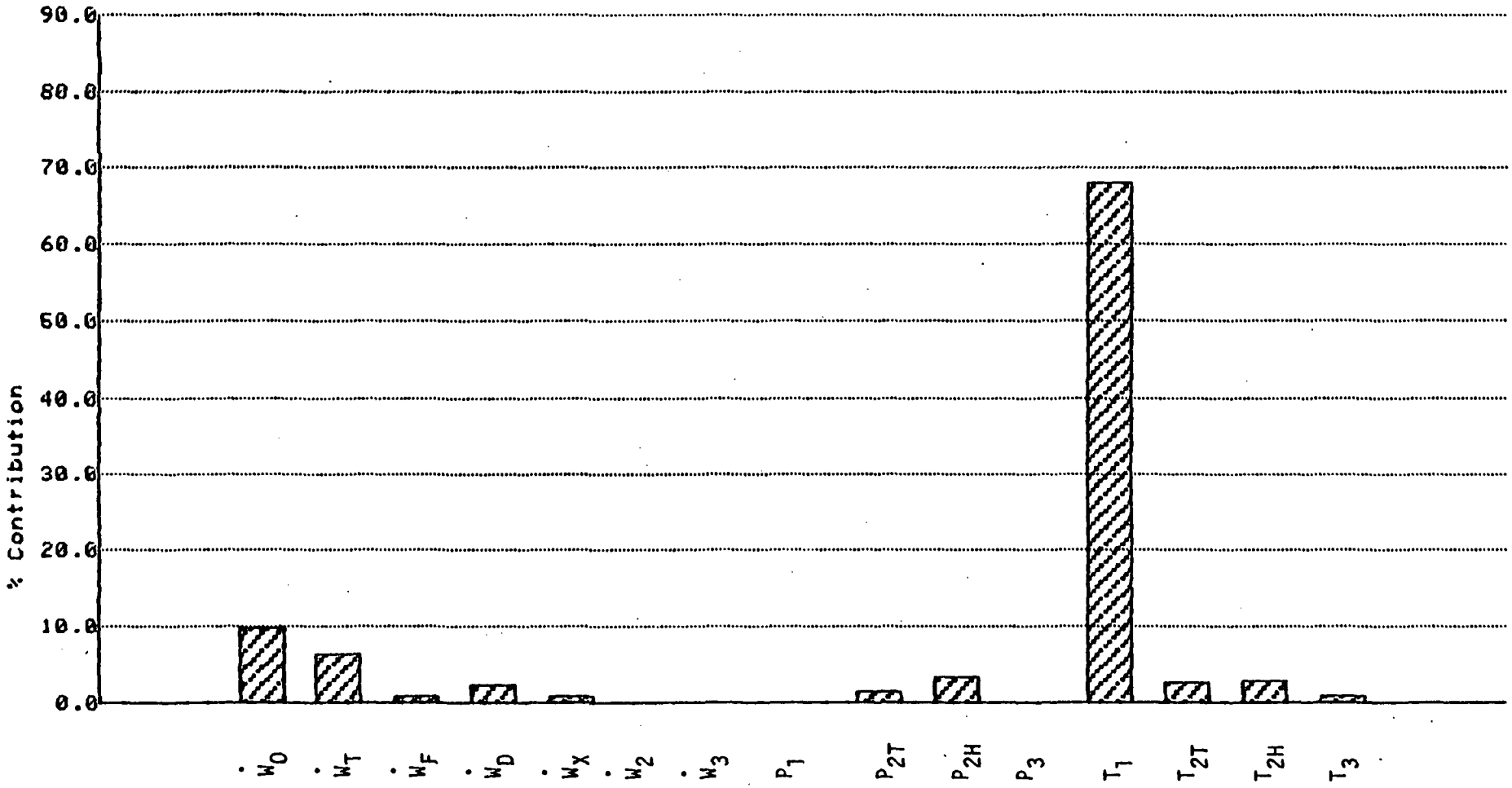

Figure 6.23 RX Measurement Contributions for a Recoverable Stall, Run 10 (SCT, dashed line; NASA, solid line)

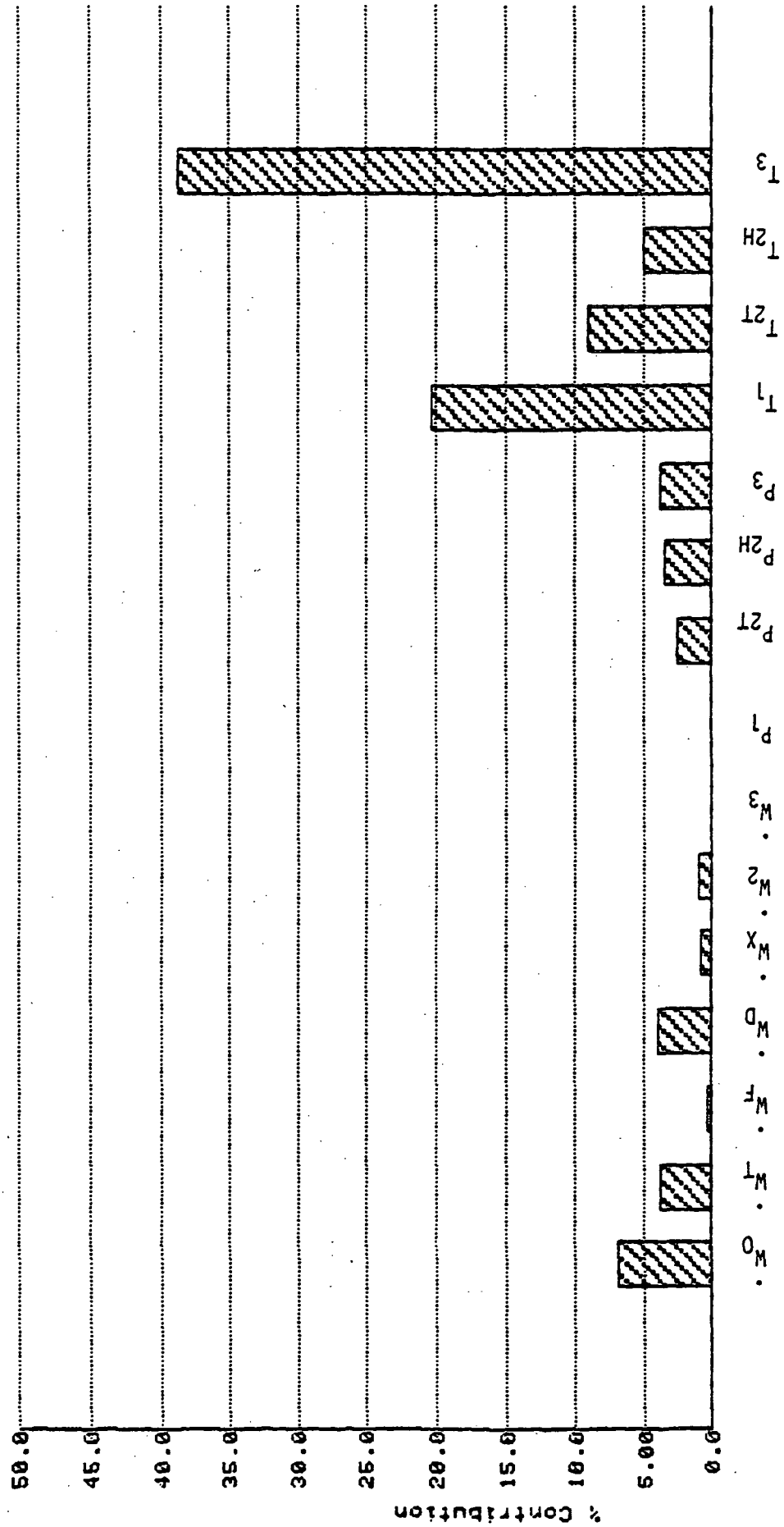

Figure 6.24 V3 Measurement Contributions for a Recoverable Stall, Run 10 (SCT, dashed line; NASA, solid line)

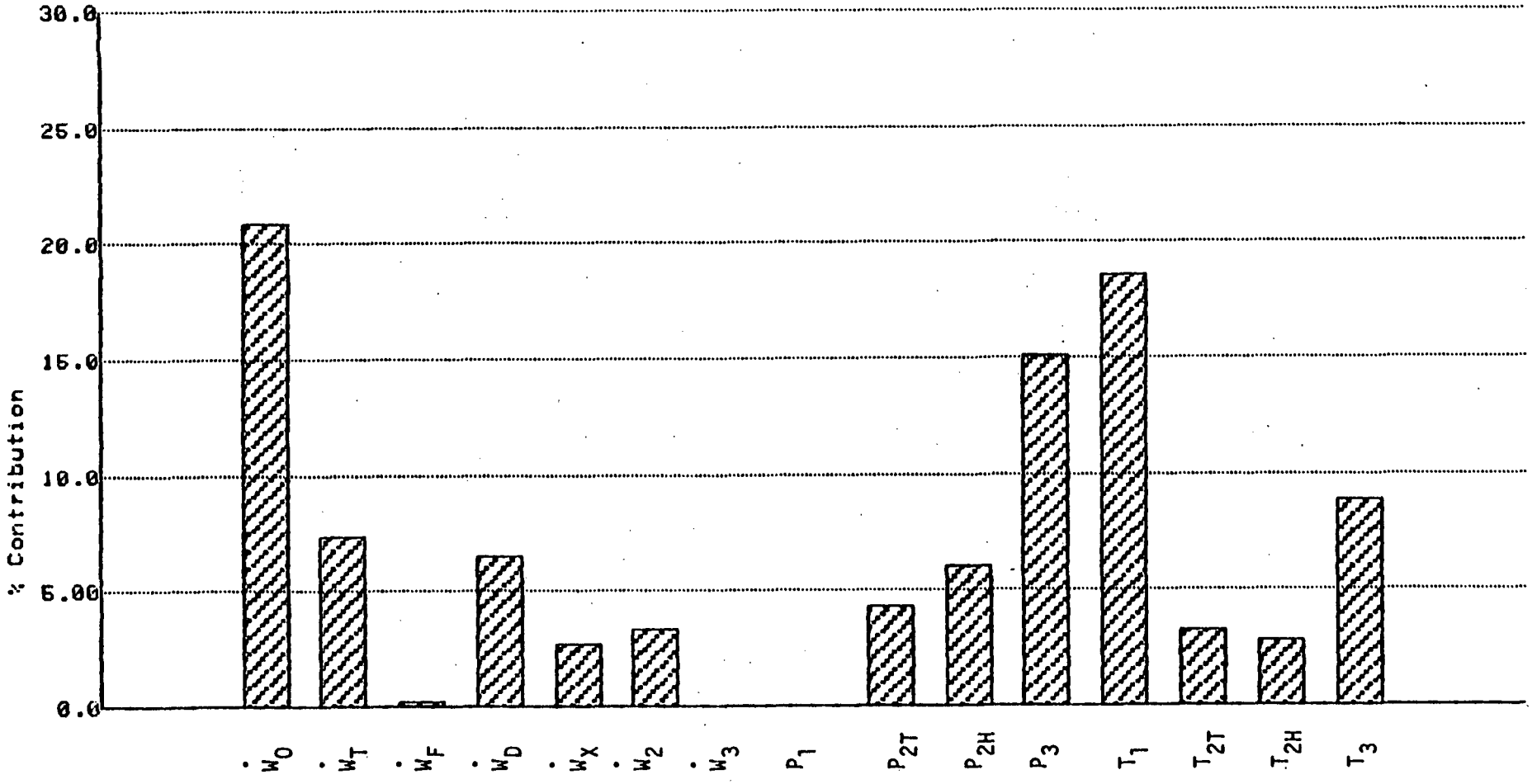

Figure 6.25 KNC Measurement Contributions for a Recoverable Stall, Run 10 (SCT, dashed line; NASA, solid line)

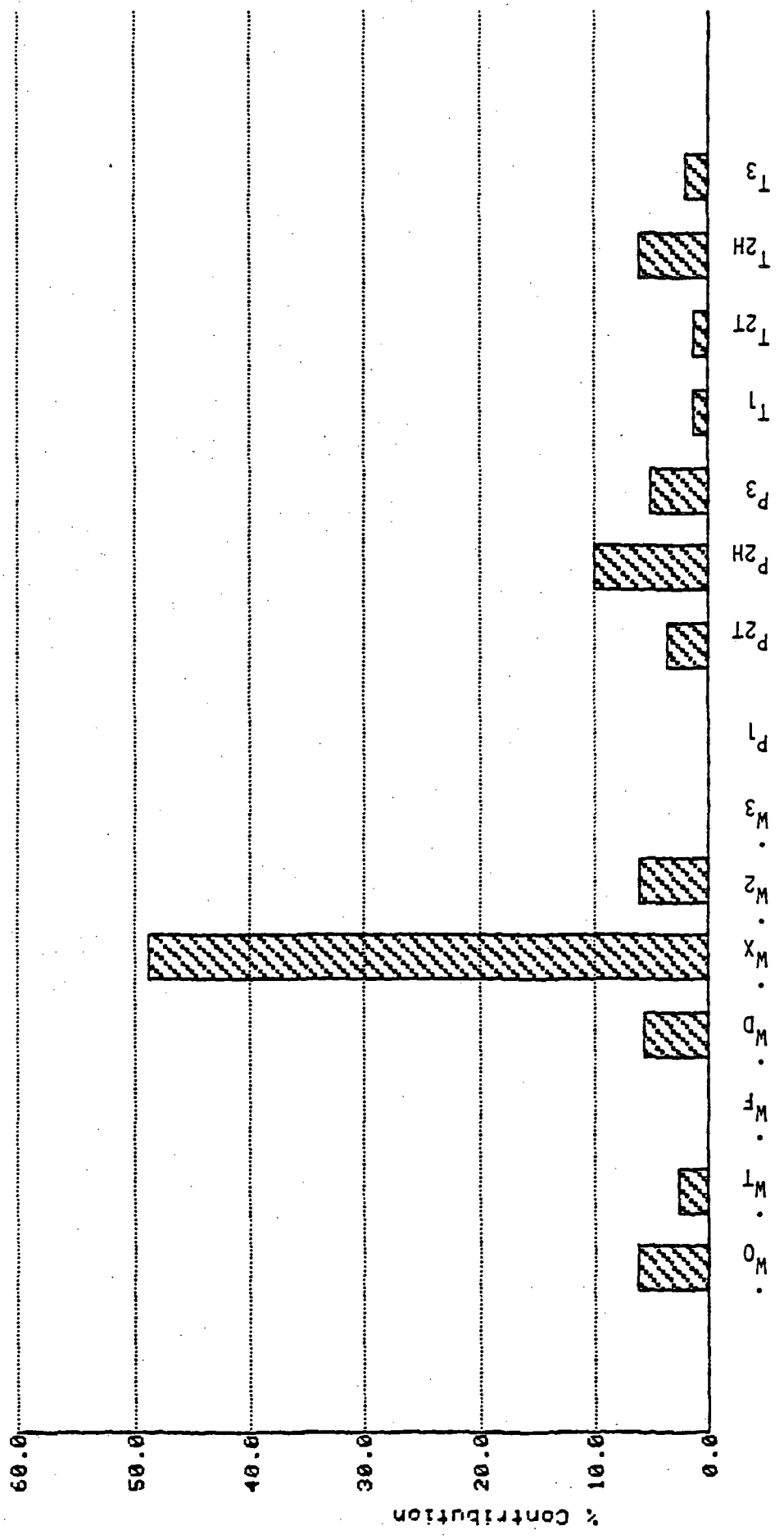

Figure 6.26 KPC Measurement Contributions for a Recoverable Stall, Run 10 (SCT, dashed line; NASA, solid line)

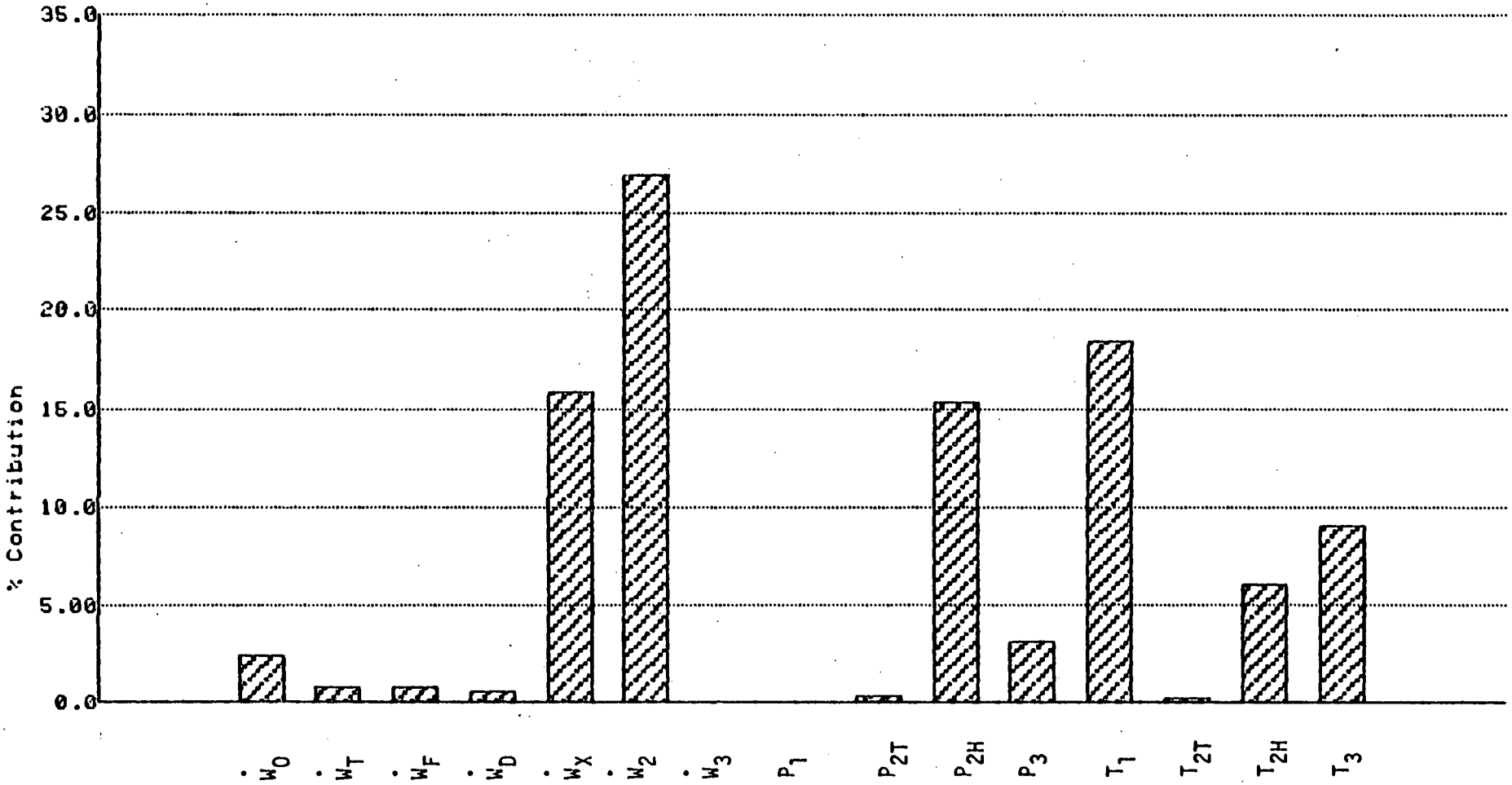

Figure 6.27 RX Measurement Contributions for a Nonrecoverable Stall, Run 10 (SCT, dashed line; NASA, solid line)

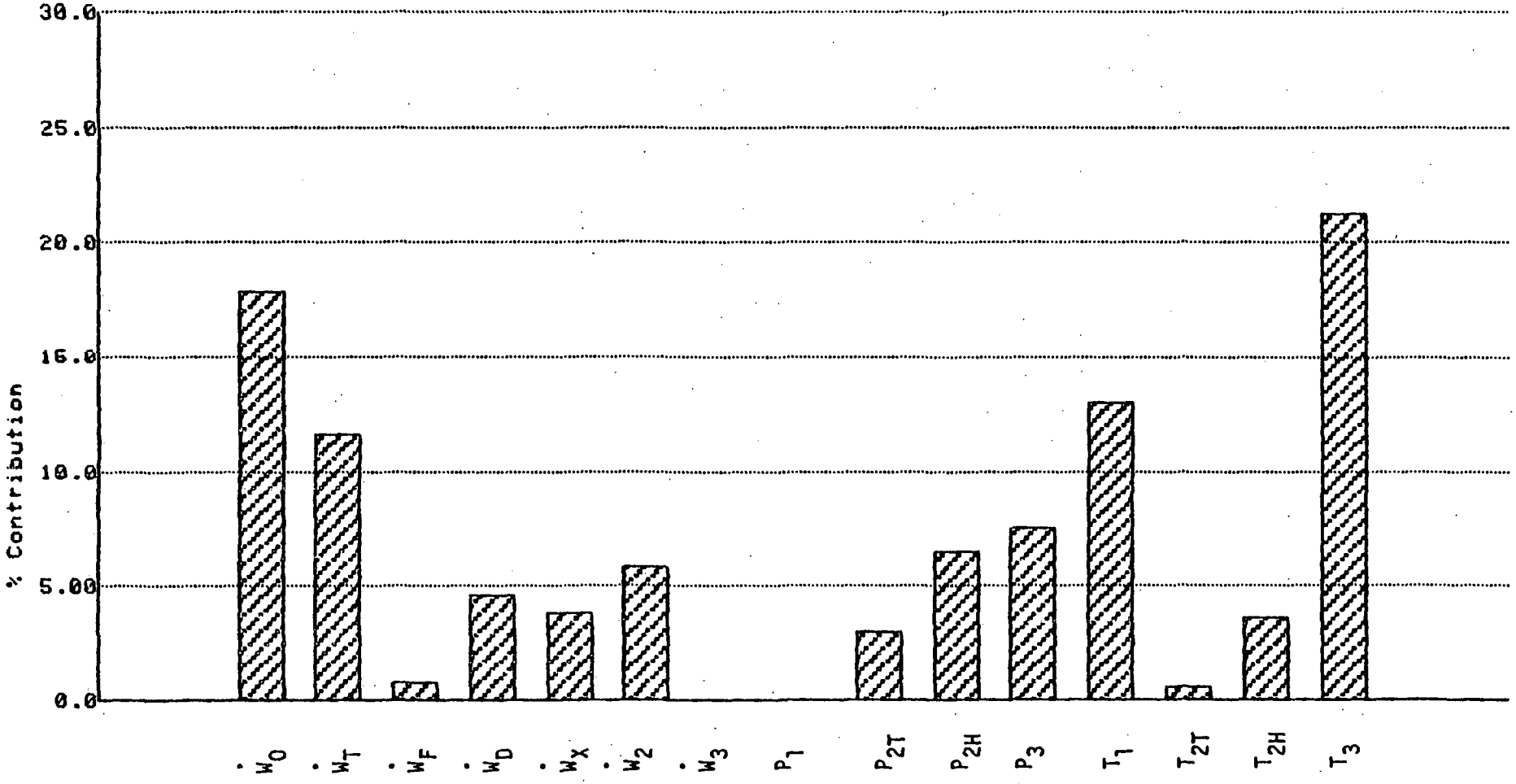

Figure 6.28 V3 Measurement Contributions for a Nonrecoverable Stall, Run 20 (SCT, dashed line; NASA, solid line)

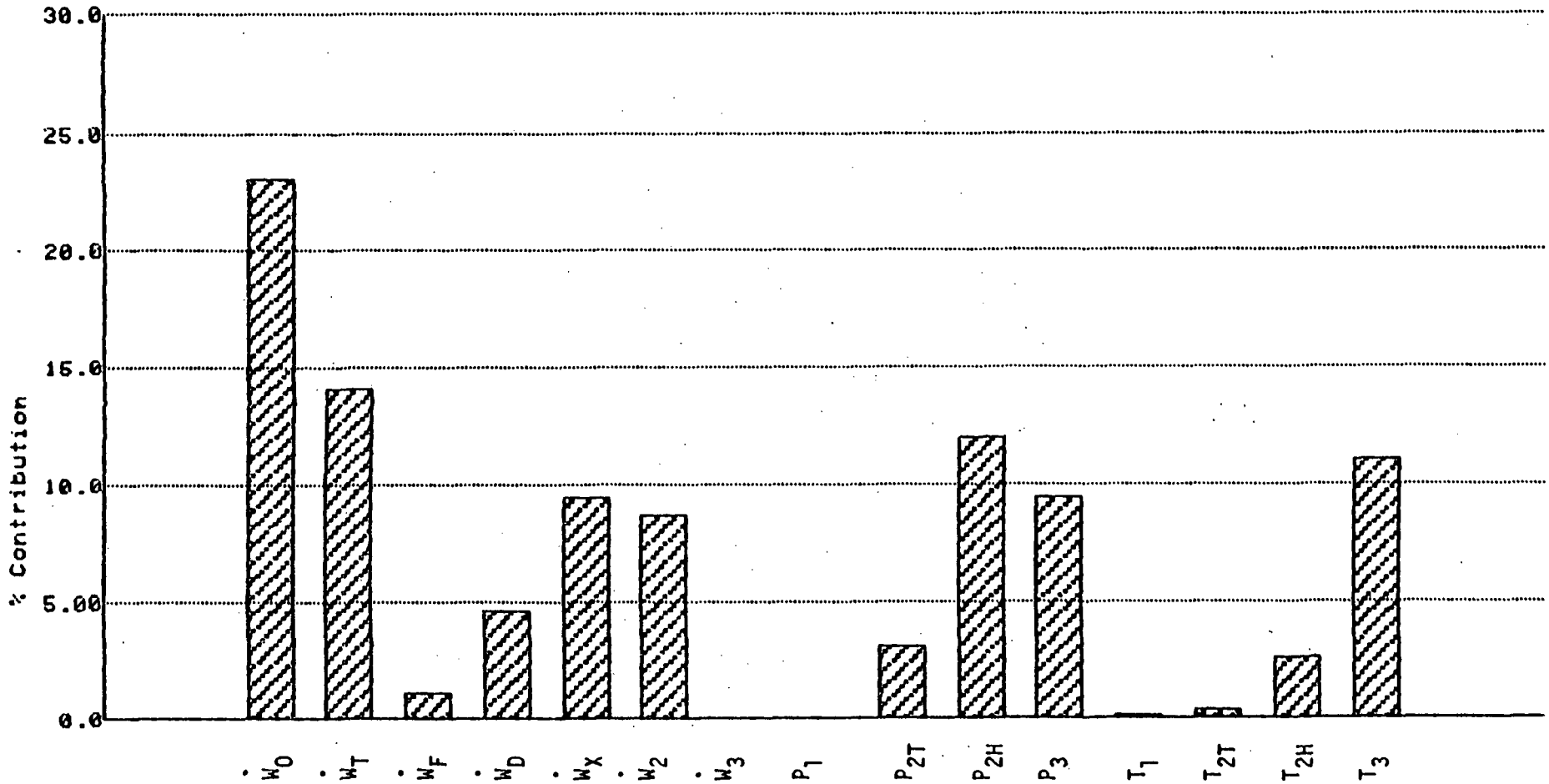

Figure 6.29 KNC Measurement Contributions for a Nonrecoverable Stall, Run 20 (SCT, dashed line; NASA, solid line)

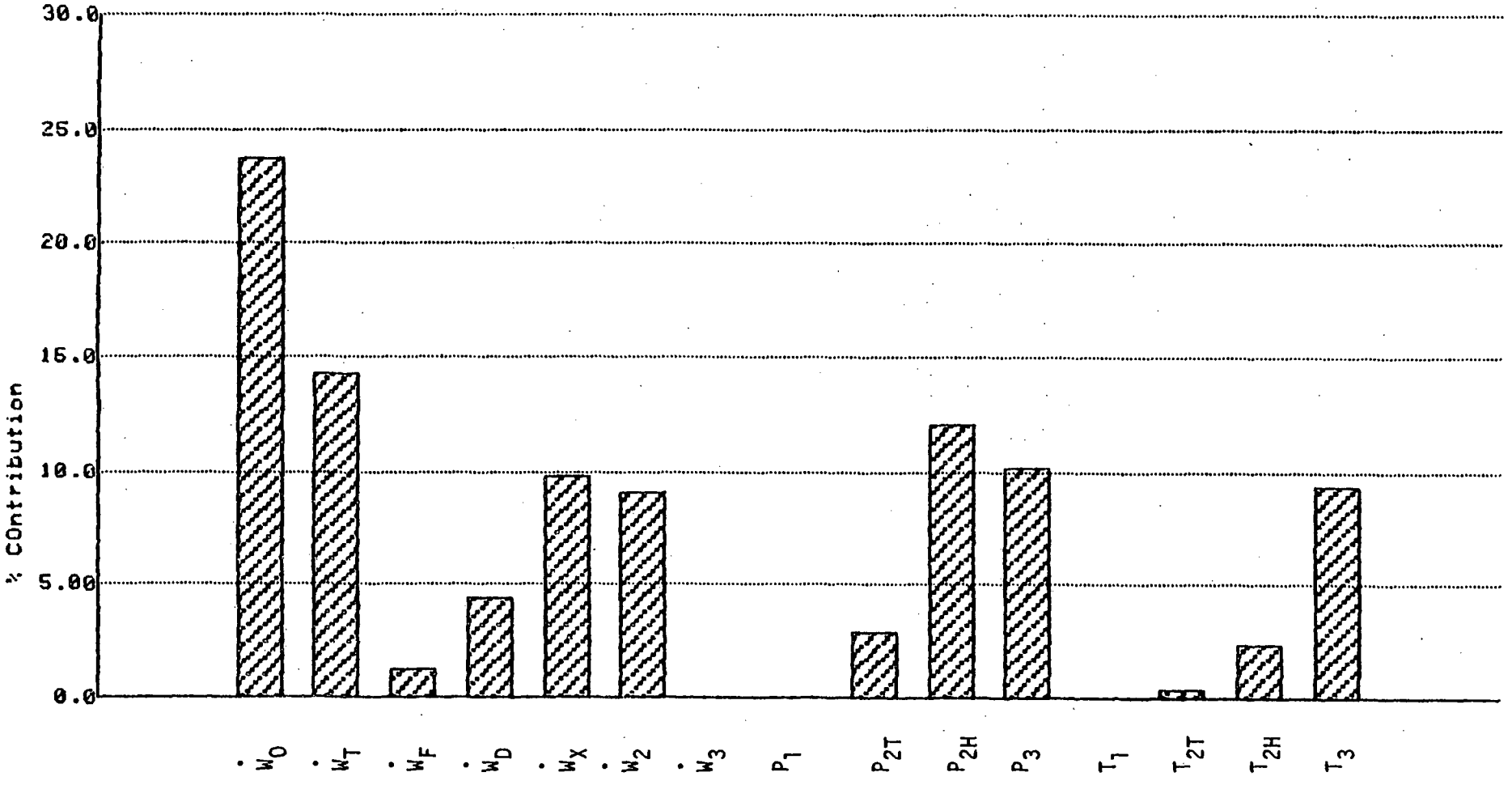

Figure 6.30 KPC Measurement Contributions for a Nonrecoverable Stall, Run 20 (SCT, dashed line; NASA, solid line)

For recoverable stall identifications both Rx and V3 are largely dependent upon temperature measurements and are independent of flow measurements. Consequently, their identifiability suffers little in the absence of flow readings.

KNC is more evenly divided in its informational dependence. It therefore sacrifices approximately half of its identifiability in the absence of flow readings.

KPC is heavily dependent upon the crossflow measurement. This measurement alone contributes 50 percent of the information pertaining to KPC, and consequently is sorely missed in the KPC second round identifications.

The scenarios change significantly in the nonrecoverable stall identifications. With nonrecoverable stall, the information is more evenly distributed among the flow, pressure and temperature measurements for all four parameters. Absence of flow measurements, although significant, usually would not be catastrophic to any single parameter identification.

6.7.2 Parameter Uncertainties

Table 6.10 summarizes engine parameter identifiabilities for four different situations. The uncertainties are based upon the noise levels given in Table 6.9.

Case	Description
1	Run 10 using all measurements. Recoverable stall.
2	Run 10 using pressure and temperature measurements only. Recoverable stall.
3	Run 20 using all measurements. Nonrecoverable stall.
4	Run 20 using pressure and temperature measurements only. Recoverable stall.

Table 6.10
Parameter Identifiabilities in Percent Standard Deviation

Case	Rx	V3	KNC	KPC
1	.1428	.0757	.3951	17.54
2	.1602	.0830	.5143	31.81
3	.0915	.0266	.0189	.0204
4	.1261	.0357	.0303	.0333

Several important generalities can be drawn from these results:

(1) All engine parameters are identifiable in all four cases with one exception: KPC is virtually unidentifiable in recoverable stall cases.

(2) Parameter uncertainty will increase from 10 percent to 50 percent if flow measurements are unavailable.

(3) Parameter identifiability improves significantly when identification is done with nonrecoverable data instead ofrecoverable data. This is strikingly true with KPC, and true for KNC as well, but to a lesser degree.

From these results, it can be determined with reasonable confidence that, had the nonrecoverable identifications been possible, the KPC identifications would have been much improved. In fact, the results in Table 6.10 predict identifiablity on par with the other three engine parameters.

6.8 NONRECOVERABLE RUN IDENTIFICATIONS

The turbofan identifications concentrated upon recoverable stall data for the turbofan study. Originally, it was planned to use both recoverable and nonrecoverable data, but difficulties in using the nonrecoverable data prevented its use.

Nonrecoverable data identification has been unsuccessful to date because of what appears to be a fundamental difference between the SCT and NASA Lewis turbofan models. Although some identification was completed using the

nonrecoverable data, it was soon determined that the model differences would produce "incorrect" identifications in some of the parameters. The following two sections document these identifications and the model-plant mismatch.

6.8.1 Model-Plant Mismatch

Figures 6.31 and 6.32 present the NASA Lewis and SCT stall responses for model Run 20. The SCT model uses the parameter values shown in Table 6.9 and should be identical to the NASA Lewis response. Obviously there is a major difference between the two responses. A second model (Run 15) was also tested to verify the differences, and it also exhibited major model-plant differences.

Table 6.11
Run 20 Nominal Engine Parameters

Run	TSTART (sec/100)	Rx (x1/100)	V3	KNC	KPC
20	1.8190	2.000	3319.	50.00	5.000

Note that the two models agree through the unstalled and negative stalled flow portions of the trajectory and that it is during the positive stalled flow that the models diverge. This suggests that the modelling error lies within the positive stalled flow portion of the model. In any event, since part of the responses do seem to agree, identification of some of the engine parameters (Rx, V3, and KNC; all but KPC which is only active during positive stalled flow) was possible.

The reason why the SCT and NASA Lewis nonrecoverable models differ could not be determined under the scope of this project. It is somewhat confusing that the recoverable stalls, although they also move through unstalled to negative stalled to positive stalled flow, do not appear to have the same modelling problems. Efforts may be made in future work to resolve these anomalies.

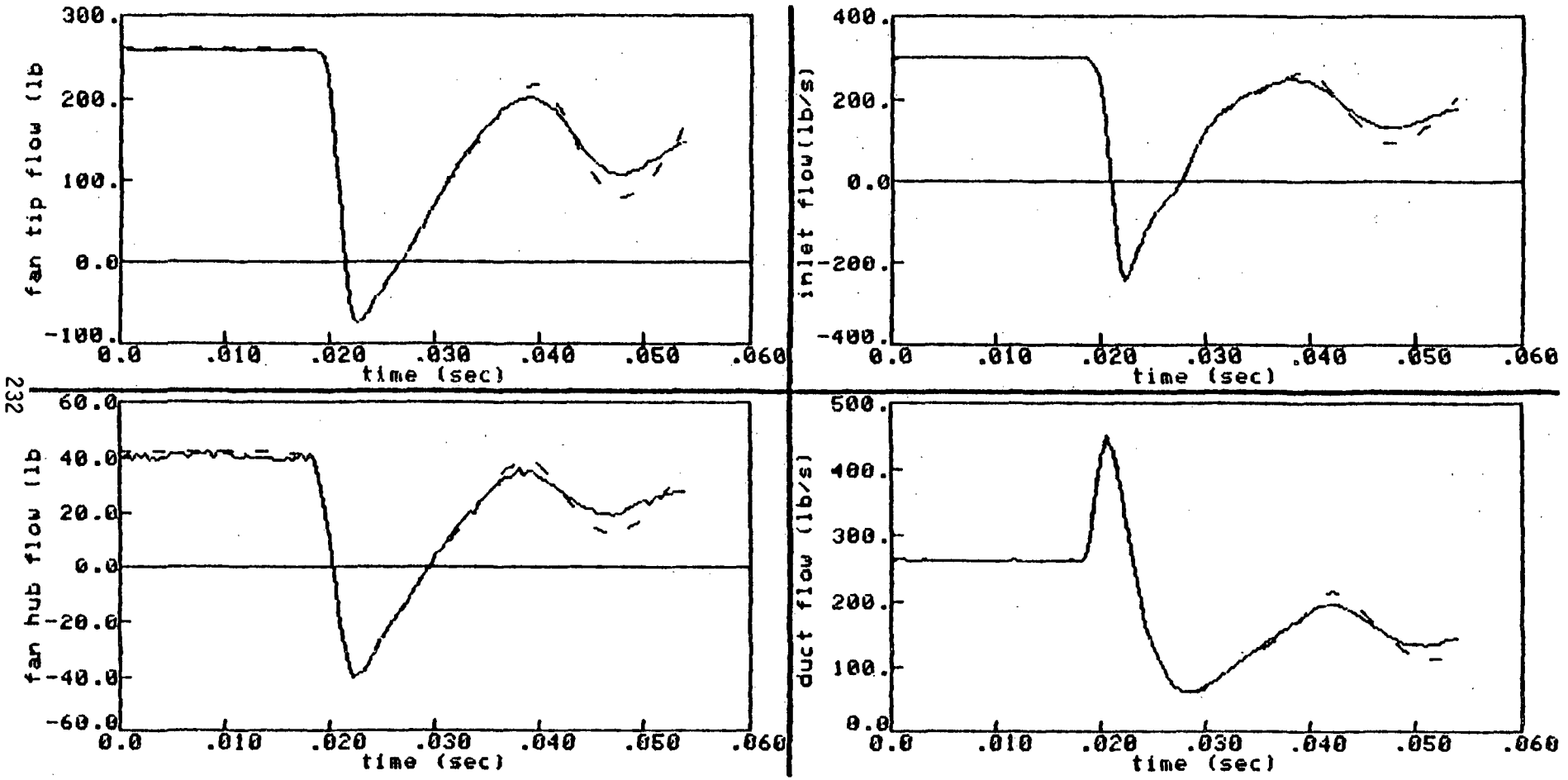

Figure 6.31 Turbofan Nominal Propagation for Nonrecoverable Stall, Run 20 (SCT, dashed line; NASA, solid line)

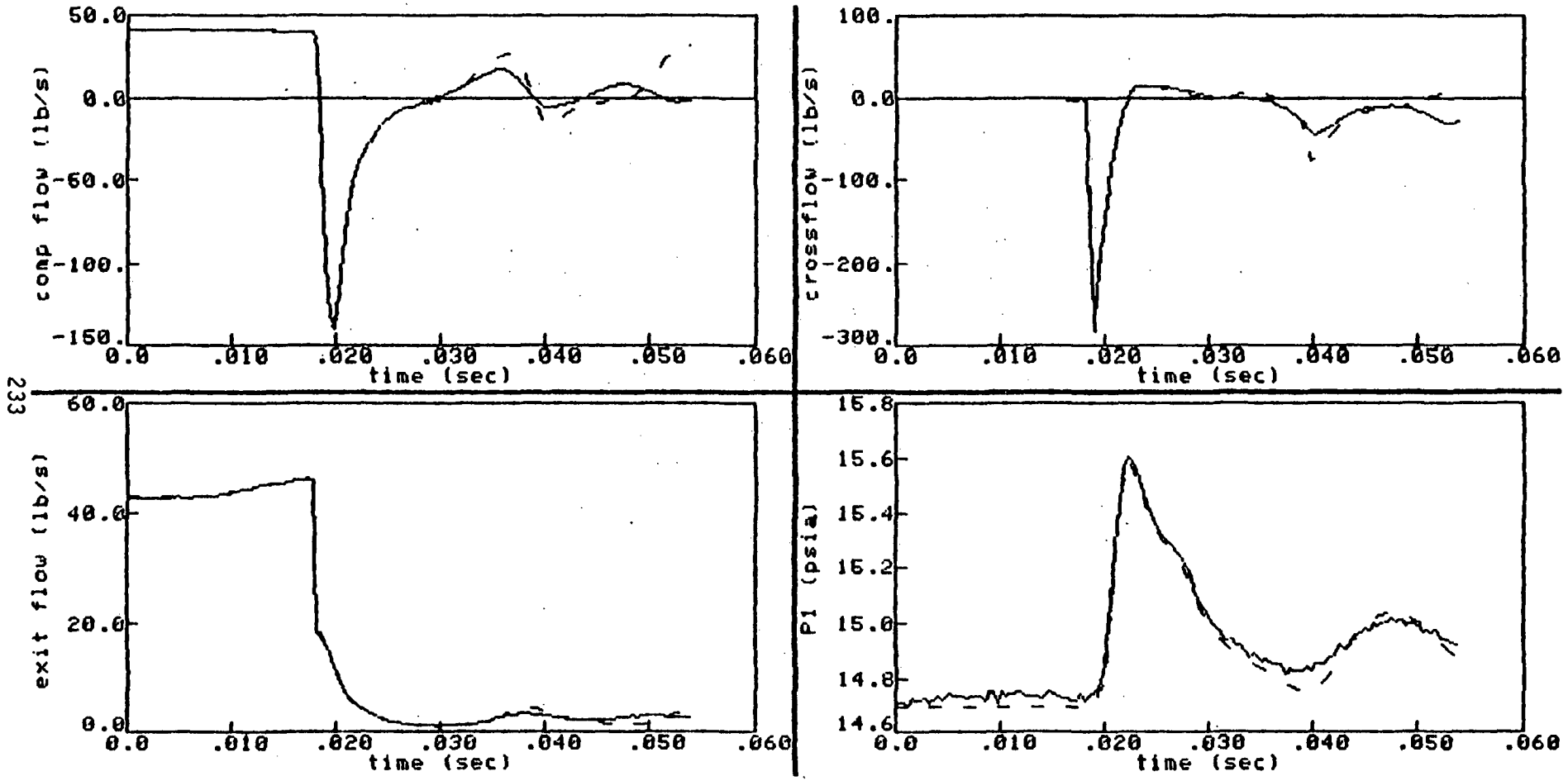

Figure 6.32 Turbofan Nominal Propagation for Nonrecoverable Stall, Run 20 (SCT, dashed line; NASA, solid line)

6.8.2 Nonrecoverable Run Identifications

Despite the problems identified above, several nonrecoverable stall identifications were successfully completed. The pre-identification model and plant are shown in Figures 6.33 and 6.34; the identified model and plant are shown in Figures 6.35 and 6.36. Identification results are summarized below in Table 6.12.

Table 6.12
Turbofan Identifications Using Noise-Free Nonrecoverable Stall Data

Run	TSTART (sec/100)	Rx (x1/100)	V3	KNC	KPC
15	1.8400	1.036	2647.*	48.84	4.586
20	1.8190	1.972*	3335.	45.74	3.217
Average		1.036	3335.	47.29	3.902
percent error		3.6	0.48	-5.42	-21.97
Average*		1.972	2647.	N/A	N/A

*identified unknown values. Not included in first average.

Table 6.13
Turbofan Identifications Original Parameter Estimates

Run	TSTART (sec/100)	Rx (x1/100)	V3	KNC	KPC
15	1.8600	1.500	2319.	25.00	2.000
20	1.8400	1.500	2319.	25.00	2.500

The procedures for the the nonrecoverable identifications were the same as those for the recoverable identifications except for one modification in step 5.2. Instead of using the entire stall trajectory in the final round of

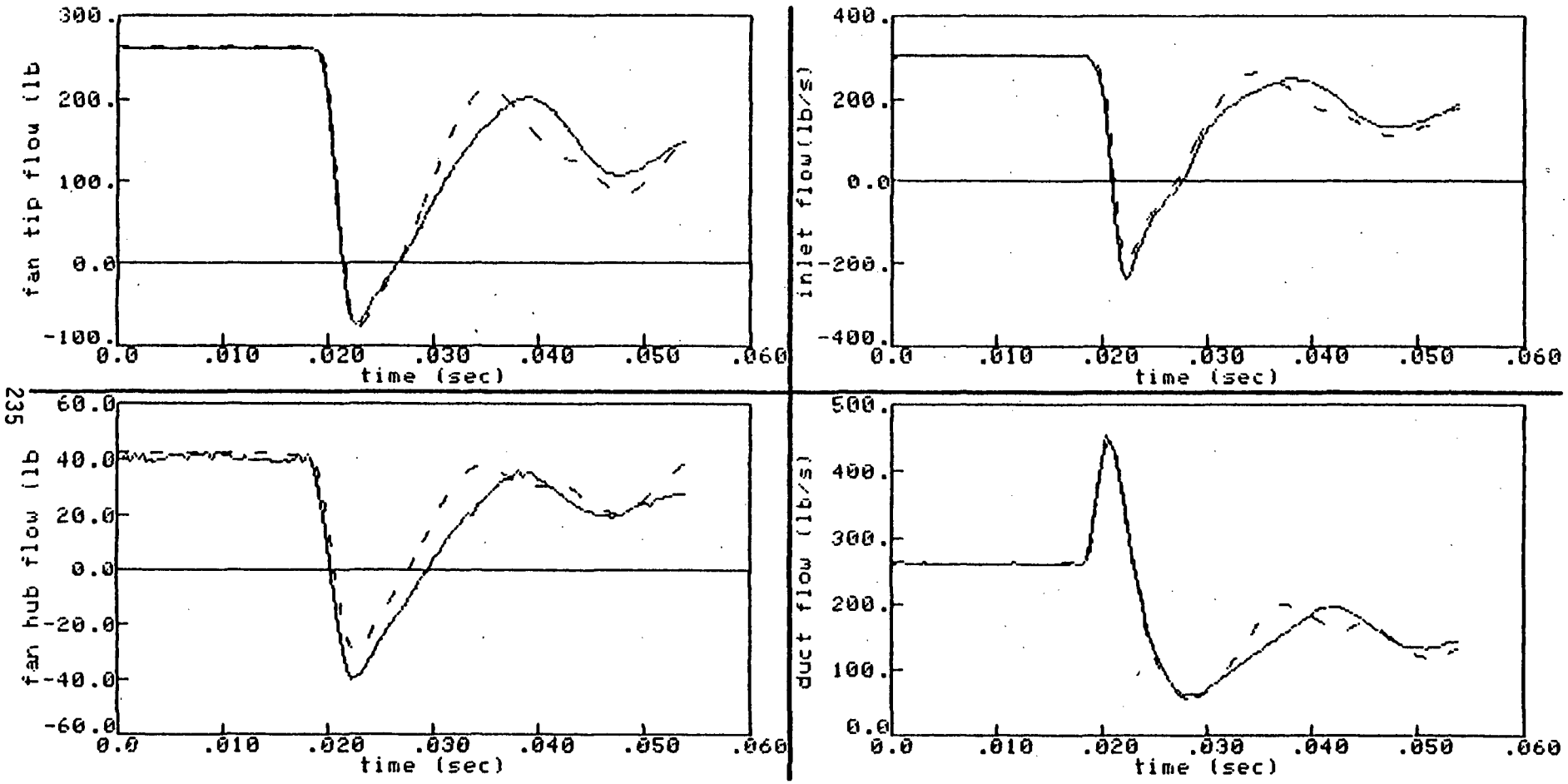

Figure 6.33 Turbofan Before Identification, Run 20 Using Original Values (SCT, dashed line; NASA, solid line)

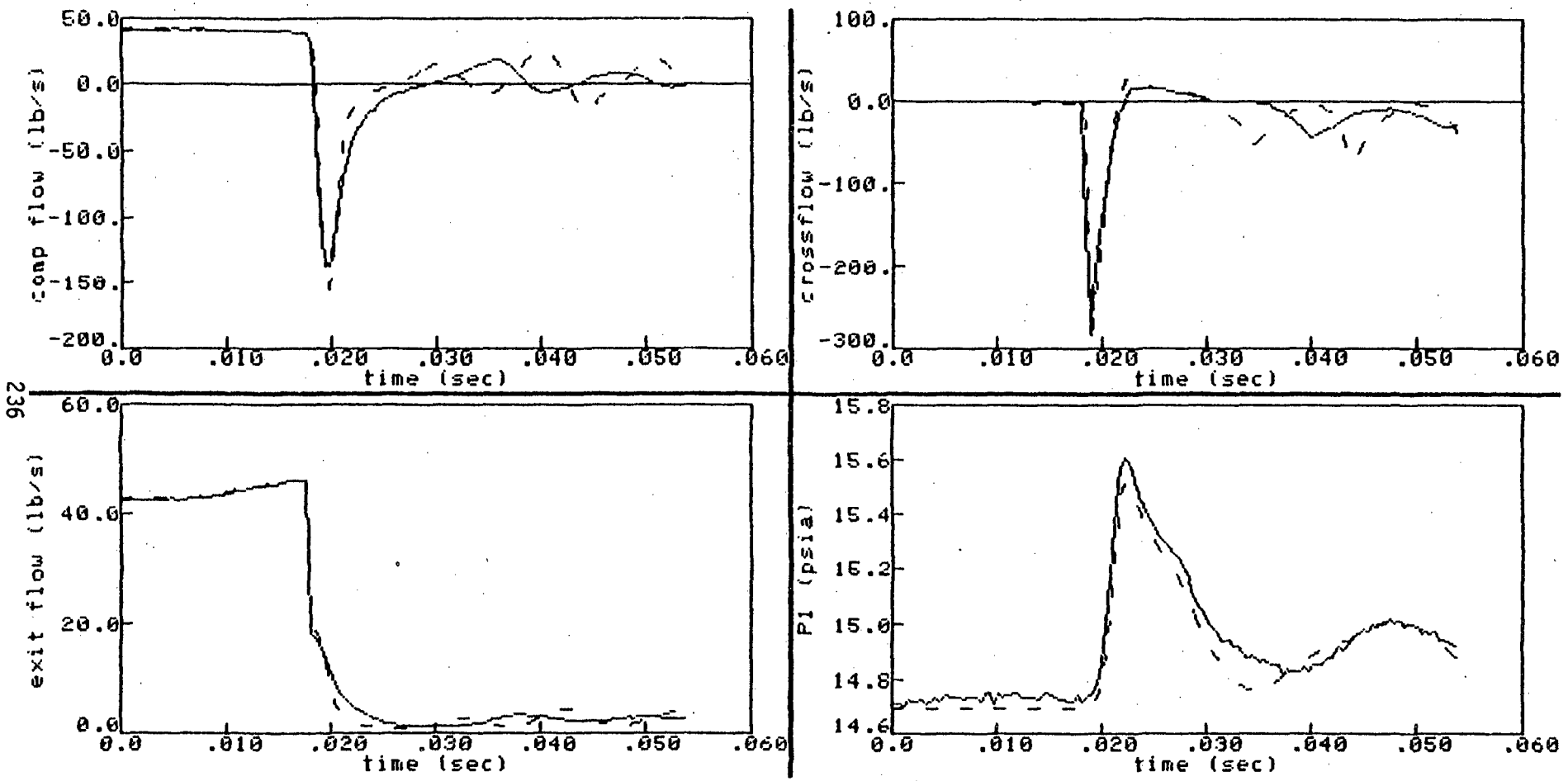

Figure 6.34 Turbofan Before Identification, Run 20 Using Original Values (SCT, dashed line; NASA, solid line)

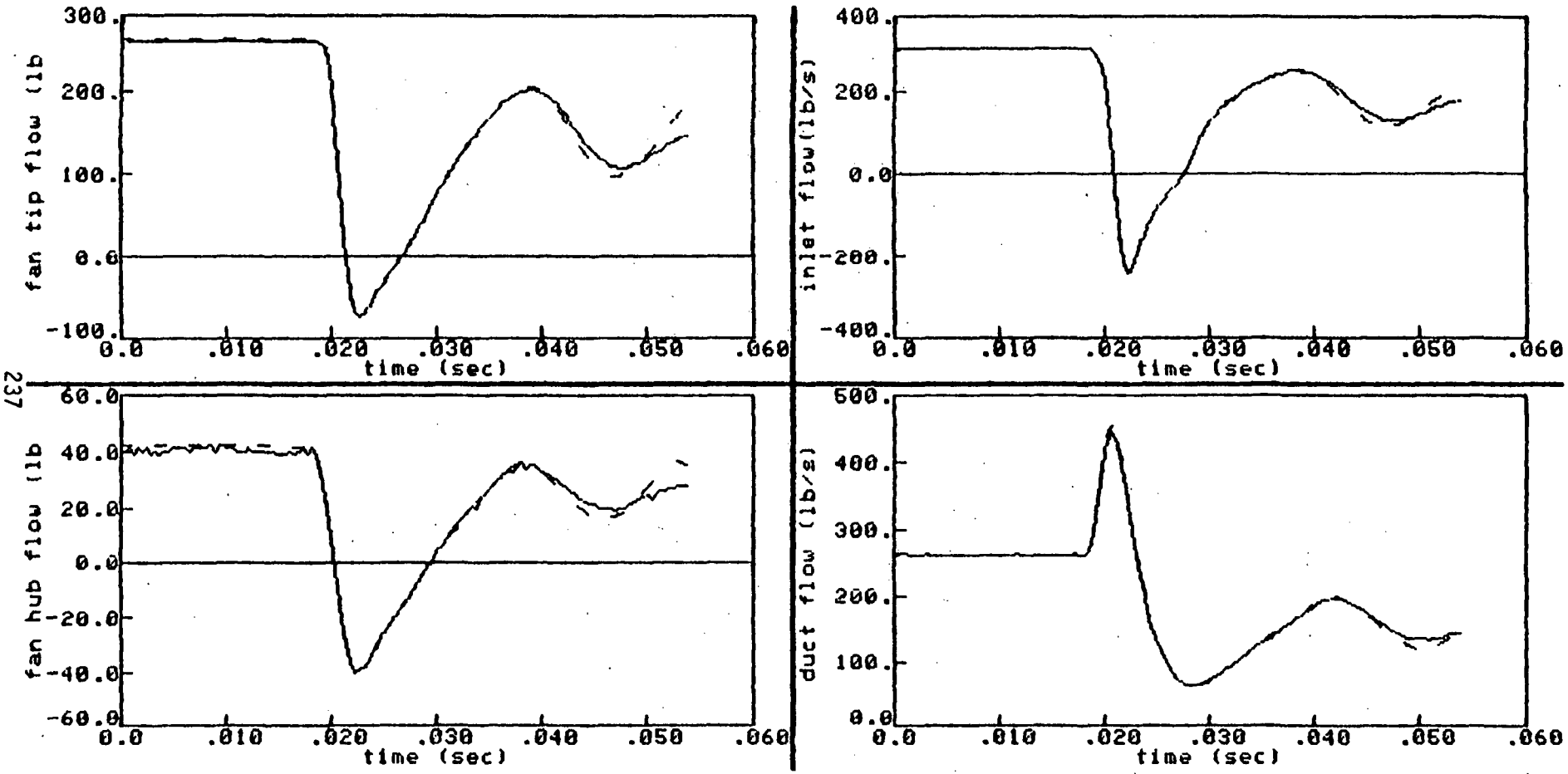

Figure 6.35 Turbofan Before Identification, Run 20 (SCT, dashed line; NASA, solid line)

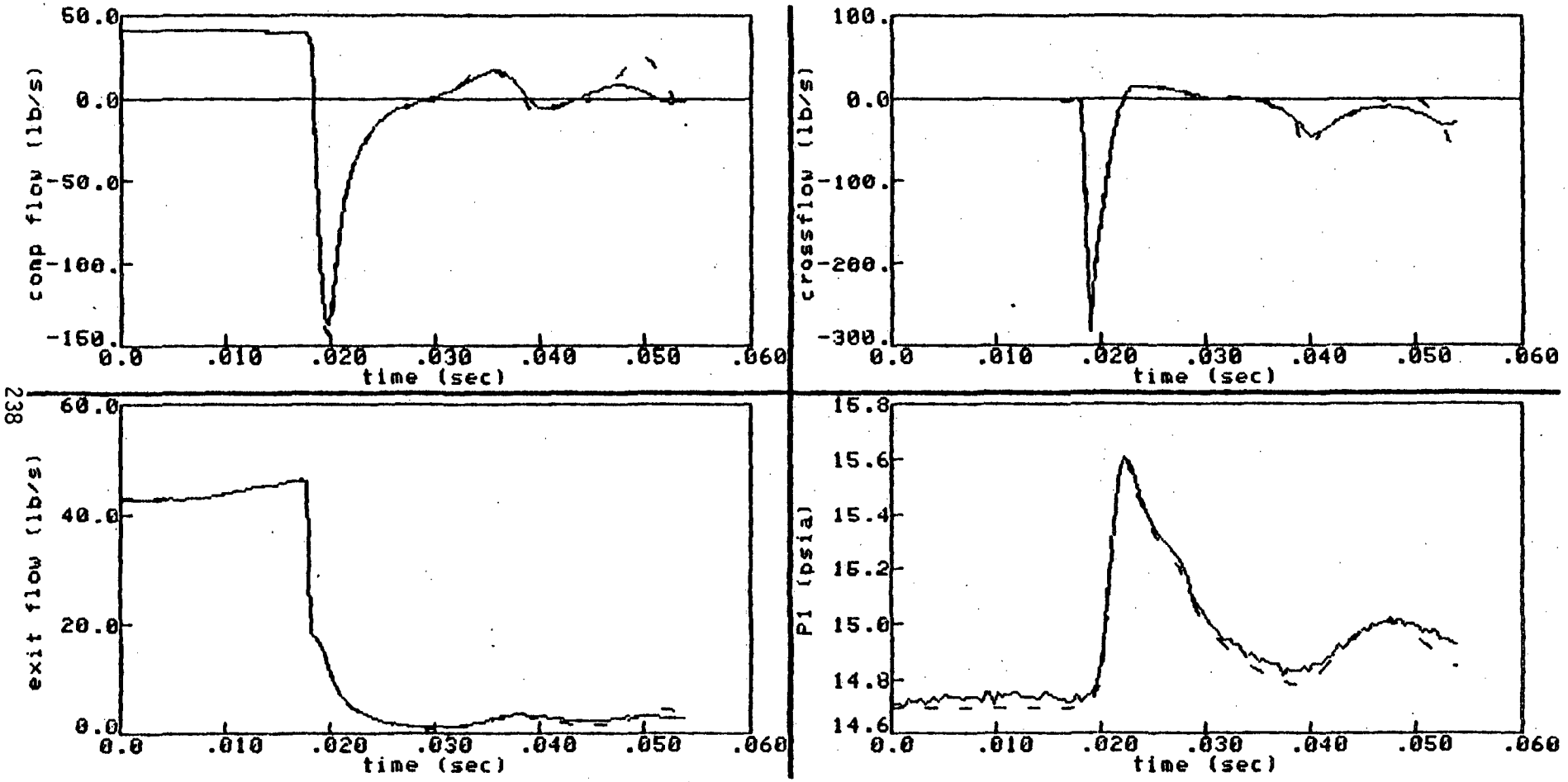

Figure 6.36 Turbofan Before Identification, Run 20 (SCT, dashed line; NASA, solid line)

engine parameter identifications, only data up to the end of the first stall cycle was used (i.e., up to the point where compressor flow becomes negative for the second time).

The trajectory of the identified model is compared to NASA data in Figures 6.35 and 6.36. Notice that the agreement is excellent up to positive stalled flow and that agreement in the first cycle is quite improved over the nominal trajectory. The indication is that a non-nominal KPC was found that produced better model-plant agreement in the first cycle than could be produced under nominal conditions. This aspect of the identification helps to support the theory that KPC identification is possible when nonrecoverable stall data are used.

6.9 SUMMARY OF RESULTS

The turbofan identifications were successfully completed by using only recoverable stall data. Final identification procedures followed the basic form outlined previously using compressor rig identification experience. The procedures worked very well, although some modifications were made in an attempt to improve the KPC identifications. The modifications did not improve the identifications.

Identifications using noise-free data were the extremely accurate, with three out of the four engine parameters being identified to within one percent. KPC was more difficult to identify and could not be identified at all from the noise-added recoverable data.

A measurement contribution analysis was made to evaluate the worth of the 15 possible measurements considered. Results revealed that only KPC in recoverable stalls was heavily dependent upon flow information and that in most other cases flow measurements could be omitted without catastrophic losses in parameter information. (Contribution results are specific to turbofan model structure and chosen noise levels.)

Uncertainty analyses were used to explain the poor identifiability of KPC when recoverable data were used. The analyses also indicated that KNC and especially KPC would show much improved identifiability if nonrecoverable data is used in identification.

The turbofan study was unable to use all of the NASA Lewis nonrecoverable stall data because of a model-plant mismatch problem; however, limited results obtained from some of the nonrecoverable data are encouraging.

VII. SUMMARY OF FINDINGS AND RECOMMENDATIONS

7.1 SUMMARY OF FINDINGS

7.1.1 Preliminary Demonstration (Task A)

The compressor rig identifications demonstrated the feasibility of compressor map parameter identification from transient data. They also provided identification experience that were used during the program to refining the compressor parameter identification procedures. A summary of the identification results is given in Table 7.1. A summary of the experiences encountered is listed in Table 7.2.

7.1.1.1 Demonstration

The compressor rig demonstration used a fifth-order turbofan model derived from a lumped parameter turbofan model developed by NASA Lewis [1]. The model actually filled a dual role. First, it was used by NASA Lewis on a hybrid computer to produce analog stall response measurements. Once the model produced stall measurements, the measurements were recorded and delivered to SCT. The model was used a second time at SCT along with the identification program, SCIDNT, to identify the rig parameters used in the NASA Lewis model. The entire process mimics an engine test, where the nature of the plant is unknown and real instrumentation effects, noise and recording effects, are included in the data.

The compressor rig identification results demonstrated several facts about the compressor map problem. First, compressor parameters can be identified from transient data. Second, the degree of identification success is dependent on a variety of conditions including number of data points, sensor noise levels, type of stall, value of the parameter being identified, etc. In general, Kn is more identifiable in the compressor rig than Kp, and in recoverable stall runs of short duration, Kp is only marginally identifiable.

Table 7.1
Compressor Rig Identifications
Noise-Added Recoverable and Nonrecoverable Runs

Run	KN actual	KN estimated	KN percent error	KP actual	KP estimated	KP percent error
5	8.00	7.94	-0.75	0.100	0.115	15.0
7	8.00	8.22	2.75	0.500	0.983	96.7
9	20.0	17.9	-10.5	0.800	0.755	-5.60
10	10.0	9.32	-6.8	0.800	0.669	-16.4
11	15.0	20.2	34.5	2.000	2.055	2.75
13	15.0	20.9	39.2	4.250	4.807	13.0
15	15.0	12.8	-14.8	1.000	0.899	-10.1
17	15.0	15.6	4.00	2.000	2.026	1.30

The results shown in Table 7.1 tell only half the story about the compressor rig identifications. The main goal of the identifications was not to maximize accuracy but to gain experience in compressor parameter identification and investigate a variety of identification procedural techniques. Hence, the identifications in Table 7.1 could have been improved had more refined techniques been used.

7.1.1.2 Experiences

A summary of experiences encountered in the compressor rig identifications is listed below in Table 7.2. These experiences were a valuable portion of the compressor rig task. They illuminate problems that had to be explained using the identifiability/sensitivity tools from Task B and were accounted for in the final procedures employed in the turbofan identifications of Task C.

Table 7.2
Summary of Compressor Rig Experiences

1. Model-Plant Differences: Time Skews

   * Observation: Due to slight differences between the model and plant, the SCT digital model stalls slightly later than the NASA hybrid model when given the same input. This delay introduces a time skew into the identification and can bias compressor parameter estimates.

   * Response: An input scaling factor, AT, was introduced to the SCT compressor model so the input could be artificially increased to hasten the onset of stall. The parameter was identified using SCIDNT until it produced synchronization between model and plant. This procedure worked fairly well but was troublesome and in some cases unsuccessful.

2. Initialization

   * Observation: The initial state values of the dynamic compressor rig model were supplied to SCT by NASA Lewis. In a normal identification situation, these values would not be availabe and would have to be estimated or identified from the data. Incorrect initial values produce steady state errors between the plant and model that could bias parameter estimates.

   * Response: Future identifications should make provisions for parameterization of initial condition values, i.e., the initial conditions should be made model parameters (under the SCIDNT definition of model parameters) and be accessible for identification.

3. Estimate Parameter Biasing:

   * Observation: If a parameter is poorly identified, that is, if it is inaccurate, then it is able to affect the estimate of other parameters. This can be understood physically in the Kn and Kp identifications. If Kn is in error, then the model and plant will be in disagreement from the inception of negative stall flow till the end of the maneuver. Since most of the positive stall flow (determined by Kp) follows negative stall flow, the Kn errors produce model-plant mismatches that affect the Kp identification.

* Response: The quantitative effects of this and other modeling "errors" is worth persuing. Certainly other errors in parameter values, lumped parameter assumptions, sensor time lags, etc., could have significant impact upon compressor map parameter identifications as well. The problem of estimation "sensitivities" is addressed in Task B (Chapter 5).

4. Information Content:

* Observation: Identifications improve with more information. Most of the compressor rig work was done using only one out every five data points. When all data points were used, identification accuracy improved.

* Observation: Noisier data decreases identification accuracy for all parameters.

* Observation: Compressor parameter identifications seem to have a predictable relationship tied to available information. For example, in recoverable stalls, there is less time spent in positive stalled flow and correspondingly, Kp identifications in recoverable stalls are marginal to poor. Kn identifications on the other hand seem to be impervious to the type of stall and are satisfactory, regardless of stall type.

* Observation: Specific sensors can be eliminated from the identification process. Through elimination of certain sensors it was found that P2 (under the present noise levels) contributes little to Kn or Kp identification.

* Response: The precise effects of sampling frequency, noise levels, type of stall and sensor set configurations require further investigation. A greater understanding of these effects will help define instrumentation requirements and help in streamlining identification procedures.

5. Separate Kn and Kp Identifications

* Observation: Kn and Kp must be identified separately because of dramatic differences in the amount of information available for each parameter. (SCIDNT normally can identify up to 50 parameters which produces more accurate identifications.) If identified together, Kn dominates the identification convergence and the Kp estimate is left unimproved.

Table 7.2 (Concluded)

* Response: Simultaneous identifications may be possible if the accuracy of the algorithm is improved. Conversion of the SCIDNT code from single (32 bit) precision to double (64 bit) precision may accomplish the desired accuracy.

6. Fixed Step Integration:

* Observation: Unreliable results have been obtained when using the variable step SCIDNT integration routine. Specifically, the calculation of Kp gradients loses fidelity under variable-step integration. Loss of fidelity is tied the fact that the Kp gradients are very small in recoverable stalls (meaning that Kp has very little effect on changing the stall trajectory when the stall is recoverable). Thus, when minor gradient errors are introduced via the variable-step integration, Kp gradient values are distorted and identification is disrupted.

* Response: SCIDNT is capable of integrating the compressor rig model using an efficient, variable-step integration package. Use of this package could produce considerable computer cost savings; however, the package cannot be used because of the accuracy problems.

  Because of the discontinuous nature of the stall-capable model, very small integration steps are needed at times. Adjusting the variable-step integration parameters of the package is not sufficient to produce an accurate integration. Therefore, a fixed-time step is required (First-order Euler integration is used.)

This concludes the summary of findings for Task A. Many of these observations were encountered throughout the text in one form or another. In the I/S study, the compressor rig observations defined areas for study; in the turbofan identifications, the observations were reflected in revised identification procedures.

7.1.2 Identifiability and Sensitivity (Task B)

The identifiability/sensitivity study served two purposes. First, the study explained the results of the compressor rig identifications, e.g., why some identifications were more accurate than others. Second, the study developed general tools from identification theory that could be used to predict 1) how identifiable a parameter is, 2) what might corrupt and identification, and 3) what sensors are needed for accurate identification, etc.

7.1.2.1 Motivation and Goals

These tools allow the user to determine before identification how well a parameter can be identified given the available sensors, noise levels, lags, etc. The tools also allow identification errors to be evaluated based upon known uncertainties in the model. For example, if a resistance is only known within 25 percent of its actual value, sensitivity tools can predict how much a Kp estimate would be biased by the error, and identifiability tools can indicate what the resulting uncertainties in parameter estimates would be.

The greatest value of the I/S tools may ultimately be found in their application to defining instrumentation requirements. Sensors important to certain parameter identifications can be identified using these tools before testing begins and minimal sensor accuracy requirements could be defined as well.

The following gives a specific outline of the I/S study goals:

(1) Determine optimal data arrangements:

  (a) study effects of sample frequency;

  (b) study effects of multiple sets of measurements;

  (c) study effects of reduced sensor sets.

(2) Determine effects of data shortcomings:

(a) study effects of sensor lags;

(b) study effects of measurement noise;

(c) study effects of asynchronizations.

(3) Determine predicted errors (resulting uncertainties) for:

(a) type of stall (e.g., non-recoverable versus recoverable);

(b) K-parameter biases.

(4) Determine optimal data weightings:

(a) study K-parameter information content as a function of time;

(b) study information contents in each sensor.

7.1.2.2 I/S Results

I/S tools were developed to address these questions and more. Under this program the tools were applied to the specific TF-34 lumped parameter compressor rig and turbofan models. The results, although they may be generally applied to other turbine engines, must be treated with caution. The important point is that the tools can be used with any engine and model; they are derived only from identification theory and are not model-dependent. (It is the results that are model-dependent.)

Because the tools are directly related to identification theory, they are precise, mathematically justified expressions. Thus, although they yield precise measures of identifiability and sensitivity, the measures are ideals. The measures do not consider errors induced by unknown modeling errors such as drift, unmodeled states, etc., and consequently, do not always represent true identifiablity and sensitivity.

The mathematical details of the I/S tools are discussed in Chapter V; a summary of a few of the I/S findings are given below. The findings are based upon study of the compressor rig model, and therefore, some of the conclusions apply only to that model (for turbofan results see Chapter VI).

(1) Kn along with most other major model parameters can be readily identified.

(2) Kp requires 200-400 times as much data to achieve the same identification accuracy as Kn identifications, and is sometimes marginally identifiable.

(3) Kp identifications are easily biased by errors in other model terms specifically, Kn.

(4) Identifiability decreases proportionally to increases in noise levels.

(5) Identifiability increases with the square root of the number of data points

(6) Individual contributions of sensors can be identified to determine those sensors that are necessary to a particular parameter identification.

(7) Kp and Kn parameters are sensitive to errors in certain model parameters (resistances, volumes, time constants, etc.) This may make identification of these parameters a necessity when identifying with real engine test data.

(8) Kp and Kn identifications are sensitive to time skews resulting from different stall onset times between model and data.

7.1.3 Final Demonstration (Task C)

The third and final program task demonstrates advanced procedures for the compressor map parameter identification using a turbofan model and measurments. Many of the experiences and knowledge gain via Tasks A and B were used in developing the identification guidelines used in the turbofan identifications. The subobjectives of the task were: first, to demonstrate compressor map parameter identification with a turbofan; second, to develop a set of comprehensive guidelines for in-stall engine identification procedure; and third, to evaluate the potentials for other turbofan identifications using I/S tools.

7.1.3.1 Demonstration

All three of these subobjectives were successfully completed in Task C. The turbofan model used was originally developed by NASA Lewis [1]. It is a twelfth-order lumped-parameter model with stalling compressor and fan maps. A summary of the identifications made on the model is shown in Tables 7.3 and 7.4. The results are from two rounds of identifications. In the first round, noise-free data is used with a total of fifteen measurements including seven flow measurements. In the second round noise was added to the data and the flow measurements were omitted.

Table 7.3
Turbofan Identifications Using
Noise-free, Recoverable Stall Data

Run	TSTART (sec/100)	Rx (x1/100)	V3	KNC	KPC
5	1.8720	1.004	3337.	51.86	6.427*
6	1.7305	.9902	3347.	50.47	4.127*
9	1.7777	.9639	3328.	95.25*	3.406
10	1.7820	.9758	3324.	99.53*	4.160
13	2.2698	1.054	2637.*	48.63	3.960
14	1.7730	1.045	2647.*	47.72	5.026
17	1.9227	2.039*	3288.	48.74	4.982
18	2.1387	2.041*	3279.	50.67	4.431
Average		1.005	3317.	49.68	4.327
Actual		1.000	3319.	50.00	5.000
percent error		0.5	-.06	-.64	-13.5
Average*		2.04	2642.	97.42	5.277

Table 7.4
Turbofan Identifications Using Noisy, Recoverable Stall Data without Flow Measurements

Run	TSTART (sec/100)	Rx (x1/100)	V3	KNC	KPC
5	1.8729	.9781	3403.	47.28	N/C
6	1.7307	.9817	3389.	47.24	N/C
9	1.7755	.9453	3483.	99.29*	N/C
10	1.7820	.9662	3398.	98.66*	N/C
13	2.2689	1.0245	2644.*	48.21	N/C
14	1.7750	1.1225	2572.*	52.22	N/C
17	1.9214	1.9356*	3387.	47.45	N/C
18	2.1367	1.9225*	3406.	45.82	N/C
Average		1.003	3411.	48.03	N/A
Actual		1.000	3319.	50.00	5.000
percent error		0.3	2.77	-3.93	N/A
Average*		1.9291	2608.	98.98	

*identified unknown values. Not included in first average.
N/C no change
N/A not applicable

A total of eight runs were made in each round. Each run represented a slightly different model since each used a different set of model parameters. With the procedural refinements brought about through compressor rig and I/S study experiences, it was possible to identify simultaneously the four engine parameters on each run. (This was not possible with the compressor rig.)

The results of the identifications were excellent. Identification of three of the engine parameters was outstanding in both rounds, with identification accuracies hovering around a few percent. The fourth engine parameter, KPC, was marginally identifiable in the noise-free data and

unidentifiable in the noisy data. I/S tools predicted this difficulty with recoverable data and also indicated that KPC is readily identifiable with nonrecoverable data. Nonrecoverable data were not used in the turbofan identifications because of a model-plant mismatch problem.

7.1.3.2 Final Identification Procedure

Despite the lack of success in the KPC identifications with recoverable data, the turbofan identifications on the whole were quite successful. The improved identification techniques simplified the process a great deal and contributed to the accuracies achieved. Some of the techniques are summarized below. Discussion of the "hows and whys" is found in Chapter VI.

Turbofan Identification Procedure

(1) Identify initial conditions. This includes the ambient conditions (TO and PO) as well as the two operating points (fan and compressor flows and speeds.)

(2) Detect time of stall. This step utilizes a test which searches for rapid drops in P3dot. A similar procedure could be used on actual test data.

(3) Identify measurement biases (optional).

(4) Incorporate preliminary identified conditions into turbofan model.

(5) Identify parameters with noise-free data.

  (a) Identify Rx, V3, KNC, and TSTART with only unstalled and negative stalled flow data. (KPC is not identified in this step because of its sensitivity to errors in KNC and TSTART. The idea is to identify the parameters that KPC is sensitive to before KPC is identified. This may reduce biases induced in the KPC estimate.)

  (b) Incorporate the identified parameters from the previous step into the model and identify Rx, V3, KNC and KPC with the entire stall maneuver.

(6) Repeat set 5 for second round using noise-supplemented data.

(7) Evaluate.

7.1.3.3 Evaluation

The final objective of Task C was to use I/S tools to evaluate the turbofan identification results. Several tools were brought to bear, but the gist of the results is summarized in Table 7.5.

The identifiabilites of the four engine parameters being tested were measured for four different cases. The identifiablity of a parameter is "a measure of the likelihood that any estimated parameter is within and specific range of the actual parameter value." In Table 7.5, that range is expressed in percent standard deviation. For example, under the conditions of case 2, there is a 95 percent probability of identifying Rx to within 0.32 percent of the actual value (2 standard deviations).

Case	Description
1	Run 10 using all measurements. Recoverable stall.
2	Run 10 using pressure and temperature measurements only. Recoverable stall.
3	Run 20 using all measurements. Nonrecoverable stall.
4	Run 20 using pressure and temperature measurements only. Recoverable stall.

Table 7.5
Parameter Identifiabilities in Percent Standard Deviation

Case	Rx	V3	KNC	KPC
1	.1428	.0757	.3951	17.54
2	.1602	.0830	.5143	31.81
3	.0915	.0266	.0189	.0204
4	.1261	.0357	.0303	.0333

Several important generalities can be drawn from these results:

(1) All engine parameters are identifiable in all four cases with one exception: KPC is virtually unidentifiable in recoverable stall cases.

(2) Parameter uncertainty will increase from 10 percent to 50 percent if flow measurements are unavailable.

(3) Parameter identifiability improves significantly when identification is done with nonrecoverable data instead of recoverable data. This is strikingly true with KPC, and true for KNC as well, but to a lesser degree.

In summary, Task C brought the demonstration of compressor map parameter identification from transient data to a successful conclusion. The engine parameters were succesfully identified, a comprehensive identification procedure was developed and demonstrated, and I/S tools were used to explain results and predict accuracies in future identifications.

7.2 RECOMMENDATIONS

The experiences of the compressor rig, I/S and turbofan studies has led to the development of a successful identification procedure outlined in Section 6.4. This outline has been extended to cover the general problem of system identification for stalling engines and inherently contains recommendations drawn from this program.

Before discussing the outline, the concept of system identification must be addressed. System identification is a phrase given to represent an iterative process by which models are developed, refined and verified; it goes well beyond simple parameter identification. The concept is represented figuratively in Figure 7.1 and is the basic approach used by SCT for system identification.

As an example application, consider the twelfth-order turbofan model used in this program. If this model were insufficient in describing actual engine test data, system identification would be employed to identify new modes and model aspects to make the model more complete. Hence, the final result of an turbofan (system) identification might produce a 20th order model in addition to identified engine parameters.

A preliminary outline for system identification of in-stall turbofan engines is given below. The outline is derived from the experiences of this program. Additional information on system identification can be found in Refs. 13 through 19.

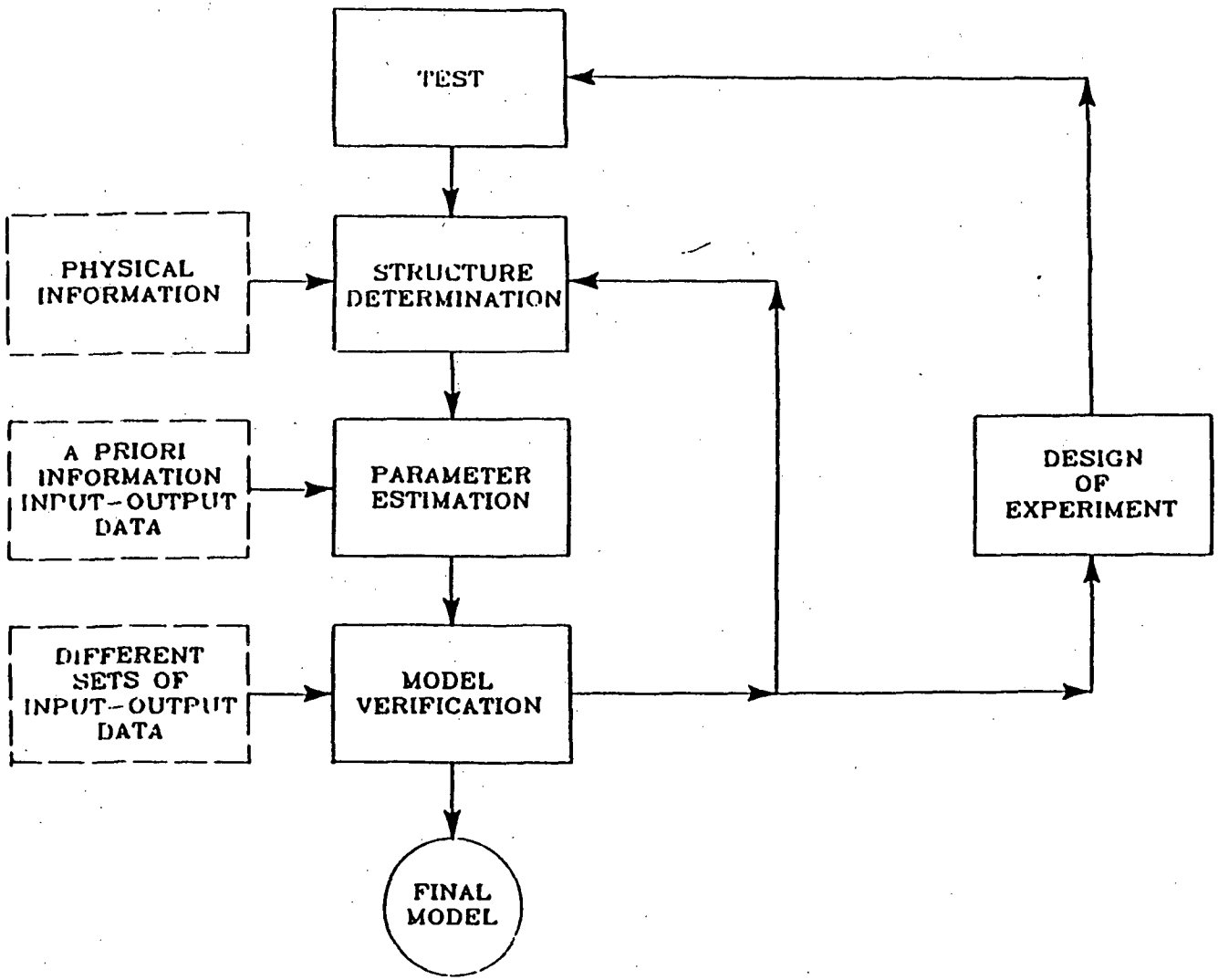

Figure 7.1 System Identification

(1) Develop an appropriate engine model for the available engine data. The model should be as complete as possible; minor features can more easily be eliminated than added.

(2) Attach the engine model to SCIDNT and modify as needed for identification considerations. Special considerations include:

   (a) Double precision code to maximize accuracy.

   (b) Fixed step integration to ensure fidelity between propagations. Step size must be small enough for accurate integration (approx. 10 microseconds).

   (c) Nonrecoverable stall data should be used whenever possible to ensure proper KPC identifications.

   (d) Engine model should stall only after a model-specified stall time; it should not stall when the model flows and speeds move beyond the stall line. (This is because an independent stall condition determination can cause significant discrepancies between model and data stall onsets.)

   (e) Stall times should be model parameters, accessible for identification.

   (f) Engine model should be constructed to initialize on ambient conditions and fan and compressor operating points (6 parameters). These initial condition values should be model parameters, also accessible for identification.

   (g) Care must be taken in writing model code to ensure that no state or measurement relies on a value not saved in X, Xdot, or Y. For example, a variable should not be dependent upon some intermediate temperature that is not saved in X, Xdot, or Y. This is because SCIDNT alters variable values in the STATE, STATIC, and MEAS routines during identification.

(3) Identify stalled compressor map parameters using 80 percent of the available engine data. (Only 80 percent of the data is used so that the remaining 20 percent can be used in model verification in the next step.) The identification process is broken into the following subtasks.

   (a) Determine the relative contributions of each of the available measurements using SENSIT or CENTS. These results will be used to reduce the sensor set for simplicity and determine which sensors should be reserved for model verification.

   (b) Determine the initial conditions of the measured plant by identifying the initial condition parameters using the unstalled, steady state portion of the engine data.

(c) Estimate the approximate stall and recovery times (if applicable) of the engine data. Include these times in the model parameter list and propagate the model.

(d) Propagate the model as necessary until the uncertain parameters produce a trajectory reasonably close to the measured response.

(e) Identify all parameters except Kp, using only the unstalled and stalled negative compressor flow portion of the data; that is, stop the identification before the engine moves into positive stalled flow.

(f) Identify all parameters including Kp, using the entire stall maneuver. (For nonrecoverable maneuvers, it may be beneficial to identify these parameters using only one stall cycle, then two, then three, etc.; thereby adding more information after each identification. This may aid the Kp identification.)

(4) Verify the identified model. Using the 20 percent of unused data, evaluate the performance of the identified model.

(a) If the evaluation is unsatisfactory, return to step 1 and consider a new model structure. Then repeat steps 2 and 3.

(b) If the evaluation is satisfactory, stop.

A large amount of background is involved in these recommendations, all of which can be found in Chapters IV through VI.

7.2.1 Other Recommendations

7.2.1.1 Identifiability/Sensitivity Studies

Once an initial engine model has been developed, an extensive I/S study of the model should be made. The goals of the study will vary depending upon the test conditions. If the data are already recorded or the instrumentation already determined, then studies examining sample rate and noise level effects would be moot. An I/S study would give valuable information on:

(1) Predicted identifiabilities of each engine parameter given present noise levels and sample rates. This could identify potential problem parameters and could also flag where additional maneuvers may be needed.

(2) Measurement contributions. Given the sensor noise levels, the relative contributions of each sensor can be measured. Those with minimal contributions could be eliminated from the model and the identification process to reduce sources of error and computational costs. Temperature sensors with lags may be strong candidates for elimination.

(3) Parameter uncertainties. The uncertainties in so-called known parameters: resistances, inductances, etc., should be studied to determine their effects on estimation. Recall from Section 5.3.1.4, that these uncertainties affect estimate uncertainties in the same way as sensor noise.

(4) Bias sources. The potential biasing effects of sensor biases, time constant errors, and nuisance parameter errors should be examined. Areas with high biasing potential should recieve special consideration, including possibly identifying the magnitude of the error.

7.2.1.2 SCIDNT Considerations

The special considerations involving the use of SCIDNT were primarily identified in Section 7.2. These considerations include the use of double precision code, simultaneous identifications, identification of initial condition parameters, and creating a special TSTART parameter that can be identified for synchronizing the onset of stall.

APPENDIX A

COMPRESSOR RIG EQUATIONS

$$P_1 = 14.8 \tag{A.1}$$

$$T_1 = 519 \tag{A.2}$$

$$\dot{W}_1 = \frac{P_1 - P_2}{R_o} \tag{A.3}$$

$$W_2 = \int_0^t (\dot{W}_1 - \dot{W}_2)dt + W_{2,i} \tag{A.4}$$

$$(WT)_2 = \gamma \int_0^t \left(\dot{W}_1 \left\{ \frac{T_1}{T_2} \right\} - \dot{W}_2 \left\{ \frac{T_2}{T_2'} \right\} \right) dt + (WT)_{2,i} \tag{A.5}$$

where: $T_2' = T_3(1 - \frac{\phi}{.7972})$

$$P_2 = \frac{R(WT)_2}{V_2} \tag{A.6}$$

$$T_2 = \frac{(WT)_2}{W_2} \tag{A.7}$$

$$\theta_2 = \frac{\left\{ \begin{matrix} T_2 \\ T_3 \end{matrix} \right\}}{519} \tag{A.8}$$

$$\delta_2 = \frac{\left\{ \begin{matrix} P_2 \\ P_3 \end{matrix} \right\}}{14.7} \tag{A.9}$$

$$PN = \frac{N/\sqrt{\theta_2}}{16042} \tag{A.10}$$

$$\phi = 7.972 \times 10^{-3} \; \frac{\dot{W}_2 \;\; \theta_2/\delta_2}{PN} \tag{A.11}$$

$$= \frac{KP}{KN} \; \phi^2 + 0.33 \tag{A.12}$$

Unstalled

$$P_3^* = P_2 \cdot F_1 \left(\frac{\dot{W}_2 \sqrt{\theta_2}}{\delta_2} , PN \right)$$

$$T_3^* = T_2 \cdot F_2 \left(\frac{\dot{W}_2 \sqrt{\theta_2}}{\delta_2} , PN \right)$$

Unstalled

$$P_3^* = \frac{P_2}{.837} (1 + .7746 \quad PN^2) \tag{A.13}$$

$$T_3^* = T_2 \left(1 + \frac{(P_3^*/P_2)^{.286} - 1}{\eta} \right) \tag{A.14}$$

$$\eta = \eta_o + F_4(PN, \eta_o) \; \phi \tag{A.15}$$

$$\dot{W}_{ST} = F_3(PN) \tag{A.16}$$

Stall if: $\dfrac{\dot{W}_2 \sqrt{\theta_2}}{\delta_2} < \dot{W}_{ST}$

Recover if: $\frac{\dot{W}_2 \sqrt{\theta_2}}{\delta_2} \geq 1.1 \dot{W}_{ST}$

$$W_3 = \int_0^t (\dot{W}_2 - \dot{W}_3)\, dt + \dot{W}_{2,i}$$

$$\dot{W}_2 = \frac{1}{L} \int_0^t (P_3^* - P_3)\, dt + \dot{W}_{2,i} \qquad (A.17)$$

$$(WT)_3 = r \int_0^t \left(\dot{W}_2 \left\{ \frac{T_3^*}{T_3} \right\} - \dot{W}_3 T_3 \right) dt + (WT)_{3,i} \qquad (A.18)$$

$$\dot{W}_3 = A \frac{P_3}{\sqrt{T_3}} \qquad (A.19)$$

$$P_3 = \frac{R(WT)_3}{V_3} \qquad (A.20)$$

$$T_3 = \frac{(WT)_3}{W_3} \qquad (A.21)$$

$$A = A_i \qquad (A.22)$$

$$= A_i - a(t - t_1) \quad \text{for } t < t_1 \text{ and } t > t_3$$

$$= A_i - a(t - t_1) + 2a(t - t_2) \quad \text{for } t_1 \leq t \leq t_2 \qquad (A.23)$$

$$\text{for } t_2 \leq t_1 \leq t_3$$

Constants

$R_o = \frac{.1}{65} = 1.538 \times 10^{-3}$

$\gamma = 1.4$

$R = 12 \times 53.3 = 639.6$

$V_2 = 42844$

$V_3 = 2570$

$N = 16042$

$KP = 1.5$

$KN = 15.0$

$L = 9.64 \times 10^{-4}$

$\eta_o = 0.10$ or 0.05

$A_i = 30.08$

$a = 40$

t_1 = arbitrary

$t_2 = t_1 + .072$

$t_3 = t_1 + .144$

APPENDIX B
TURBOFAN EQUATIONS

Note: * denotes state equations
** indicates where inputs enter

B.1 Equations

$$P_1 = \frac{R(WT)_1}{V_1} \tag{B.1}$$

$$P_{2T} = \frac{R(WT_{2T})}{V_{2T}} \tag{B.2}$$

$$P_{2H} = \frac{R(WT_{2H})}{V_{2H}} \tag{B.3}$$

$$T_1 = \frac{WT_1}{W_1} \tag{B.4}$$

$$T_{2T} = \frac{WT_{2T}}{W_{2T}} \tag{B.5}$$

$$T_{2H} = \frac{WT_{2H}}{W_{2H}} \tag{B.6}$$

$$W_3 = W_{AS} + W_{FS}$$

$$P_3 = \frac{RT_3\ W_3}{V_3} \tag{B.7}$$

$$T_3 = \frac{WH_3}{C_P M_3} \qquad (C_P = \text{last } C_P) \tag{B.8}$$

* $$\dot{W}_2 = (P_o - P_1)/R_o \tag{B.9}$$

* $$\dot{W}_1 = \dot{W}_i - \dot{W}_{FT} - \dot{W}_{FH} \tag{B.10}$$

$$\dot{W}_F = \dot{W}_{FT} + \dot{W}_{FH} \tag{B.11}$$

$$\theta_1 = T_1/T_{STD} \tag{B.12}$$

$$\delta_1 = P_1/P_{ST} \tag{B.13}$$

$$PNF_C = PNF/\sqrt{\theta_1} \tag{B.14}$$

$$\dot{W}_{FC} = \dot{W}\sqrt{\theta_1}/\delta_1 \tag{B.15}$$

$$P^*_{2T} = f(\dot{W}_{FC}, PNF_C, T_1, P_1) \tag{B.16}$$

(B.17)

$$T^*_{2T} = f(\dot{W}_{FC}, PNF_c, T_1, P_1) \tag{B.18}$$

$$P^*_{2H} = f(\dot{W}_{FC}, PNF_c, T_1, P_1) \tag{B.19}$$

$$T^*_{2H} = f(\dot{W}_{FC}, PNF_c, T_1, P_1) \tag{B.20}$$

* $$W_{FT} = (P^*_{2T} - P_{2T})/L_T \tag{B.21}$$

* $$\ddot{W}_{FH} = (P^*_{2H} - P_{2H})/L_N \tag{B.22}$$

$$\dot{WT}_1 = \gamma(T_a \dot{W}_2 - T_b W_{FT} - T_c \dot{W}_{FH}) \tag{B.23}$$

$$T_a = T_o \text{ if } \dot{W}_i > 0$$

$$= T_1 \text{ if } \dot{W}_i < 0$$

$$T_b = T_1 \text{ if } \dot{W}_{FT} > 0$$

$$= T_{2T} \text{ if } \dot{W}_{FT} < 0$$

$$T_c = T_1 \text{ if } \dot{W}_{FH} < 0$$

$$= T_{2H} \text{ if } \dot{W}_{FH} > 0$$

$$\dot{W}_D = (P_{2T} - P_{EXIT})/P_{DUCT} \tag{B.24}$$

$$\dot{W}_x = (P_{2T} - P_{2H} - P_x)/R_x \tag{B.25}$$

$$\theta_2 = T_{2H}/T_{STD} \qquad \begin{cases} \theta_2 = T_3/T_{STD} \\ \delta_2 = P_3/P_{STD} \end{cases} \quad \text{if } \dot{W}_c < 0 \tag{B.26}$$

$$\delta_2 = P_{2H}/P_{STD} \tag{B.27}$$

$$PNC_c = PNC/\sqrt{\theta_1} \tag{B.28}$$

$$\dot{W}_{cc} = \dot{W}_c \ \overline{\theta_2}/\delta_2 \tag{B.29}$$

$$P_3^* = f(\dot{W}_{cc}, PNC_c, P_{2N}, T_{2N}) \tag{B.30}$$

$$T_3^* = f(\dot{W}_{cc}, PNC_c, P_{2N}, T_{2N}) \tag{B.31}$$

* $$W_c = (P_3^* - P_3)/L_c \tag{B.32}$$

$$Q_{metal} = hA(T_{2H} - 1.11\ T_o) \tag{B.33}$$

* $$\dot{U}_{2T} = \gamma(T_a\ \dot{W}_{FT} - T_b\ \dot{W}_x - T_{2T}\ \dot{W}_D) \tag{B.34}$$

where:

$$T_a = T_{2T} \quad \dot{W}_{FT} > 0$$
$$= T_{2T} \quad \dot{W}_{FT} < 0$$

$$T_b = T_{2T} \quad \dot{W}_c > 0$$
$$= T_{2T} \quad \dot{W}_c < 0$$

$$* \qquad \dot{U}_{2H} = \gamma(T_a \dot{W}_{FH} - T_b \dot{W}_c - T_c \dot{W}_x) \tag{B.35}$$

where:

$$\begin{cases} T_a = T_{2H} & \dot{W}_{FH} > 0 \\ \quad = T_{2H} & \dot{W}_{FH} < 0 \end{cases}$$

$$\begin{cases} T_b = T_{2H} & \dot{W}_c > 0 \\ \quad = T_3 & \dot{W}_c < 0 \end{cases}$$

$$\begin{cases} T_c = T_{2T} & \dot{W}_x > 0 \\ \quad = T_{2H} & \dot{W}_x < 0 \end{cases}$$

$$f/a = W_{fs}/W_{as} \tag{B.36}$$

$$a/f = 1/(f/a) \tag{B.37}$$

$$G = 1 - \frac{a/f}{STOi} \tag{B.38}$$

$G = 1$ if $G > 1$

$G = 0$ if $G < 0$

$$\dot{W}_{fb} = (1 - G)\, \dot{W}_f \tag{B.39}$$

$$Q_{burn} = (.95)(HV)\, \dot{W}_{fb} \tag{B.40}$$

$$\dot{W}_e = K_{noz}(1 + \Delta A)\, P_3/\sqrt{T_3} \qquad \begin{cases} \Delta A = 0 & \text{normal} \\ \Delta A = dA \text{ if } \Delta AP_3 < 0 & \end{cases}$$

ΔAP_3 is measured input (B.41)

$$C_p = aT_{ave} + b \qquad T_{ave} = (T_3^* + T_3)/2 \qquad \left.\right\} \text{if } \dot{W}_c > 0 \tag{B.43}$$

$$* \quad \dot{W}_{as} = \dot{W}_e - \dot{W}_c/(f/a + 1) \tag{B.44}$$

$$* \quad \dot{W}_{af} = \dot{W}_f - \frac{f/a}{(f/a + 1)} \dot{W}_c \tag{B.45}$$

$$* \quad \dot{W}H_3 = r[C_p(T_3^* \dot{W}_c - T_3\dot{W}_e) + Q_{burn}] \tag{B.46}$$

$$* \quad \dot{W}_{as} = -(\dot{W}_c - \dot{W}_c)/(f/a + 1) \qquad \left.\right\} \text{if } \dot{W}_c < 0 \tag{B.47}$$

$$* \quad \dot{W}_{fs} = \dot{W}_f - \frac{f/a}{(fa + 1)} (\dot{W}_e - \dot{W}_c) \tag{B.48}$$

$$* \quad \dot{W}H_3 = \gamma[C_p(T_3 \dot{W}_c - T_3 \dot{W}_e) + Q_{burn}] \tag{B.49}$$

$$C_p = aT_3 + b \tag{B.50}$$

Note: (*) denotes a state equation.

B.2 Functions: Fan (f_1, f_2, f_3, f_4)

$$(\text{If } \dot{W}_{Fc}/PNF_c < 280\text{: stall}) \tag{B.51}$$

$$\phi = 1.630\ 10^{-3}\ \dot{W}_{Fc}/PNF_c \tag{B.52}$$

$$\psi = K\phi^2 + 0.11 \begin{cases} K = KPF\ \dot{W}_{Fc} > 0 \\ K = KNF\ \dot{W}_{Fc} < 0 \end{cases}$$

$$P_{2T}^{*},\ P_{2H}^{*} = (1.073)(P_1)\left(1 + \frac{PNF_c^2}{.9916}\right) \tag{B.53}$$

$$\text{if } \dot{W}_{Fc}/PNF_c > 350\text{: recover} \tag{B.54}$$

$$P_{2T}^{*} = P_1(1 + PNF_c \text{ factor}) \qquad \text{factor} = F_1(\dot{W}_{Fc}/PNF_c) \tag{B.55}$$

$$P_{2H}^{*} = P_1(1 + PNF_c \text{ factor}) \qquad \text{factor} = F_2(\dot{W}_{Fc}/PNF_c) \tag{B.56}$$

$$T_{2T}^{*},\ T_{2H}^{*} = 1.11\ T_1 \tag{B.57}$$

B.3 Functions: Compressor

$$\left(\text{if } \dot{W}_{cc}/PNC_c < 31\text{: stall}\right)$$

$$\phi = 1.714 \times 10^{-2}\ \dot{W}_{cc}/PNC_c \tag{B.58}$$

$$\psi = k\phi^2 + 1.54 \begin{cases} K = KPC\ \dot{W}_{cc} > 0 \\ K = KNC\ \dot{W}_{cc} < 0 \end{cases} \tag{B.59}$$

$$P_3^{*} = (1.206)\ P_{2H}\ (1 + 0.8528\quad PNC_c^2) \tag{B.60}$$

$$T_3^* = T_{2H}\left[1 + PNC_c^2 \frac{\left(\left(\frac{P_3^*}{P_{2H}}\right)^{.286} - 1\right)}{\eta}\right] \tag{B.61}$$

$$\eta = \eta_o + m_\eta \phi \tag{B.62}$$

$$m_\eta = .4031 \tag{B.63}$$

$$\left(\text{if } \dot{W}_{cc}/PNC_c > 33\text{: recover}\right)$$

$$P_3^* = P_{2H}\ (1 + PNC_c^2\ \text{factor}) \qquad \text{factor} = F_3\ (\dot{W}_{cc}/PNC_c) \tag{B.64}$$

$$T_3^* = T_{2H}\ (1 + PNC_c^2\ \text{factor}) \qquad \text{factor} = F_4\ (\dot{W}_{cc}/PNC_c) \tag{B.65}$$

Note: All functions F_i are 1-dimensional interpolations

B.4 Parameters

$P_o = 15.2$

$P_{exit} = 14.7$

$P_x = 0.48$

$T_o = 519.$

$R = 640.$

$r = 1.4$

$P_{STD} = 14.7$

$T_{STD} = 519.$

$R_o = 1.6458 \times 10^{-3}$

$R_{DUCT} = 2.1756 \times 10^{-2}$

$R_x = 1.0 \times 10^{-2}$

$V_1 = 20000.$

$V_{2T} = 109189$

$V_{2H} = 2641$

$V_3 = 3319$

$L_T = 4.299 \times 10^{-5}$

$L_H = 2.679 \times 10^{-4}$

$L_C = 1.427 \times 10^{-3}$

$PNF = .899$

$PNC = 1.052$

$KPF = 0.5$

KNC = 50.0

hA = 0.6672

η_o = 0.1

Stoi = 15.

a = 2.629×10^{-5}

b = 0.2246

HV = 18400.

K_{noz} = 8.49

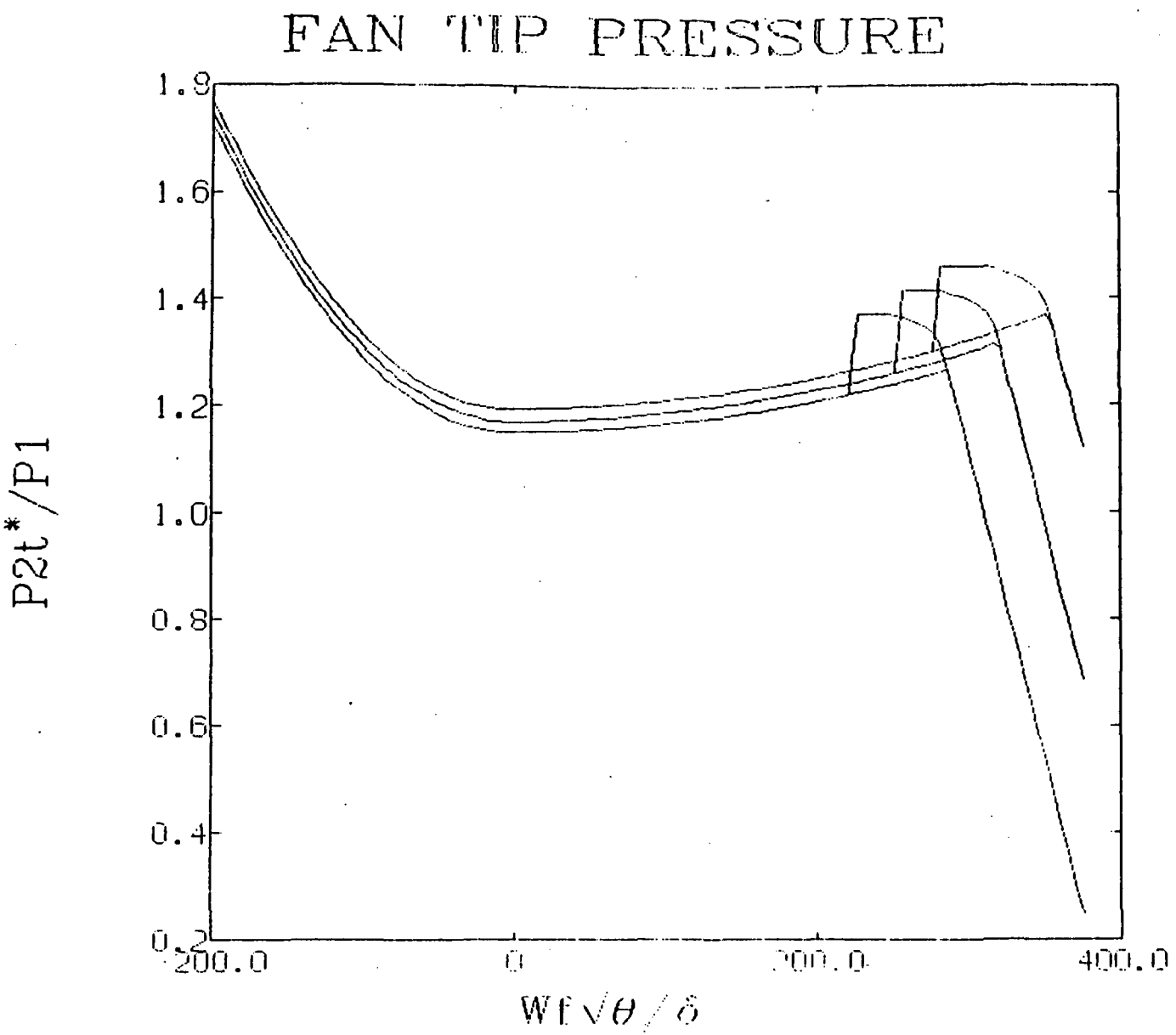
FAN TIP PRESSURE
P2t*/P1
1.8
1.6
1.4
1.2
1.0
0.8
0.6
0.4
0.2
-200.0
0
200.0
400.0
Wf√θ/δ

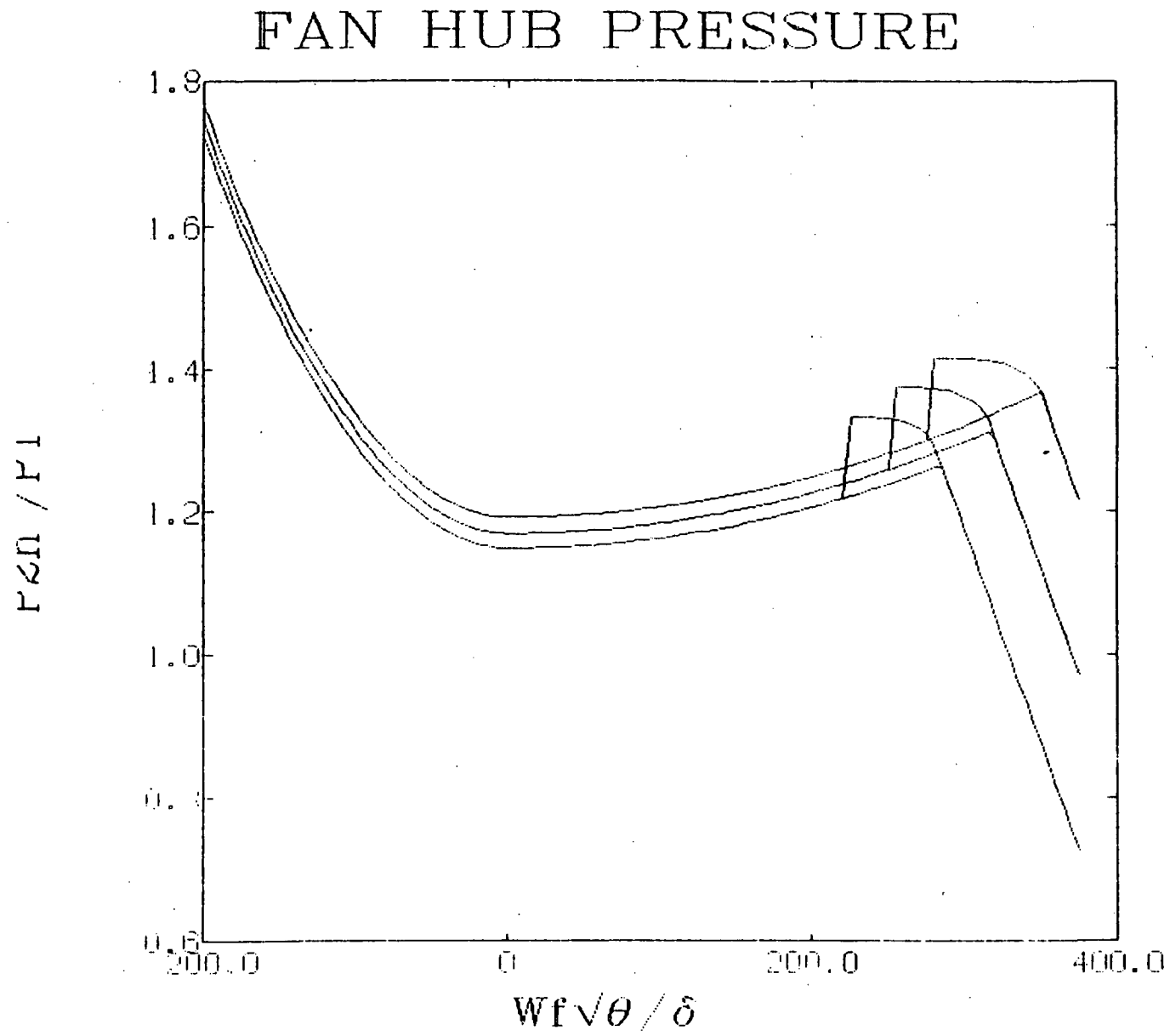
FAN HUB PRESSURE
1.8
1.6
1.4
1.2
1.0
0.8
200.0
0
200.0
400.0
Wf√θ / δ

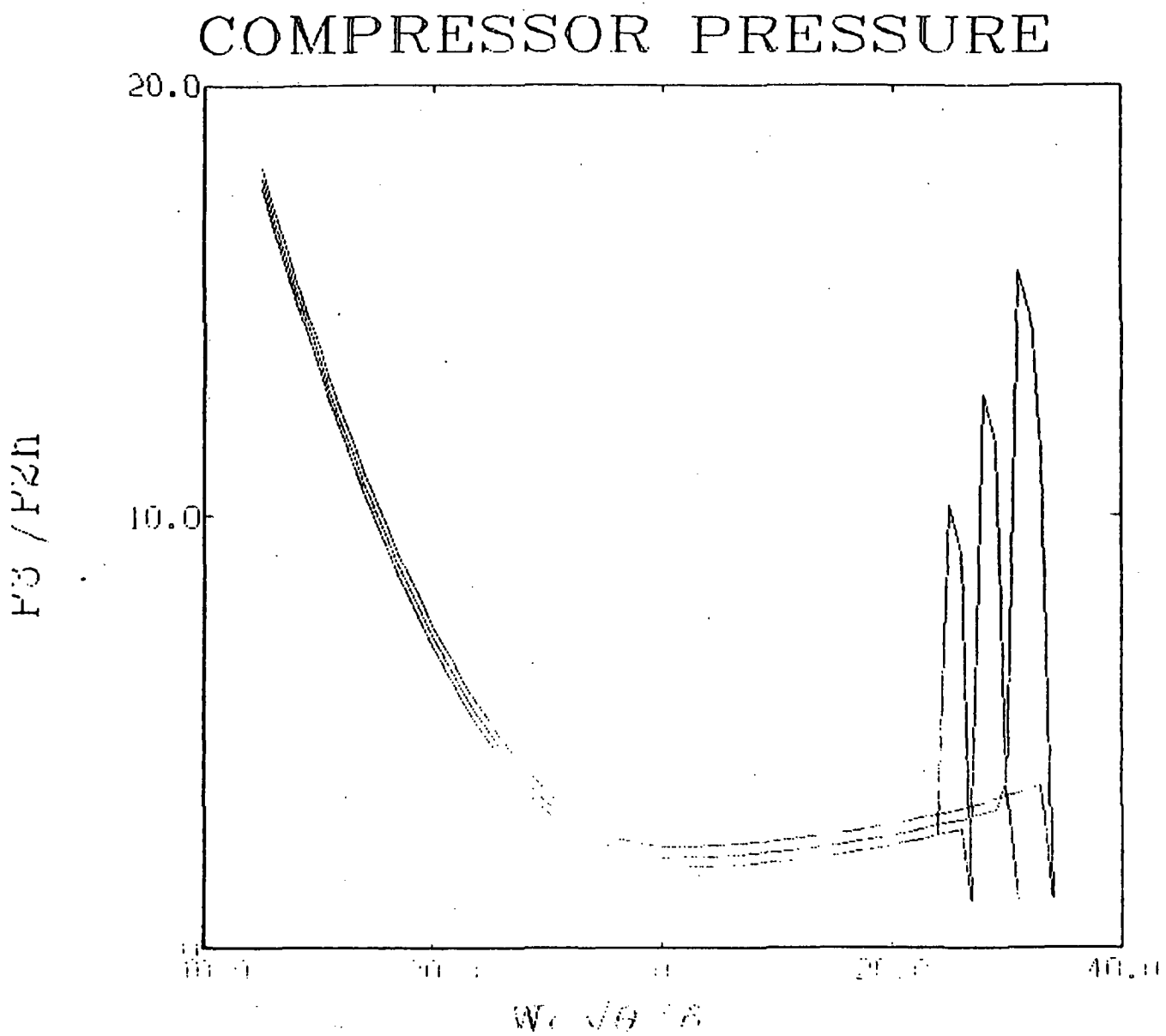
COMPRESSOR PRESSURE
20.0
10.0
P3 / P2R
40.0

REFERENCES

1. Ward, C.G., "Compressor Stability Assessment Program," Technical Report AFAPL-TR-74-107, Vols. I and II, 1974.

2. Johnson, I.A. and Bullock, R.O., eds., Aerodynamic Design of Axial Flow Compressors, NASA SP-36, 1965.

3. Wenzel, L.M., Bruton, W.M., "Analytical Investigation of Nonrecoverable Stall," NASA TM 82792, February 1982.

4. Allen, D.M., "Mean Square Error of Prediction as a Criterion for Selecting Variables," Technometrics, Vol. 13, No. 3, Aug. 1971, pp 469, 475.

5. Trankle, T.L., "Practical Aspects of System Identification," ASME Paper 79-WA/DSC-23, presented at Winter Annual Meeting, New York, December 3, 1979.

6. Lawson, C.L., and Hanson, R.J., Solving Least Square Problems, Prentice-Hall, 1974.

7. Marquardt, D.W., "An Algorithm for Least Squares Estimation of Nonlinear Parameters," J. Soc. Indust. Appl. Math., Vol. 11, No. 2, 1963, pp 431-441.

8. Kalman, R.E., Bucy, R., "New Results in Linear Filtering and Prediction," Trans. ASME, Vol. 83D, 1961, p. 95.

9. Luenberger, D.G., "Observing the State of a Linear System," IEEE Trans. Military Electronics, Vol. MIL-8, 1964, pp 74-80.

10. Fisher, R.A., "Two New Properties of the Mathematical Likelihood," Proc. Roy. Soc., London, Vol. 144, 1934.

11. Trankle, T.L., Vincent, J.H., Franklin, S.N., "System Identification of Nonlinear Aerodynamic Models," prepared for NATO AGARDOGRAPH "The Techniques and Technology of Nonliner Filtering and Kalman Filtering," February 1982.

12. Forsythe, G., Moler, C.B., Computer Solution of Linear Algebraic Systems, Prentice-Hall, 1967.

13. Bierman, G.J., Factorization Methods for Discrete Sequential Estimation, Academic Press, New York, 1977.

14. Maine, R.E. and Iliff, K.W., "User's Manual for MMLE3, A General FORTRAN Program for Maximum Likelihood Parameter Estimation," NASA TP-1563.

15. Hall, Jr., W.E., "System Identification - An Overview," Naval Research Reviews, Vol. 30, No. 4, April 1977, pp.1-20.

16. Gustavsson, I., "Survey of Applications of Identification in Chemical and Physical Processes," Proceedings of the 3rd IFAC Symposium, The Hague/Delft, The Netherlands, 12-15 June, 1973, pp 67-85.

17. Baeyens, R., Jacquet, B., "Applications of Identification Methods in Power Generation and Distribution," Proceedings of the 3rd IFAC Symposium, The Hague/Delft, The Netherlands, 12-15 June 1973, pp 1107-1121.

18. De Hoff, R.L., "Identification of a STOL Propulsion Plant Model," J. of Guidance and Control, Vol. 2, No. 3, May-June 1979.

19. Bekley, G.A., Benken, J.E.W., "Identification of Biological Systems: A Survey," Automatica, Vol. 14, No. 1, Jan. 1978, pp 41-47.

20. Chow, G.C., "Identification and Estimation in Econometric Systems: A Survey," IEEE Trans. on Automatic Control, Vol. AC-19, No. 6, Dec. 1974, pp 855-861.

21. Gersch, W., and Foutch, D.A., "Least Squares Estimates of Structural System Parameters Using Covariance Function Data," IEEE Trans. on Automatic Control, Vol. AC-19, No. 6, Dec. 1974, pp 898-903.